Multiple Photon Reactions of Organic Molecules in Solution

by

Jeffrey T. Banks

A thesis
presented to the University of Ottawa
in partial fulfillment of the degree of
Ph. D. in Chemistry

ISBN 0-612-00516-X

UNIVERSITÉ D'OTTAWA
UNIVERSITY OF OTTAWA

Acknowledgements

I would like to thank my thesis advisor, Dr. J. C. (Tito) Scaiano, for all his help and advice. I consider myself fortunate to have been a member of his group during the past four years. Thanks to Dr. Waldemar Adam for allowing me to work at his lab in Würzburg and Dr. Rolf Shulte Oestriche for his invaluable assistance during my stay there. Drs. B. R. Arnold, J Andraos, H. Garcia, M. A. Miranda and Ms. N. deLucas have also collaborated with me in some parts of the research described in this thesis and their help is greatly appreciated. I would also like to thank NSERC for financial support.

I would also like to thank the past and present members of Tito's group, all of whom have helped at one time or another. In particular I would like to thank: S. E. Sugamori and Drs. M. Barra, R. W. Redmond, P. F. McGarry, C. Bohne, and B. R. Arnold (again) who showed me how things worked when I first arrived; A. Berinstain and A. Simard who set up the majority of the LFP system at the University of Ottawa; R. Boch who started at the same time I did and C. Sturino (from Dr. Fallis' group) who was my synthetic advisor. I would be remiss if I did not mention Dr. M. T. H. Liu and the rest of the Chemistry Department at the University of Prince Edward Island, your undergraduate program is second to none.

Special thanks to Mónica (Number One) for putting up with me as a neighbor and for being a good friend.

I would also like to thank my parents for all the help they have been over the years. Finally, I must thank Marion and Alexis. Alexis you are truly a wonderful daughter; it was you who inspired me to return to school and continue my education. Marion, I must apologize because words cannot express my gratitude for what you have done for me. I am sure that without you none of this would have happened. I look forward to the future that we shall share, we have worked hard to make it bright.

Table of Contents

		Page
	Acknowledgements	i
	Table of Contents	ii
	List of Tables	v
	List of Figures	vi
	Abstract	xi
Chapter 1	Introduction	1
1.1	Preliminaries	1
1.2	Current Methods to Study the Photochemistry of Transient Intermediates	8
1.2.1	Low Temperature Matrix Techniques	9
1.2.2	High-Intensity Techniques	9
1.2.2.1	Two-Laser Two-Colour Laser Flash Photolysis	10
1.2.2.2	Laser Jet Photolysis	14
1.3	Purpose of this Thesis	16
Chapter 2	Laser Techniques and General Instrumentation	18
2.1	Introduction	18
2.2	Laser Flash Photolysis	18
2.2.1 .	Two-Laser Two-Colour Laser Flash Photolysis	24
2.3	Preparative Multi-photon chemistry	25
2.3.1	Laser-Jet Photolysis	26
2.3.2	Laser-Drop Photolysis	29
2.4	Nanosecond Photography	32
2.5	General Instrumentation	34
Chapter 3	Use of Two-Laser Two-Colour Laser Flash Photolysis and Laser-Jet Photolysis to Study the Thermal and Photochemical Fragmentation Pathways of α,α-Dialkoxybenzyl Radicals	37
3.1	Introduction	37
3.2	Results	42

3.2.1	Absorption Spectroscopy of Dialkoxybenzyl Radicals	42
3.2.2	Bleaching of Dimethoxybenzyl Radicals.	45
3.2.3	Thermally Initiated Experiments on the Fragmentation of Unsymmetric Dialkoxybenzyl Radicals	50
3.2.4	Low-Intensity Irradiations With Predominant Thermal Fragmentation of Unsymmetric Dialkoxybenzyl Radicals	51
3.2.5	Laser-Jet Experiments	52
3.3	Discussion	53
3.4	Conclusion	55
3.5	Experimental	56
Chapter 4	Development of the Laser-Drop Technique to Induce Multiple Photon Chemistry: Examples Involving the Photochemistry of Diphenylmethyl Radicals	62
4.1	Introduction	62
4.2	Results	65
4.2.1	Description of the Experiment	65
4.2.2	Photochemistry of 1,1-Diphenylacetone	68
4.3	Discussion	75
4.3.1	The Diphenylmethyl Radical System	76
4.4	Conclusion	79
4.5	Experimental	80
Chapter 5	Examples of Multi-Photon Chemistry of Organic Molecules in Solution	82
5.1	Introduction	82
5.2	α,α-Disubstituted Benzyloxyl Radicals	83
5..2.1	Results	90
5.2.1.1	Photochemistry of Dicumyl Peroxide	90
5.2.1.2	Photochemistry of 1,1-Diphenylethyl-t-butyl Peroxide	94
5.2.2	Discussion	99
5.2.2.1	The Cumyloxyl Radical System	99

5.2.2.2	The 1,1-Diphenylethoxyl Radical System	101
5.2.3	Conclusion	106
5.3	Photochemistry of 1,5-Diiodoalkanes: Evidence for the Formation of a Bridged Iodine Radical	107
5.3.1	Results	111
5.3.2	Discussion	119
5.3.3	Conclusion	124
5.4	Laser-Drop Photolysis of 2-Diazo-1,3-Indandione: Evidence for a Propadienone Intermediate	124
5.4.1	Results	128
5.4.2	Discussion	131
5.4.3	Conclusion	135
5.5	The Two-Photon Chemistry of ortho-Methylbenzophenone	135
5.5.1	Results	141
5.5.2	Discussion	146
5.5.3	Conclusion	148
5.6	Experimental	149
Chapter 6	Investigations Concerning Drop Explosion During Laser-Drop Experiments	152
6.1	Introduction	152
6.2	Results	159
6.2.1	Fluorescence Spectra in Drops	159
6.2.2	Nanosecond Photography	162
6.3	Discussion	173
6.4	Conclusion	178
6.5	Experimental	179
Chapter 7	Final Comments and New Directions	180
	Claims to Original Research	185
	References	186

List of Tables

		Page
Table 2.1	Available lasers at the University of Ottawa	20
Table 3.1	Fragmentation ratios k1/k2 of the radicals **6** obtained under various experimental conditions.	52
Table 4.1	Photolysis of diphenylmethyl radical precursors in CCl_4	71
Table 4.2	Photolysis of diphenylmethyl radical precursors in methanol	74
Table 5.1	Photolysis of **2** in acetonitrile and in methanol.	94
Table 5.2	Photolysis of **5** in acetonitrile.	98
Table 5.3	Product Distributions for LDP and Lamp Photolysis of **16** and **25**.	118
Table 5.4	Photolysis of **43** in oxygenated benzene.	144

List of Figures

		Page
Figure 1.1	Potential energy diagram for two excited states of the same multiplicity. Diagram shows the overlap of the vibrational levels due to the small energy gap.	3
Figure 1.2	Transient spectrum obtained 500 ns after a 308 nm laser pulse. The band centered at 335 nm is attributed to **2** and the band at 480 nm to **3**. Inset shows the decay trace for **2** as monitored at 335 nm.	12
Figure 1.3	Two-laser two-colour LFP of **1** in acetonitrile. Arrows show the timing and wavelengths of the lasers. (a) Monitored at 325 nm. (b) Monitored at 480 nm.	13
Figure 2.1	Voltage on the PMT during the course of one laser pulse. Note the logarithmic time scale.	22
Figure 2.2	Schematic diagram for laser-jet photolysis.	28
Figure 2.3	Different behavior of drops suspended from (a) Near horizontal needle and (b) Vertical needle.	31
Figure 2.4	Schematic diagram showing nanosecond photographic experimental setup.	33
Figure 3.1	Transient spectrum obtained 1 μs after 308-nm laser pulse for a 1.500 mM solution of **1** in benzene. (a) Flow cell. (b) Static cell.	43
Figure 3.2	Decay trace monitored at 420 nm for 308-nm LFP of 1.50 mM solution of **1** in benzene.	45
Figure 3.3	(a) Transient spectrum of the α,α-dimethoxybenzyl radical produced according to reactions 3.7 and 3.8. Inset shows the growth of the radical monitored at 420 nm. (b) Transient spectrum for α-methoxy-α-ethoxybenzyl radical produced according to reactions 3.7 and 3.8. Inset shows the decay of the radical monitored at 420 nm. Both spectra corrected for acetal photolysis; see text.	46

Figure 3.4	Absorption signal (ΔOD) as a function of laser intensity for 308 nm LFP of **1** as monitored at 420 nm. %100 laser power corresponds to ~25 mJ.	47
Figure 3.5	(Top) Bleaching of dimethoxybenzyl radical upon excitation with a dye laser (420 nm). The dye laser was fired 3 μs after the synthesis laser (308 nm). Radical produced from a solution of 0.33 M benzaldehyde dimethyl acetal and 0.28 M di-tert-butyl peroxide in benzene (monitored at 390 nm). (Bottom) Bleaching of **8** to form **7** upon excitation with a dye laser (420 nm). The dye laser was fired 3 μs after the synthesis laser (308 nm). **8** was formed from a solution of **7** in toluene (monitored at 494 nm). Inset shows expansion of the region in which the dye laser was fired.	48
Figure 3.6	Arrhenius plot for the relative rates (k_1/k_2) of the two fragmentation pathways for the α-methoxy-α-ethoxybenzyl radical.	51
Figure 4.1	Schematic diagram of the timing sequences for laser-drop irradiations.	66
Figure 4.2	Diagram of the cell employed for laser-drop experiments. The overall length is 12 in. and the cell is equipped with removable quartz windows.	67
Figure 4.3	Transient spectra recorded upon 308 nm excitation of a 2 mM solution of **5** in acetonitrile recorded immediately (a) and 0.5 μs (b) after excitation. The increase in peak intensity in b is due to decay of excited radical (**5***) leading to ground state repopulation.	69
Figure 4.4	(a) Decay of the excited diphenylmethyl radical **6*** monitored at 355 nm. (b) Decay of the ground state diphenylmethyl radical **6** monitored at 335 nm.	70
Figure 4.5	Trace showing the repopulation of the ground state radicals at short time scales. Monitored at 335 nm.	71
Figure 4.6	(Top) Fluorescence spectrum for excited diphenylmethyl radicals **6*** in drops of methanol. (Bottom) Decay trace for the excited radical monitored by its emission at 535 nm.	73
Figure 5.1	Transient spectrum obtained by 266 nm excitation of a 1 mM solution of **2** in acetonitrile.	91

Figure 5.2	(a) Decay trace of cumyloxyl radical **3** in acetonitrile (monitored at 485 nm). (b) Decay trace of cumyloxyl radical **3** in methanol (monitored at 485 nm).	92
Figure 5.3	Quenching plot of the decay (k_{obs}) of radical **3** as a function of the concentration of methanol in the 0 to 10 M range. Monitored at 485 nm. Solvent: acetonitrile.	93
Figure 5.4	Transient spectra obtained after 248 nm excitation of peroxide **5** in acetonitrile at 100 ns and 1 μs time delays. The UV band grows in concurrently with the decay of the visible band.	95
Figure 5.5	Effect of oxygen on the decay of the signals. (Top) Monitored at 320 nm. Note the initial jump in the signal under nitrogen due to a UV absorption of the alkoxyl radical **6**. (Bottom) Monitored at 520 nm.	96
Figure 5.6	Arrhenius plot for the decay of the visible signal produced upon 248 nm excitation of **4**.	97
Figure 5.7	AM1-UHF calculated reaction coordinate for reactions 5.9 to 5.11. All values in kcal/mol.	103
Figure 5.8	Transient spectrum recorded upon 266 nm excitation of a 2 mM solution of **21** in cyclohexane.	113
Figure 5.9	Decay of signal produced upon 266 nm excitation of **21** in cyclohexane. Monitored at 320 nm.	113
Figure 5.10	Transient spectrum obtained upon 248 nm excitation of 50 μM solution of **16** in cyclohexane.	114
Figure 5.11	Decay of the signals produced upon 308 nm excitation of 0.39 mM solutions of **16** in cyclohexane when bubbled with nitrogen or oxygen. Monitored at 350 nm.	114
Figure 5.12	Absorption signal (ΔOD) as a function of laser intensity for 308 nm LFP of 0.39 mM **16** in cyclohexane as monitored at 350 nm. %100 laser power corresponds to ~60 mJ.	115
Figure 5.13	Bleaching of the signal from 248 nm LFP of 50 μM **16** in cyclohexane upon excitation with an excimer laser (308nm). The excimer laser was fired 1 μs after the synthesis laser (248 nm).	115

Figure 5.14	Transient spectrum obtained upon 248 nm excitation of 10 mM solution of **22** in cyclohexane.	116
Figure 5.15	Decay of the signals produced upon 248 nm excitation of 10 mM solutions of **22** in cyclohexane when bubbled with nitrogen or oxygen. Monitored at 350 nm.	117
Figure 5.16	Transient spectrum obtained from 308 nm LFP of 0.10 mM solutions of **30** in acetonitrile.	129
Figure 5.17	Transient spectrum obtained from 308 nm LFP of 0.10 mM solutions of **30** in methanol.	129
Figure 5.18	(Top) Growth of the enol ester **33** formed by trapping of the ketene **32** by methanol, monitored at 390 nm. (Bottom) Decay of **33** as monitored at 390 nm.	130
Figure 5.19	Ratio of the **37**-to-**34** as a function of laser power. 100 % laser power corresponds to ~100 mJ/pulse. The line in the graph is an arbitrary fit.	131
Figure 5.20:	Transient spectra obtained from the 308 nm LFP of 0.50 mM deaerated solutions of **43** in methanol.	142
Figure 5.21	Transient spectra obtained from 308 nm and 308 + 440 nm TLTC-LFP of 0.50 mM deaerated solutions of **43** in methanol. Spectra obtained 100 ns before (triangles) and 100 ns after (diamonds) the firing of the second (440 nm) laser.	142
Figure 5.22	Decay traces from TLTC-LFP of 0.50 mM **43** in methanol. (Top) Jump in signal as monitored at 355 nm. (Bottom) Bleach of signal as monitored at 455 nm.	143
Figure 5.23	AM1-RHF calculated geometries and bond orders for the central rings for E-**45**, E-**45***, and **46**.	145
Figure 6.1	Plot showing typical behavior of etch depth with laser fluence.	154
Figure 6.2	Fluorescence spectra of 160 μM pyrene in hexanes. Under normal and laser-drop conditions.	160

Figure 6.3	Fluorescence decays of the monomer and excimer emissions from 160 μM pyrene in hexanes. (a) Under laser-drop conditions. (b) In a LFP cell under normal LFP conditions.	161
Figure 6.4	Scanned image of Polaroid photograph of acetonitrile 1 μs after the LDP laser pulse; a) actual size, b) enlarged ~8 times.	165
Figure 6.5	Photograph of hexane drop containing 160 μM pyrene. No flash laser used (see text).	166
Figure 6.6	Nanosecond photographs of acetone and acetonitrile at delay times of: a) 1 μs, b) 2 μs, c) 5 μs, d) 10 μs. Arrow at the top of the pictures indicates the direction of the laser.	167
Figure 6.7	Nanosecond photographs of acetonitrile at delay times of: a) 30 μs, b) 100 μs, c) 2 ms. Arrow at the top of the pictures indicates the direction of the laser.	168
Figure 6.8	Nanosecond photographs of acetone at delay times of: a) 30 μs, b) 200 μs, c) 2 ms. Arrow at the top of the pictures indicates the direction of the laser.	169
Figure 6.9	Nanosecond photographs of hexane drops with 9-bromophenanthrene at delay times of: a) 1 μs, b) 3 μs, c) 4 μs, d) 8 μs, e) 15 μs, f) 30 μs. Arrow at the top of the pictures indicates the direction of the laser.	170
Figure 6.10	Nanosecond photographs of hexane drops with 9-bromophenanthrene at delay times of: a) 100 μs, b) 1 ms. Arrow at the top of the pictures indicates the direction of the laser.	171

Abstract

This thesis presents the results from numerous studies on the multiple photon reactions of organic molecules in solution. The initial investigations on the selectivities of radical fragmentation reactions from ground and excited states required the use of both pulsed and continuous wave laser techniques. Laser flash photolysis techniques were used to determine that α,α-dimethoxybenzyl radicals undergo fragmentation from the excited state with a quantum yield which is close to one. High intensity laser-jet photolysis was used to determine the selectivities for the excited state fragmentation of unsymmetrically substituted α,α-dialkoxybenzyl. It was found that the excited radicals show no selectivity upon fragmentation whereas the ground state radical fragmentations are governed by the thermodynamic stability of the radical products.

Lack of a suitable method for the production of semi-preparative amounts of multiple photon reaction products in our own laboratory led us to develop a new technique which utilizes pulsed lasers. By irradiating small droplets of solution with the focused output from a pulse laser we were able to induce multiple photon reactions with efficiencies which are comparable to the laser-jet technique. A direct comparison was made for the case of diphenylmethyl radicals in carbon tetrachloride and methanol.

This method, dubbed laser-drop photolysis, was used, along with laser-flash photolysis techniques and conventional lamp irradiations, to investigate and compare the chemistry for several transient species from both the ground and excited states. A number of unique reaction pathways

have been found to occur from the excited states of the transient intermediates. For example, ground state 1,1-diphenylethoxyl radicals undergo a neophyl-like rearrangement to yield 1-phenoxy-1-phenylethyl radicals. From the excited state this radical undergoes β-scission, a process which does not occur from the ground state radical.

Irradiation of small drops of liquid by the focused output from high powered pulse lasers results in their destruction in a manner similar to the ablative photodecomposition of organic polymers. We have investigated the dynamics of the drop explosion by taking Polaroid photographs with a time resolution of ~20 ns by using a second pulsed laser as the flash for the camera. The destruction of the drops occurs in the μs time scale and a model has been proposed which is consistent with the dynamics of drop explosion. Further, pyrene has been used in attempts to probe the temperature increase inside the drop just prior to its explosion.

Chapter 1: Introduction.

1.1 Preliminaries.

That chemical reactions can be initiated by light has been known for centuries.[1] In the early 19th century von Grotthuss, and later Draper, were able to show that light must be absorbed in order to induce a chemical transformation. Although this seems obvious to the modern chemist, the implications of this conclusion (known as the Grotthuss-Draper law) formed the basis for later investigations which related the intensity of the light absorbed by a system to the rate of photochemical reactions.[2]

In 1873 Sestini and Cannizzaro reported one of the earliest known organic photochemical reactions. This involved the photolysis of santonin in 80% acetic acid to produce photosantonic acid. It is interesting, considering the title of this thesis, that this reaction was later shown to involve the absorption of three photons to produce the final product[1] (Scheme 1.1). Although the intermediates involved in this reaction are all isolable molecules, it can still be considered a multiple photon reaction.

At the turn of the twentieth century the appearance of quantum theory and the realization of the dual nature of light led Stark, and later Einstein, to relate the number of photons absorbed by a system to the number of molecules transformed in a photochemical reaction. They proposed that the amount of radiation absorbed is limited to one photon per molecule taking place in the reaction. This law, known as the law of photochemical equivalence (also known as the Stark-Einstein Law), was not easily accepted; this is because it was not known at the time that an excited molecule could be deactivated by processes other than chemical transformations

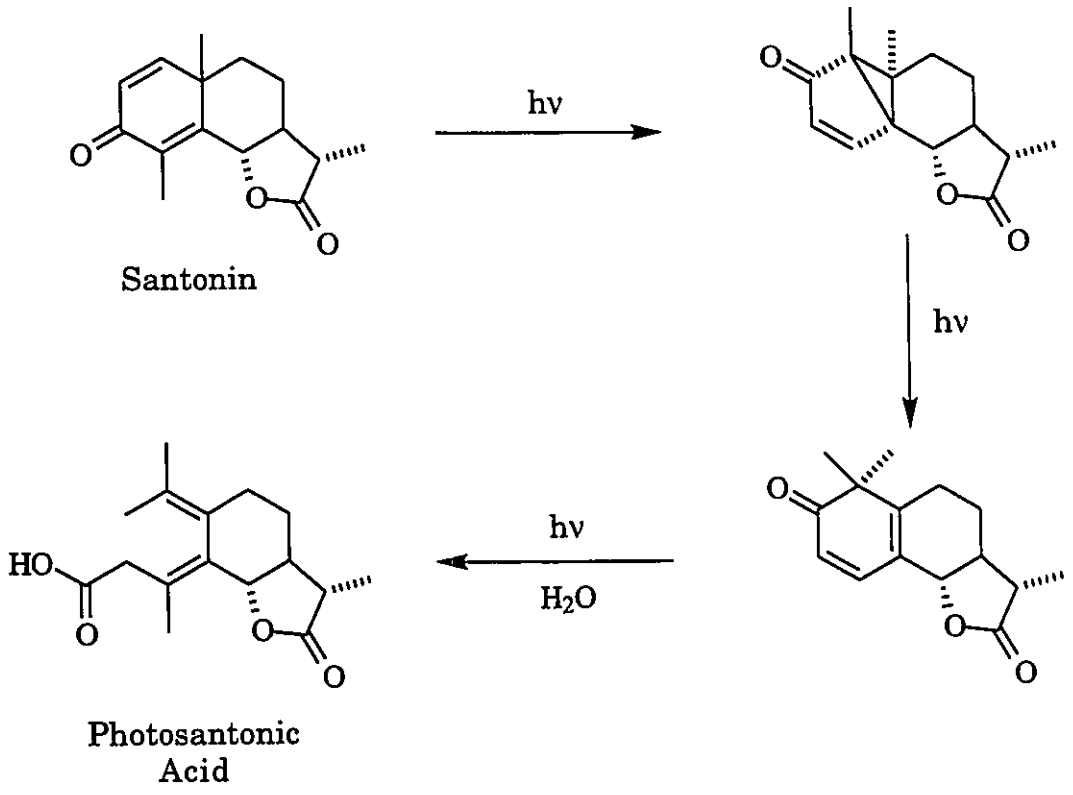

Santonin

Photosantonic Acid

Scheme 1.1

and the failure to recognize the difference between primary and secondary photochemical processes[2] (such as the chain reactions of free radicals).

The law of photochemical equivalence is a result of the short lifetimes of excited species, often only a few tens of nanoseconds or less for excited singlet states. With ordinary radiation it is unlikely that a molecule which has been excited by the absorption of a photon will absorb a second photon before it has been deactivated. As a consequence of this law, it had been generally accepted that the products of photochemical reactions were not altered by changes in the intensity of the light used.[3]

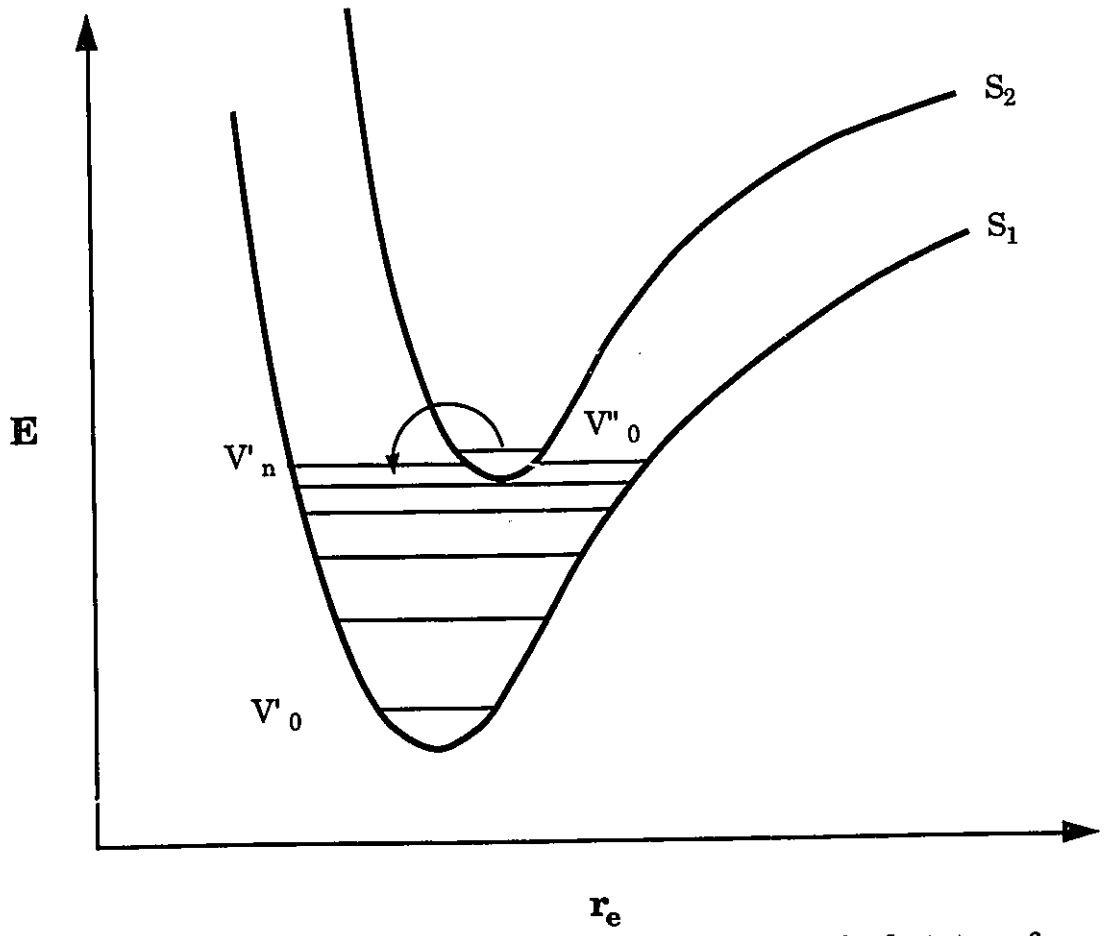

Figure 1.1: Potential energy diagram for two excited states of the same multiplicity. Diagram shows the overlap of the vibrational levels due to the small energy gap.

Another factor which influenced the belief that light intensity had little consequences on the outcome of a photochemical reaction was first postulated to explain the fact that the fluorescence spectra of molecules in solution were almost insensitive to the wavelength used for excitation. Kasha postulated that molecules which are excited to upper electronic states (other than S_1 or T_1) would undergo nonradiative transitions to the vibratonally relaxed first excited states much faster than radiative transitions or photochemical transformations. He reasoned that the energy gap between the ground and lowest excited states is usually much larger

than the gap between two excited states of the same multiplicity. Thus, the potential energy curves of two upper electronic states are usually close enough in energy so that the vibrational manifolds of the two states overlap, this allows molecules in an upper excited state to decay through vibrational levels and reach the lowest excited state. The smaller the energy gap between two states the faster is the nonradiative decay [4] (Figure 1.1). This postulate has become known as "Kasha's Rule".

In 1949, Norrish and Porter[3] published the first report on intensity dependent photochemistry using a gas-discharge flash-lamp. These authors found that the course for several bimolecular gas phase reactions could be altered by changing the intensity of the irradiating source. The most striking example was that the photochemical reaction of chlorine gas with carbon monoxide to produce phosgene, which is normally quite efficient, was completely suppressed under high intensity conditions. Under low-intensity conditions the reaction proceeds through a free radical chain (Scheme 1.2) initiated by the photochemical decomposition of chlorine gas to give chlorine atoms.[5,6] Under high-intensity conditions, the concentration of free radical species is so large that the termination reactions, which produces chlorine gas and carbon monoxide, become the dominate reactions of the radical species and thus suppresses the chain. Although this reaction does not break the law of photochemical equivalence or Kasha's rule, it demonstrated that the outcome of a photochemical reaction can be controlled by the intensity of the irradiating source.

Organic chemists have a great interest in transient intermediates because they provide a means by which the chemical transformations they wish to undertake may be understood. Once the mechanism of a reaction is understood, it may be possible to alter the parameters of the reaction so that

the yield of products is optimized. For instance, if it can be established that a chemical reaction proceeds through the intermediacy of a carbon centered radical, the diligent organic chemist will take great pains to eliminate oxygen from his reaction system to avoid the formation of peroxy radicals which may provide an alternate, usually undesirable, pathway for the ultimate fate of the carbon-centered radicals.

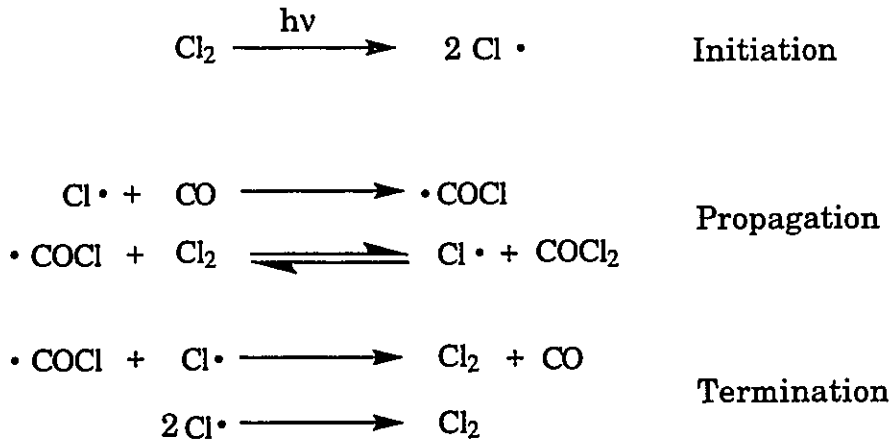

Scheme 1.2

Photochemists have played an integral part in developing methods to elucidate reaction mechanisms by characterizing the spectroscopic properties of the transient intermediates which lie on the reaction pathway between reactants and products. The rotating sector technique, first described in 1926 by Briers, Chapman and Walter,[7] was perhaps the first method to take advantage of the ability of light energy to produce short-lived reactive intermediates which could then be studied spectrophotometrically. The advent of gas-discharge flash-lamps led to the development of flash photolysis[8] which enabled the detection of transient species with lifetimes as short as a few hundreds of microseconds. The appearance of pulsed

lasers extended this technique into the nanosecond regime.[9,10] Recent advances in laser and electronic technology have reduced the available time domain to the picosecond regime.[11]

With the ever expanding knowledge base on the properties of transient intermediates, it has become evident that these short-lived species, which are molecules in their own right, often have suitable absorption properties so that they themselves can undergo electronic excitation. During the past few decades there has been a growing interest among photochemists concerning the fate of transient intermediates which are subject to excitation by electromagnetic radiation. Much like excited state molecules (which are included as transient intermediate species), it is the short-lived nature of these species which makes the absorption of light an unlikely event. The most efficient method of producing a large population of transient species at ambient temperatures is to photolyse a suitable precursor with high-intensity electromagnetic radiation. In order to excite the transient produced, it must absorb a second photon during its short lifetime. Thus, two photons will have been absorbed (one by the precursor, and one by the transient intermediate) to produce the excited transient.

As one can imagine, the intensity of light needed to initiate a multi-photon reaction is very much larger than that which can be produced by conventional light sources. With the advent of high powered lasers it has become possible to provide a sufficient flux of photons so that a transient intermediate may absorb a second photon before it has had time to be deactivated. When a transient intermediate undergoes electronic excitation, it finds itself in a high energy electronic state which may not be

normally accessible, and the fate of this species may be quite different than that of the ground-state transient intermediate.

From the above discussion, it can be seen that the ultimate fate of a photochemical reaction may be dependent on the intensity of the irradiating source. Wilson and Schnapp[12] have suggested that photochemical reactions may be partitioned into three domains depending on the intensity of light used and the behavior of the transient intermediates produced. These domains are characterized as follows: 1) The single-photon domain obeys the law of photochemical equivalence and is accessed by conventional, low-intensity sources of radiation. 2) The multiple-photon domain usually requires light intensities greater than about 10^{23} photons/cm^2 s. In this domain sequential multiple-photon processes become important and the law of photochemical equivalence is no longer valid. 3) The plasma domain requires even higher light intensities, $\geq 10^{28}$ photons/cm^2 s, and results in simultaneous double-photon absorption, dielectric breakdown and plasma formation.

There are other consequences of irradiation in the second domain besides multiple photon reactions, and since it is this domain that is the subject of this thesis, a brief description of the two major processes which occur is given here: 1) Intertransient reactions quite often occur in this domain because the large concentration of transient species (typically 0.1 to 10 mM) increases the probability that two transient species will encounter each other before they have reacted by another pathway. This is the type of reaction which was reported by Norrish and Porter[3] as the first intensity dependent photochemical reaction (discussed above). 2) Intratransient reactions become possible if transient lifetimes, absorption properties and concentrations allow them to compete with the precursor for the incident

photons. Note that, in order for a transient to undergo the absorption of a photon, it must absorb in the region of the irradiating source.

It should also be pointed out that the multiple photon processes which occur in the second domain arise from the sequential absorption of one or more photons by conventional transient species. The simultaneous multiple photon processes which occur in the third domain are a fundamentally different event. In this case, there is insufficient energy in the first photon to produce a stable excited state, but a pseudostate may exist for a time period which is governed by the uncertainty principle ($\leq 10^{-12}$ s); if this psuedostate absorbs a second photon within this time period it may produce a stable, conventional excited state.[12]

1.2 Current Methods to Study the Photochemistry of Transient Intermediates.

There are two strategies in studying the photochemistry of reactive intermediates: 1) Supply a sufficient number of photons to both produce and excite the transient intermediates. 2) Prolong the lifetime of the transient intermediate so that it is possible to further excite it with a second photon from a conventional light source; The first of these strategies falls into the category of high-intensity irradiations. The second has not been used during the course of the investigations described in this thesis, however, low temperature matrix isolation techniques must be mentioned here because of the large contribution they have made to the study of the photochemistry of transient intermediates[13-15] (and the study of transient intermediates in general).

1.2.1 Low Temperature Matrix Techniques.

The technique of low temperature matrix isolation spectroscopy was first described in 1954 by Pimentel et al.[16] and Norman and Porter.[17] Since that time it has become a well established technique in the study of reactive species.[18-20] Quite simply, this technique incorporates suitable photochemical precursors to reactive intermediates into a low temperature matrix (organic glasses, or low temperature inert gas matrices) and then subjects these to electromagnetic radiation from either a conventional or laser source to produce the target intermediate to be studied. This species is then characterized by appropriately adapted, conventional spectroscopic instruments (UV-Vis, IR, ESR etc.). The target species can then be further irradiated, usually at a different wavelength than that used to produce it, and the products from this 'second' irradiation characterized in a similar manner.

Because this technique uses conventional spectroscopic methods to characterize the target species, much more spectroscopic information can be obtained than with time resolved techniques. In fact, it is often possible to identify the structural features of the intermediate without having to isolate the products. Unfortunately, the reactivity of a species at the low temperatures used (from about 4 K to 77 K depending on the matrix material used) is different than that of the same species at room temperature, especially if the reaction is bimolecular or thermally activated.

1.2.2 High-Intensity Techniques.

Prior to the development of laser-drop photolysis,[21] described in detail in Chapter 4, two methods had been developed which could effectively study

multiple-photon reactions in solution. These two techniques attack the problems associated with the study of multiple-photon reactions from two different vantage points, one is a primarily spectroscopic/kinetic technique while the other is a semi-preparative method. Both techniques have been used during the course of the research described in this thesis and the experimental details are given in Chapter 2.

1.2.2.1 Two-Laser Two-Colour Laser Flash Photolysis.

This technique, as the name suggests, is an extension of laser flash photolysis and was developed in the early eighties by Scaiano and coworkers.[22-25] In this type of experiment two lasers are used in succession to produce, and then excite, the transient intermediate to be studied. The first laser is used to produce the transient to be studied and is dubbed the 'synthesis' laser. At a preset time interval after the synthesis laser has been fired, a second laser, the 'photolysis' laser, is fired into the photolysis cell to excite the transient. Experimental details for laser-flash photolysis (LFP) and two-laser two-colour laser flash photolysis (TLTC-LFP) can be found in Chapter 2.

While two-photon processes can frequently be initiated by single-pulse laser excitation, this does not provide sufficient control of the experiment to adequately understand the mechanisms or reaction kinetics. By utilizing two lasers, the timing, wavelength, and energy dose for each laser can be independently controlled. The wavelength of the synthesis laser is usually lower than the photolysis laser, in a region where the precursor to the transient to be studied absorbs. The photolysis laser must be in a region where the transient absorbs, and the precursor to the transient does not. If the precursor absorbs at the wavelength of the

photolysis laser (the second laser) further production of the transient may occur. Finally, the transient of interest must be sufficiently long-lived (typically ≥ 1 μs) so that there is suitable absorption at the time the second laser is fired.

Excitation of a transient intermediate by a second laser pulse will result in the formation of an excited transient. There are several scenarios possible as a consequence of exciting the transient intermediate. Whether or not the excited transient can be detected will depend on its lifetime and absorption spectrum. If the excited transient absorbs in a region of the spectrum where neither the transient intermediate nor its precursor absorb, and is sufficiently long lived to be detected, there will be an increase in the optical density in this region which decays as the excited transient is deactivated. Quite often, the lifetime of the excited transient is too short to be detected, however, if the ultimate fate of exciting the transient results in the depletion of the ground state transient a decrease in the absorption signal due to the ground state transient will be seen.

A good example to illustrate one possible outcome of a TLTC-LFP experiment can be seen during the one-, and two-laser photolysis of 2-keto-3,3-diphenyl-7-octene (**1**). LFP (308 nm) of **1** results in the spectrum shown in Figure 1.2, the absorption centered at 335 nm is due to the 1,1-diphenylhex-5-enyl radical (**2**), this radical absorbs a second 308 nm photon during the course of the laser pulse, resulting in the formation of the fluorenyl type radical (**3**), which absorbs in the 480 nm region. When a 337 nm laser pulse is fired ~2 μs after the 308 nm laser, an instantaneous decrease in the absorption signal at 325 nm can be seen (Figure 1.3a).

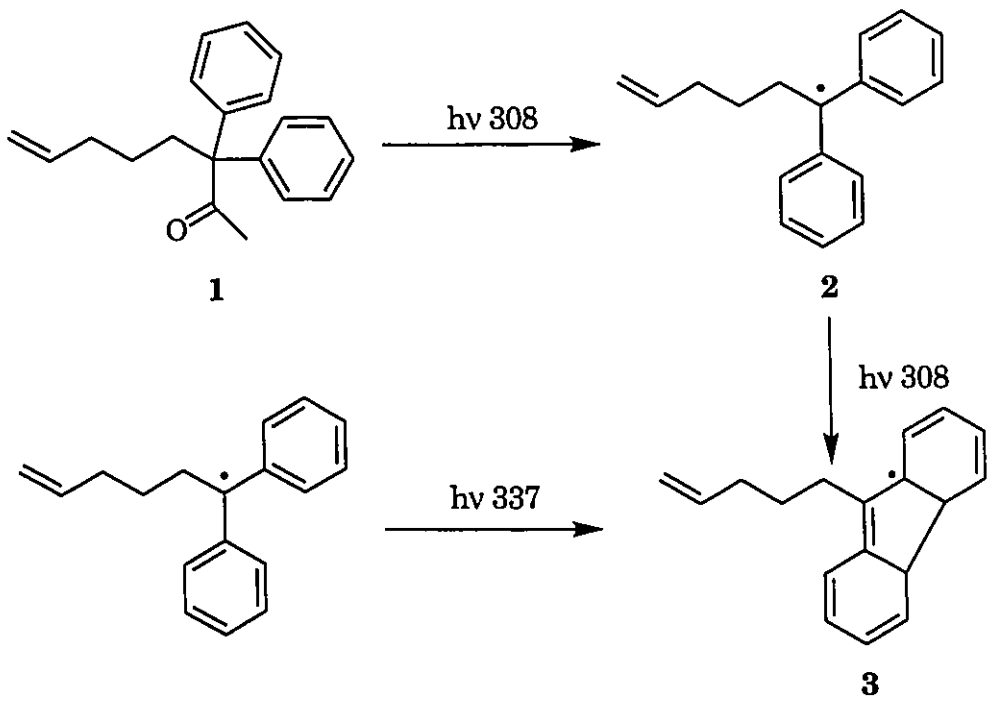

Scheme 1.3

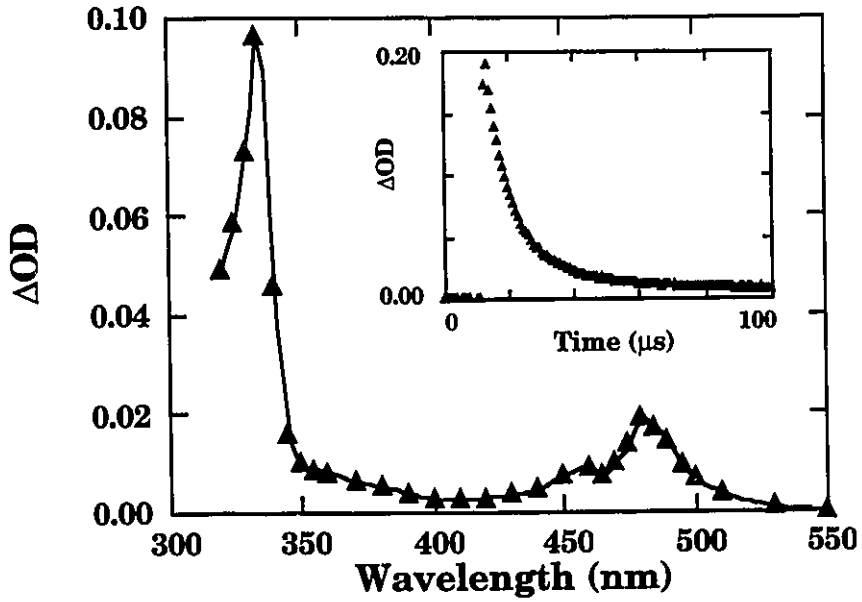

Figure 1.2: Transient spectrum obtained 500 ns after a 308 nm laser pulse. The band centered at 335 nm is attributed to **2** and the band at 480 nm to **3**. Inset shows the decay trace for **2** as monitored at 335 nm.

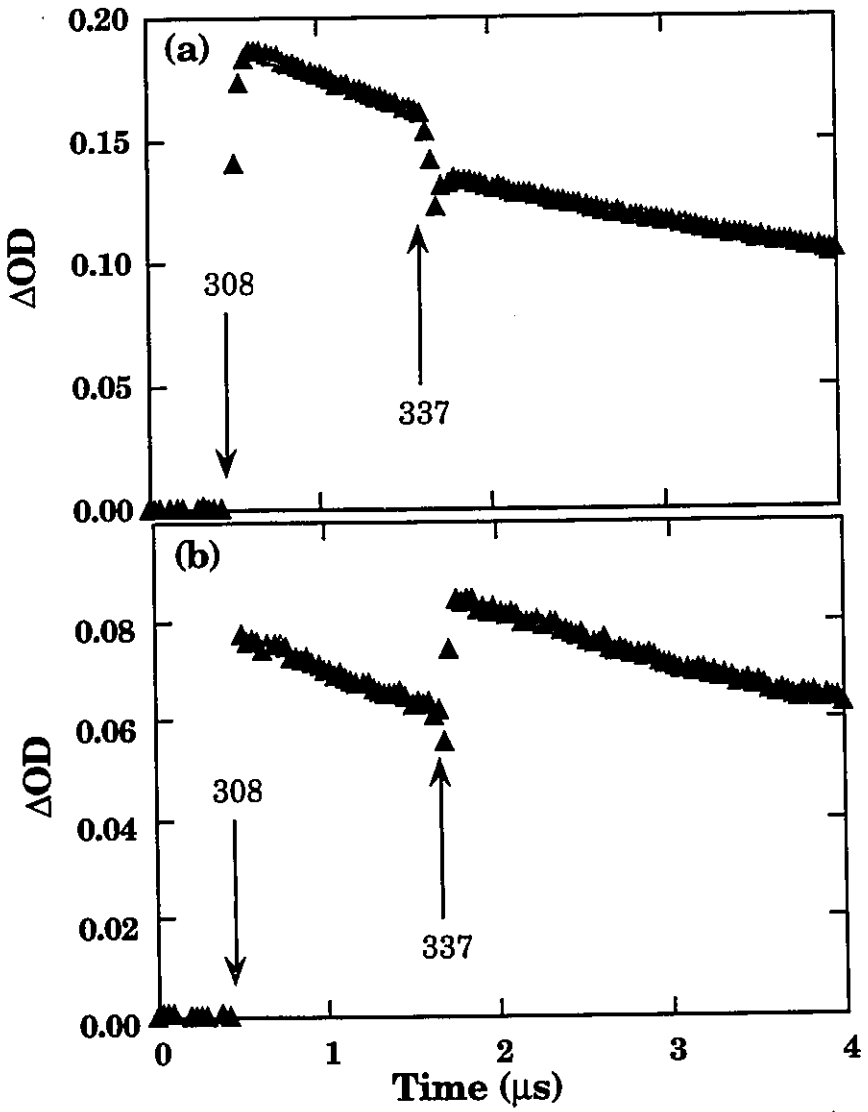

Figure 1.3: Two-laser two-colour LFP of **1** in acetonitrile. Arrows show the timing and wavelengths of the lasers. (a) Monitored at 325 nm. (b) Monitored at 480 nm.

Concurrent with the 'bleaching' at 325 nm, an instantaneous growth in the signal can be seen at 480 nm (Figure 1.3b). In this example, the excited radical, **2***, cannot be detected, but the consequences of excitation of the radical are readily detectable as a bleaching of the signal at 325 nm due to **2** and a concurrent jump in the signal at 480 nm due to **3**. The mechanism for the two-photon chemistry of **1** is shown in Scheme 1.3.

Variations of TLTC-LFP experiments have been described in the literature. Meisel and coworkers[26,27] have substituted pulse radiolysis for the synthesis laser in the study of the photochemistry of several diarylmethyl radicals. And Itoh and coworkers[28,29] have replaced absorption detection with fluorescence detection to monitor the excited intermediates in two laser experiments. Redmond, Wayner and coworkers[30] have done two-laser two-colour photoacoustic calorimetric experiments to determine the quantum yield of fluorescence for diphenylmethyl radicals.

As already discussed, the spectroscopic, and sometimes kinetic, results of TLTC-LFP experiments are readily obtainable. However, in order to determine the exact mechanism responsible for the outcome of these experiments it is crucial to know the structure of the final products. Products can sometimes be obtained in isolable amounts by irradiating a sample with a few thousand pairs of laser pulses. But this is difficult and time consuming for even the most favourable cases and becomes impossible for less well behaved systems.

1.2.2.2 Laser Jet Photolysis.

Laser-jet photolysis (LJP), a technique developed by Adam and Wilson,[31-33] utilizes a continuous wave argon ion laser. In these types of experiments the output from the laser is focused on a high velocity microjet (50 to 100 μm in diameter) of a solution containing the substrate to be studied. It has been shown that microbodies can effectively amplify light intensities by as much as a factor of 10^6 over that which would normally be obtained by focusing the same amount of light into a macro-amount of identical material.[34-38] The microjet serves as a resonance cavity which

traps the light as modes of concentric rings by total internal reflection around the outer rim of the microjet cross-section. Modes whose circumference correspond to an integral number of the light wavelengths will interfere constructively, which in turn intensifies the light. It must be kept in mind that the total number of photons does not increase (conservation of energy) but rather, there are regions inside the microjet which have a much higher density of photons due to constructive interference. The light intensity normally achieved by the focused output from an argon ion laser is in the range of about 10^{22} photons/cm^2 s. If the development of the modes within the jet are taken into consideration, this intensity may reach as high as 10^{28} photons/cm^2 s. These high light intensities place the laser-jet in the multiple-photon domain of light intensities.

The microjet is created by pumping the photolysis solution through a thin capillary (usually 50 to 100 μm) with an HPLC pump, typical flow rates are 1 to 5 ml/min. Because this technique couples a continuous wave laser with a continuous flow of substrate, large volumes of solution can be processed. If the conversion of starting material is low, and the products are photostable at the wavelengths of the laser, the photolysate can be recycled as many times as necessary to achieve an adequate conversion. Because of these capabilities, the laser-jet has proven to be an efficient method to obtain isolable amounts of multiple-photon reaction products, which can then be characterized by conventional spectroscopic methods.

Because of the limited range of wavelengths available from the argon ion laser, (333 to 364 nm) the target transient must absorb in this region, this limits the number, and type, of transient species which can be studied with this method. Another disadvantage of this method is that it provides

no spectroscopic information about the species which are produced during the course of the experiment. This limits the mechanistic insights it can provide to conjecture based on the structure of the products. Furthermore, the only kinetic information which can be attained is limited to systems that are suitable for competitive product studies, which is complicated by the lack of information on the concentration and structure of the intermediates involved.

1.3 Purpose of this Thesis.

Research in the area of multiple-photon chemistry of organic molecules in solution has been done in a systematic manner only during the last decade.[12,24] This is largely due to the technological developments which have led to the commercial availability of high power lasers necessary to attain the light intensities required to both produce and excite transient intermediates; and the electronic components needed to carry out two-laser two-colour laser flash photolysis and related experiments.

The reactivity-selectivity principle is a fundamental axiom of organic chemistry.[39,40] While the validity of this principle has been questioned,[41-44] it has generally been found to hold in cases where the competing reactions proceed through similar transition states and are not governed by stereoelectronic or geometric constraints. The thermal fragmentation reactions of unsymetrically substituted dialkoxyethyl radicals[45] and t-alkoxyl radicals[46] are largely governed by the thermodynamic stabilities of the leaving radical and therefore obey the reactivity-selectivity principle. Reports of similar radical fragmentation reactions concerning radicals with suitable absorption properties in the UV and visible regions of the electromagnetic spectrum led us to undertake an investigation on the effect

of electronic excitation upon the selectivities of the fragmentation pathways of these types of radicals.

During the course of these investigations it became evident that the methods available in our laboratory were unsuitable to carry out the product studies necessary to complement the kinetic and spectroscopic information we had been able to obtain. In order to carry out these product studies we collaborated with Dr. Waldemar Adam and his group at the University of Würzburg in Germany. This collaboration led to an appreciation of the value of a semi-preparative method for high-intensity irradiations and the realization that any future studies into multiple-photon reactions necessitated an alternate means to generate multiple-photon products in semi-preparative amounts in our own laboratory.

This thesis describes the development and implementation of a new method of semi-preparative high-intensity photochemistry which utilizes pulsed, rather than continuous wave, lasers. We have used this method (dubbed 'laser-drop photolysis'), along with the previously established high-intensity methods described earlier, to study the reactions of electronically excited free radicals. The reactions of other electronically excited transients such as ketenes and photoenols will also be described, as well as some of the physical consequences of high-intensity pulsed irradiation on small liquid drops. Given the ubiquitous nature of pulsed lasers in laboratories which study the chemistry of transient intermediates it is hoped that the 'laser-drop photolysis' method of high-intensity irradiation will generate interest among other groups into the processes involved in multiple-photon reactions in solution.

Chapter 2. Laser Techniques and General Instrumentation.

2.1 Introduction.

The laser lab at the University of Ottawa is one of the best equipped labs in Canada for the study of reactive intermediates, rivaled only by the facilities at the Steacie Institute for Molecular Sciences located at the Sussex Drive laboratories of the National Research Council of Canada. Besides conventional nanosecond laser flash photolysis and two-laser two-colour LFP this lab also has the equipment to study short lived intermediates by conventional flash photolysis,[47] single photon counting,[48] diffuse reflectance LFP,[49] time resolved conductance,[50] singlet oxygen emission,[51] photoacoustic calorimetry,[52] and has recently acquired a picosecond laser which is set up for pump-probe OMA detection as well as a Hamamatsu picosecond fluorimeter. The work described in this thesis has added laser-drop photolysis[21] and nanosecond photography to the arsenal of techniques which are available to researchers at these laboratories.

As the title of this chapter suggests, the focus will be on the detailed descriptions of the various laser techniques and instruments used during the course of the research described in this thesis. The more general experimental procedures (synthetic, analytical, purification, etc.) will be described in the sections where they apply.

2.2 Laser Flash Photolysis.

Some of the earlier laser flash photolysis experiments described in this thesis were performed at the National Research Council laboratories at Sussex Drive. Details of the LFP system used there can be found in previous

theses,[53,54] and have also been described in the literature.[22,55] The LFP facilities at the University of Ottawa have not been described before.

Any flash photolysis apparatus can be thought of as a spectrophotometer with very fast time resolution coupled with a pulsed excitation source to produce the species to be monitored. The excitation source is used to produce the transient species from an appropriate precursor, which, providing there is a change in absorptivity, will change the optical density of the sample. This change in optical density is monitored by the spectrophotometer as a function of time and the data collected in order to extract the kinetic information.

Laser flash photolysis uses a pulsed laser as the excitation source, the two LFP systems in our laboratory can be used with any of six available lasers with power outputs in the UV ranging from 6 mJ/pulse for the nitrogen laser to as much as 150 mJ/pulse (at 308 nm) for the EX 530 excimer laser. The pulse widths for all of the above mentioned lasers are less than ~10 ns. See Table 2.1 for a complete listing of the lasers and their specifications. The laser pulses are directed towards, and concentrated (but not focused) on, the sample at right angles with respect to the monitoring beam by a series of prisms and lenses. In the case of some of the lower powered lasers a better signal to noise ratio may be obtained by irradiating in a small angle "front face" alignment.[56] The concentration of the sample is such that the absorbance in the laser cell is between 0.20 and 0.40 at the wavelength of the laser to be used. It is best to keep the absorbance on the low end to avoid shock waves and/or a concentration gradient of the transient species. Excitation of the sample results in a large population of transient intermediate species which can be monitored by the detection system. The lasers are usually operated at 1 or 2 Hz and shutters are placed

between the laser and the sample so as to avoid irradiating the samples unless data is being acquired. Laser cells are made from 7 x 7 mm^2 suprasil quartz tubing. For substrates which undergo a net chemical reaction upon irradiation samples are flowed through specially constructed sample cells to avoid sample depletion and/or product build-up.

Table 2.1: Available lasers at the University of Ottawa

Laser	Type (Mixture)	λ (nm)	Duration (ns)	Energy mJ/pulse	Notes
Nitrogen	Gas	337.1	6-8	6	
Excimer	(KrF)	248	12	<200	Power and pulse width also dependent on the buffer gas.
	(XeCl)	308	8-10	<150	
Nd/YAG	Solid	266	5-10	<10	Wavelength varied by frequency doubling, tripling, etc.
		355		<30	
		532		<100	
		1064		<300	
Dye	Liquid	-	<20	<30	Pumped at 308 nm by excimer laser. Energy is dependent on the efficiency of the dye used.

The detection system ("spectrophotometer") consists of a pulsed 150 Watt xenon lamp as the monitoring light, a high intensity monochromator and a photomultiplier tube (PMT) which operates on six dynodes. The monitoring lamp is pulsed so that the intensity of the beam is increased by a factor of 20 - 100 during a few ms. This enhances the signal-to-noise ratio and is especially important for small and/or short-lived (≤100 ns) signals.

The output from the monitoring lamp is focused into the sample and the light which is transmitted focused onto the monochromator slit which selects the wavelength of light to be monitored. This light is then allowed to impinge upon the PMT which yields a current signal terminated into an appropriate load resistor (typically 93 Ω) that converts the current to a voltage signal. The voltage signal changes in time and is captured by a Tektronix 2440 digital storage oscilloscope equipped with pre-trigger capabilities.

The LFP systems are interfaced with Macintosh computers equipped with National Instruments control cards and LabVIEW-2.2 software. These control the experiment, capture and process the raw data from the oscilloscope, and provide a means for long term data storage and future processing. The 'master' of the LFP system is the line synchronizer, which sends out TTL pulses to the various components of the LFP system (shutters, lamp pulser, laser, etc.) in the proper time sequences. The line synchronizer also synchronizes the TTL pulses so that they originate at the same point on the 60 Hz AC sine wave inherent to all North American electrical systems (hence its name).

Figure 2.1 shows a plot of PMT output versus time for the period from one second before to one second after a particular laser pulse. The LFP operator instructs the computer to allow the experiment to begin, this opens the gates which allow the TTL pulses from the line synchronizer to reach the various components of the LFP system. The first event is the opening of the shutters which allows some light into the monochromator slit, then the lamp is pulsed, causing a sharp increase in the PMT output. The scope is then armed which allows it to continuously collect and eject data. This is followed by the firing of the laser. The collection of data is started when the

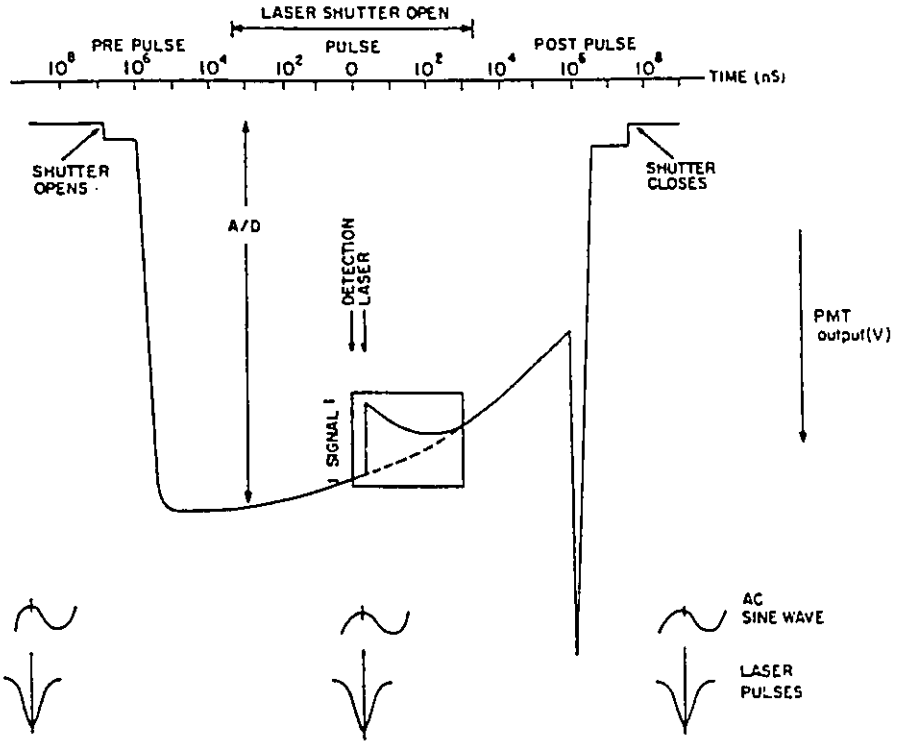

Figure 2.1: Voltage on the PMT during the course of one laser pulse. Note the logarithmic time scale.

laser beam strikes a fibre-optic cable which triggers the scope to save the signal from the PMT, this is the signal represented in the small box in Figure 2.1. Because the scope has pre-trigger capabilities, it saves a preset number of channels from before it had been triggered. The total PMT voltage is also collected in the second channel without any offset on the scope and corresponds to the intensity of the monitoring beam, I_0. Finally, the charges on the lamp capacitors are dumped, producing the spike shown at the right in Figure 2.1, and the shutters are closed.

The raw data from the scope is captured and processed by the computer which converts the voltage signals from the PMT to change in absorbance (ΔOD signal) by equation 2.1. Typically a kinetic trace is constructed by averaging the data collected from several laser shots. The

ΔOD is then plotted as a function of time to provide a kinetic trace such as that shown in the inset in Figure 1.2. Transient absorption spectra are constructed by acquiring kinetic traces at several wavelengths and plotting the ΔOD for each as a function of the monitoring wavelength. Figure 1.2 also shows a good example of a transient absorption spectrum. Because the transient absorption spectra are built from a series of kinetic traces it is also possible to build three dimensional spectra with time as the third axis. It is usually more convenient to show the transient absorption spectra from two or more time delays on one traditional, two-dimensional plot.

$$\Delta OD = -\log(1 - \text{Signal}/I_0) \tag{2.1}$$

In order for the ΔOD values at different wavelengths to be comparable it is important that the I_0 values are similar at the different wavelengths. This is accomplished by averaging several shots for each kinetic trace and a programmable PMT power supply. The user enters the desired PMT output (I_0) along with acceptable minimum and maximum values. If the I_0 is not at the desired level after the first shot, the PMT power supply is adjusted by the computer to provide a more suitable voltage for the next shot. The supply voltage for each of the next shots is determined by the intensity from the previous shot. If the level is outside of the given range, that particular trace is not included in the set of data that is finally averaged. The operator also has the option of controlling the supply voltage manually.

Further improvement of data quality can be made by applying correction shots for either background noise or fluorescence from the sample. Background noise is usually corrected for at longer time scales (≥2 μs/division) because the baseline from the pulsed monitoring lamp may not

be flat (as in the small box in Figure 2.1). This is done by acquiring data in the normal way, however, the laser shutter is not opened, the signal from the background correction shot is then subtracted from the signal for the data LFP shot. At shorter time scales (≤ 2 μs/division) baseline drift is not a problem, however, fluorescence and scattered light from the laser cell may be. Fluorescence is corrected for in the same manner as background noise except that in this case the laser is allowed to hit the sample but the monitoring light is not. Corrections are introduced by alternating signal and correction shots.

One element of LFP which is not immediately obvious and must be pointed out is that the signal from a flash photolysis experiment is reported in units of ΔOD rather than the absolute optical density typically observed in a conventional spectrophotometer. The reason for this is intrinsic to the experimental arrangement. The spectrophotometer in a flash photolysis apparatus is essentially a single beam spectrophotometer and the reference solution is the sample prior to irradiation by the excitation source.

It is also possible to acquire fluorescence traces from the LFP systems in a manner similar to a fluorescence correction shot, that is, with the monitoring beam blocked. Because the response from the PMT may not be the same at different wavelengths, interpretation of fluorescence spectra must be done carefully. It is best to use a known fluorescence spectrum in the same region as a reference.

2.2.1 Two-Laser Two-Colour Laser Flash Photolysis.

This technique has been discussed in Chapter 1 and has also been reviewed in the literature.[24] These experiments are a simple modification of the conventional LFP experiment as described above using two lasers

fired in sequence. In this case the first laser, called the "synthesis" laser, produces a transient intermediate which is then further excited by the second laser, called the "photolysis" laser. One can see that the second laser must emit at a wavelength that is absorbed by the transient produced by the first laser, but not by the original precursor, (*vide supra*). A good example for TLTC-LFP has been discussed in Chapter 1 and shown in Figure 1.2.

These experiments are exactly as described in section 2.2 except that the TTL pulse from the line synchronizer which is used to fire the laser is instead sent to a Stanford Research Systems Inc. Model DG535 4 channel Digital Delay/Pulse Generator. The delay generator then sends a TTL pulse to fire the first laser, and at a preset time interval, sends a second TTL pulse to fire the second laser. The beams from the lasers are positioned so that they overlap with each other as well as the monitoring beam. The second laser can be positioned to be almost collinear with the first, or fired at the front of the LFP cell in a front faced alignment.

2.3 Preparative Multi-photon chemistry.

In order to prepare isolable amounts of multi-photon products in solution it is necessary to have adequate photon flux so that the probability that a transient species (which itself is produced upon the absorption of a photon) will absorb a photon is high. As was discussed in Chapter 1, the minimum amount of flux needed to both produce and excite short lived species is relatively high and cannot be attained by conventional light sources. Presently, the only sources of such high intensity light are lasers, as will be seen both continuous wave and pulsed lasers may be used.

A further problem which hinders preparative multi-photon chemistry is that when a photon flux of the necessary magnitude is achieved, the material with which the solution is contained often undergoes ablative damage. Even high quality quartz has been shown to undergo ablative damage by pulsed lasers which emit a frequency of light to which the quartz is apparently transparent.[57] In order to avoid this problem it is essential that the vessel either has no walls, or alternatively, the light used is focused with a long focal length lens so that the flux is much lower where it passes the walls of the vessel than where the irradiation of the solution occurs.

Two methods of preparative multi-photon chemistry were used during the course of the experiments described in this thesis: i) Laser-jet photolysis (LJP) and ii) Laser-drop photolysis (LDP). The experiments using LJP were performed at the Institute of Organic Chemistry, University of Würzburg , Würzburg, Germany, under the direction of one of the developers of this technique, Dr. Waldemar Adam. The LDP technique was developed at the University of Ottawa as an alternative to the LJP method for preparative experiments of this type. Detailed descriptions of both techniques follow.

2.3.1 Laser-Jet Photolysis.

This is a recently developed technique and has been described in the literature.[32,33] The principles which have been proposed to be involved in the production of ultra-high intensities achieved with this technique were discussed in the last chapter. The purpose of this section is to describe the necessary components and experimental arrangement required to perform successful laser-jet experiments.

The laser-jet apparatus consists of two separate subsystems; i) the excitation/optic system and ii) the delivery/containment system. The first is simply a continuous wave laser source, in this case an argon ion laser, and the necessary optical components used to direct and focus the output from the laser. The laser used in Würzburg is capable of delivering ~6 Watts of UV light with lines at 333, 351 and 364 nm. An 80 mm focal length quartz lens mounted on an x-y-z micropositioner is used to focus and position the laser beam into the liquid microjet of the photolysis solution.

The delivery/containment system is used to generate and maintain a thin laminar flow of the photolysis solution and collect the photolysate after it has passed through the focal region of the laser. This system consists of a Bischoff 2200 HPLC pump which pumps the photolysis solution through a capillary nozzle to generate the microjet. The capillary is placed so that the microjet is injected into a reaction chamber which is kept under a positive pressure of inert gas. The laser beam enters the reaction vessel through a vacant window port and irradiates the microjet, which is collected in a receiving flask. Since the microjet scatters a considerable amount of the irradiating light this provides an easy method to insure that the laser beam is incident upon the microjet by using a piece of paper as a projection screen behind the apparatus and observing the light projected upon it. The photolysate can be recycled by placing the HPLC inlet directly in the receiving flask after the desired amount has been collected. A schematic diagram for the laser-jet apparatus is shown in Figure 2.2.

An important parameter when performing laser-jet irradiations is the residence time of the photolysis solution in the focal region of the laser. The residence time, t_{res}, is determined by the diameter of the capillary nozzle, d, the width of the laser at the microjet, l (typically 100 μm), and the

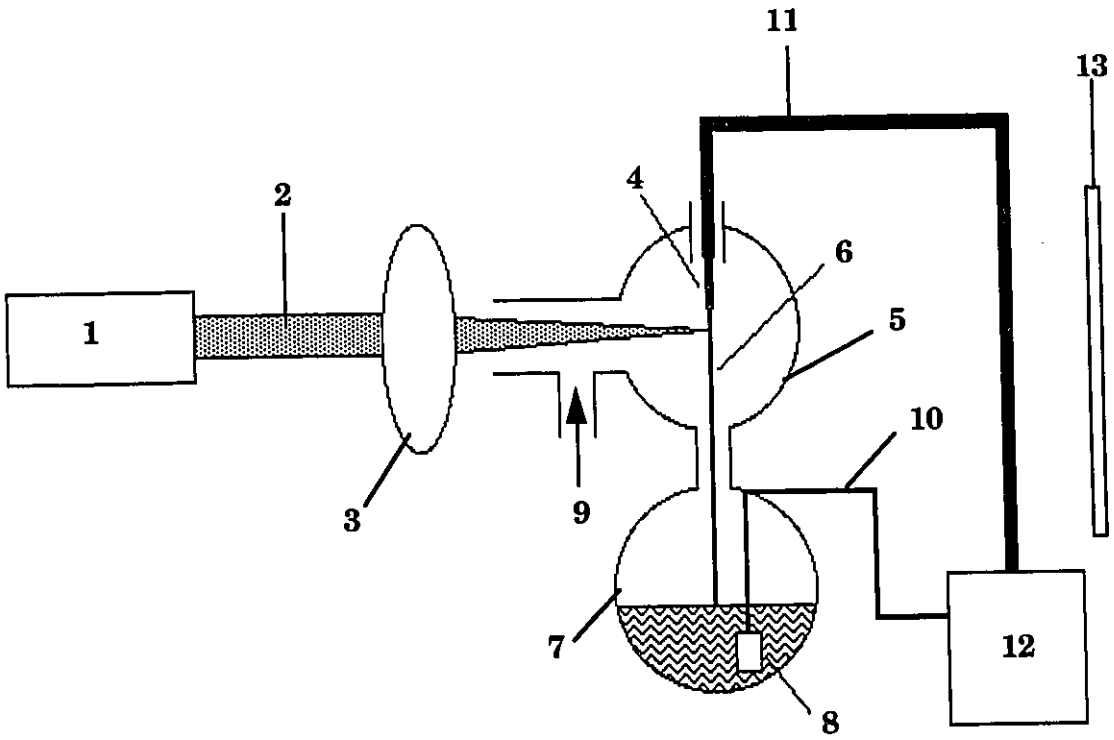

1 - Argon Ion Laser
2 - Laserbeam
3 - Lens on Motor Positioner
4 - Capillary
5 - Glass Bulb
6 - Jet Stream
7 - Collecting Flask
8 - Filter
9 - Inert Gas Supply
10 - Low Pressure Tubing
11 - High Pressure Tubing
12 - HPLC Pump
13 - Projection Screen

Figure 2.2: Schematic diagram for laser-jet photolysis.

flow rate of the solution through the nozzle, F (equation 2.2). Thus, there are two ways in which the residence time can be controlled, by adjusting the flow rate of solution, or by changing the capillary nozzle. It is usually

preferable to adjust the flow rate because it is a simple matter to do so, and, changing the size of the capillary also changes the photon flux inside the microjet. The residence time in the laser focal region for a capillary nozzle of 100 μm diameter and a flow rate of 1 ml/min is ~50 μs.

$$t_{res} = \pi l d^2/4F \qquad (2.2)$$

2.3.2 Laser-Drop Photolysis.

The difficulties associated with preparative two-laser chemistry, (*vide infra*, Chapter 4) and the unavailability of a continuous wave laser appropriate for laser-jet experiments, led us to try and develop an alternative preparative technique utilizing pulsed lasers. A further incentive for a technique of this type is the ubiquitous nature of pulsed lasers in laboratories which study short-lived species. The development of this technique, dubbed laser-drop photolysis, has been published[21] and is described in later chapters of this thesis. This section describes the experimental details of laser-drop photolysis.

Like the laser-jet apparatus, the laser-drop also consists of an excitation/optic system and a delivery/containment system. In this case the excitation source is a pulsed laser (usually a Lumonics EX-530 excimer laser with a Xe/HCl gas mixture in a neon buffer, 308 nm, ~6 ns, 80-150 mJ/pulse) which is passed through a quartz prism and a 200 mm focal length quartz lens. The prism is mounted on an x-y positioner and is used to position the laser beam so that the focal point of the laser excites a drop of solution suspended from the tip of a 6 inch syringe needle.

The photolysis solution is delivered by a syringe through a 20 gauge syringe needle. The flow of solution is controlled by a Sage Instruments

Model 355 syringe pump. The needle is placed in the laser-drop cell by inserting it through a rubber septum, keeping the end of the needle just slightly tipped from horizontal (<10°). The solution is delivered at a rate which is slow enough so that drops form on the needle, when the drop is slightly larger than the area of the cross section of the laser beam near the focal point it is irradiated by a single laser pulse. This causes the drop to disintegrate into smaller drops and a mist which are contained by the walls of the cell. With the laser induced removal of the irradiated drop a new drop begins to form. The size of the drop can be controlled by the flow rate of the syringe pump or the repetition rate of the laser. We found it best to run the laser at a constant repetition rate (usually 1-5 Hz) and adjust the flow rate with the syringe pump so that the drop was only slightly larger than the irradiated area.

The irradiation cell was constructed from an Ace Glass Ltd. photochemical cell; 300 mm in length and 50 mm in diameter, with removable quartz windows at both ends. Two septa inlets were placed near the top, in the center of the cell, to insert the solution input needle and inert gas relief needle. A gas inlet was placed at the top of the cell near the front window. The input needle was bent at ~135° so that the end was horizontal. Figure 4.2 (Chapter 4) shows a drawing of the laser-drop cell. Losses of solution during handling and irradiation are similar as those for the laser jet technique, typical loses after several cycles are usually in the 10-20% range *Caution: These irradiations must be carried out in an inert atmosphere. If the laser beam hits the tip of the syringe needle air-saturated mixtures can explode readily. At least one rubber septum must be employed in the cell, to provide a safety pressure release should these precautions fail.*

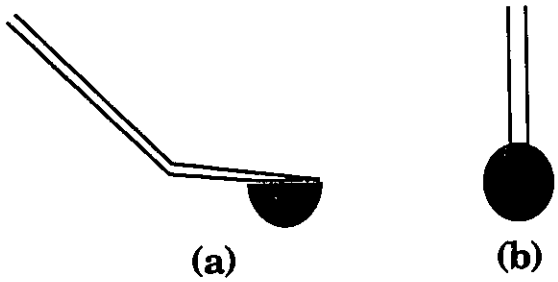

Figure 2.3: Different behavior of drops suspended from (a) Near horizontal needle and (b) Vertical needle.

During the course of experiments that led to the final design of the laser-drop cell a number of problems were encountered which are worth mentioning so that they may be avoided in future attempts at improvement on this design. It has been suggested that the experiments could be made easier if the needle were held in a vertical, rather than horizontal, position. However, this is not possible since drops formed on a vertically positioned needle are held by surface tension above the bottom of the needle and irradiation of the drop without hitting the needle is not possible. When a horizontal position is used the drop hangs from the needle and irradiation of just the drop is possible (see Figure 2.3). The long cell design of Figure 4.2 is important so that the windows are located away from the focal point of the laser beam. When this is not the case repetitive irradiation causes ablation of the quartz windows and eventually leads to perforations. Lasers that have a wide cross-section, such as the excimer lasers used here, are particularly well suited for these types of experiments. When a laser with a small coherent beam, such as a Nd-YAG laser, is used it may be necessary to defocus the laser then refocus it with a long focal length lens just before it enters the cell to avoid the above mentioned ablation problems. Finally, the placement of the inert gas inlet at the front of the cell helps to keep the mist

from being deposited on the front window, this helps to avoid the carbonization of organic solvents on the quartz window.

2.4 Nanosecond Photography.

As mentioned above, irradiation of small droplets of solution with the focused output from a pulsed laser leads to the rapid destruction of the drops. Investigations as to the physical processes responsible for this phenomenon are reported in Chapter 6. As part of these investigations photographs were taken of the drops as they were destroyed using a very short (~10 ns) photographic "flash". In this way the actual destruction of the drop can be "stopped" in time and the events leading to the total destruction of the drop can be viewed as a series of photographs. This method of "nanosecond photography " is a modification of the method used by Srinivasan to study the events which occur during the ablation of thin polymer films.[58-61]

This experiment is done in much the same manner as a TLTC-LFP experiment. The laser-drop cell is placed on a narrow table. A Mamiya RB67 camera equipped with a macro lens, a Polaroid Land Pack and Polaroid 6000 Black and White film is set up at right angles to the axis of the laser-drop cell and focused on the needle. A picture of the needle is taken to insure proper focusing and depth of field. A 25 mm diameter quartz test tube is filled with a solution of 30 mM Coumarin 460 dye in methanol and placed directly behind the cell in line with the needle and the camera lens. A drop is allowed to form on the needle, then the shutter for the camera is opened and the drop is irradiated by an excimer laser, a second laser (either another 308 nm excimer or 248 nm laser) is fired at a preset time interval after the first laser into the dye in a direction slightly off the axis of

the test tube, needle and camera lens. The fluorescence from the dye illuminates the drop for 10 ns, after which the camera shutter is allowed to close. Since the fluorescence lifetime of the dye is shorter than the laser pulse, the fluorescence from the dye is just slightly longer than the laser pulse. There is also a 345 nm cut off filter placed between the cell and the camera to filter out any stray light from either the laser-drop or flash lasers. Figure 2.4 shows a schematic diagram of the experimental setup used for nanosecond photography.

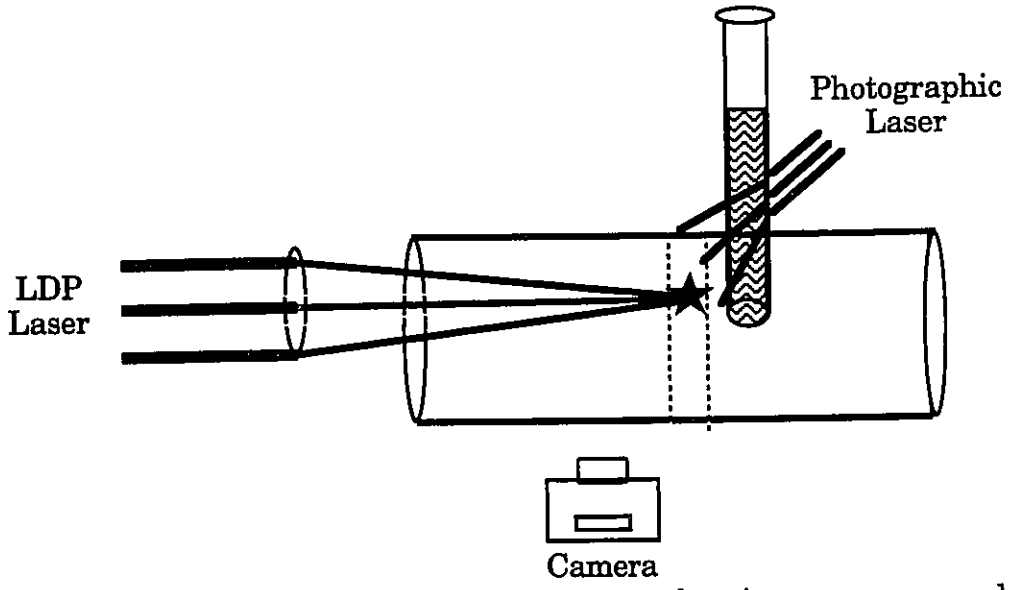

Figure 2.4: Schematic diagram showing nanosecond photographic experimental setup.

Pictures were also taken with a 35 mm SLR camera with 1000 asa film. However, this requires processing of the film and proper film exposure may be a problem. If the flash laser has too much power it may be necessary to attenuate the beam with a neutral density filter before it enters the dye to avoid overexposure of the film; this is easily determined with Polaroid film by taking pictures and allowing them to develop immediately afterwards, filters may then be added as required. We found that the best

results were obtained by setting the F-stop of the camera at 22 and attenuating the flash laser until the proper exposure was attained. By using the smallest available lens aperture the best depth of field is attained, this minimizes problems due to improper focusing of the camera. It should also be mentioned that the LFP line synchronizer was used to send the TTL pulse to the delay generator which in turn fires the lasers. Timing of the lasers was calibrated by performing a "calibration" TLTC-LFP experiment. This was necessary to determine the settings needed by the delay generator to fire the two lasers simultaneously, this corresponds to the zero time for the photographs and the flash laser could then be delayed at known time intervals from the laser-drop laser.

2.5 General Instrumentation.

Gas Chromatography. Analytical gas chromatography was done with a Perkin-Elmer Model 8320 capillary gas chromatograph equipped with a DB-5 bonded phase column of 15 m length (from J&W Scientific) and an FID detector. Where possible an internal standard was used (usually 1,4-di-t-butylbenzene) to provide accurate determination of the conversion of starting material and product yields.

HPLC. These experiments were performed with a Varian Model 9010 HPLC pump, 9065 autosampler, Model 9090 diode array detector, and a 25 cm Techsphil C-18 column. The HPLC instruments were interfaced to a 386 computer equipped with Varian Star Workstation software. Analytical experiments were done with an internal standard which was chosen so as to have suitable absorption properties for the particular system under study. The diode array also provided an additional means for product

identification by comparing the UV spectra and retention times of products with authentic samples.

UV-Visible Spectrophotometer. All UV-visible spectra were recorded on a Hewlett-Packard Model 8451 diode array spectrophotometer.

Low-Intensity Irradiation. These were carried out in a homemade reactor with three separate irradiation chambers. Each irradiation chamber was equipped with either nine RPR-2540, RPR-3000 or RPR-3500 lamps, these correspond to wavelength maxima of 254, 300, or 350 nm with a full-width at half-maximum of about 25 nm. The temperature in the irradiation chambers was in the 30 - 35 ^{o}C range. All samples were deaerated by purging with a slow stream of nitrogen for 20 - 40 minutes unless stated otherwise.

Molecular Modeling. Molecular modeling calculations were done on a MacIntosh II vx computer equipped with a Tektronix 88K coprocessor and CAChe Scientific modeling software (version 3.5.1). This software package includes several graphical and computational application programs. The computational programs include semi-empirical methods such as MNDO, AM1, PM3, INDO/S, Extended Hückel, etc., as well as a classical mechanical program (Mechanics) which utilizes MM2 force field parameters.

Molecule files are built using the "Editor". These files can then be used as input files for any of the computational applications. Once a file has undergone a particular computation (geometry optimization, SCF energy calculation, etc.) the results can be viewed graphically in the Editor. Isosurfaces for molecular orbitals, electron density, electrostatic potential, etc. can be constructed from the quantum mechanical calculations by a program called "Tabulator". These isosurfaces must be viewed in another

program called "Visualizer+", this program also allows electronic and vibrational spectra calculated from the semi-emperical programs to be viewed.

The general method we have used for molecular modeling is as follows; 1) The molecule file was built using the Editor. 2) The geometry was first optimized with Mechanics. 3) This geometry was then used as input for optimization by one of the semi-empirical methods. Any further calculations which may have been done used a geometry which was optimized by one of the semi-empirical methods as the input file.

Chapter 3: Use of Two-Laser Two-Colour Laser Flash Photolysis and Laser-Jet Photolysis to Study the Thermal and Photochemical Fragmentation Pathways of α,α-Dialkoxybenzyl Radicals.

3.1 Introduction.

2,2-Dimethoxy-2-phenylacetophenone (1, commercially known as Irgacure-651™ from Ciba-Geigy) is a very efficient and frequently used free radical photoinitiator. The primary photoprocess in this molecule involves Norrish Type I photocleavage to yield α,α-dimethoxybenzyl (2) and benzoyl radicals (3), reaction 3.1.

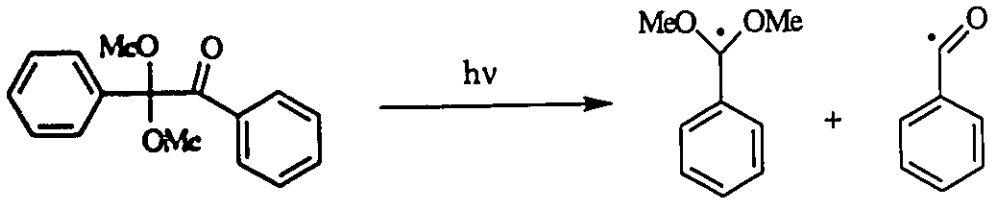

1 2 3 (3.1)

It has been known for many years that one of the forms of decay from 2 involves its fragmentation to give methyl radical (4) and methyl benzoate (5), reaction 3.2.[62-64]

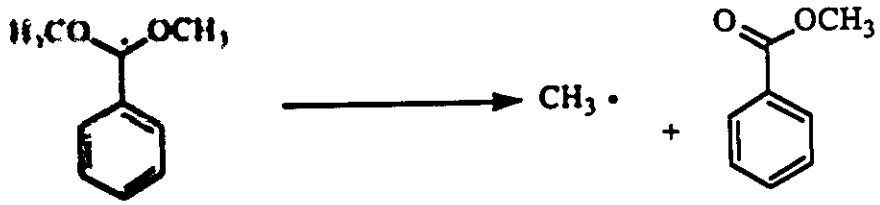

2 4 5 (3.2)

The mechanism and yield of this reaction has been the subject of considerable discrepancies and inconsistencies in the literature. A spin trapping study by Baumann and coworkers[65] revealed that the radicals **2** and **3**, but not **4**, could be trapped by N-t-butyl-α-phenylnitrone. Steady-state ESR experiments[66] employing low radical concentrations (radical lifetimes of 500 μs) also showed radicals **2** and **3**; **4** appeared only as a very weak signal when the temperature was greater than 70 °C. These investigations indicate that reaction 3.2 is slow and should contribute little to the products, especially under high intensity conditions where radical concentrations would be high, and where radical-radical reactions should be the predominant mode of decay for both **2** and **3**. However, product studies under moderate light intensities (450 Watt medium-pressure mercury lamp) showed that methyl benzoate accounted for 57% of the products from the dimethoxybenzyl radical.[67]

An ^{1}H CIDNP investigation by Borer et al.[68] found emission signals from acetophenone (methyl, 2.12 ppm) which were attributed to an in-cage radical recombination of methyl radicals formed by reaction 3.2 and benzoyl radicals formed from the Type I cleavage of **1**. This indicates that reaction 3.2 competes with cage escape of the initially formed geminate radical pair. Fouassier and Merlin[69] reported a lifetime of 17 μs for the decay of **2** in benzene, with an absorption maximum at ~460 nm. Furthermore, Groenboom et al.[70] reported that radicals **2** and **4**, but not **3** could be detected by ESR, and that addition of dodecanethiol does not prevent the fragmentation by trapping radical **2** to form the corresponding acetal. However, in the same paper these authors also report that α-methoxybenzyl radicals, which do not undergo fragmentation to a significant degree (*vide infra*), are not scavenged by dodecanethiol. A later time resolved ESR study

showed the formation of all three radicals 0.3 μs after the laser pulse.[71] This indicates that demethylation is even faster than that reported by Foussier.[69] However, the ESR signals from the methyl radical did not increase as the signal from **2** decayed as would be expected if reaction 3.2 were responsible for the decay of **2**. In fact, 1.8 μs after the laser pulse the methyl radical was no longer detected while the substituted benzyl radical showed well defined hyperfine structure.

Fischer and coworkers[72] re-examined the photochemistry of **1**, also using time-resolved ESR. They showed that the ratio of the signals from **2** and **4** at a fixed time after the laser pulse increased with increasing photolysis laser intensity. If the signal from the methyl radical were due to the thermal decay of **2**, the ratio of the signals should remain constant. These authors concluded that the signal for the methyl radical must be due to a photofragmentation of the dimethoxybenzyl radical.

A subsequent, more extensive investigation by Fischer et al[66] utilized product analysis, CIDNP, and optical spectroscopy to further support their photofragmentation mechanism. They found that the % yield of methyl benzoate first decreases, then increases with increasing light intensity. If the demethylation reaction was solely a thermal process it would be expected that radical-radical reactions would become the predominant mode of decay for **2** and the % yield of methyl benzoate would continue to decrease. CIDNP experiments showed a linear dependence on photolysis intensity for the net nuclear polarization of products containing one methyl group and a quadratic dependence for the polarization of ethane, which results from the combination of two methyl radicals. These results are also consistent with a photofragmentation pathway for the demethylation of **2**.

Fischer's work clearly establishes that radical **2** is a highly photosensitive species and that reaction 3.2 can occur either thermally or photochemically. The relative importance of these two pathways is a function of the light intensity and excitation wavelength employed; notably, the photofragmentation pathway can contribute significantly even at moderately low light intensities.

Reactions of this type are not unique for radical **2**. The fragmentation of α-alkoxybenzyl and dialkoxyethyl radicals are well known. Huang et al.[73] compared the ratio of dimerization to fragmentation products for a number of α-alkoxybenzyl radicals (reactions 3.3 and 3.4) to determine the relative stabilities for a number of alkyl radicals. They found that the dimerization-to-fragmentation product ratio changes from 4.4 for R=methyl to 0.33 for R=t-butyl and no dimerization products could be found when R was either benzyl or diphenylmethyl. They concluded that the fragmentation pathway becomes more facile as the leaving radical becomes more stable. A later study by Ong and Chick[74] placed the stability of the adamant-1-yl radical between that of methyl and ethyl (dimerization/fragmentation ratio=2.4) by utilizing the same reactions (3.3 and 3.4). In a similar study, Huyser et al.[45] studied the fragmentation of 1-alkoxy-1-butoxyethyl radicals (reactions 3.5 and 3.6). They also found that the product ratios could be predicted on the basis of radical stabilities, that is, cleavage of the carbon-oxygen bond favors production of the more stable radical.

With Fischer's finding of the easy photofragmentation of dialkoxybenzyl radicals,[66,72] and the dependence of radical stability on the thermal fragmentation of dialkoxyalkyl radicals,[45] we thought that these types of reactions would provide a method of comparing the selectivity for

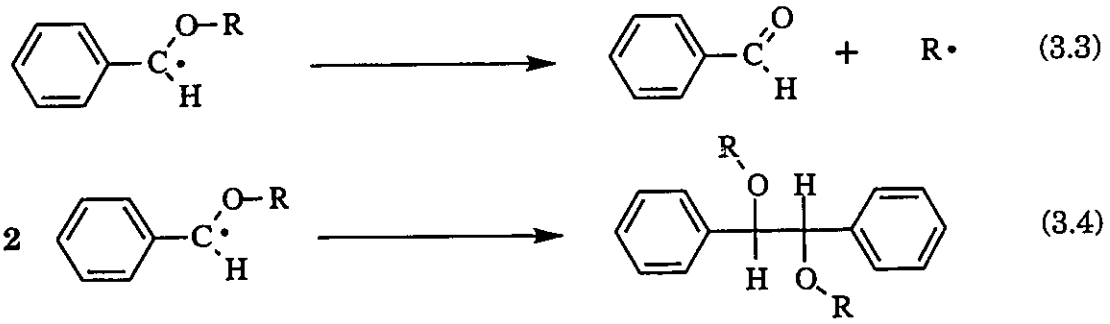

(3.3)

(3.4)

(3.5)

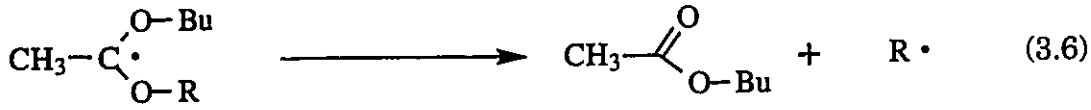

(3.6)

the fragmentation of ground and excited state radicals of general structure **6**, where $R^1 \neq R^2$. The study of these reactions required the use of a variety of laser techniques and this report provides a rare direct comparison of photoreactions under conditions of (pulsed) laser flash photolysis and the (cw) laser-jet technique. In addition, we have verified that the photofragmentation of the dimethoxybenzyl radical is indeed an efficient process with a quantum yield approaching unity.

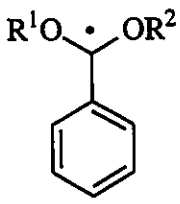

6

3.2 Results.

3.2.1 Absorption Spectroscopy of Dialkoxybenzyl Radicals.

α,α-Dimethoxybenzyl radicals may be generated by direct photolysis of **1** (reaction 3.1) or by hydrogen abstraction of the benzylic hydrogen of benzaldehyde dimethyl acetal (reaction 3.8 R^1=R^2=Me) by t-butoxyl radicals produced upon photolysis or thermolysis of di-t-butyl peroxide (reaction 3.7).[62,63]

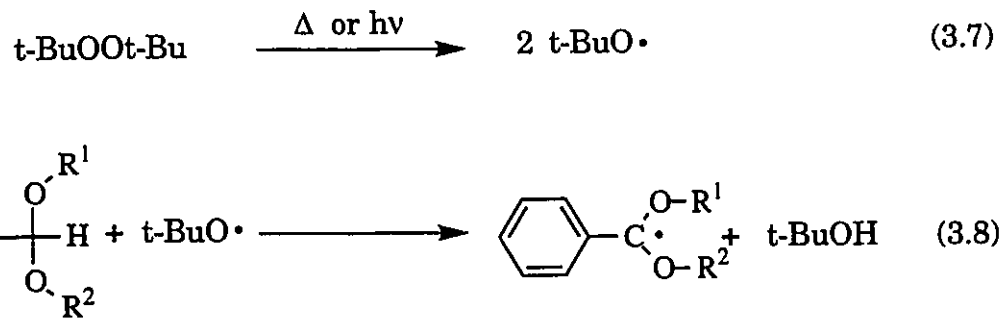

Fischer et al.[66] reported that the transient spectra obtained upon photolysis of **1** may be contaminated by contributions from other species. Figure 3.1 shows the spectra obtained by laser flash photolysis (1 μs after the laser pulse) of a 1.50 mM solution of **1** in benzene by employing for excitation the pulse from an excimer laser (308 nm). Figure 3.1(a) displays the spectrum obtained when the solution is allowed to flow through the photolysis cell, thus, this ensures that a fresh sample of **1** is irradiated by each pulse from the laser. This spectrum agrees well with that obtained by Fischer,[66] with λ_{max} at 420 nm. Figure 3.1(b) shows the spectrum from the same solution but where a static cell was employed. It must be pointed out that these spectra are obtained on a point by point basis; thus, the sample

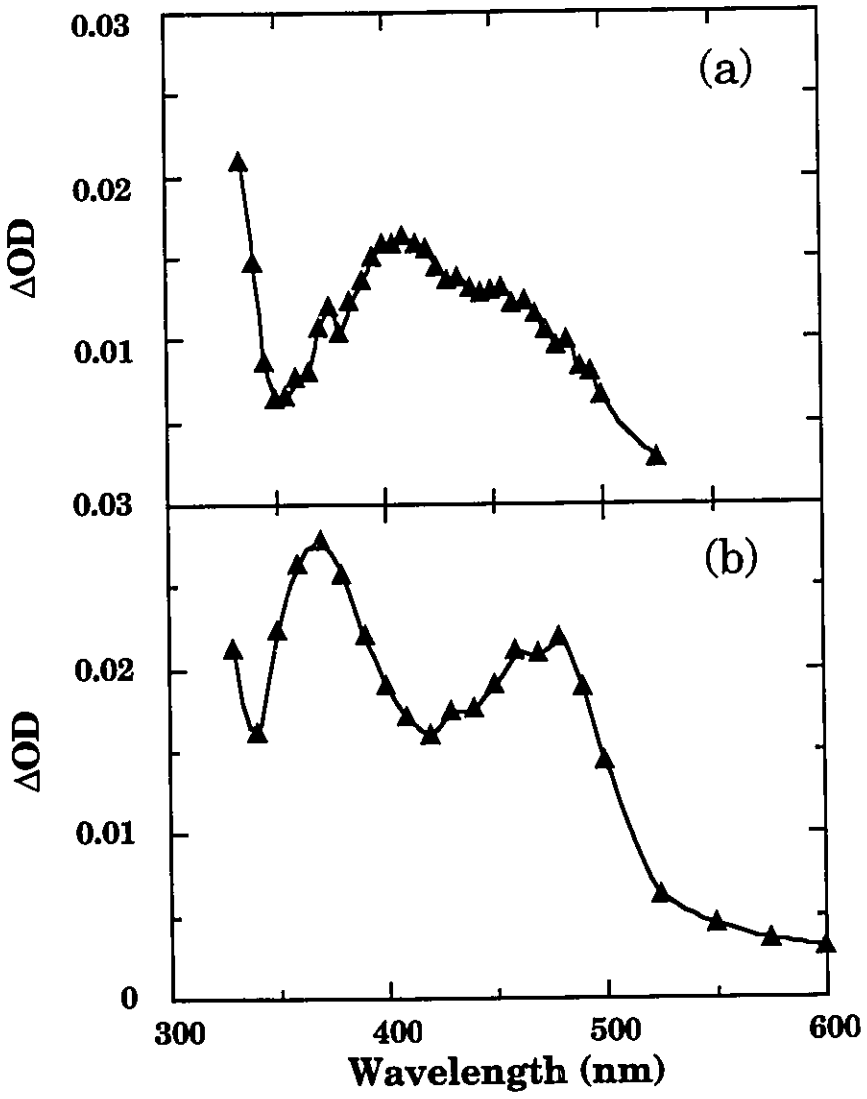

Figure 3.1: Transient spectrum obtained 1 μs after 308-nm laser pulse for a 1.500 mM solution of **1** in benzene. (a) Flow cell. (b) Static cell.

received six shots of the laser for each point as the spectrum is scanned from longer to shorter wavelengths. By the time the points below 520 nm are obtained, the sample had received at least forty laser shots. The spectrum in Figure 3.1(b) has absorption maxima at 370 and 480 nm; this is similar to the triplet-triplet absorption spectrum for benzil,[75] a product which may be formed by the recombination of benzoyl radicals and which will accumulate

as the irradiation proceeds. It is also noteworthy that the spectrum in Figure 3.1(b) is similar to that found upon LFP of **1** by Fouassier[69] which the authors assigned to **2** and **3**. Although Fischer[66] attributed the differences between the spectrum obtained in his work and that of Fouassier's to photolysis of **2** by the monitoring light, it now seems likely that they are due to the formation of benzil as mentioned above. The spectra in Figure 3.1 show the importance of using a flow cell for LFP experiments, especially when there are products formed as a result of photolysis.

Osborn and Sandner[64] reported that the triplet from **1** could not be quenched by numerous triplet quenchers and determined that the lifetime for the triplet was less than 1 μs. The CIDNP investigation by Borer et al.[68] showed that the radicals are formed from the triplet state of **1**. Figure 3.2 shows the decay trace for the signal obtained upon 308 nm LFP of **1** monitored at 420 nm. This signal is formed instantaneously on the time scale of detection by our system, ~30 ns. Thus, we can conclude that the triplet for **1** must be shorter lived than 30 ns. This is consistent with the failure to quench its triplet state.[64]

Figure 3.3(a) shows the transient spectrum obtained upon laser flash photolysis (308 nm, 1.2 μs after the laser pulse) of a benzene solution which contained 0.28 M di-t-butyl peroxide and 0.33 M benzaldehyde dimethyl acetal; this is similar to Figure 3.1(a), except that the maximum is located at 400 nm. Figure 3.3(b) shows the transient spectrum obtained upon laser flash photolysis (337 nm, 1.7 μs after the laser pulse) of 0.33M benzaldehyde ethyl methyl acetal in a 1:2 (v/v) mixture of benzene/di-t-butyl peroxide and is attributed to the α-ethoxy-α-methoxybenzyl radical. In both spectra, 3.3(a) and 3.3(b), some spectral contamination was caused by the direct photolysis of the acetals. This was corrected for by subtracting the spectrum recorded

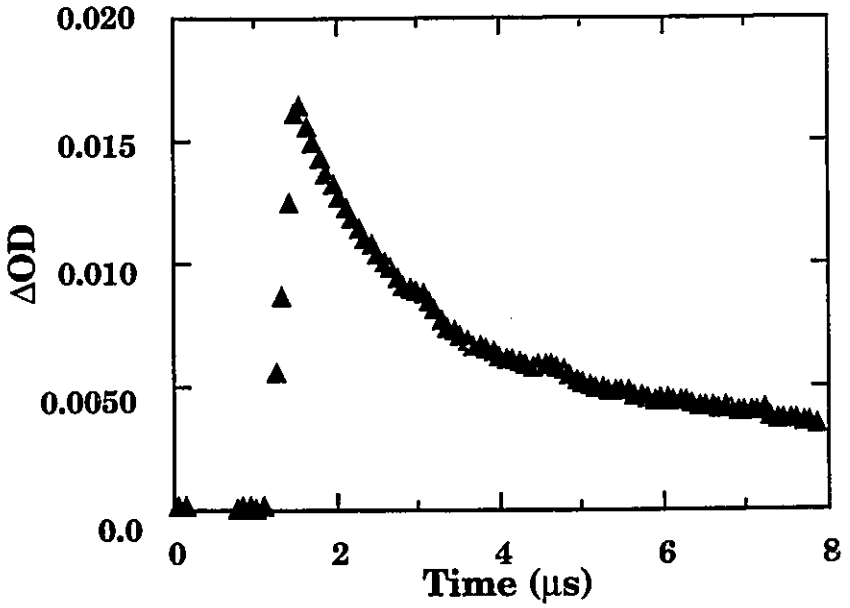

Figure 3.2: Decay trace monitored at 420 nm for 308-nm LFP of 1.50 mM solution of 1 in benzene.

at times less than 100 ns after the laser pulse from that obtained at times > 1 μs. The two spectra are identical, with maxima at 400 nm. The decay traces for all the above spectra could not be fitted to first or second order kinetics. This is an indication that the radicals disappear by mixed first (fragmentation of dialkoxybenzyl radicals) and second (radical-radical reactions) order processes.

3.2.2 Bleaching of Dimethoxybenzyl Radicals.

A preliminary experiment to investigate the possibility of the photofragmentation of the dimethoxybenzyl radical was performed by comparing the change in absorption signal (ΔOD) as a function of the laser intensity for the laser flash photolysis of **1** (%100 corresponds to ~30 mJ/pulse). A plot of ΔOD vs. % laser power, in which the laser was attenuated by passing the beam through precalibrated neutral density

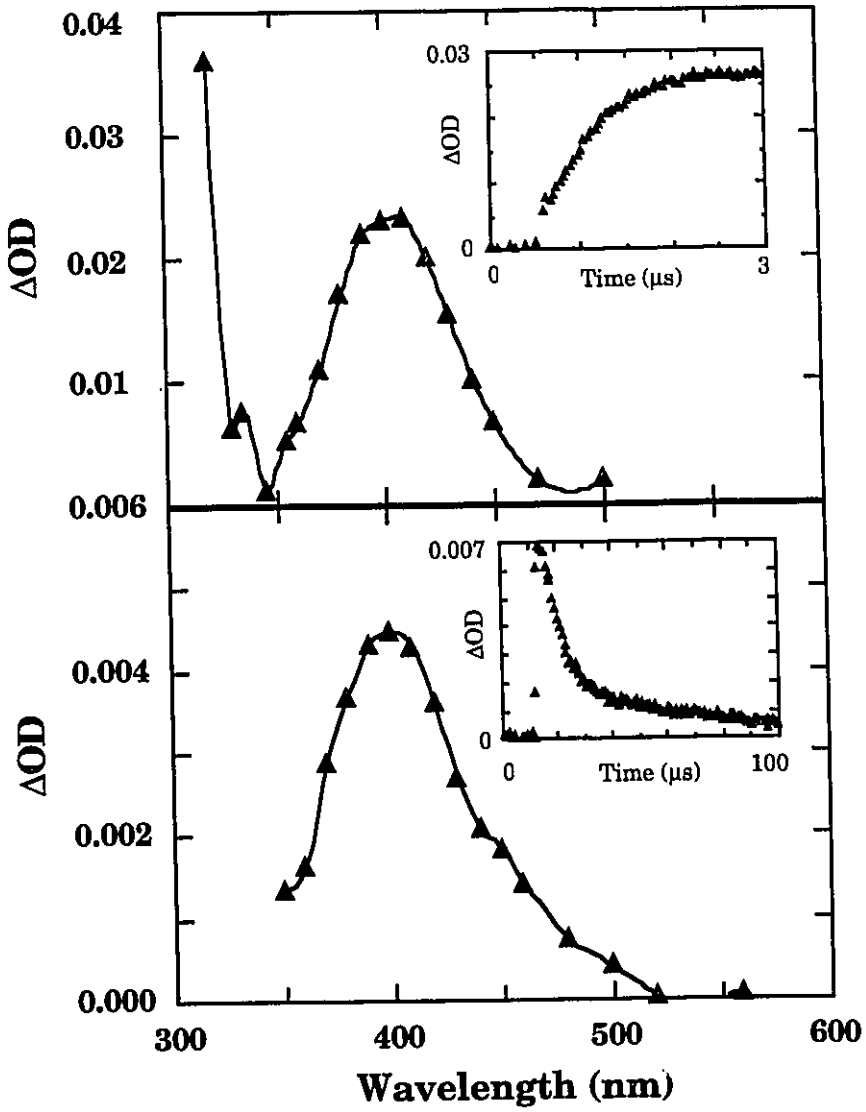

Figure 3.3: (a) Transient spectrum of the α,α-dimethoxybenzyl radical produced according to reactions 3.7 and 3.8. Inset shows the growth of the radical monitored at 420 nm. (b) Transient spectrum for α-methoxy-α-ethoxybenzyl radical produced according to reactions 3.7 and 3.8. Inset shows the decay of the radical monitored at 420 nm. Both spectra corrected for acetal photolysis; see text.

filters, is shown in Figure 3.4. There is a definite downward curvature as the laser power is increased, which indicates secondary photolysis of the radical during the laser pulse. This is further evidence that a

photofragmentation of the dimethoxybenzyl radical is responsible for the increased production of methyl benzoate upon increased laser intensity, as reported by Fischer.[66]

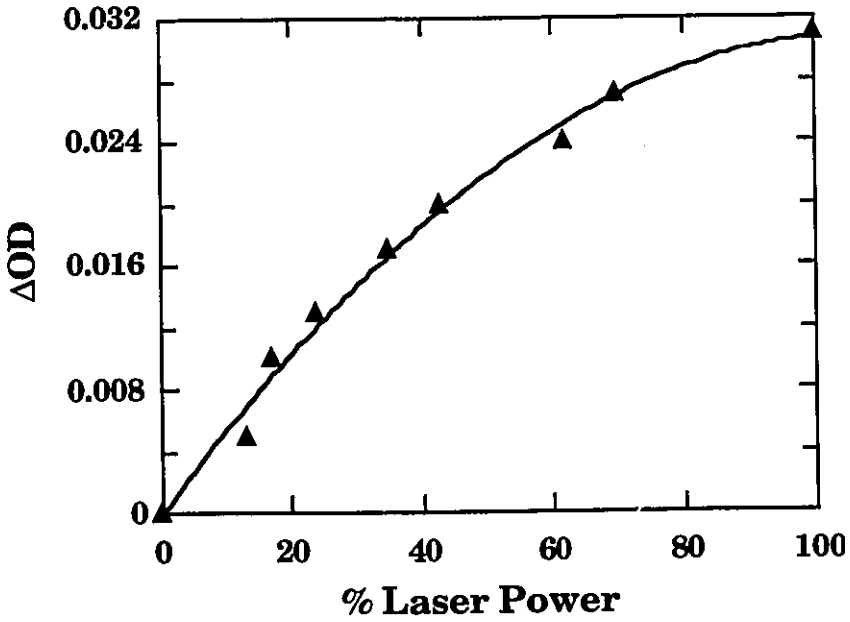

Figure 3.4: Absorption signal (ΔOD) as a function of laser intensity for 308 nm LFP of **1** as monitored at 420 nm. %100 laser power corresponds to ~25 mJ.

TLTC-LFP experiments were performed to provide further evidence for the photofragmentation and to measure its quantum yield. The dimethoxybenzyl radical was generated by reaction of t-butoxy radicals and benzaldehyde dimethyl acetal in benzene by 308 nm excimer laser excitation and then excited with the pulses from a dye laser at 420 nm. The dye laser pulse led to efficient and irreversible bleaching (Figure 3.5 Top) of the dimethoxybenzyl radical, which was monitored at 390 nm.

Transient bleaching quantum yields were determined by using Aberchrome-540 actinometry as described in the Experimental Section and

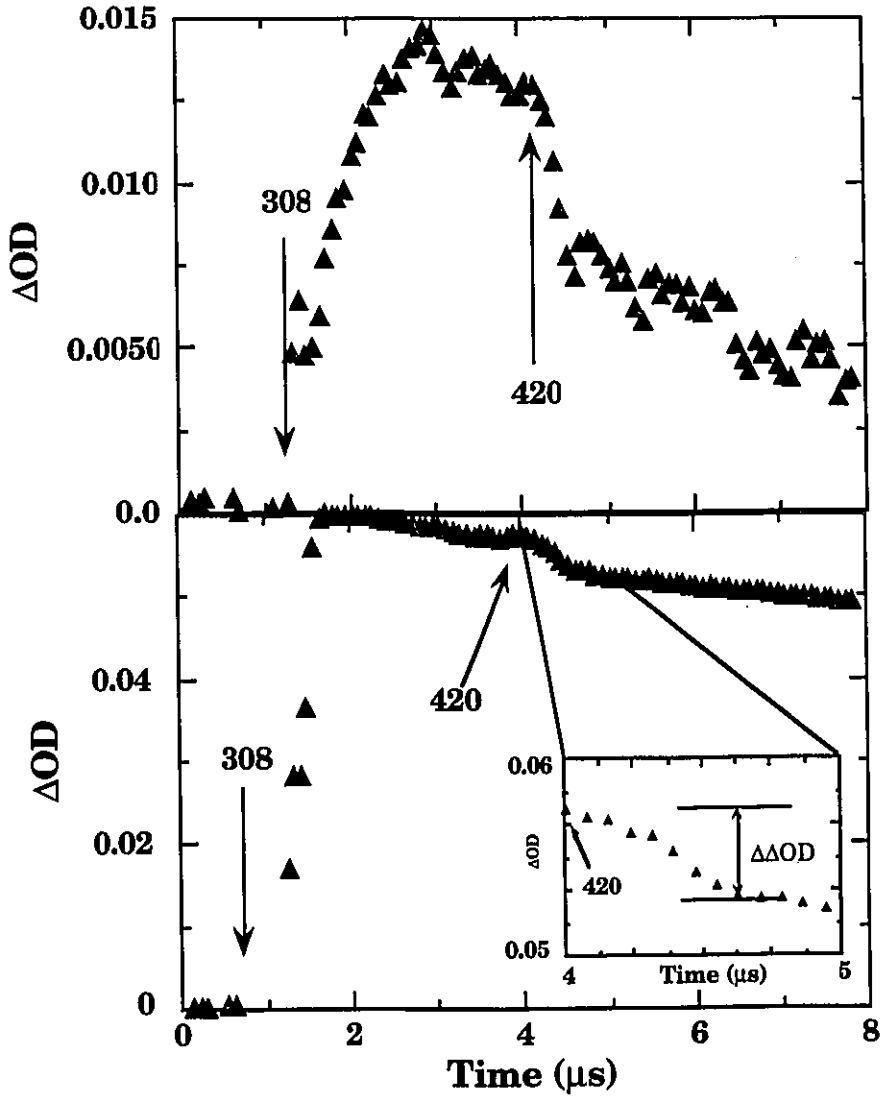

Figure 3.5: (Top) Bleaching of dimethoxybenzyl radical upon excitation with a dye laser (420 nm). The dye laser was fired 3 μs after the synthesis laser (308 nm). Radical produced from a solution of 0.33 M benzaldehyde dimethyl acetal and 0.28 M di-tert-butyl peroxide in benzene (monitored at 390 nm). (Bottom) Bleaching of **8** to form **7** upon excitation with a dye laser (420 nm). The dye laser was fired 3 μs after the synthesis laser (308 nm). **8** was formed from a solution of **7** in toluene (monitored at 494 nm). Inset shows expansion of the region in which the dye laser was fired.

in earlier reports.[76] The extinction coefficient for **8** is 8200 $M^{-1}cm^{-1}$ at 494 nm, and the bleaching quantum yield at 420 nm is 0.0772.[77] The extinction coefficient for the dimethoxybenzyl radical at 390 nm was estimated to be 1000 $M^{-1}cm^{-1}$ from the transient absorption spectrum (Figure 3.2(a)) and the extinction coefficient at 418 nm (800 $M^{-1}cm^{-1}$) reported by Fischer.[66] The changes in optical densities were the values obtained from the two-laser experiments. The bleaching of the dimethoxybenzyl radical and the fulgide **8** are shown in Figures 3.5(a) and 3.5(b) respectively. The optical densities for the transient involved were matched at 420 nm, the wavelength of the dye laser. A value of 0.80 ± 0.16 was obtained for the bleaching quantum yield of the dimethoxybenzyl radical in benzene.

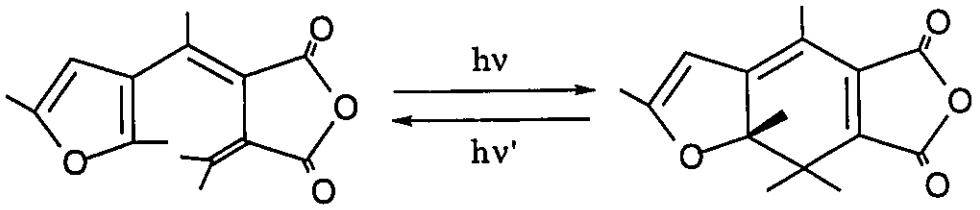

7 **8**

Scheme 3.1

Errors in these experiments tend to be moderately large,[76] not only due to the complexity of the two-laser experiment, but also because the errors in the extinction coefficients are incorporated in the quantum yields. The error limits given above (± 20 %) are slightly smaller than those estimated in earlier work, which reflects the availability of an independent determination of the extinction coefficient for the dimethoxybenzyl radical.

3.2.3 Thermally Initiated Experiments on the Fragmentation of Unsymmetric Dialkoxybenzyl Radicals.

The present study centers on a comparison of thermal and photoinduced fragmentations of unsymmetric dialkoxybenzyl radicals such as that produced in reaction 3.8 above. These fragmentations lead to two different alkyl benzoates as indicated in reaction 3.9.

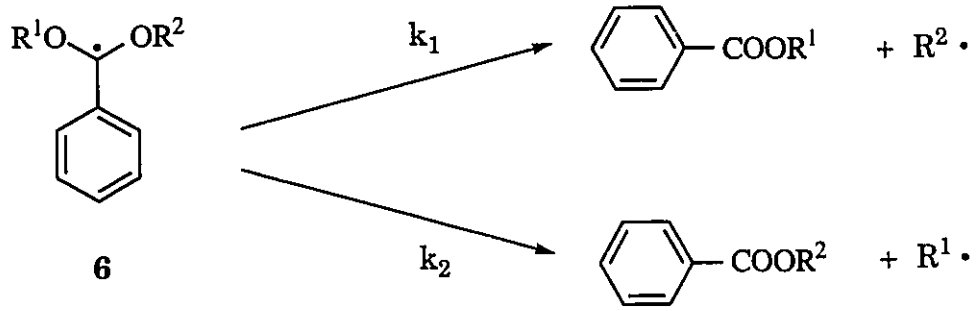

6 (3.9)

In order to determine k_1/k_2 ratios, several acetals were allowed to react with either di-t-butyl peroxide or di-t-butyl hyponitrite as sources of t-butoxy radicals, as indicated in the Experimental Section. We note that while reaction 3.8 may be accompanied by hydrogen abstraction processes at other positions, such reactions are not expected to yield the alkyl benzoates used to determine the k_1/k_2 values. These side reactions are expected to be more important when the substituents carry labile hydrogens, such as in the case of isopropyl derivatives. The methoxy-ethoxy benzyl derivative was mostly free from any significant problems related to side reactions and allowed the determination of k_1/k_2 values over a range of temperatures. The corresponding Arrhenius plot is shown in Figure 3.6 and leads to a difference of –1.4 kcal/mol in the activation energies and a ratio of 0.77 for the preexponential factors (ethyl-to-methyl fragmentation).

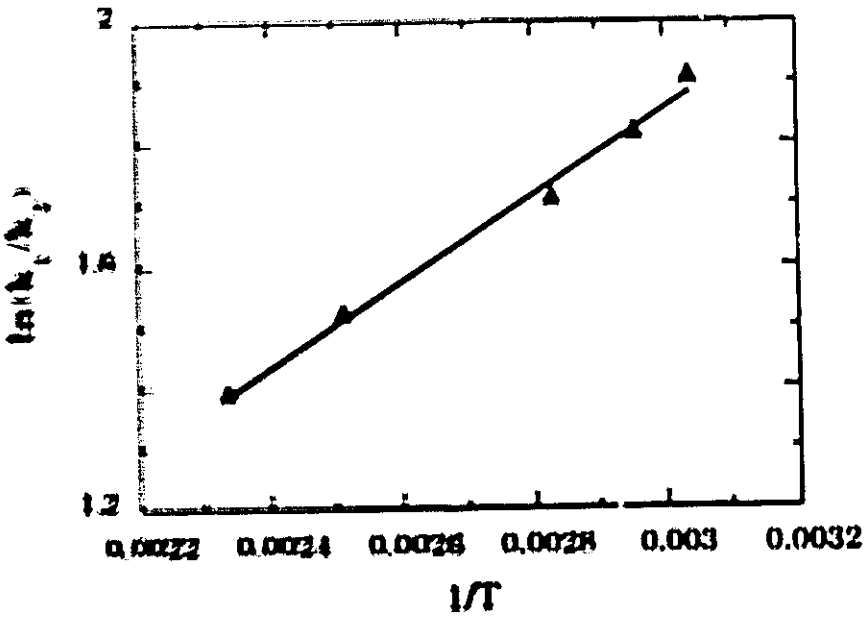

Figure 2.6 Arrhenius plot for the relative rates (k_1/k_2) of the two fragmentation pathways for the α-methoxy-α-ethoxybenzyl radical.

The plot of Figure 2.6 gives a ratio of rate constants of 7.6 at room temperature and of 6.3 at 56 °C, the temperature at which other derivatives were examined (see Table 2.1). For the methyl-isopropyl system, we were unable to detect isopropyl benzoate by gas chromatography. Given our analytical sensitivity, this places the corresponding k_1/k_2 ratio as greater than 80.

2.2.3 Low-intensity irradiations with predominant thermal fragmentation of unsymmetric dialkoxybenzyl radicals

In these experiments the radicals were generated by low intensity (long wavelength) irradiation of the AIBN peroxide. While the process is initiated photochemically, the fragmentation of the radicals is expected to be a predominantly thermal process. The selectivities observed, as measured by

the k_1/k_2 ratio suggest a mixture of thermal and photoinduced radical decay, (Table 3.1). Clearly, even under conditions of very low-intensity illumination, close to one half of the radicals undergo photolysis.

Table 3.1: Fragmentation ratios k_1/k_2 of the radicals **6** obtained under various experimental conditions.

		Fragmentation ratios k_1/k_2 [a]		
Radicals 6		**Thermolysis 56° C**	**Low intensity photolysis 35° C**	**Laser-jet photolysis ≤40 °C**
R^1	R^2			
CH_3	C_2H_5	6.5[b]	4.2	0.90
CH_3	i-C_3H_7	>40	25	1.25
C_2H_5	i-C_3H_7	12	6.4	1.10

a: Error ca. ± 10% of stated values.
b : Value derived from the plot in Figure 3.6.

3.2.5 Laser-Jet experiments.

The laser-jet technique employs a high velocity microjet (~ 100 μm in diameter) which is irradiated with the focused output from an argon-ion laser.[31-33] The microjet intensifies the light by trapping it as a standing wave within the stream. Under these conditions photogenerated transients may undergo further photolysis. Further details of these experiments have been given in Chapters 1 and 2.

The values of k_1/k_2 were determined by chromatographic analysis of the benzoate ratios and are given in Table 3.1. Clearly the photoinduced radical fragmentation shows virtually no selectivity.

It is interesting to note that we originally considered the two-laser, two-color approach already described in the determination of quantum yields in order to study product ratios from the fragmentation of the excited radicals. However, we found that increased absorption at 308 nm (the laser wavelength) upon irradiation prevented high conversion experiments. Attempts to carry out similar experiments with the 337 nm pulses from a nitrogen laser (where product absorption was not a problem) were unsuccessful due to the low and insufficient power of this laser. This shows the value of the laser-jet technique as a complementary tool for the examination of two-photon processes.

3.3 Discussion.

The work reported here on the fragmentation reactions of dialkoxybenzyl radicals illustrates the high sensitivity of these radicals to photodecomposition, a characteristic feature already observed in other laboratories.[66,72] Even low-intensity irradiation (see Table 3.1) tends to cause extensive light-induced fragmentation. Extensive photodecomposition even under conditions of very low-intensity irradiation reflects a combination of various factors, e.g., the lifetime and absorption characteristics of the radicals. Further, the di-t-butyl peroxide, used as a source for t-butoxy radicals and as cosolvent, has a very low extinction coefficient in this wavelength region (~1 M^{-1} cm^{-1}) and thereby acts as an inefficient internal filter. On the other hand, the dialkoxybenzyl radicals exhibit a relatively strong absorption and compete efficiently for the incident photons. Effective

absorption is assisted by their long lifetime, which is only limited by slow thermal fragmentation. Thus, nearly every absorbed photon induces cleavage, as indicated by the high quantum yields for fragmentation. Consequently, even under the conditions of mild low-intensity irradiation the photolysis of the intermediates competes with that of the t-butyl peroxide and a combination of photochemical and thermal fragmentation is observed.

In order to elucidate the structural influence on the fragmentation aptitudes, the thermal reactions under exclusion of light were examined. In these thermolysis the differences in reactivity arise almost exclusively from activation energy differences, as revealed by the results for the ethoxy-methoxy case in Figure 3.6. If one assumes that merely the stability of the resulting radical controls the fragmentation, independently of the structure of the second alkyl group in the molecule, then the expected k_1/k_2 ratio for the CH_3/i-C_3H_7 system would be ~78,[78] which is well in line with the value >40 observed experimentally. The same holds true for the intermediate case, the C_2H_5/i-C_3H_7 combination. Thus, as expected, the more stable the incipient radical species, the lower the activation energy and the more pronounced the fragmentation is.

Comparison of our fragmentation ratios (Table 3.1) with the rate constant reported by Fischer[66] for the fragmentation of the dimethoxybenzyl radical allows us to estimate the absolute rate constants for the fragmentation of the ethyl and isopropyl radicals. The rate constant for the methyl fragmentation is 260 s^{-1} at room temperature and with the help of Fischer´s estimate of the Arrhenius parameters[66] one calculates a value of 426 s^{-1} at 56 °C, which corrected for the statistical factor (i. e. the presence of two methoxy groups) leads to 213 s^{-1} per methoxy group. Substitution of this

value in the k_1/k_2 ratios (Table 3.1) leads to the absolute rate constants of 1,380 s^{-1} and 16,600 s^{-1} for the thermal cleavage of ethyl and isopropyl at 56 °C. In view of the high rate constants for thermal isopropyl cleavage it is rather remarkable that for this case (last entry in Table 3.1) considerable photolytic radical fragmentation takes place even under low-intensity irradiation.

Contrasting results were obtained in the laser-jet photolyses experiments (Table 3.1). Under the high intensity of the laser-jet experiments the radicals undergo exclusively photoinduced fragmentation with low selectivity, i.e. k_1/k_2 ca. unity. The deviations from unity in these ratios are most probably within the experimental error. Thus, the excitation of the radicals **6** provides enough energy (351 nm represents 81.5 kcal/mol) to overcome the ground state activation barriers and the lack of selectivity for the fragmentation of these electronically excited radicals is not surprising. This report provides one of the first examples on the selectivities of electronically excited radicals.

3.4 Conclusion.

The efficiency of the photocleavage for α,α-dialkoxybenzyl radicals helps to explain the efficiency of **1** as an initiator for photopolymerization systems since it is the very reactive methyl radical which is produced as a result. This could also have important consequences as to the intensity of light used for particular photopolymerization processes.

Finally, the laser-jet and two-laser two-color techniques provide complementary information on the photochemistry of transient species. Together they provide a quantitative description of the kinetics, quantum yields and product characterization of two-photon processes. The value of a

similar technique that could utilize pulsed lasers, of which we have many, did not escape our attention. The development of just such a technique is described in Chapter 4.

3.5 Experimental.

Materials. 2,2-Dimethoxy-2-phenylacetophenone (Aldrich) (**1**) was recrystallized twice from ethanol before use. Di-t-butylperoxide (Aldrich) was passed through a column of alumina to remove hydroperoxides before photolysis. Aberchrome-540 (Aberchromics Ltd., Cardiff, U. K.), benzaldehyde dimethyl acetal (Aldrich), and all solvents (acetonitrile, benzene and toluene; BDH Omnisolv) were used as received.

Methyl benzoate p-toluenesulfonyl hydrazone[79] was prepared from trimethyl orthobenzoate and (p-toluenesulfonyl)hydrazide. In a typical preparation, 10.0 g (55 mmol) of trimethyl orthobenzoate and 10.0 g (54 mmol) of p-toluenesulfonyl hydrazide were refluxed for 4 h in 60 mL of methanol. This solution was then placed in the freezer overnight, the resulting amorphous powder was collected by filtration and washed with 10 mL of cold methanol to yield 14.2 g (86 %) of white powder, m. p. 84 - 88 ^{o}C.

Ethyl benzoate p-toluenesulfonyl hydrazone[79] was prepared from triethyl orthobenzoate and p-toluenesulfonyl hydrazide as above. A solution of 12.0 g (54 mmol) of triethyl orthobenzoate and 10.0 g (54 mmol) of p-toluenesulfonyl hydrazide was refluxed in 60 mL of ethanol for 4 h. This solution was then placed in the freezer overnight, the resulting crystals were collected by filtration and washed with 10 mL of cold ethanol to yield 13.7 g (80 %) of white amorphous powder, m. p. 114 -118 ^{o}C

Benzaldehyde ethyl methyl acetal[79] was obtained by adding 10.0 g (32.7 mmol) of methyl benzoate p-toluenesulfonyl hydrazone to a solution of

potassium (1.3 g, 33.2 mmol) in 100 mL absolute ethanol and irradiated at room temperature. Initially, a yellow solid was formed and gas was evolved. After about 48 h, gas evolution had ceased and a small amount of a yellow and white solid was remained. The solid was removed by filtration and the ethanol evaporated (rotary evaporator) to leave a white paste. The acetal was extracted with 20 mL of ether and washed with 30 mL of water. The aqueous phase was extracted with 2 x 10 mL of ether and the combined organic phases washed with 4 x 20 mL of distilled water. The ether extract was dried with $MgSO_4$ and the solvent removed to give 4.2 g of a clear yellow liquid. Vacuum distillation of the residue yielded 3.3 g (61 %) of benzaldehyde ethyl methyl acetal; b.p. 39-40 ^oC (0.20 mm); ^1H NMR ($CDCl_3$) δ (ppm): 1.2-1.3 (t, 3H), 3.3 (s, 3H), 3.5-3.7 (q, 2H), 5.5 (s, 1H), 7.3-7.5 (m, 5H); ^{13}C NMR ($CDCl_3$) δ: 15.2 (CH_3), 52.4 (CH_3), 61.2 (CH_2), 102.1 (CH), 126.7 (CH), 128.1 (CH), 128.2 (CH), 138.6 (C).

Benzaldehyde isopropyl methyl acetal[79] was prepared as above, except that 2-propanol was used in place of ethanol. Yield 3.4 g (58 %); b.p. 42-43 ^oC (0.15 mm); ^1H NMR ($CDCl_3$) δ (ppm): 1.17-1.12 (d, 3H), 1.23-1.26 (d, 3H), 3.4 (s, 3H), 3.8 - 4.0 (m, 1H), 5.5 (s, 1H), 7.3-7.5 (m, 5H); ^{13}C NMR ($CDCl_3$) δ: 22.2 (CH_3), 23.0 (CH_3), 51.9 (CH_3), 68.4 (CH), 101.1 (CH), 126.7 (CH), 128.1 (CH), 128.2 (CH), 138.6 (C).

Benzaldehyde ethyl isopropyl acetal[79] was prepared as above except that ethyl benzoate p-toluenesulfonyl hydrazone was used in place of methyl benzoate p-toluenesulfonyl hydrazone. Yield 3.6 g (57 %); b.p. 59-60 ^oC (0.20 mm); ^1H NMR ($CDCl_3$) δ (ppm): 1.15-1.25 (t, 3H), 1.16-1.19 (d, 3H), 1.22-1.25 (d, 3H), 3.4-3.5 (q, 2H), 3.8-4.0 (m, 1H), 5.5 (s, 1H), 7.3-7.5 (m, 5H); ^{13}C NMR ($CDCl_3$) δ: 15.2 (CH_3), 22.3 (CH_3), 23.1 (CH_3), 60.0 (CH_2), 68.5 (CH), 100.2 (CH), 126.7 (CH), 128.1 (CH), 128.2 (CH), 139.6(C).

Di-t-butyl hyponitrite[80] was prepared from t-butyl bromide and sodium hyponitrite. Anhydrous zinc chloride was added to a mixture of t-butyl bromide (5 mL) and ether (5 mL) followed by 0.6 g (5.7 mmol) of sodium hyponitrite, which was added slowly (5 minutes) with swirling and occasional cooling to insure that the temperature of the reaction mixture was kept below 45°C. After allowing the reaction mixture to stand for 75 min, the inorganic salts were removed by filtration and the organic phase washed with 5 mL water. The wash was extracted with 4 mL of ether and the organic phases combined, washed with 4 x 5 mL of water and dried over $MgSO_4$. The solvent was removed under reduced pressure to give 0.80 g (80 %) of an off-white solid. Recrystallization from pentane gave 0.60 g of pure white needles.

Thermally-initiated reactions. To examine the effects of temperature on the thermal fragmentation of α-ethoxy-α-methoxybenzyl radicals, t-butoxyl radicals were generated thermally from either di-t-butyl hyponitrite (temperatures below 100 °C), or di-t-butyl peroxide (temperatures above 100 °C). Stock solutions were made containing 10% di-t-butyl hyponitrite in benzaldehyde ethyl methyl acetal or 10% di-t-butyl peroxide in benzaldehyde ethyl methyl acetal. In a typical run, 200 µl of stock solution was placed in a glass ampoule and degassed by 5 freeze-pump-thaw cycles. After degassing, the ampoule was sealed and placed in a refluxing solvent to maintain constant temperature. The reaction was allowed to remain in the refluxing solvent for at least five half-lives of the t-butoxy radical source.[81,82] The reaction was then stopped and the ampoule broken and washed with 2 mL of ether. The ether solution was treated with 1 mL of concentrated HCl to convert the acetal to benzaldehyde. The acid was neutralized with sodium bicarbonate and the organic layer separated, which was washed with 3 x 2

mL of water. The organic layer was analyzed by GC and the ratio of the benzoate products determined from the integrated areas.

Laser-Jet Experiments. In order to ensure that the dialkoxybenzyl radicals underwent a significant degree of photofragmentation, it was necessary to use a method of irradiation capable of delivering a high photon flux. The technique of Laser-Jet photochemistry provides the photon flux necessary to photoexcite transient species and lead to sequential two photon processes.[32,33]

In a typical experiment, 5 mL of a 75 mM solution of acetal in di-t-butyl peroxide was passed through the Laser-Jet and recycled until approximately 30% of the acetal had been depleted (ca. 3 h, 22 cycles). The samples were degassed by purging with a slow stream of dry argon for 20 min and the irradiation chamber was kept under a positive argon gas pressure. The ratio of the benzoate products were determined by GC.

Low-intensity photolysis. To make a direct comparison of the thermal and photochemical product yields, it was necessary that the temperatures of the reactions were also comparable. Since higher than ambient temperatures are required to produce t-butoxy radicals from either di-t-butyl peroxide or di-t-butyl-hyponitrite, it was decided to use low intensity irradiation as an alternative method, thus, the steady-state concentration of the dialkoxybenzyl radicals would be small and we anticipate that only a minimal fraction of the radicals would fragment photochemically. In fact this fraction turned out to be somewhat higher than we had expected (*vide supra* , see Table 3.1).

In a typical experiment, 1.0 mL of a degassed solution of 75 mM acetal in di-t-butyl peroxide was photolysed by irradiation with 300 nm Rayonet lamps until all of the acetal had been depleted (approximately 30

min). The ratio of the benzoate products was then determined by gas chromatography.

Laser flash photolysis (LFP). Early experiments in this work were carried out at the National Research Council Laboratories in Ottawa (Canada) with the system described in earlier work.[22,55] A Lumonics TE-860 excimer laser filled with Xe/HCl/He mixture (~6 ns, ≤ 20 mJ/pulse) or a Molectron UV-24 nitrogen laser (~ 8 ns, ≤ 10 mJ/pulse) were used for sample excitation, while a Candela Dye Laser with Stilbene-420 dye (~250 ns, ≤ 80 mJ/pulse) was employed to excite the radicals in the two-color, two-laser experiments. More recent experiments were carried out at the University of Ottawa on the laser system described in Chapter 2. Static samples (usually 2 mL) were contained in cells made of 7 x 7 mm^2 square Suprasil tubing. Flow experiments employed a flow cell constructed of the same tubing. Unless otherwise indicated, the samples were deaerated by bubbling with oxygen-free nitrogen and experiments were carried out at room temperature.

The quantum yield for the bleaching of the dimethoxybenzyl radical in benzene was measured with Aberchrome-540 (**7**) as a two-color actinometer.[76]

Aberchrome-540 is the commercial name for the fulgide, **7**[77] which is isomerized to **8** with a quantum yield of 0.20 in toluene and has been widely used as an actinometer for steady-state irradiations.[77,83] The Aberchrome-540 system has been shown to be photoreversible with a quantum yield that depends linearly upon the irradiation wavelength.[77] This reaction may be conveniently used as an actinometer for the measurement of transient extinction coefficients and for the determination of bleaching quantum yields for transients in two-laser experiments.[76] The latter requires the

parallel generation of both the colored form **8** of Aberchrome-540 and the transient to be bleached with the first laser pulse and the matching of the optical densities of these two at the wavelength and time of the second laser. Both the transient of interest and **8** are then excited with the second laser. The quantum yield for bleaching (Φ_{bl}) of the transient can then be evaluated according to equation 3.10, where ε_8 and ε_R are the extinction coefficients at

$$\Phi_{bl} = \frac{\varepsilon_8}{\varepsilon_R} \frac{\Delta OD_R{}^0}{\Delta OD_8{}^0} \frac{\ln(\Delta OD_R{}^0/\Delta OD_R{}^d)}{\ln(\Delta OD_8{}^0/\Delta OD_8{}^d)} \Phi_8 \qquad (3.10)$$

the wavelengths for which they were monitored for **8** and the dimethoxybenzyl radical **6**, $\Delta OD_8{}^o$ and $\Delta OD_8{}^d$ are the changes in optical densities before and after the dye laser pulse for **8** (monitored at 494 nm), $\Delta OD_R{}^o$ and $\Delta OD_R{}^d$ are the changes in optical densities before and after the dye laser pulse for the dimethoxybenzyl radical (monitored at 390 nm) and Φ_8 is the quantum yield for the photoconversion of **8** to **7** at the wavelength of the dye laser (420 nm).

Chapter 4. Development of the Laser-Drop Technique to Induce Multiple Photon Chemistry: Examples Involving the Photochemistry of Diphenylmethyl Radicals.

4.1 Introduction.

TLTC-LFP, as has been mentioned, is an invaluable tool for obtaining kinetic and mechanistic information involving the reaction pathways for short-lived intermediates in solution. Use of this technique for the production of isolable amounts of multi-photon reaction products is, at best, cumbersome. Scaiano and Johnston[84] were able to show that **4** is the two-photon product of **1** (Scheme 4.1). However, in order to obtain 1 mg of this product, it was necessary to irradiate a solution of 24 mg of **1** in 25 mL of benzene with 9000 pairs of laser shots (308 nm pulse followed 100 ns later by a 337 nm pulse). This represents a 4% isolated yield and a full day investment of time.

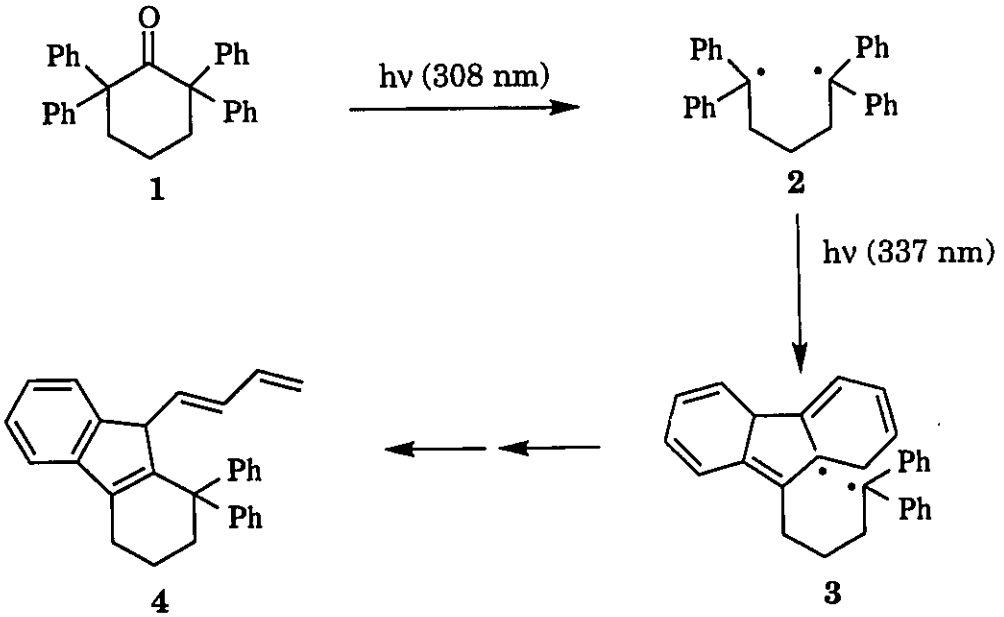

Scheme 4.1

The LJP technique developed by Adam, Wilson and co-workers[32,33] has proven to be a more pragmatic approach for the production of isolable amounts of multiple photon products which can then be characterized by conventional spectroscopic methods. These workers were able to isolate > 40 mg of **4** upon LJP of 100 mg of **1** in a single afternoon. As is easily seen this is a much more efficient method of preparative multi-photon chemistry. This technique however is limited in the mechanistic insights it provides and for all practical purposes cannot yield any kinetic information.

Thus, one can see that the strengths and limitations of the TLTC-LFP and LJP techniques are complimentary and, as was shown in the previous chapter, may be used in a symbiotic fashion to elucidate the reaction mechanisms from which multiple photon products are derived. However, there is at present no laboratory which is equipped to carry out both types of experiments "in house". In fact, the investigation of α,α-dialkoxybenzyl radicals[85] is a unique example in the literature providing a direct comparison of these two techniques in the same paper.

For the numerous laboratories that use pulsed lasers for transient studies setting up the laser jet technique would represent a major investment. We reasoned that what the laser jet technique achieves by using a continuous laser and a continuous flow, could perhaps also be achieved with a pulsed laser by using it in conjunction with a "pulsed" flow. Thus the idea of employing pulsed lasers to irradiate small droplets of solution.

In order to "test" this hypothesis, which we have called laser-drop photolysis (LDP), we reasoned that the diphenylmethyl radical (**6**) would provide an ideal system. This radical can be produced photochemically from a number of precursors such as, 1,1-diphenylacetone, (**5**), 1,1,3,3-

tetraphenylacetone,[22,86,87] the diphenyl acetic acid ester of N-hydroxypyridine thione,[88] and by hydrogen abstraction from appropriate donors by diphenylcarbene produced upon photolysis of diphenyldiazomethane.[22] The radical has a large extinction coefficient near 308 nm, 88,000 M^{-1} cm^{-1} at 330 nm and 40,000 M^{-1} cm^{-1} at 315 nm.[87] The excited radical, **6***, is readily produced in a single laser pulse with an appropriate precursor,[22,86,87] and also has a large extinction coefficient near 308 nm, 80,000 and 24,000 M^{-1} cm^{-1} at 360 and 270 nm respectively.[87] The lifetime of the excited radical in acetonitrile has been reported to be about 260 ns and about 235 ns in several alcohols.[22,26]

Ground state **6** is a relatively inert radical and does not readily abstract hydrogen atoms from most solvents, but prefers to undergo radical-radical recombinations in the absence of oxygen. Although **6*** does show some increased reactivity towards hydrogen donors such as 1,4-cyclohexadiene and tri-N-butyltin hydride,[86] it is a surprisingly poor hydrogen abstracting species, even though this reaction would be more exothermic than abstraction of hydrogen by a phenyl radical. The reactivity towards tri-N-butyltin hydride is five times less than that of t-butyl radicals.[22] This species can be quenched by oxygen to give singlet oxygen and ground state radicals.[89] The excited radical also reacts with electron acceptors; Scaiano et al.[86] have shown that the diphenylmethyl cation can be generated in this manner in acetonitrile, thus proving that full electron transfer occurs with suitable electron acceptors. The reaction of **6*** with halogenated compounds is known to also involve electron transfer, the net result of such a reaction being the abstraction of the halogen to produce benzhydryl halide and the corresponding radical[22,86] *vide supra* .

The [illegible] gives a strong emission in the 500 – 600 nm region with a quantum yield of [illegible].[illegible] In fact, this emission has recently been reported [illegible] detected [illegible].[illegible]

A recent publication by [illegible] and [illegible][illegible] describes the laser-jet photochemistry of [illegible] which allows the direct comparison of the laser-drop technique with that of LJP. This chapter describes the successful implementation of this [illegible] sample technique using the [illegible] system.

[illegible] Results

[illegible] Description of the Experiments

[illegible] that one could [illegible] a pulsed laser at high frequency and [illegible] Depending on [illegible] only [illegible]% of the solution would be [illegible] conditions.

The idea of [illegible] falling drops of solution was [illegible] The simplest approach [illegible] Chapter 2 [illegible] solution [illegible]

Chapter 6). Once the drop has been destroyed, a new drop begins to form. Figure 4.1 shows a schematic representation of the timing of a laser-drop experiment.

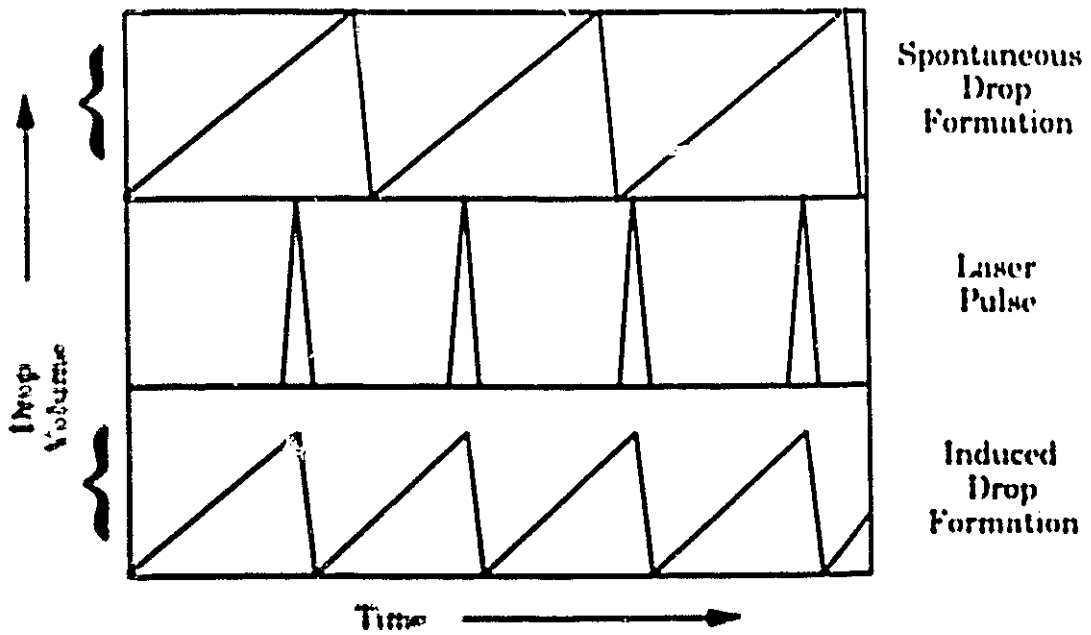

Figure 4.1: Schematic diagram of the timing sequences for laser-drop irradiations

Several aspects of the experiment must be taken into account for the design of an adequate laser-drop cell: i) Because the droplets explode upon irradiation, the ejected material must be contained to ensure that the photolysate can be efficiently collected. ii) Ablation of quartz is not minimum under these irradiation conditions[1] and the drop must be far enough away from the cell window to keep the focal point of the laser from destroying the quartz window. iii) It is usually desirable to keep the photolysis efficient under an inert atmosphere to avoid oxygen contamination, and so if for some reason there is sufficient oxygen present, the solvent may ignite and cause an explosion. In this case it is prudent to have a pressure release panel to avoid rupture of the container

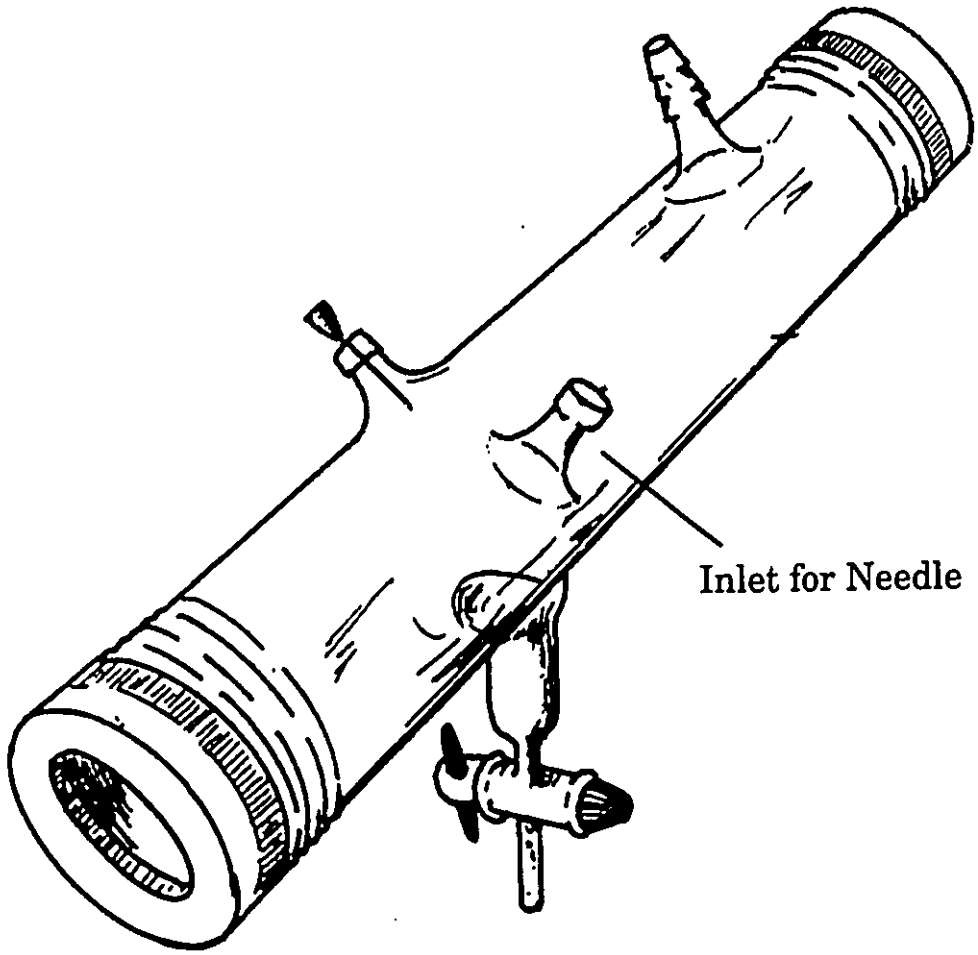

Figure 4.2: Diagram of the cell employed for laser-drop experiments. The overall length is 12 in. and the cell is equipped with removable quartz windows.

and possible injury to the experimenter. Figure 4.2 shows the design for the laser-drop cell built and used for these studies. It must be stressed that there is the possibility for explosion during the course of these experiments. However, provided the experimenter is aware of this and takes the necessary precautions, this technique is no more dangerous than many typical synthetic organic procedures. Complete details for cell design and experimental procedures for laser-drop experiments are provided in Chapter 2.

4.2.2 Photochemistry of 1,1-diphenylacetone (5)

1,1-Diphenylacetone, (5), was chosen as the precursor for 6 because it is commercially available and, at the wavelength of the laser used (308 nm), it is possible to produce and excite the radical within a single laser pulse.

In order to fully characterize our excitation conditions, a few laser flash photolysis experiments were carried out on the same solutions employed for the laser-drop experiments. Figure 4.3 shows the transient spectra recorded upon 308 nm laser excitation of a deaerated solution of 5 (2 mM) in acetonitrile. Figure 4.3a corresponds to the spectrum immediately after excitation, and Figure 4.3b after a delay of ~0.5 μs. The short lived species (Figure 4.4a) has a lifetime of 232 ns and λ_{max} 355 nm and can be confidently assigned to excited diphenylmethyl radicals (6*).[22,26,27] The long lived species that has a half-life in excess of 10 μs under our experimental conditions and λ_{max} 334 nm is due to the ground state radical, 6 (Figure 4.4b).

Note that the ΔOD at ~334 nm in Figure 4.3a is smaller than that of Figure 4.3b, which was taken at a later time. This is due to repopulation of the ground state radical from the excited state and can be seen by the growth of the ground-state radical after an initial absorption caused by the laser pulse. The growth at 330 nm (Figure 4.5) has the same lifetime as the decay of the excited radical as monitored at 355 nm.

The products of the laser-drop photolysis of a solution containing 10 mM 5 in carbon tetrachloride show benzhydryl chloride (7) as the main (>98%) reaction product. In contrast, lamp photolysis yields very little 7, while tetraphenylethane (8) and 1,1,1,-trichloro-2,2-diphenylethane (9) are now the main products. Product distributions for the irradiation of 5 are

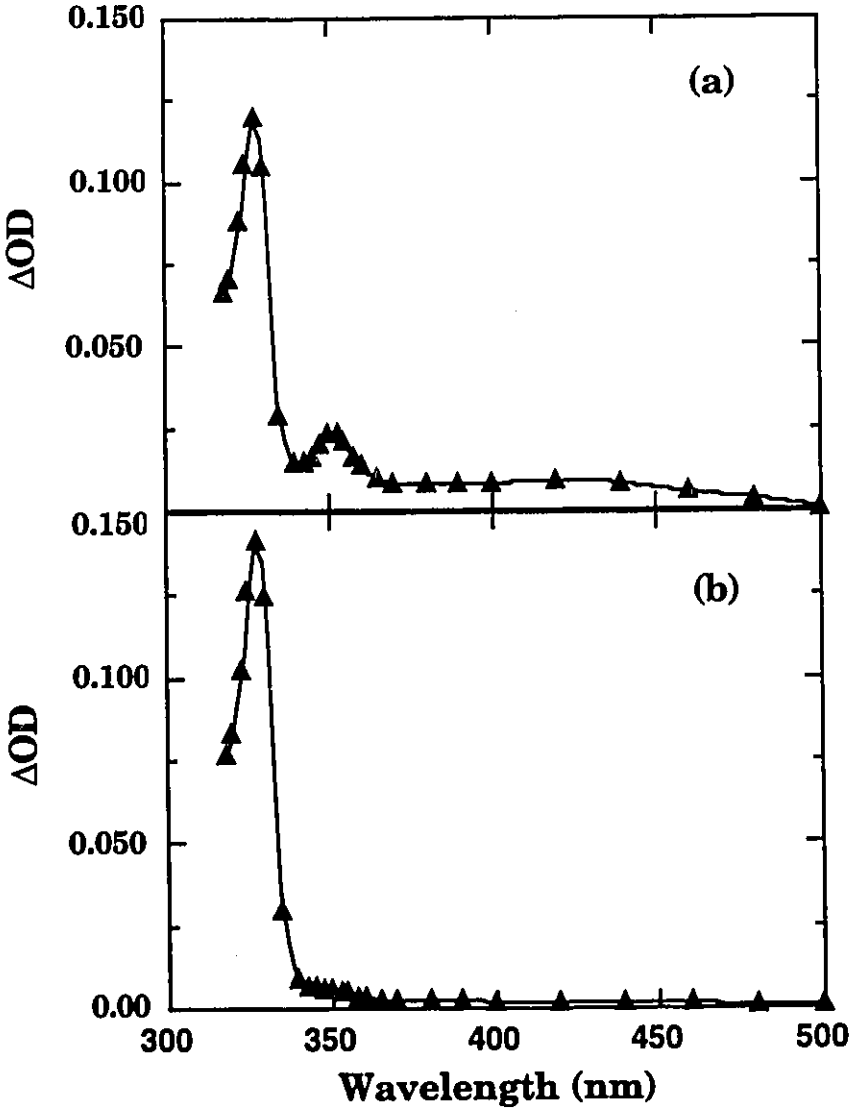

Figure 4.3: Transient spectra recorded upon 308 nm excitation of a 2 mM solution of **5** in acetonitrile recorded immediately (a) and 0.5 μs (b) after excitation. The increase in peak intensity in b is due to decay of excited radical (**5***) leading to ground state repopulation.

given in Table 4.1. While the acetyl radical products were not quantified, it is evident that **9** results from the combination of **6** with trichloromethyl radicals, which under lamp irradiation would be the expected product of reactions of acetyl radicals with the solvent according to reaction 4.1.

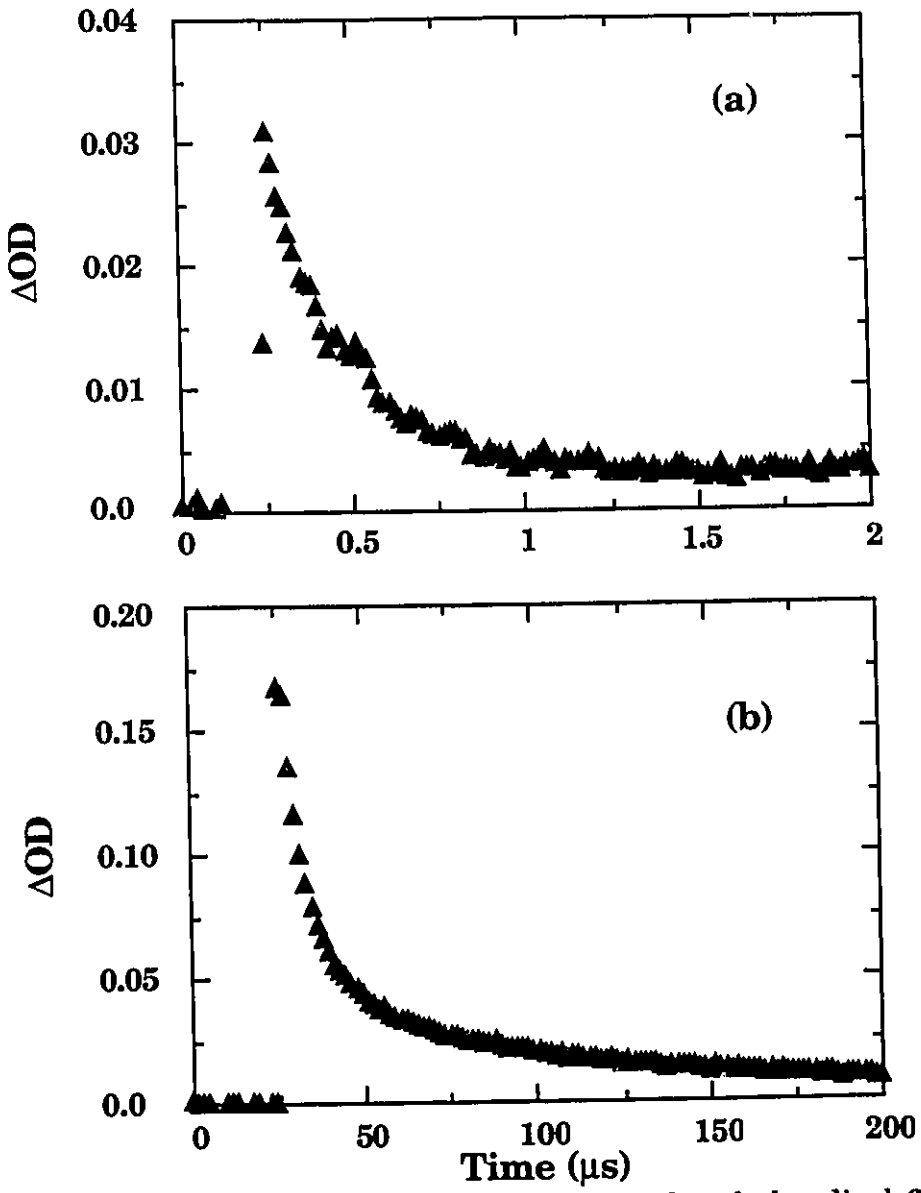

Figure 4.4: (a) Decay of the excited diphenylmethyl radical **6*** monitored at 355 nm. (b) Decay of the ground state diphenylmethyl radical **6** monitored at 335 nm.

$$CH_3\dot{C}O + CCl_4 \longrightarrow CH_3COCl + CCl_3^{\bullet} \qquad (4.1)$$

Recent reports employing time resolved infrared spectroscopy have demonstrated the reactivity of acyl radicals towards the C–Cl bond. Ingold

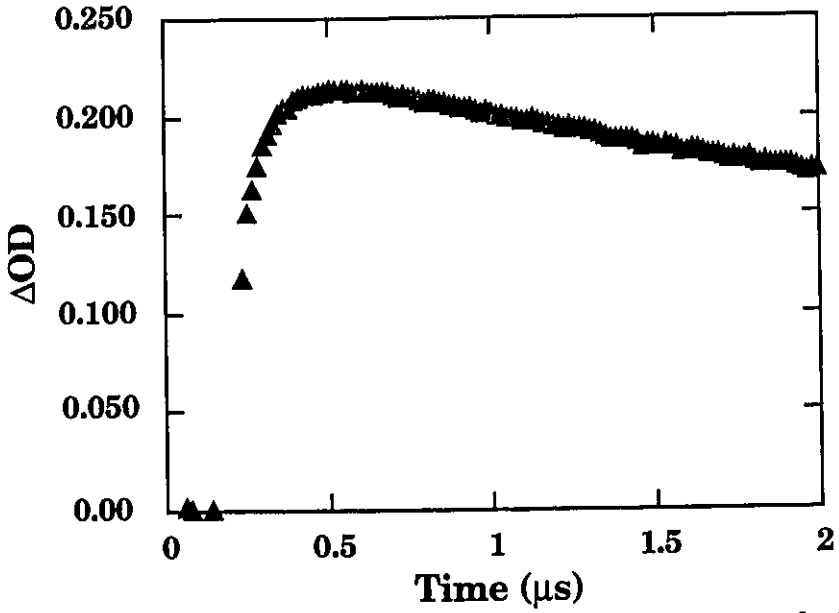

Figure 4.5: Trace showing the repopulation of the ground state radicals at short time scales. Monitored at 335 nm.

Table 4.1 Photolysis of diphenylmethyl radical precursors in CCl_4

Method	Precursor	%Conv.	7	8	9
Rayonet [a]	5	87	10	38	52
Laser jet [b]	11	22	96	5	--
Laser-drop	5	15	>98	<2	--

[a]Lamp irradiation at 300 nm. [b]Data from ref. 90.

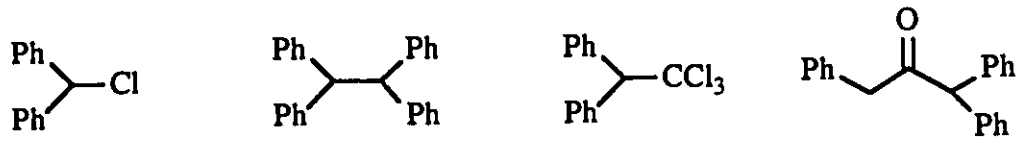

7 8 9 11

and co-workers[91] report a rate constant of 5.6×10^4 M^{-1} s^{-1} for abstraction of chlorine from carbon tetrachloride by benzoyl radicals. It is expected that

the acetyl radical would be at least as reactive towards a C-Cl bond as the benzoyl radical, and probably more so. We note that the absence of **9** under laser jet and laser-drop excitation conditions cannot be due to failure to produce $CCl_3\bullet$, since in fact excited diphenylmethyl radicals abstract a chlorine to provide an additional source of $CCl_3\bullet$ under these conditions.[22,86]

Preparative experiments for LDP of **5** in carbon tetrachloride were done by recycling the photolysate four times. Two separate experiments were performed; i) deaerating the photolysate between cycles, and ii) deaerating only before the first cycle. The % conversions were 57% and 52% respectively with product distributions similar to that listed in Table 4.1. No additional products were detectable.

The effect of drop size on product distribution was also investigated by LDP of CCl_4 solutions of **5**. This was done by altering the flow rate of the solution while the repetition rate of the laser was kept constant. It was found that drop size (5 to 25 μl) had little effect on product distribution as long as the energy of the laser was kept constant and the drops remained in the same focal region of the laser. Drop size did however have a direct effect on the percent conversion, with the smaller drops having the largest degree of conversion. This is not surprising since the drops are always larger than the laser cross section at the focal point. Drop size effects were not investigated further, other than to keep the drops as small as possible while remaining slightly larger than the cross section of the focused laser.

When drops of a deaerated 10 mM solution of **5** in methanol were irradiated by the focused output from a 308 nm excimer laser, a strong green fluorescence was readily visible. Figure 4.6 shows the emission spectra and fluorescence decay obtained by laser-drop irradiation of **5** in

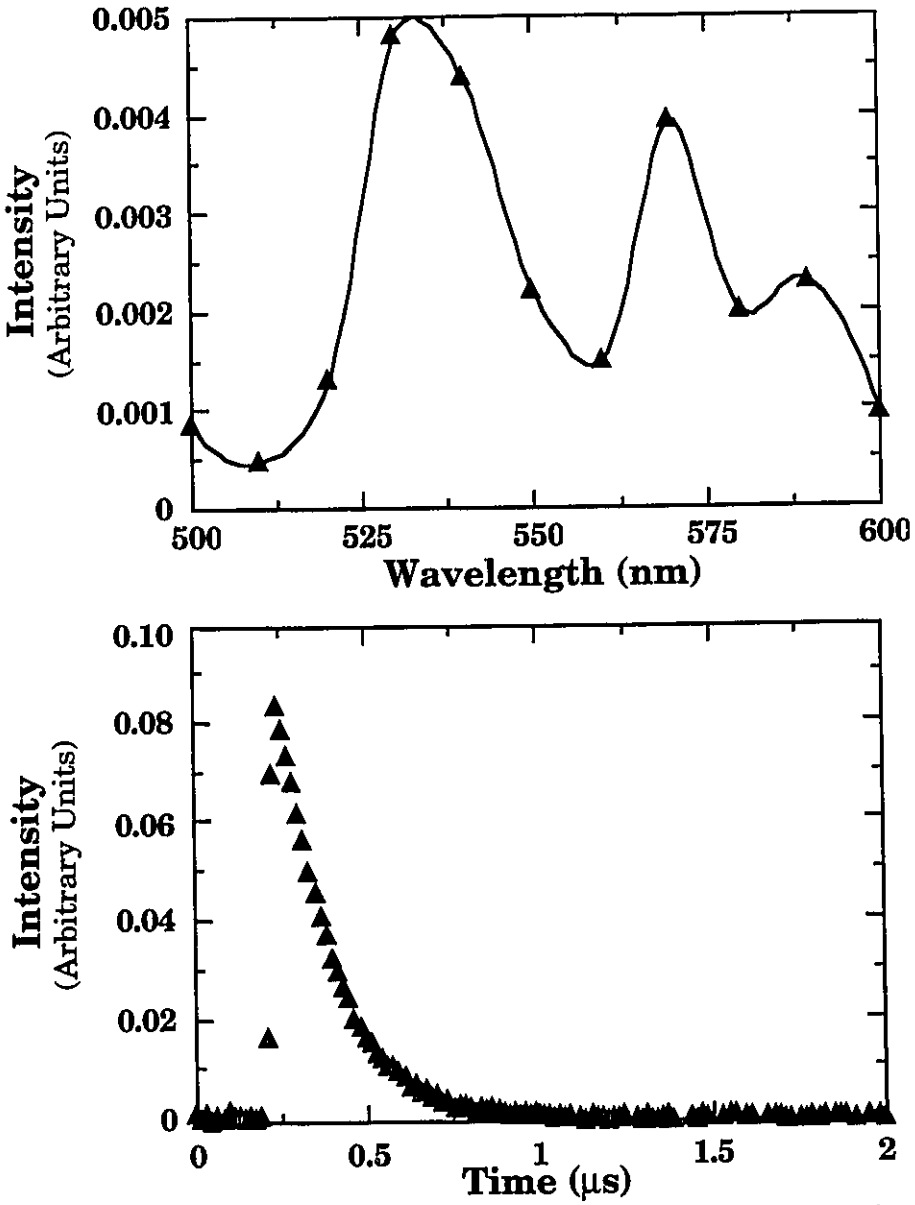

Figure 4.6: (Top) Fluorescence spectrum for excited diphenylmethyl radicals **6*** in drops of methanol. (Bottom) Decay trace for the excited radical monitored by its emission at 535 nm.

methanol. This spectrum agrees well with that reported by Bromberg et al.[26] and Scaiano et al.[92] for the excited diphenylmethyl radical **6***. It is interesting that the lifetime for the excited radical in this case is considerably shorter than that found under normal LFP conditions (τ=160

ns). This is probably due to a bimolecular self quenching of the excited radicals due to the high concentration produced under LDP conditions. A similar phenomenon has been observed in micellar solution.[93]

Table 4.2: Photolysis of diphenylmethyl radical precursors in methanol

Method	Precursor	%Conv.	**8**	**10**
Rayonet [a]	**5**	98	>98	--
Laser jet [b]	**11**	27	59	34
Laser-drop	**5**	19	8	92

[a]Lamp irradiation at 300 nm [b]Data from ref. 90.

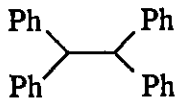

8

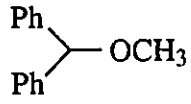

10

The photolysis products of **5** (10 mM) in methanol again showed a strong dependence on light intensity. Under lamp irradiation the major product (>98%) is 1,1,2,2-tetraphenylethane (**8**), formed by the combination of radicals **6**, while under laser-drop conditions the ether **10** accounts for 92% of the products. Product distributions for the photolysis of **5** in methanol are given in Table 4.2. A solution of **5** in methanol-d_1 was also irradiated under laser-drop conditions and analyzed by GC-MS. The $m^+/(m^++1)$ ratio for the ether **10** was 3.7 as compared to a ratio of 6.4 for the ether produced upon LDP of **5** in undeuterated methanol.

4.3 Discussion

Laser excitation of small absorbing droplets leads to the rapid ejection of material in an apparent explosion of the drop. One may question the process (or processes) which are responsible for drop explosion and whether or not it is these processes which are responsible for the changed chemistry during laser-drop irradiation rather than the absorption of light by the initially formed transient. We have done experiments to address some of these issues and to show that the ejection of material occurs on the microsecond time scale. As well, we have evidence, by way of "chemical thermometers", that the temperature increase of the drops during irradiation is small. These experiments and their results are discussed in Chapter 6.

One could envisage a large temperature increase in the drop after the deposition of the energy from the laser pulse. A simple calculation shows that the ejection of material most probably is not due to thermal effects. If 100 mJ are deposited and converted into heat in a 10 μl droplet the temperature change would be 4° in methanol (specific heat, C= 0.60 cal/K.g) and 12° for carbon tetrachloride (C= 0.20 cal/K.g). As has been mentioned, the actual volume of the drop which is irradiated is smaller than the total volume of the drop; while this in theory would lead to even greater temperature changes than those calculated, one can see from the high conversion of **5** to **10** in methanol (19%), a three photon process (*vide supra*), that a large number of photons are required to induce chemical change, and not to generate heat. It must also be noted that a significant amount of light is scattered at the surface of the drop. This can easily be seen by performing the LDP experiment in the dark and holding a piece of paper at

several positions around the drop. Further, specific heats for common solvents are unlikely to be lower than for carbon tetrachloride. Under most conditions, the actual temperature change should be between 2 and 6 degrees.

Another question of interest relates to the actual concentration of intermediate that could be generated under laser-drop conditions. At 308 nm the energy corresponds to approximately 93 kcal/mol. A simple calculation indicates that a 100 mJ pulse incident on a 10 mL droplet would lead to a transient concentration of 0.025 M if it was totally absorbed and the process occurred with a quantum yield of one. While these criteria may not be always met, one can anticipate that initial transient concentrations could approach 10^{-2} M.

4.3.1 The diphenylmethyl radical system

In a recent paper Adam and Schulte Oestrich[90] examined the high intensity photochemistry of benzhydryl phenyl ketone ($Ph_2CHCOPh$, **11**) in carbon tetrachloride and in methanol. The process involves the intermediacy of excited electronic states of the diphenylmethyl radical, **6***. Adam's results[90] on the laser jet photolysis of **11** are very similar to those recorded by us for the laser-drop photolysis of **5** (see Tables 4.1 and 4.2). In CCl_4 the formation of **7** can be readily explained by the reaction of **6*** with the solvent, reaction 4.2.

$$Ph_2\dot{C}H^* + CCl_4 \longrightarrow Ph_2CHCl + CCl_3\bullet \qquad (4.2)$$

It has been reported that reaction 4.2 occurs with a rate constant of 1.6×10^8 M^{-1} s^{-1} at room temperature and that the lifetime of **6*** in CCl_4 is

less than 5 ns.[22] It was proposed several years ago that quenching of **6*** by CCl_4 probably involves charge transfer interactions.[22] Arnold et al.[87] have recently been able to prove unequivocally this mechanism by characterizing the corresponding carbocation, Ph_2CH^+, as an intermediate in the reaction in acetonitrile. In non-polar media (e.g. in CCl_4 solvent) geminate recombination of the ions (Ph_2CH^+ and Cl^-) may predominate and account for the high yield of **7** (>98%).

When the solvent is methanol, the charge transfer mechanism is no longer efficient for **6***, and its lifetime is 236 ns, a value quite close to those typically observed in inert solvents.[22,27] Under high intensity excitation conditions (laser jet or laser-drop) a significant yield of ether **10** was formed (see Table 4,2). Meisel et al.,[27] and later Arnold et al.,[87] showed that **6*** can be further excited to **6****. Meisel[27] suggested that **6**** may lose a hydrogen atom to form diphenylcarbene. In this case one would expect the carbene to insert into the O–H bond of methanol to form ether **10**, reaction 4.3. However, no deuterium incorporation in **10** was detected under laser jet[90] excitation of **11** in a 5% solution of methanol-d_1 in benzene. Laser-drop photolysis of **5** in neat methanol-d_1 shows some deuterium incorporation, as shown by the change in the $m^+/m^+{+}1$ ratio. However, the incorporation is small and could result from proton exchange of the ether with the deuterated solvent after photolysis. Since the insertion of diphenyl carbene into the O-D bond would result in deuterium incorporation these results suggest that the ether is formed by the nucleophilic trapping of the cation, **6⁺**, by methanol. That this is the case is further supported by Steenken's report on the photoionization of aryl substituted methyl radicals,[94] and a report by Redmond et al.[95] on the photoionization of diphenylketyl radicals in polar solvents.

$$Ph_2C: + MeOH(D) \longrightarrow Ph_2CH(D)OCH_3 \qquad (4.3)$$

Adam was also able to show that the ratio of products **10/7** increased as a function of laser intensity when the laser jet photolysis of **11** was carried out in a 1:99 mixture of CCl_4 and methanol.[90] This result indicates that the reaction with methanol, to form **10**, requires more photons than the reaction with carbon tetrachloride to form **7**. Thus, different species must be responsible for the different product distributions which result from increasing the light intensity. This experiment, combined with Meisel's observation of irreversible photobleaching of **6*** in methanol, suggests that the formation of **10** results from the successive absorption of three photons. Thus, we find that the photochemistry of **5** under laser-drop conditions parallels that observed by Adam[90] for **11** under laser jet conditions. The origin of the products of laser-drop photolysis of **5** is outlined in Scheme 4.2.

Ether **10** accounted for 92% of the diphenylmethyl radical products under laser-drop irradiation of **5**, compared with 34% reported for the photolysis of **11** under laser jet conditions (see Table 4.2). We note that the conversion of the 10 mM solution of starting material is similar for both laser-drop and laser jet experiments, suggesting at least comparable efficiencies for both the laser-drop and laser jet techniques in producing multiple-photon products. In fact, the conversion to three photon products is much higher in the laser-drop technique, probably suggesting that this method should be preferred for processes requiring more than two-photons. It is also noteworthy that both methods can recycle the photolysate to increase the conversion of starting material. Although our experiments indicate that oxygen contamination is not a problem when recycling (the

photolysate is kept under an inert atmosphere), transfer of the photolysate should be done with care to avoid any problems since radicals, triplets, carbenes and other reactive intermediates are often reactive towards oxygen, and oxygen contamination would result in competing oxidative pathways for the reactions of these species.

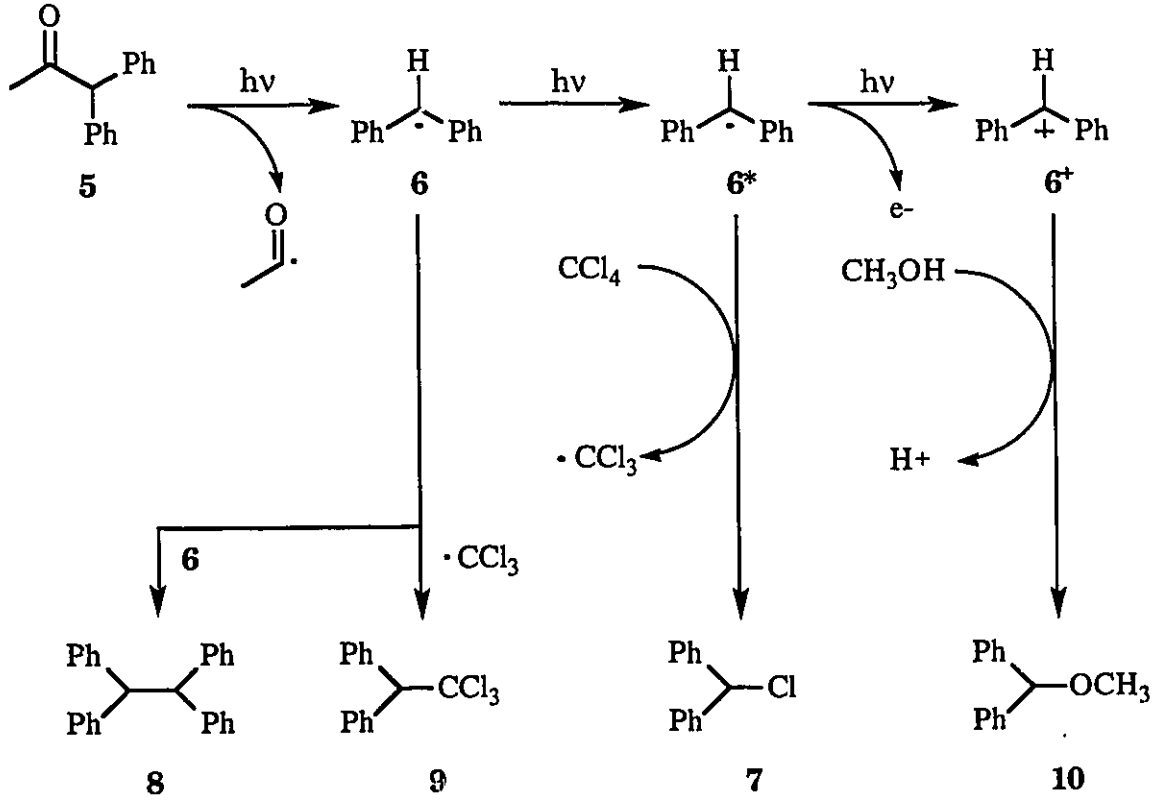

Scheme 4.2

4.4 Conclusion

The laser-drop and laser jet techniques offer similar, if certainly not identical, capabilities for the preparation of multiphoton products. One may wonder if there is an obvious reason why one or the other should be preferred. The most obvious answer is that the choice should reflect the availability of lasers on-site. Given an available laser, the cost of either

technique is minimal compared with the cost of the lasers. We feel this should be the main reason for choice. There is at least one situation where the laser-jet must be used, i.e. when the species to be irradiated by a "second" photon is not produced in less than a few nanoseconds. When this is the case, the laser pulse is over before there is significant absorption due to the transient species. This is often the case with a species which is produced as the result of a bimolecular reaction such as the production of the dialkoxybenzyl radicals produced by hydrogen abstraction from the corresponding acetal as reported in the previous chapter.

In summary, the laser-drop technique offers the possibility of carrying out preparative multiphoton chemistry in a simple way with equipment readily available in laboratories that routinely carry out laser flash photolysis experiments. Our results for the diphenylmethyl radical system are in line with those reported using the laser jet technique.

Experimental

Materials. 1,1-Diphenylacetone (Aldrich) was recrystallized twice from methanol and no impurities could be detected by GC. All solvents were spectral grade (BDH, Omnisolv) and used as received.

General Techniques. Products of photolysis of **5** were identified by GC-MS analysis provided by the Mass Spectroscopy lab at the University of Ottawa. The product distributions were quantified by capillary gas chromatography employing 1,4-di-t-butylbenzene as internal standard.

Laser Flash Photolysis. Details for the LFP instrumentation are given in Chapter 2. The LFP experiments were done in flow cells to avoid interference from possible product build-up. It was necessary to attenuate

the laser with a 25% neutral density filter to keep the ΔOD signals below ~0.20.

Laser-Drop Photolysis. Details for these types of experiments and the design and construction of the cell are given in Chapter 2. The experiments were carried out using a Lumonics EX-530 excimer laser with a Xe/HCl gas mixture in a Ne buffer (308 nm, ~6 ns, 80-130 mJ/pulse).

Fluorescence measurements were carried out by replacing the sample holder on the LFP optical table by the laser-drop cell so that the drops were at the same level as the slit for the monochromator. The drops were irradiated by the laser at an angle of 90° with respect to the monochromator. The voltage across the PMT was controlled manually so that the signals could be captured by the oscilloscope set at 20 mV/div at the maximum emission. The spectrum was obtained, point by point, by scanning the monochromator (keeping the voltage across the PMT constant) across the wavelength region for emission and recording the fluorescence decay.

Chapter 5: Examples of Multi-Photon Chemistry of Organic Molecules in Solution.

5.1 Introduction.

The previous two chapters of this thesis introduced the two primary techniques (TLTC-LFP and LDP) used in this laboratory for the investigation of the photochemistry of short lived organic species in solution. As mentioned in the introductory chapter, it is the short lived nature of these species which makes their photochemistry a difficult subject to study. We have shown that the combination of preparative and time-resolved methods greatly enhances our understanding of multi-photon reaction mechanisms. This chapter combines these two techniques, along with conventional nanosecond laser flash photolysis and low intensity product studies, to investigate the multi-photon chemistry for a number of examples.

In order to successfully implement the laser-drop photolysis technique for the preparation of multi-photon products, the substrates (both the precursor and reactive intermediate) must meet several criteria. It is prudent at this point to list these criteria: i) The precursor molecule must absorb at the wavelength of the photolysis laser; ii) The reactive intermediate must be produced within the duration of the laser pulse in order to absorb a 'second' photon; iii) The reactive intermediate must become the major absorbing species within the laser pulse (again, at the wavelength of the laser used); and iv) If it is necessary to recycle the photolysate, the products must be photostable at the wavelength of the laser, and they should not become the major absorbing species in the photolysate.

5.2 α,α-Disubstituted Benzyloxyl Radicals.

Alkoxyl radicals are important intermediates in biological,[96] atmospheric,[97,98] and organic[99,100] chemistry and have been the subject of numerous studies. The vast majority of studies have centered on the reactions of t-butoxyl radicals, probably due to the fact that several thermal and photochemical sources for this radical are readily available. Cumyloxyl radicals have also received considerable attention because of their involvement in the autoxidation of cumene,[101] a major industrial process used in the synthesis of phenol and acetone.

Alkoxyl radicals usually decay by one of two pathways, either hydrogen atom abstraction from a suitable donor (reaction 5.1) or β-scission to produce a ketone and an alkyl radical (reaction 5.2). Although other reactions have also been studied, such as addition to the carbon-carbon double bond in alkenes,[102] reactions 5.1 and 5.2 usually compete with other processes which limits their synthetic utility.

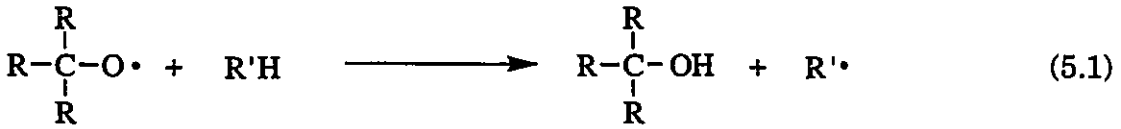

(5.1)

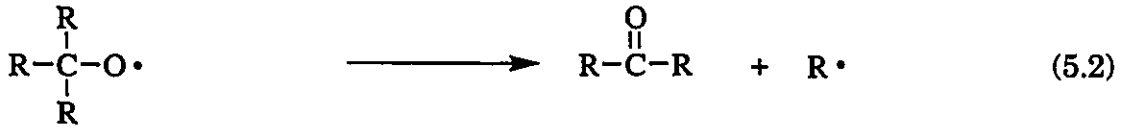

(5.2)

Tertiary alkoxyl radicals have provided much information on the relative stability of several carbon centered organic radicals. One method involves the competitive chlorination of organic substrates by t-butyl

hypochlorite. This is a free-radical chain process usually initiated by the photochemical cleavage of the O-Cl bond in the hypochlorite. The propagation steps in this reaction are the abstraction of hydrogen from the substrate by t-butoxyl radicals (reaction 5.4) and the transfer of chlorine from hypochlorite to alkyl radicals (reaction 5.5). When two different substrates R^1H and R^2H are used, the relative yields of R^1Cl and R^2Cl are a measure of the ratio $k_4{}^1/k_4{}^2$ (providing the concentrations of the two substrates are equal). With the known relative rate constants, application of the reactivity-selectivity principle provides some insight into the relative stabilities of the radicals formed by abstraction of hydrogen. During the 1960's this method was used to measure the relative rate constants for a large number of organic substrates,[103] and it was found that the relative reactivity towards carbon-hydrogen bonds followed the accepted trends of radical stability.

$$\text{t-BuOCl} \xrightarrow{h\nu} \text{t-BuO}\bullet + \text{Cl}\bullet \qquad (5.3)$$

$$\text{RH} + \text{t-BuO}\bullet \longrightarrow \text{R}\bullet + \text{t-BuOH} \qquad (5.4)$$

$$\text{R}\bullet + \text{t-BuOCl} \longrightarrow \text{RCl} + \text{t-BuO}\bullet \qquad (5.5)$$

Intuitively, one might expect that the β-scission reaction of t-alkoxyl radicals would also provide a means to assess the relative stability of alkyl radicals. As one can see, in a highly substituted t-alkoxyl radical of general structure **1** it is theoretically possible for three fragmentation reactions to occur (Scheme 5.1), and it would be expected that fragmentation to produce the most stable radical would predominate. It is also necessary that the

stabilities of the ketone products are similar and do not play a major role in the overall differences in the thermochemistry of the fragmentation reactions. Indeed, this has been found to be true in the case of unsymmetrical radicals with simple alkyl groups.[46]

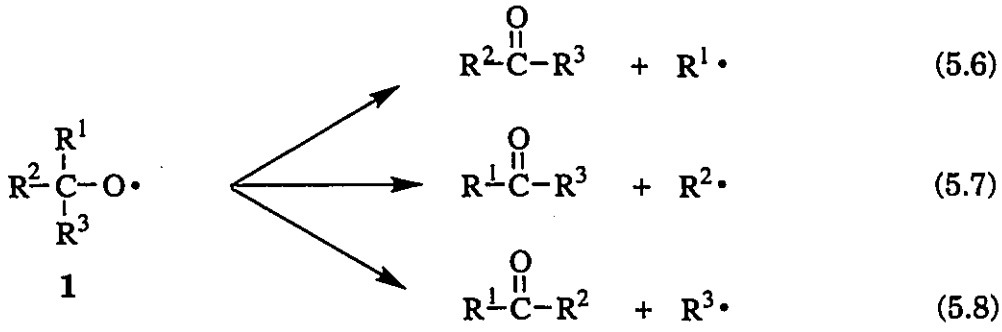

(5.6)

(5.7)

(5.8)

Scheme 5.1

However, Walling et al.[104] found that the relative rates for β-scission followed the order methyl < ethyl < benzyl < i-propyl < t-butyl , this rate order seems to imply that isopropyl and t-butyl radicals are more stable than benzyl, which is not the case according to thermochemical determinations of radical stability. It should be pointed out that Walling's[104] data were determined by comparing the ratio of the rate constant for hydrogen abstraction (k_a) from cyclohexane by α,α-dimethyl-α-alkylmethoxy radicals, (**1a**; $R^1 = R^3$ = methyl, R^2 = alkyl), to the rate constant for β-scission (k_β) of the same radicals. Thus, their data is based on the ratio k_β/k_a for a series of radicals of general structure **1a**. The authors attributed the anomalous placement of the benzyl radical to the relief of steric strain because the difference in activation energy (E_β - $E_{abst.}$) for cleavage to yield the benzyl radical was actually smaller than either i-propyl or t-butyl. Support for this was also found in the ratio of pre-

exponential factors; A_β/A_a was substantially smaller for benzyl (0.006 M^{-1}) than for i-propyl (1.15 M^{-1}). Implicit in this argument is the assumption that the rate constant for hydrogen abstraction remains the same for the entire series of radicals investigated, if this is not the case, comparison of the relative rate constant ratios is invalid for the placement of the β-scission reaction rates.

Further investigations by Walling's group[104,105] found that the ratio of the rate constant for β-scission to the rate constant for hydrogen abstraction from a substrate RH by t-butoxyl radicals, k_β/k_a, changes dramatically with solvent, becoming larger with increasing solvent polarity. In the case of cyclohexane as substrate, this ratio changes by a factor of 8 between $CFCl_2CF_2Cl$ and acetic acid as solvents.[105]

At the time, only the relative rate constants could be obtained experimentally and it could not be determined conclusively whether the increase in this ratio with increasing solvent polarity was due to an increase in the rate of β-scission, a decrease in the rate of hydrogen abstraction, or a combination of the two. They argued however that solvent effects on competitive radical reactions (in this case a competition between a unimolecular fragmentation and a bimolecular hydrogen abstraction) should reflect the degree of solvation of the transition state rather than that of the radicals themselves. Furthermore, these effects must be small for the abstraction of hydrogen by alkoxyl radicals since solvent molecules should be sterically excluded from the alkoxyl radical in the transition state. Thus, they concluded that the effect of solvent polarity on the ratio of the rate constants must reflect a polar contribution to the transition state for the β-scission reaction such as that shown for the transition state for β-scission of cumyloxyl radical, **3**‡.

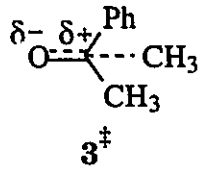

3‡

There has been further support for Walling's proposal; Neta et al.[106] found that the absolute rate constant for the β-scission of cumyloxyl radicals in water was 1 x 10^7 s^{-1} at room temperature. This can be compared to the value measured in CCl_4 at room temperature of 2.3 x 10^5 s^{-1} by Ingold and co-workers.[107] More recently, Ingold, Lustyk and co-workers[108] have published an extensive report which gives absolute rate constants for both hydrogen abstraction from cyclohexane, and β-scission of cumyloxyl radicals in several solvents of varying polarity. In this report the authors showed that the rate constant for abstraction was virtually identical (within experimental error) in the solvents studied, whereas the rate constant for β-scission varied from a value of 3.4 x 10^5 s^{-1} in carbon tetrachloride to a value of 22 x 10^5 s^{-1} in acetic acid. These findings support Walling's hypothesis.[105]

When more than one of the substituent groups in alkoxyl radicals of general structure **1** are aryl, the β-scission reaction no longer occurs. Instead there is migration of an aryl group to produce the corresponding phenoxymethyl radical, presumably according to reactions 5.10 and 5.11 in Scheme 5.2. It is interesting to note that the migration of a phenyl group in triphenylmethoxyl radicals to form phenoxy-diphenylmethyl radicals was the first reported free-radical rearrangement.[109] The 1,2-migration of an aryl group in free radicals, known as the neophyl rearrangement, has been extensively studied.[110-112] Although it is generally accepted to occur via a

bridged-radical intermediate, direct evidence for this type of intermediate is scarce. ESR [110,111] and CIDNP[112] studies for the rearrangement of 2-arylpropyl type radicals failed to detect signals for any bridged-radical intermediates.

The question as to whether the bridged intermediate is a true intermediate or a transition state[110] has been solved in at least one case by the detection of the bridged intermediate radical (spiro[2-2-dimethylcyclopropyl-1,3-cyclohexadienyl], **4**) that mediates the parent reaction.[113] This intermediate, prepared by hydrogen abstraction from the corresponding cyclohexadiene, has a weak absorption maximum at 560 nm. This radical is believed to have the same structure as would be expected for the intermediate of a neophyl rearrangement.

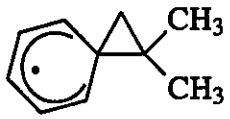

4

Recently, Schuster and co-workers[114] have reported the detection of an intermediate with λ_{max} = 535 nm and a lifetime of ~310 ns in acetonitrile upon 266 nm LFP of 1,1-diphenylethyl-t-butyl peroxide, (**5**), at room temperature. These authors assigned this intermediate to the bridged radical **7**. This assignment was based upon the similarity to the absorption of the spiro[2.5]octadienyl radical mentioned above,[113] and the fact that "no known alkoxyl radicals possess absorptions in the visible region of the spectrum."[114]

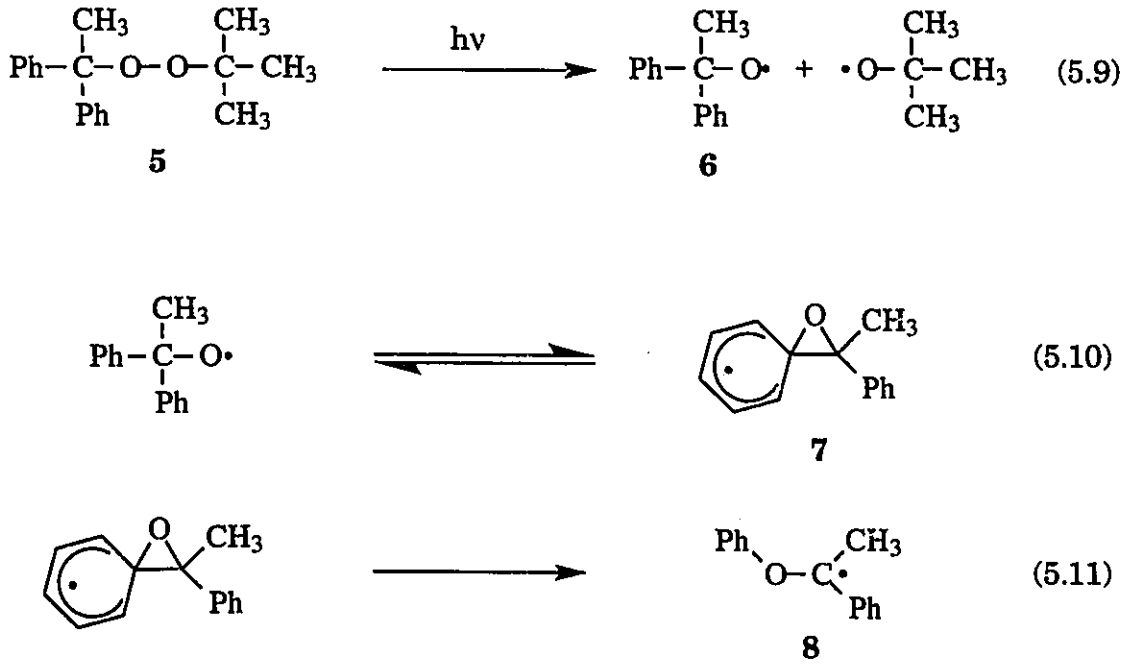

Scheme 5.2

Schuster and coworkers[114] also found that the absorption at 535 nm was quenched by 1,3-dioxolane with a rate constant of 4.4 x 10^6 M^{-1} s^{-1}. Steady-state photolysis of **5** in 1,3-dioxolane or isopropanol gave 1,1-diphenylethanol as the sole product. They proposed that **7** must be in equilibrium with **6** to account for this product. Picosecond absorption spectroscopy showed that the visible absorption was formed in less than 17 ps, the rise time of their system.

A later study by Avila et al.[115] found that benzyloxyl and substituted benzyloxyl radicals do have an absorption band in the visible region of the spectrum. Because this band is red-shifted by electron donating groups at the para position on the ring, the authors suggest there may be some contribution from a charge transfer resonance structure which is responsible for the previously undetected visible absorption band.

Upon consideration of the visible absorption band found for benzyloxyl type radicals,[115] we have reinvestigated the photochemistry of 1,1-diphenylethyl-t-butyl peroxide (**5**) and provide evidence that the intermediate which Schuster[114] attributed to the bridged radical, **7**, is due to the diphenylethoxyl radical, **6**. Also, considering the charge transfer contribution to the transition state for β-scission of t-alkoxyl radicals, *vide supra*,[104,105,108] and the charge transfer absorption band for the cumyloxyl radical,[115] we thought that it may be possible to induce β-scission for α,α-disubstituted benzyloxyl radicals photochemically under conditions where the thermal pathway for this reaction is suppressed. This section also describes the successful implementation of LDP experiments for cumyloxyl (**3**), and diphenylethoxyl (**6**) radicals.

5.2.1 Results.

5.2.1.1 Photochemistry of Dicumyl Peroxide (2).

As mentioned previously, cumyloxyl radicals (**3**) have recently been reported to have absorption bands in the UV and visible (λ_{max} 485 nm) regions.[115] Figure 5.1 shows the spectrum recorded upon 266 nm laser flash photolysis of a 1 mM deaerated solution of **2** in acetonitrile. Typical lifetimes under these conditions were around 1.5 μs for both the visible and UV absorption bands and agree well with recently reported values.[107,108,115] When the solvent is methanol the lifetime of the cumyloxyl radicals (**3**) are reduced to ca. 165 ns as a result hydrogen abstraction from the solvent. Figure 5.2 shows the decay of cumyloxyl radicals in acetonitrile (5.2a) and methanol (5.2b).

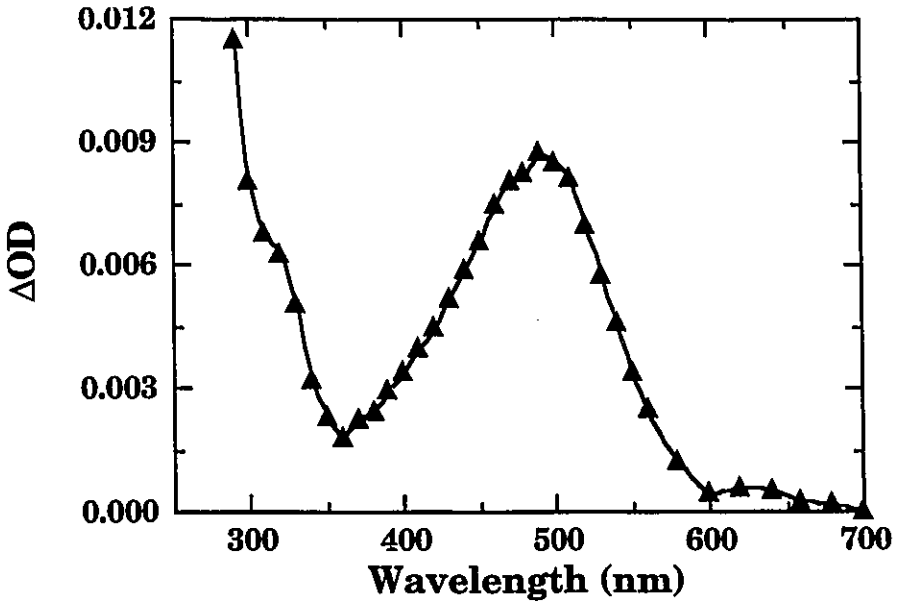

Figure 5.1: Transient spectrum obtained by 266 nm excitation of a 1 mM solution of **2** in acetonitrile.

Addition of methanol in the 0-1 M range to solutions of **2** in acetonitrile leads to a shortening of its lifetime (monitored at 500 nm) and follows clean first order kinetics. The experimental rate constant for radical decay, k_{expl}, is given by equation (5.12), where k_q is the bimolecular rate constant for the reaction of cumyloxyl radicals with methanol, and k_o is the sum of all first and pseudo first order processes. Figure 5.3 shows a

$$k_{expl} = k_o + k_q[MeOH] \qquad (5.12)$$

plot of k_{expl} as a function of methanol concentration, from which we obtain $k_q = (3.0 \pm 0.1) \times 10^5\ M^{-1}\ s^{-1}$. For comparison the reported value for reaction of t-butoxyl with methanol is $2.9 \times 10^5\ M^{-1}\ s^{-1}$.[116]

Lamp irradiation (300 nm) of a 10 mM solution of **2** in acetonitrile gave acetophenone, (**9**), as the only major aromatic product (98%). The

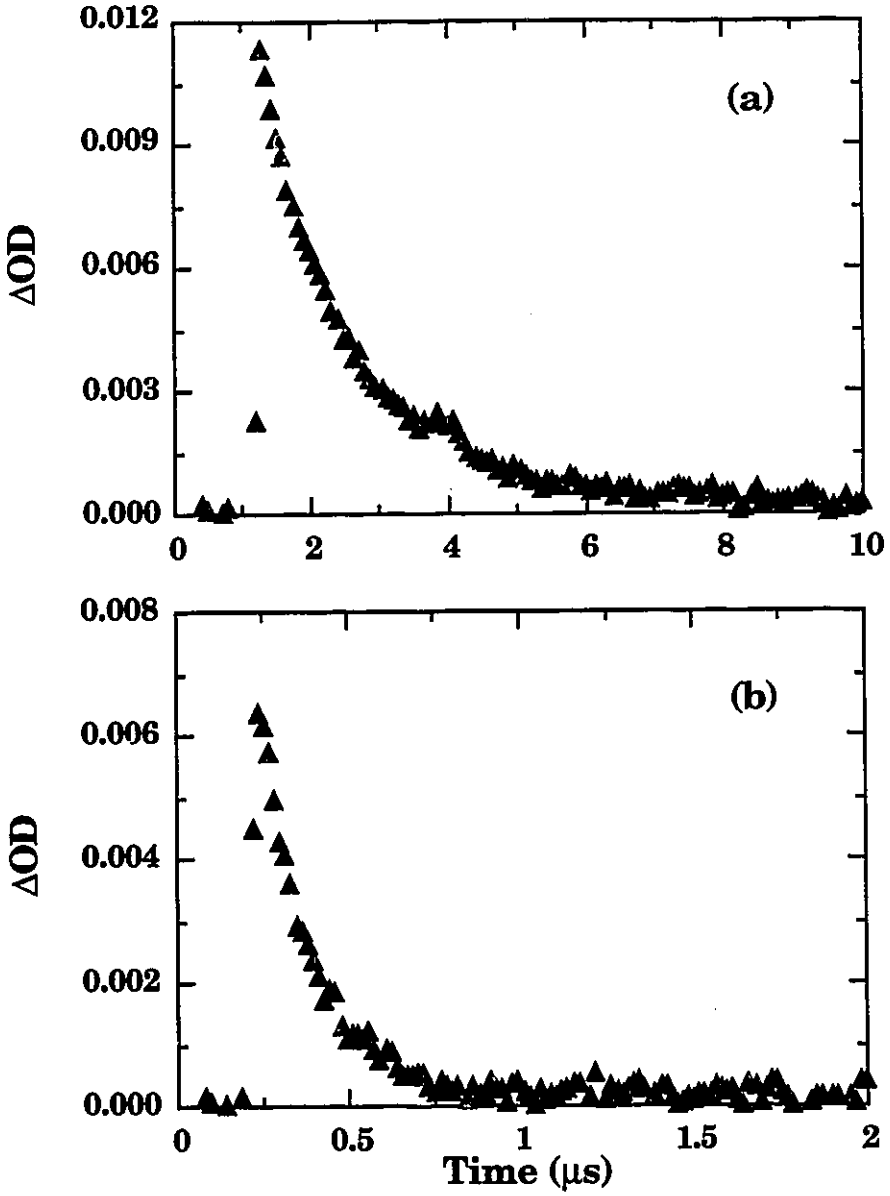

Figure 5.2: (a) Decay trace of cumyloxyl radical **3** in acetonitrile (monitored at 485 nm). (b) Decay trace of cumyloxyl radical **3** in methanol (monitored at 485 nm).

β-scission of cumyloxyl radical in the absence of readily abstractable hydrogens is well documented.[107,117] When the photolysis is carried out in methanol as solvent, cumyl alcohol (**10**) becomes the only major aromatic product (> 98%), with only a small amount of acetophenone (**9** < 2%). We

attribute this behavior to hydrogen abstraction by **3** from the solvent, as expected from the reactivity observed in the laser flash photolysis experiments (*vide supra*).

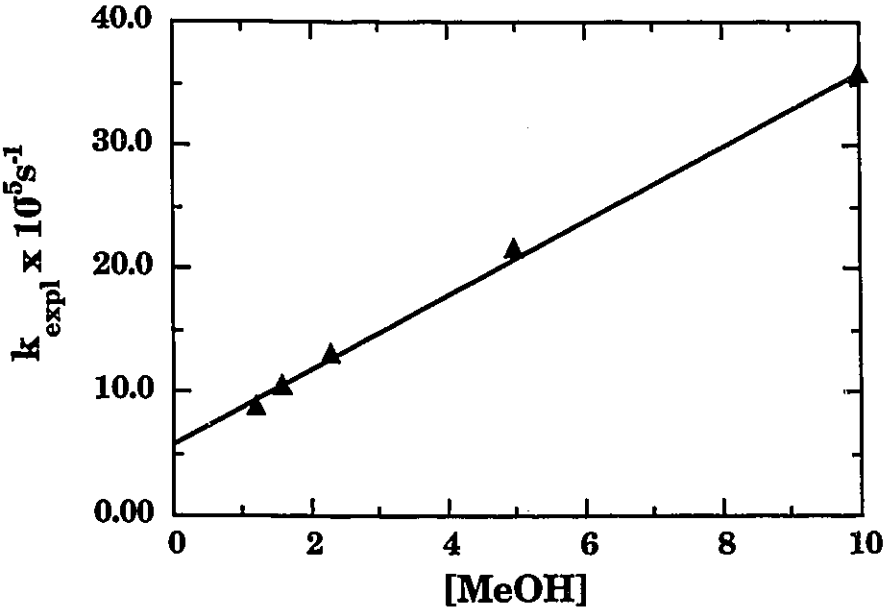

Figure 5.3: Quenching plot of the decay (k_{obs}) of radical **3** as a function of the concentration of methanol in the 0 to 10 M range. Monitored at 485 nm. Solvent: acetonitrile.

Cumyloxyl radicals have significant absorption at 308 nm (see Figure 5.1). In contrast, the precursor peroxide (**2**) absorbs very weakly at this wavelength (ε_{308} ~ 5.7 M^{-1} cm^{-1}, corresponding to A = 0.04 for a 10 mM solution in a cell with 7 mm optical path). It was possible to use the 308 nm excimer laser for the laser-drop photolysis of **2** by recycling the solution several times until a sufficient concentration of products had accumulated. Five cycles of laser-drop irradiation of 10 mM solutions of **2** in methanol lead to an almost equimolar mixture of **9** and **10**. At this point the conversion was ca. 10%. No other products were detected by HPLC Table 5.1 gives the product yields for lamp and laser-drop photolysis of **2**.

Table 5.1. Photolysis of **2** in acetonitrile and in methanol.

Method	Solvent	%Conv.	**9**	**10**
Rayonet [a]	acetonitrile	39	>98	--
Rayonet [a]	methanol	48	<2	>98
Laser-drop [b]	methanol	10	54	46

a: Lamp irradiation at 300 nm. b: 5 cycles.

5.2.1.2 Photochemistry of 1,1-Diphenylethyl-t-butyl Peroxide (5).

Laser excitation of deaerated 1 mM solutions of peroxide **5** in acetonitrile with the 248 nm laser pulses from an excimer laser leads to the transient spectrum of Figure 5.4. The visible band decays with a lifetime of ~400 ns; concurrently with this decay, a band with λ_{max} 320 nm grows in, indicating that the intermediate absorbing at 535 nm is a precursor to that absorbing at 320 nm. We assign the 320 nm transient to the carbon centered radical **8**; benzylic radicals frequently have strong absorptions in this region.[118,119] Consistent with this assignment, the growth of the 320 nm band is absent in oxygen-saturated solutions, indicating that **8** reacts readily with oxygen, as expected.[120] Under these conditions the traces at 320 nm reveal a decay with a similar lifetime of that observed at 535 nm, indicating that **6** also has some absorption in the ultraviolet region. Figure 5.5 shows 320 nm traces under nitrogen and under oxygen . Note that the 320 nm trace includes some "instantaneous" absorption, in agreement with the results under oxygen. The traces at 535 nm, show only moderate sensitivity to oxygen, with a lifetime of ca. 320 ns under 1 atm of oxygen;

this is consistent with the assignment of this intermediate as the alkoxyl radical **6**. In contrast, we would expect the carbon-centered radical **7** to show a much higher reactivity towards oxygen. Thus, we conclude that the signals in the 535 nm region are due to **6** and not **7**. This assignment also avoids the need to invoke an equilibrium between **6** and **7** as suggested by Schuster[114] since hydrogen abstraction by **6** can compete with the migration of the phenyl group.

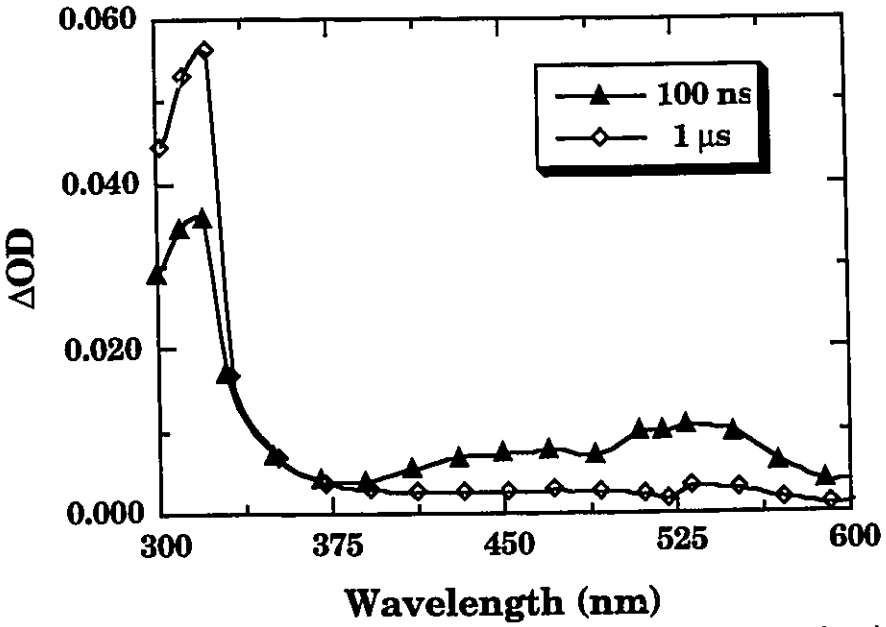

Figure 5.4: Transient spectra obtained after 248 nm excitation of peroxide **5** in acetonitrile at 100 ns and 1 μs time delays. The UV band grows in concurrently with the decay of the visible band.

The temperature dependence for the decay kinetics of **6**, monitored at 535 nm, were also examined. These experiments were carried out in acetonitrile in the –38 to +22 °C range. The data yield an excellent Arrhenius dependence (see Figure 5.6), corresponding to an activation energy of 5.9 kcal/mol and a pre-exponential factor of 5.7×10^{10} s^{-1}. These values can be compared with the known values for the migration of phenyl

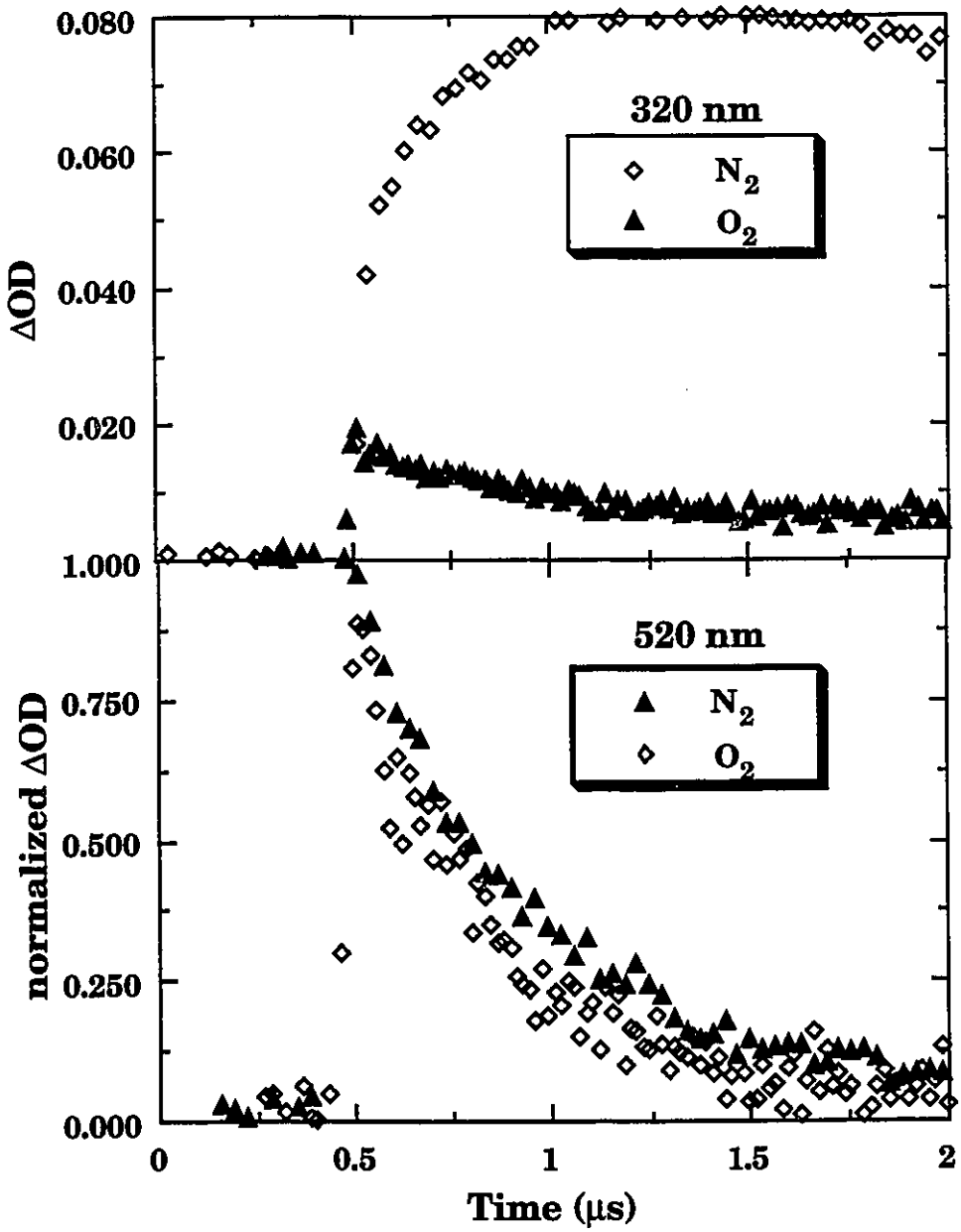

Figure 5.5: Effect of oxygen on the decay of the signals. (Top) Monitored at 320 nm. Note the initial jump in the signal under nitrogen due to a UV absorption of the alkoxyl radical **6**. (Bottom) Monitored at 520 nm.

from the 2-phenyl-2-methylpropyl radical.[110] The reported activation energy is 10.8 kcal/mol for this rearrangement with a preexponential factor of 1.0 x 10^{11} s^{-1}. It is expected that the activation energy for the rearrangement for

6 would be less due to resonance stabilization of the benzylic radical product and the greater reactivity of an oxygen centered radical. This pre-exponential factor is also indicative of an entropy loss; note that given the reported errors, the two values are not significantly different.

The fact that the decay kinetics for **6** (at 535 nm) are consistent with the formation kinetics for **8** (at 320 nm) suggests that the lifetime of **7** must be short in the time scale of these experiments. A reasonable estimate based on our results indicates that **7** must live less than 100 ns. Molecular calculations suggest that this is a conservative limit in view of the low activation energy estimated for reaction 5.11, *vide infra* .

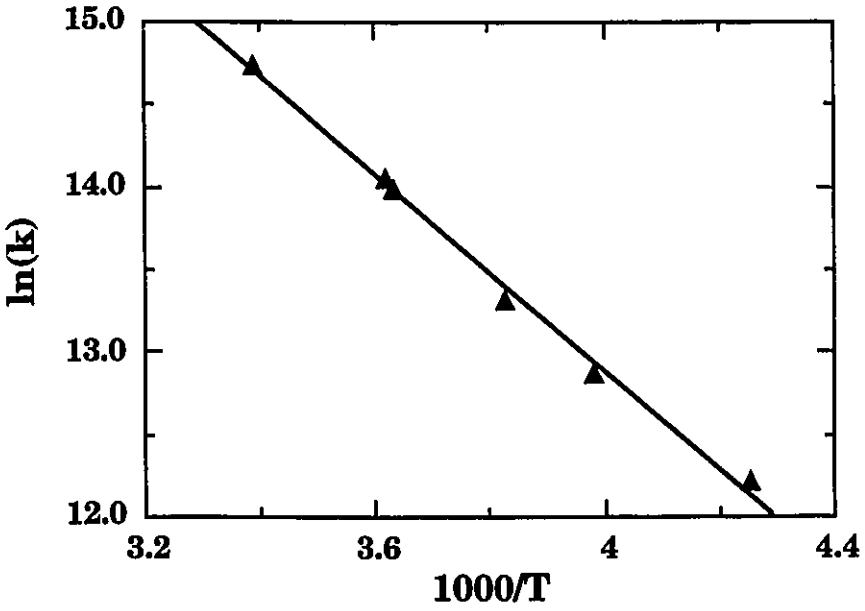

Figure 5.6: Arrhenius plot for the decay of the visible signal produced upon 248 nm excitation of **5**.

Lamp photolysis (300 nm, <20 min.) of deaerated 10 mM solutions of **5** in acetonitrile leads to the dimer **12** (formed by the recombination of radicals **8**) as the major product. As long as the conversion was kept below about 10%, no acetophenone or benzophenone (products from β-scission)

could be detected. Under prolonged irradiation (12 hrs., complete consumption of starting material) the reaction mixture becomes quite complex and a significant amount of acetophenone is formed. This is probably due to oxygen contamination since Ingold[121] has shown that acetophenone, phenol and p-benzoquinone are formed in a complex mechanism when oxygen is present. Benzophenone is not formed at all under lamp irradiation. Further, acetophenone or benzophenone were not produced when peroxide **5** was decomposed thermally at 169 °C.

Like the cumyloxyl radical, 1,1-diphenylethoxyl radicals also have significant absorption at 308 nm, while the precursor peroxide **5** absorbs only weakly, although it does absorb significantly more than dicumyl peroxide **2** (ε_{308} ~ 20 M^{-1} cm^{-1}, corresponding to A = 0.14 for a 10 mM solution in a cell with 7 mm optical path), thus it was not necessary to recycle the photolysate from laser-drop photolysis in order to obtain ~7% conversion. Laser-drop photolysis of deaerated 10 mM solutions of **5** in acetonitrile (under nitrogen atmosphere) leads to the formation of acetophenone (**9**) and benzophenone (**11**) in a 1-to-0.8 ratio. No other products were detected by HPLC. Table 5.2 gives the product yields for lamp and laser-drop photolysis of **5**.

Table 5.2. Photolysis of **5** in acetonitrile.

Method	% Conv.	**9**	**11**	**12**
Rayonet [a]	10	-	-	~100
Laser-drop [b]	7	56	44	-

[a]Lamp irradiation at 300 nm [b]One cycle.

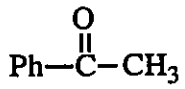

9

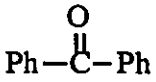

11

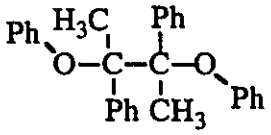

12

5.2.2 Discussion.

From the LFP studies of **2** and **5**, it can be seen that these peroxides are suitable to study the photochemistry of the alkoxyl radicals, **3** and **6**, using the laser-drop technique. The peroxides have small but adequate absorption coefficients at 308 nm, the wavelength of the laser. The quantum yield for the production of alkoxyl radicals from peroxides has been reported to be 0.85.[122,123] And, the alkoxyl radicals have absorption coefficients large enough so that the radicals can compete with the precursors in the latter part of the laser pulse. For the cumyloxyl radical, ε_{485} has been estimated to be ~1300 M^{-1} cm^{-1}.[115] From the spectrum in Figure 5.1 we estimate the extinction coefficient to be ~1000 M^{-1} cm^{-1} at 308 nm. Furthermore, peroxides are thought to cleave from a dissociative state, implying that cleavage of the O-O bond is, for all practical purposes, instantaneous,[124] thus satisfying the condition that they are produced during the early part of the laser pulse.

5.2.2.1 The Cumyloxyl Radical System.

Photolysis of dicumyl peroxide **2** yields two cumyloxyl radicals (**3**), which in the absence of a suitable hydrogen donating species, undergo β-scission to give acetophenone, **9**, and methyl radicals. In order to insure that **9** was a photoproduct of the cumyloxyl radicals, it was necessary to suppress the thermal β-scission reaction. This was easily done by using a

good hydrogen donating solvent such as methanol. Thus, low-intensity irradiation of **2** in methanol yields cumyl alcohol, **10**, as the major product with only small amounts of **9** (< 2%). In contrast, laser-drop irradiation produces almost equimolar amounts of **9** and **10**. This represents a greater than 23 fold increase in the relative yield of acetophenone under laser-drop conditions, indicating that **3** undergoes a photoinduced β-scission reaction. Scheme 5.3 shows the main reaction paths taking place in the laser-drop photolysis of dicumyl peroxide in methanol.

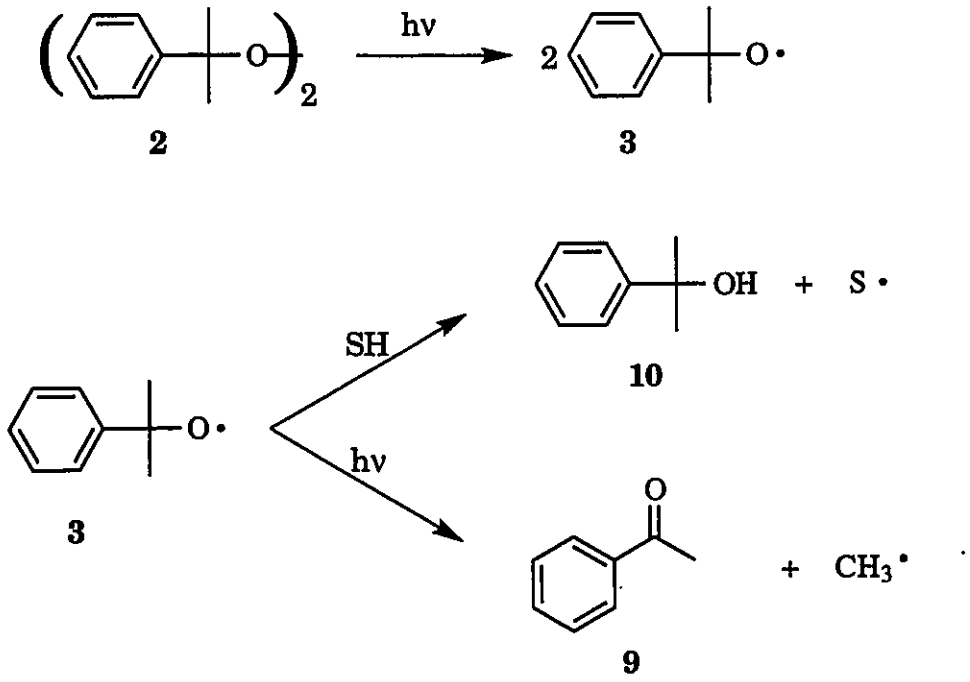

Scheme 5.3

Two-laser two-colour laser flash photolysis experiments were also attempted to see if bleaching of **3** could be detected spectroscopically. The radical was produced with a pulse from the 266 nm laser and irradiated 250 ns later with either a 308 nm pulse from the excimer laser or a 480 nm pulse from the dye laser, no bleaching could be found in either experiment.

Lusztyk and co-workers also attempted to bleach this radical with similar results.[125] Failure to detect bleaching of the signal from a second laser does not necessarily imply that a photocleavage cannot occur. Under laser-flash conditions the ΔOD due to the radicals at the wavelengths of the second lasers is small, 0.008 or less, which corresponds to a concentration on the order of about 10 μM, under laser-drop conditions the concentration of radicals may be in the mM range. Also, if the excited state of the radicals are very short-lived it is possible that, under laser-drop conditions, the radicals are re-excited several times during the laser pulse.

5.2.2.2 The 1,1-Diphenylethoxyl Radical System.

One of the major reasons Schuster and coworkers[114] assigned the transient formed upon LFP of 1,1-diphenylethyl-t-butyl peroxide (**5**) to the bridged radical **7** was the visible absorption band centered at 515 nm. At the time, alkoxy radicals were neither known nor expected to absorb in the visible region of the spectrum. The later discovery that aryl-substituted alkoxyl radicals have an absorption band in the visible region of the spectrum[115] provided some indication that this transient could be due to the 1,1-diphenylethoxyl radical (**6**). We have shown, upon further examination of the photochemistry of **2**, that this is indeed the case. The growth in the UV portion of the spectrum, which is concurrent with the decay of the visible transient, is consistent with this assignment. The fact that this growth is suppressed by oxygen while the visible transient is only slightly affected allows us to confidently assign the UV band to the 1-phenoxy-1-phenylethyl radical (**8**).

There are only two minor discrepancies between our investigation and Schuster's, these authors report a long-lived residual absorption in the

410 nm region of the spectrum which they attributed to the radical **8**. We could find no residual absorptions in this region. There is also a minor difference between the lifetime of **6**, 310 ns in their report and 400 ns by ours. The synthesis of the peroxide was carried out exactly as described by Schuster[114] and the peroxide appeared pure by ^{1}H NMR analysis. However, HPLC analysis of the peroxide revealed an impurity which absorbed out to about 290 nm. Although this impurity was most likely small in molar terms, spectrally it accounted for about 10% of the absorption at 266 nm, the wavelength used for LFP by Schuster.[114] Passing the peroxide through a column of silica and recrystalyzation from methanol was adequate to eliminate this impurity. We tentatively suggest that this impurity was responsible for the residual absorption and the reduced lifetime reported by Schuster.

The temperature dependence for the decay of the visible band gives further evidence for the assignment of the radical **6** to this transient. The pre-exponential factor shows a significant loss of entropy in the transition state, consistent with reaction 5.10. If reaction 5.11 were the rate limiting step it would be expected that there would be an entropy gain reaching the transition state. The activation energy for this reaction (5.9 kcal/mol) is also in agreement with that reported[110] for the migration of phenyl in the parent neophyl rearrangement.

A series of AM1-UHF calculations[126] were also carried out on the intermediates and transition states involved in reactions 5.10 and 5.11. The geometries were obtained using the eigenvector-following search algorithm as described by Baker.[127] Note here that the transition state for the reaction **6**→**7** could not be fully optimized, however, no structure along the reaction surface could be found which corresponds to the 'true' transition state. The

transition state for **7**→**8** was fully optimized and only one imaginary vibrational mode found when a force calculation was done. The reaction coordinate as described by the AM1 calculations is shown in Figure 5.7. From the reaction coordinate it can be seen that **7** is expected to be a true intermediate, but reaction 5.11 would be too fast for the experimental technique employed.

The laser-drop experiments show a remarkable change in the chemistry of **6**. Low intensity photolysis of **5** give only the dimers **12** (meso and *d,l*) from the recombination of the rearranged radicals **8**. When the

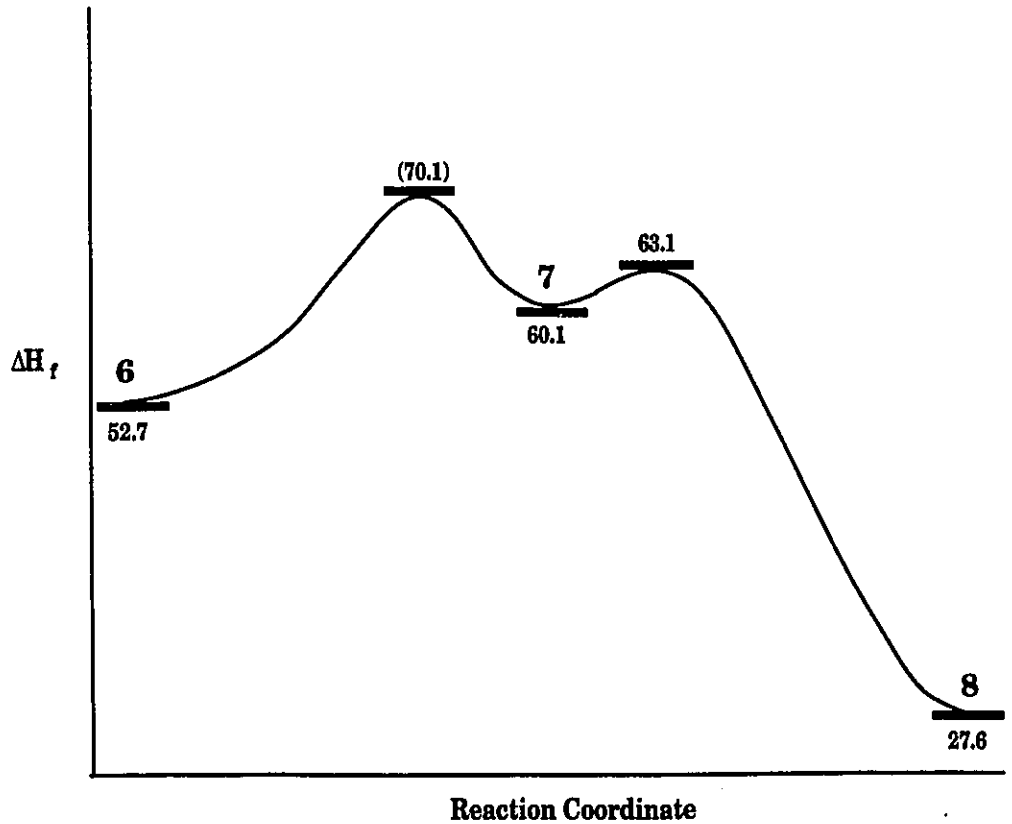

Figure 5.7: AM1-UHF calculated reaction coordinate for reactions 5.9 to 5.11. All values in kcal/mol.

photolysis is carried out under laser-drop conditions these dimers are no longer formed, instead acetophenone (**9**) and benzophenone (**11**) are formed

in a 1.25 ratio. These results suggest that the β-scission reactions (reactions 5.13 and 5.14) take place under laser-drop conditions.

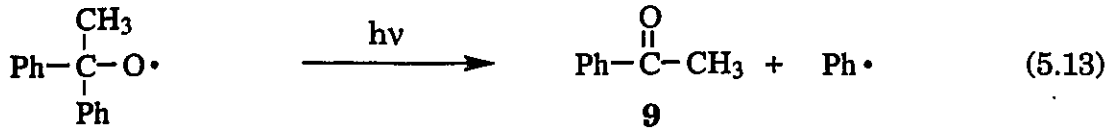

9 (5.13)

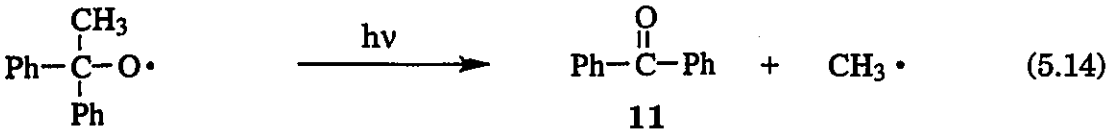

11 (5.14)

It is interesting that the phenyl migration is completely suppressed during laser-drop photolysis of **5**. This suggests that the geometry for the excited radical (either **6*** or **7***) is such that it is allowed to crossover to the reaction surface for β-scission, but cannot crossover to the reaction surface which leads to phenyl migration. Of course there is also the possibility that the reaction proceeds entirely on the excited state surface. While we cannot rule this out, it would still require that the geometry for the excited radical is such that it is committed to proceed to β-scission rather than phenyl migration. Since the geometry of the excited species responsible for the ketone products must be very similar to the transition state geometry for β-scission of radical **6**, it is likely that this is the radical photolyzed during laser-drop photolysis.

Schuster and coworkers[114] have suggested that the alkoxyl radical **6** is in equilibrium with the cyclohexadienyl radical **7**, and that the cyclohexadienyl radical is responsible for the visible absorption band from LFP of **5**. This is still possible even if it is the alkoxyl radical which is excited by a second 308 nm photon during LDP. If there is an equilibrium

between **6** and **7**, then it would be reasonable to assume that the visible absorption band produced upon LFP of dicumyl peroxide is due to a similar cyclohexadienyl radical in equilibrium with the cumyloxyl radical. Avila[128] has shown that ΔOD(485 nm)/ΔOD(320 nm) remains constant (0.71) for the LFP of **2** at temperatures from 248 to 346 K, this is definitive proof that the same species is responsible for both the visible and UV absorptions since an increase in temperature would shift the equilibrium to the less thermodynamically favoured species (LeChatelier's Principle). In light of the fact that the both peroxides (**2** and **5**) give alkoxyl radical β-scission products upon LDP, we assign the visible absorption bands to the corresponding alkoxyl radicals.

The cleavage of α,α-dialkoxybenzyl radicals discussed in Chapter 3 showed that electronic excitation of the radicals resulted in a complete lack of selectivity in the fragmentation reaction as compared to the ground state radicals. If the excited radical **6*** showed no selectivity between reactions 5.13 and 5.14, the ratio of the ketones would be expected to be 2 in favour of acetophenone (because one of two phenyl radicals can be formed), this is very close to the experimental value of 1.25. Although these reactions do not occur thermally, and it is impossible to compare the effect of electronic excitation on the selectivity of the radical fragmentation to that of the thermal β-scission reactions (5.13 and 5.14), the ground state β-scission reaction of cumyloxyl radicals forms only acetophenone. This implies that thermal fragmentation to produce phenyl radicals from **6** would also be unfavourable. The lack of selectivity for the β-scission reaction of **6*** suggests that the photoinduced β-scission of the cumyloxyl radical should also show little selectivity, and that acetone and phenyl radicals should be produced as well as acetophenone and methyl radicals. However, HPLC

showed only acetophenone and cumyl alcohol as LDP products of **2** in methanol. Both acetone and benzene (the expected product from the phenyl radical) would be detectable by HPLC, in fact, benzene was used as an internal standard in some cases to quantify the conversion of starting materials but could not be found in the product mixtures during qualitative runs (no internal standard).

5.2.3 Conclusion.

The photochemistry for 1,1-diphenylethoxyl-t-butyl peroxide (**5**) has been re-examined and the visible absorption band, produced upon LFP, previously attributed to the spiro-cyclohexadienyl radical (**7**) has been assigned to the 1,1-diphenylethoxyl radical (**6**). This assignment is based on several factors; 1) The similarity between the visible absorption band produced upon LFP of dicumyl peroxide (**2**) and **5**.[115] 2) Concurrent with the decay of the visible band is a growth in the UV region of the spectrum, this is assigned to the 1-phenoxy-1-phenylethyl radical **8**. 3) The Arrhenius parameters for the decay of the visible band indicate a loss of entropy during the transition state; this is more consistent for reaction 5.10 than 5.11, where a gain in entropy would be expected. 4) The UV and visible bands belong to the same intermediate. 5) LDP produces the alkoxyl radical β-scission products, and, 6) AM1 calculations indicate that **6** is 7.6 kcal/mol lower in energy than **7**.

Laser-drop photolysis of the two peroxides (**2** and **5**) show surprising selectivities for the fragmentation reactions of the excited radicals. In the case of dicumyloxyl radical the fragmentation gives only the methyl radical from both the excited and ground states. For 1,1-diphenylethoxyl radical there is little selectivity between the two β-scission reactions from the

excited radical, however, the phenyl migration, which is the sole reaction pathway for the ground state radical, is not a competitive process from the excited radical. Reactions 5.13 and 5.14 provide a good example where high-intensity laser photochemistry leads to new products, distinct from those obtained under conditions of lamp irradiation.

5.3 Photochemistry of 1,5-Diiodoalkanes: Evidence for the Formation of a Bridged Iodine Radical.

The photochemistry of alkyl iodides has been well studied for many decades,[129,130] this is mainly due to the long wavelength of the $n \rightarrow \sigma^*$ transition of the carbon-iodine bond (relative to other alkyl halides).[131] The primary step upon photolysis is the homolytic cleavage of the C-I bond to produce an alkyl radical and an iodine atom. In polar solvents, electron transfer competes efficiently with escape from the solvent cage to produce an ion pair.[132,133] For bicyclic iodides it has been proposed that the ion pair forms a polar bond association which leads to solvolysis at the bridgehead carbon when methanol is used as solvent.[30,133-135] However, in non-polar solvents electron transfer becomes unfavourable and escape from the solvent cage leads to radical products.[136,137]

An interesting feature of the halogen atoms is their ability to form halonium ions. These are divalent compounds of electron deficient halogens. Diaryliodonium ions are probably the most investigated of the halonium ions because of their synthetic utility in the arylation of nucleophiles under mild conditions.[138] and their industrial importance as photoinitiators for free radical and cationic polymerizations.[139-141]

The mechanism for the arylation of nucleophiles is not clear, but it has generally been accepted to occur by one of two possible mechanisms;

i) trapping of the diaryliodonium ion by the nucleophile to form a trivalent iodine intermediate followed by reductive elimination to form the arylated nucleophile and aryl iodide (Scheme 5.4)[138] or ii) one electron reduction of the diaryliodonium ion to form a divalent iodine radical intermediate which subsequently cleaves to produce an aryl radical and aryl halide, the aryl radical then combines with the oxidized nucleophile to form products (Scheme 5.5).[142-144]

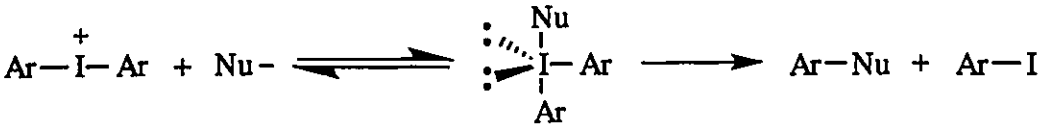

Scheme 5.4

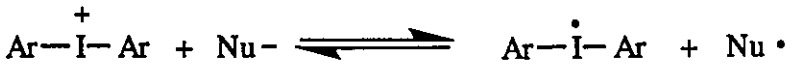

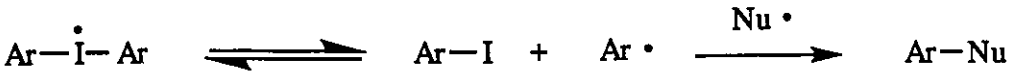

Scheme 5.5

Support for a divalent iodine radical intermediate was provided in an elegant paper by Tanner et al.[145] in which they showed that the kinetics for the transfer of iodine from an aryl iodide to an aryl radical did not fit a simple atom abstraction model. They proposed that a symmetrical transition state with partial bonding between the aryl groups and the iodine atom was not a part of the mechanism, but rather that the divalent iodine radical was an intermediate. Further evidence found in their study was the

production of benzenes during the arylation of phenoxide with mono substituted diphenyl iodonium ion. A photo-CIDNP study by DeVoe and co-workers[146] gave direct evidence for the existence of phenyl radicals during the anthracene sensitized photolysis of diphenyliodonium hexafluorophosphate in acetonitrile-d_3. They concluded that the divalent iodine radical intermediate was formed by electron transfer from the anthracene triplet, this leads ultimately to phenylated anthracenes and phenyl iodide as products.

A recent communication by Farnham and Calabrese[147] reported the isolation and x-ray structure for the iodinanide anion **13** (isolated as the lithium salt complexed with two equivalents of tetramethylethylenediamine). These compounds had been postulated previously by Wittig and Schöllkopf[148] and given some kinetic evidence by Reich and co-workers.[149] Although iodinanide species are rare, their existence, along with iodonium cations, demonstrates the ability of divalent iodine to exist in two extreme oxidation states. Thus, it may be expected that an intermediate oxidation state of divalent iodine could be observable.

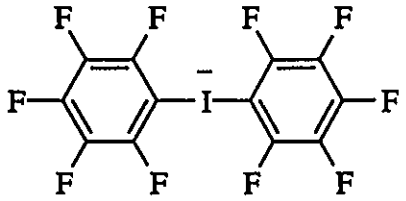

13

Hypervalent sulfur radicals are well known in the literature.[150,151] In fact, Martin and Perkins[152] have shown that sulfuranyl radicals **15** are

in equilibrium with their dimers with $K_{eq} = 5.55 \times 10^{-2}\ M^{-1}$ at 20 °C (Scheme 5.5).

To date, there has been no conclusive evidence for the existence of divalent halogen radicals, although there have been many instances where such a complex has been invoked to explain anomalous results for the

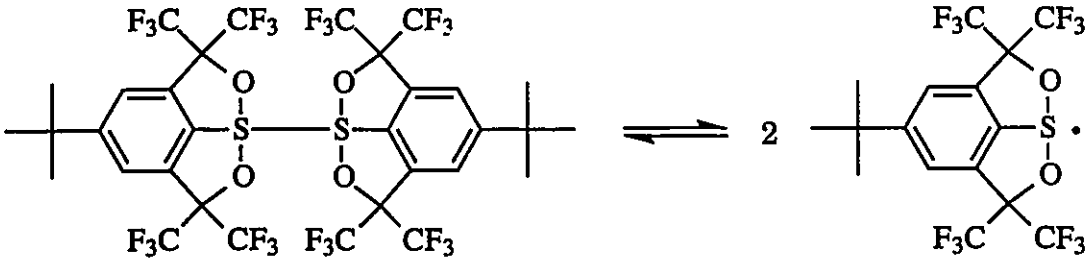

14 **15**

Scheme 5.5

reactions of haloalkyl radicals. Thaler[153] reported that bromination of bromoalkanes leads to a much higher yield of 1,2-dibromoalkanes than would be expected from thermodynamic considerations. Skell and Shea[154] were able to show that, during the course of bromination of (+)-1-bromo-2-methylbutane with DBr, a significant amount of starting material undergoes hydrogen-deuterium exchange with retention of configuration at the asymmetric carbon. They postulated that a bridged radical intermediate was responsible for this result.

Although dialkyl iodonium ions are known,[155] and one can envisage a divalent iodine radical as the one electron reduction product of such ions, there has been only one report for the detection of such a radical in the literature.[156] We report here evidence for such radicals resulting from the

photolysis of 1,5-diiodopentanes using steady-state photolysis, laser flash photolysis (LFP) and laser-drop photolysis (LDP).[21]

5.3.1 Results

Low intensity photolysis. Lamp irradiation (300 nm Rayonet, Pyrex filter, 1 hr) of a 0.50 mM deaerated solution of 1,5-diiodo-1,5-diphenylpentane (**16**) led to complete consumption of starting material, and the formation of a mixture of 1,5-diphenyl-1-iodopentane (**17**), 1,5-diphenylpentane (**18**), 1,5-diphenyl-1-pentene (**19**, E and Z), and 1,5-diphenyl-5-iodo-1-pentene (**20**, E and Z) (Scheme 5.6). Under similar conditions, 1,5-diphenyl-1-iodopentane (**17**) was partially converted into 1,5-diphenylpentane (**18**) and 1,5-diphenyl-1-pentene (**19**). By contrast, the photolysis of 1,5-dichloro-1,5-diphenylpentane (**21**) led to a complex mixture containing more than 11 products, which can be explained by the expected homolytic cleavage of a carbon-chlorine bond followed by hydrogen abstraction from solvent by chlorine atoms, radical-radical recombination and some secondary photolysis of monochlorinated products.[85]

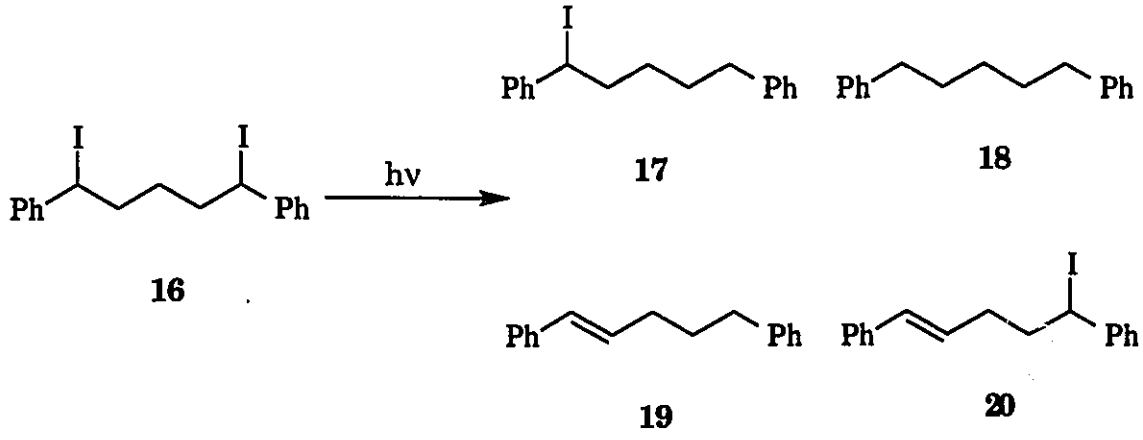

Scheme 5.6

Laser flash photolysis. LFP (266 nm) of a deaerated solutions of **21**, the dichloro analog of **16**, yields a very narrow spectrum centered at 320 nm (Figure 5.8) which decays by complex kinetics (Figure 5.9). This absorption is readily quenched by oxygen. In contrast to the spectrum obtained by photolysis of **21**, 248 nm LFP of a deaerated, ~50 μM solution of **16** in cyclohexane leads to an instantaneous (on our time scale), broad absorption in the UV, from 260 nm out to about 450 nm, with local maxima at 290, 320, 350 and 370 nm and a strong band continuing into the deep UV (Figure 5.10; compare with Figure 5.8). This absorption decays with the same kinetics over the entire spectrum, and follows first order (or pseudo-first order) kinetics with a lifetime of 4.4 ± 0.3 μs under these conditions. A similar spectrum is obtained upon 308 nm LFP of a 0.39 mM solution of **16** in cyclohexane. Oxygen saturated solutions of **16** in cyclohexane have a lifetime only slightly shorter than the same solutions deaerated by nitrogen (2.4 and 2.9 μs respectively for 308 nm LFP, Figure 5.11).

An investigation of the effects of light intensity on the lifetime of the transient and the size of the signal was done by attenuating the laser beam with precalibrated neutral density filters. The lifetime increases as the laser power is decreased, indicating that the transient does not decay by true first-order kinetics. As can be seen in Figure 5.12, there is distinct downward curvature in a plot of ΔOD vs. % laser power. This type of curvature is often found when the initial transient formed undergoes further photolysis during the laser pulse[85] (see also Figure 3.4) Two-laser two-colour LFP was done using one excimer with 248 nm pulses to form the transient and a second laser with 308 nm pulses to photolyse the transient.[24] Photolysis of the transient at 308 nm leads to permanent and irreversible bleaching as monitored at 320 nm(Figure 5.13).

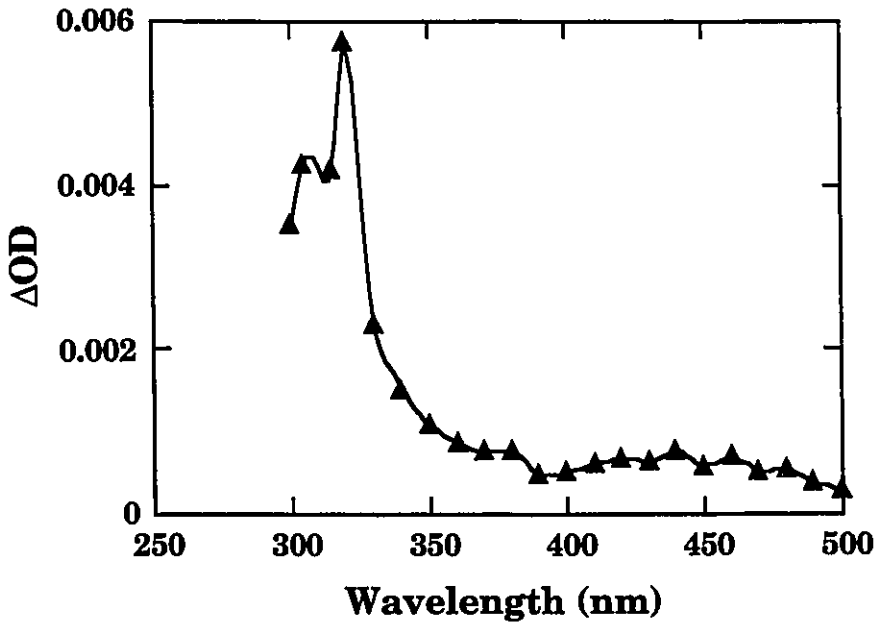

Figure 5.8: Transient spectrum recorded upon 266 nm excitation of a 2 mM solution of **21** in cyclohexane.

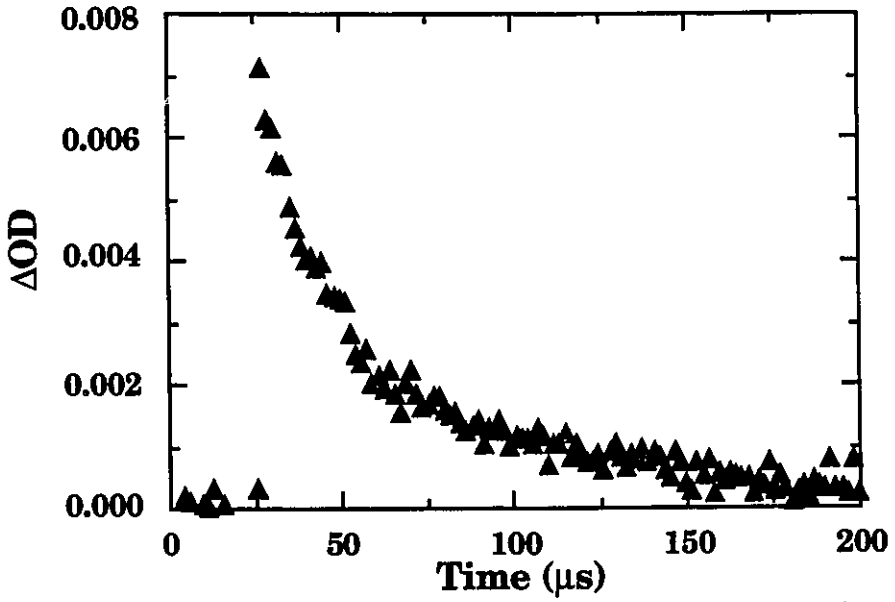

Figure 5.9: Decay of signal produced upon 266 nm excitation of **21** in cyclohexane. Monitored at 320 nm.

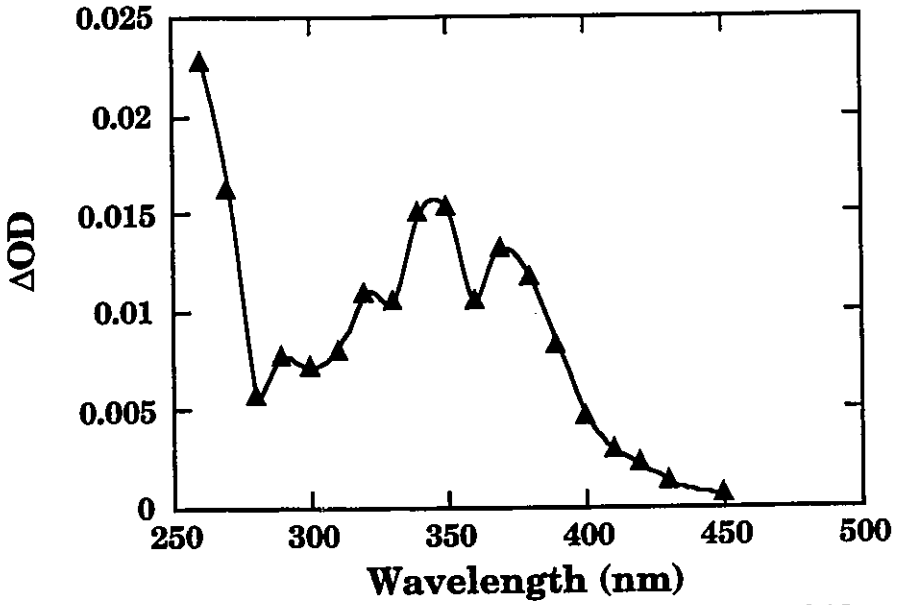

Figure 5.10: Transient spectrum obtained upon 248 nm excitation of 50 μM solution of **16** in cyclohexane.

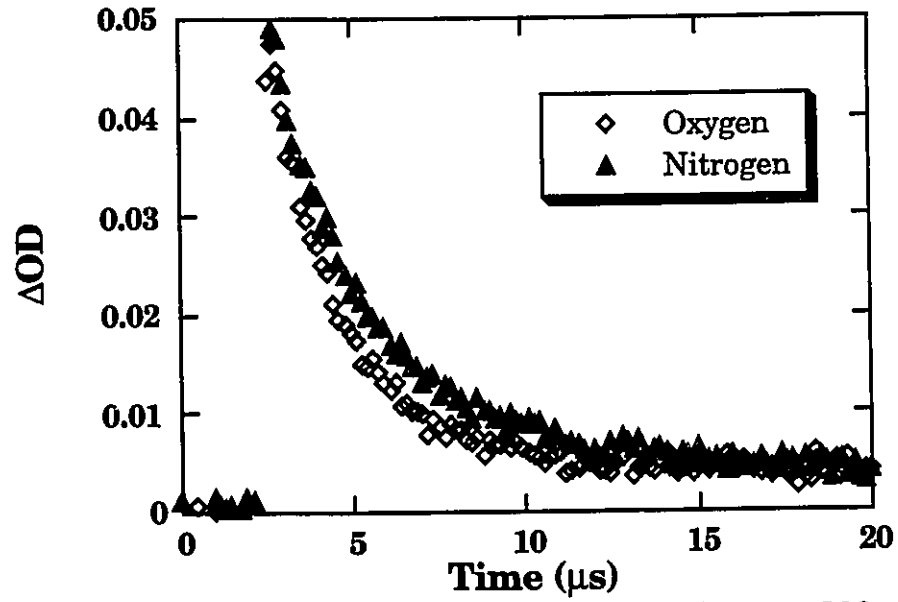

Figure 5.11: Decay of the signals produced upon 308 nm excitation of 0.39 mM solutions of **16** in cyclohexane when bubbled with nitrogen or oxygen. Monitored at 350 nm.

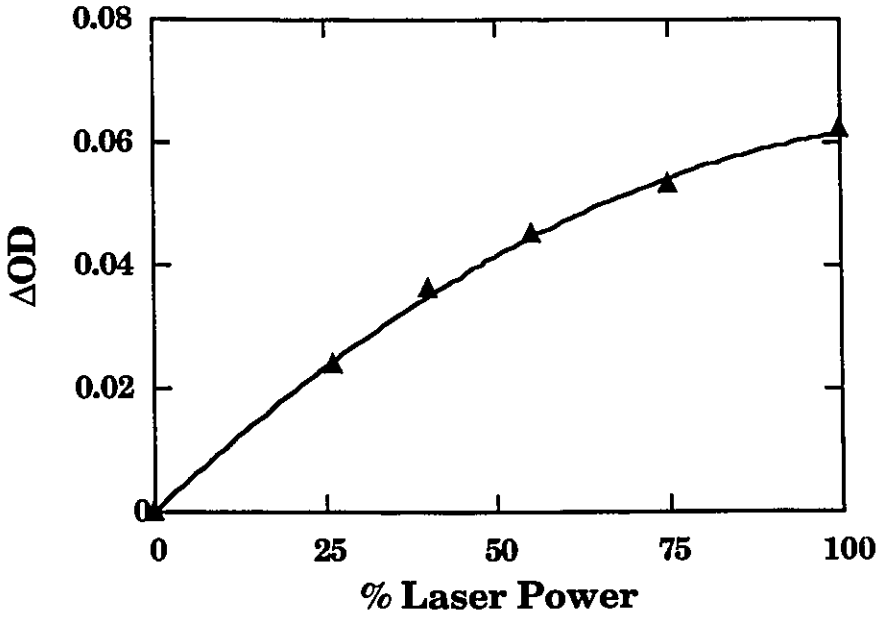

Figure 5.12: Absorption signal (ΔOD) as a function of laser intensity for 308 nm LFP of 0.39 mM **16** in cyclohexane as monitored at 350 nm. %100 laser power corresponds to ~60 mJ.

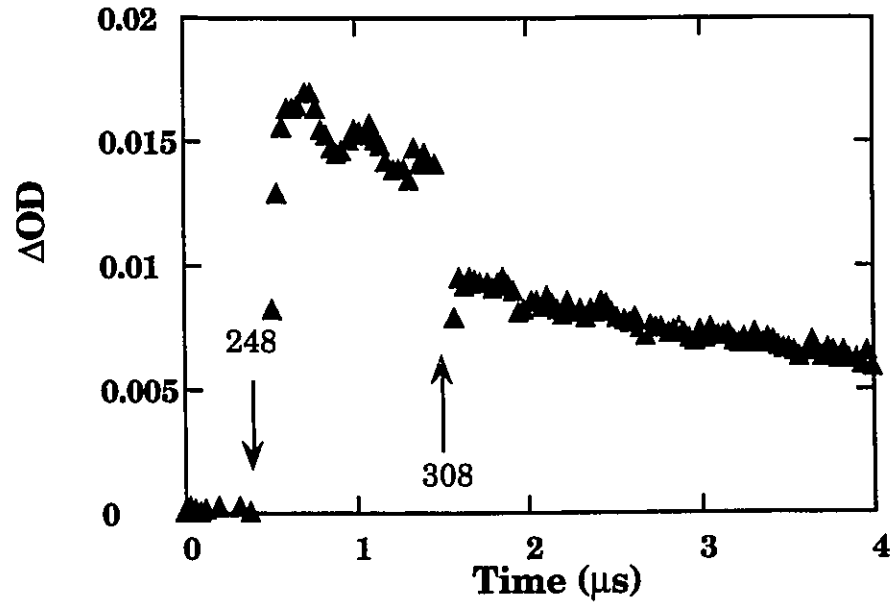

Figure 5.13: Bleaching of the signal from 248 nm LFP of 50 μM **16** in cyclohexane upon excitation with an excimer laser (308 nm). The excimer laser was fired 1 μs after the synthesis laser (248 nm).

LFP (248 nm) of a 2.0 mM solution of 1,5-diiodopentane (**22**) in cyclohexane leads to an instantaneous absorption band centered at 300 nm with a shoulder at 360 nm and a much weaker absorption which grows in at 570 nm. After irradiation the solutions remain a pale violet colour, this suggests that the growth at 570 nm is due to the formation of molecular iodine. The spectrum for the LFP of **22** at 0.6 and 29 μs is shown in Figure 5.14. The signal at 300 nm decays with complex kinetics and does not decay back to the baseline in the time frame of the experiment (100 μs). The shoulder at 360 nm returns to the baseline with the same kinetics. Oxygen saturated solutions of **22** in cyclohexane decay slightly faster than the same solutions deaerated with nitrogen, with lifetimes of 3.1 and 4.1 μs respectively, when fitted to first order kinetics (Figure 5.15).

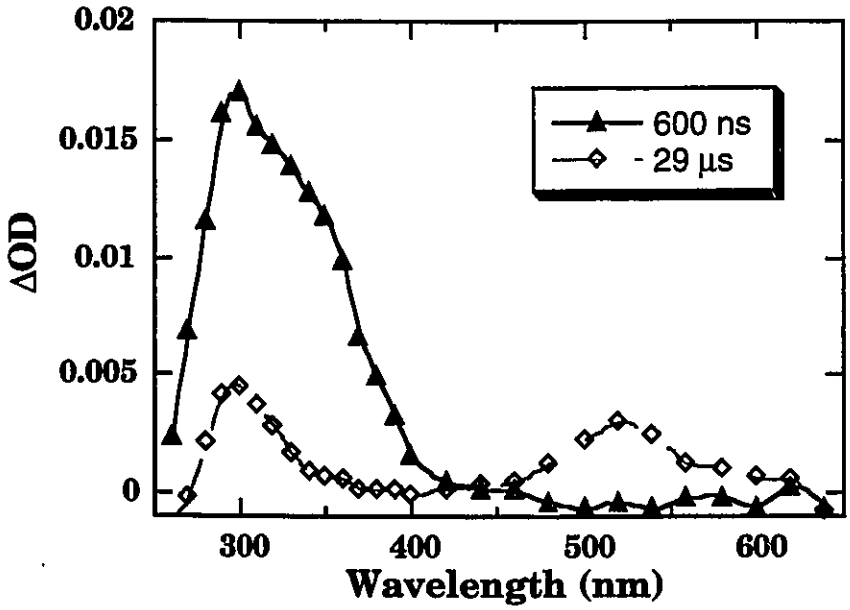

Figure 5.14: Transient spectrum obtained upon 248 nm excitation of 10 mM solution of **22** in cyclohexane.

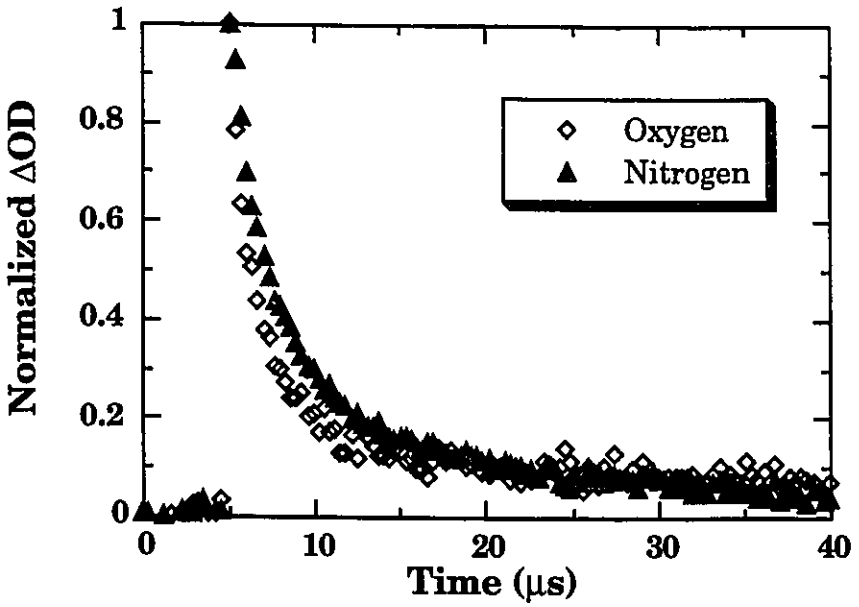

Figure 5.15: Decay of the signals produced upon 248 nm excitation of 10 mM solutions of **22** in cyclohexane when bubbled with nitrogen or oxygen. Monitored at 350 nm.

Laser-drop photolysis. When drops of deaerated 0.60 mM solutions of **16** in cyclohexane were irradiated by the focused output from a 308 nm laser (8-10 ns/pulse 80 - 130 mJ), the products change dramatically. The major products are 1,2-diphenylcyclopentane (cis- and trans-**23** in approximately equimolar amounts), with minor amounts of the olefins **19** (≤ 15% of products) when the laser power was 80 mJ (because **16** undergoes decomposition in the GC injector, product distributions were determined by ^{1}H NMR). When the laser power was increased to 130 mJ/pulse, the cyclopentanes (**23**) were the only major product detected, the amount of olefins in this case was too small to be quantified.

The products from the laser-drop experiments imply that both iodine atoms are extruded during the laser pulse to produce 1,5-diphenylpentadiyl biradical (**24**). This biradical can be produced alternatively by the photolysis of 2,6-diphenylcyclopentanone (**25**) and is known to give **19** (two isomers)

and **23** (two isomers) as products.[157] Lamp irradiation of the ketone **25** gave the same products as LDP of **16**, however, the olefins accounted for ~55% of the products as analyzed by GC. Rüchardt and coworkers[157] reported that the ratio of cyclic to olefinic products changed with both temperature and solvent. These authors did not use cyclohexane as a solvent, but found that the ratio of products changes as a function of temperature in n-pentane as solvent. It is expected that a similar temperature dependency would occur in a similar solvent such as cyclohexane. We decided to do a control experiment with **25** to see if the small amount of olefinic products from LDP of **16** could be due to elevated temperatures within the drop. LDP of **25** in cyclohexane gave approximately the same product distribution as the low intensity photolysis, in this case the olefins accounted for 60% of the products. Table 5.3 shows the product distributions for the low and high intensity photolysis of **16** and **25**.

Table 5.3: Product Distributions for LDP and Lamp Photolysis of **16** and **25**.

Substrate	Method	Conversion (%)	Mass Balance	Products (%)
16	Rayonet	~100	91	**17** (30), **18** (24), **19** (31), **20** (15)
16	LDP	≥ 25 [a]	na	**19** (15), **23** (85)
25	Rayonet	25	95	**19** (55), **23** (45)
25	LDP	22	92	**19** (60), **23** (40)

[a]-Based on the amount of products.

We had hoped that the temperature dependency reported for the photolysis of **25**[157] might provide a "chemical thermometer" which could be used to measure the temperature of the drops during LDP, however, there

seemed to be no correlation between the temperature and the olefin/cyclopentane ratio as reported by Rüchardt.[157] These authors also mentioned that the olefins are not photostable, and that they accounted for a smaller percentage of the products at longer irradiation times (higher conversion) along with a decrease in the mass balance. We tried irradiations (Rayonet, 300 nm) at low conversion (≤ 20%), but the product ratios at temperatures above 35 °C varied from one experiment to the next. We suggest that the laser-drop photolysis of **25** gives a more accurate product ratio for the primary photoproducts, and that steady-state irradiations result in the secondary photolysis of the olefins.

5.3.2 Discussion

The spectra of benzylic radicals are well known in the literature[158] and have a characteristically narrow absorption at around 320 nm. Indeed, they have often been studied by the photolysis of benzyl chlorides.[118,119,159] This combined with the quenching of the signal in Figure 5.8 with oxygen[120] allows us to confidently assign the transient from photolysis of **21** to the benzylic radical **26** as shown in reaction 5.15. There are a number of anomalies which cannot allow us to assign the transient in Figure 5.10 to the corresponding benzylic radical **27**: i) The broad absorption is uncharacteristic of benzylic radicals. It is not expected that iodine substitution four σ-bonds away from the radical center would have such an effect on the absorption spectrum. ii) The decay of this transient is only slightly affected by the presence of oxygen. It is well known that benzylic radicals react with oxygen at near the diffusion controlled rate.[120] And, iii) although the products from the photolysis of **16** could all be accounted for by invoking a benzylic radical intermediate, it would be expected that the

reaction mixture would be more complex. Notably missing are radical dimers, which are extremely common products under high intensity conditions as a result of the high concentration of radicals.[160]

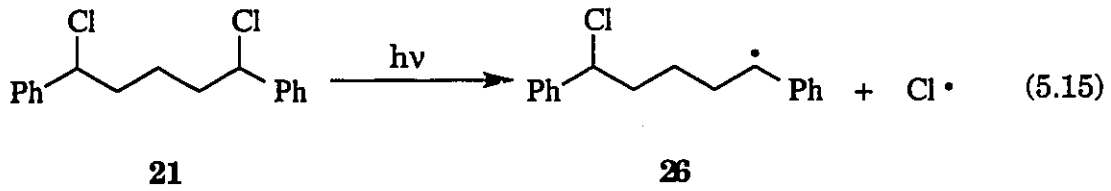

(5.15)

21 **26**

An alternative assignment for the spectrum in Figure 5.10 is the hypervalent intramolecular iodine complex **28** (Scheme 5.9). Good evidence for such an intermediate is provided by the product distributions from the laser-drop experiments. If the cyclopentanes (**23**) were produced by the photolysis of the benzylic radical **27** by way of "free" biradical **24**, one could expect a much higher yield of the olefins **19**. This is because spin statistics determine that three quarters of the biradicals produced in such a process would have to be triplets and the lowest energy conformation of the benzylic radical would be the 'stretched' linear chain. Previous investigations have shown that the triplet biradical gives a significant yield of the olefins, along with the cyclopentanes, as products.[157]

Perhaps even more compelling evidence for such an intermediate is provided by the spectrum obtained from the photolysis of **22**, no known alkyl radicals absorb in this region of the spectrum. In fact, a simple primary alkyl radical would not be expected to absorb at wavelengths accessible to our LFP system ($\lambda \geq 260$ nm). As in the case with alkyl substituted benzyl radicals, an iodine atom four carbons away from the radical center would not be expected to cause such a long wavelength absorption in a primary alkyl radical. Therefore the intermediate responsible for the absorption

spectrum cannot be the carbon-centered radical, and the formation of the hypervalent iodine radical **29** seems a likely candidate (Scheme 5.8).

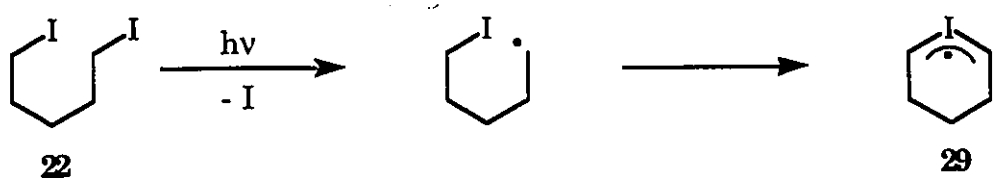

22 **29**

Scheme 5.8

We have shown in this study that the olefins are produced in a 60% yield when the triplet biradical precursor **25** is photolyzed. LDP of **25** shows that the olefins are produced even under these extreme conditions, thus, it cannot be argued that elevated temperatures within the drop during its explosion upon irradiation are responsible for the lack of olefinic products for LDP of **16**.

We propose that LDP of **16** results in formation of the divalent iodine radical intermediate **28**, which undergoes absorption of a second photon to produce predominantly the cyclic product and an iodine atom. It is difficult to ascertain whether absorption of a photon by **28** results in the concerted formation of a carbon-carbon bond along with the extrusion of an iodine atom or formation of the biradical **24** upon extrusion of iodine. One cannot dismiss the biradical as an intermediate because of the lack of olefinic products since the incipient biradical would be in a conformation which favours cyclization. Turro and co-workers[161,162] have shown that intersystem crossing (isc) due to spin-orbit coupling is facilitated by small end-to-end distances of the biradical termini. It is also possible that isc could be further enhanced by the presence of an iodine atom in the solvent cage. External heavy-atom effects are well documented in the case of heavy

atom solvents.[163-165] Thus, even though spin statistics determine that three quarters of the biradicals formed in such a process would be triplets, any triplet biradicals formed may not live long enough to undergo the rotations which would lead to a conformation which would allow formation of the olefins before isc to the singlet state occurs.

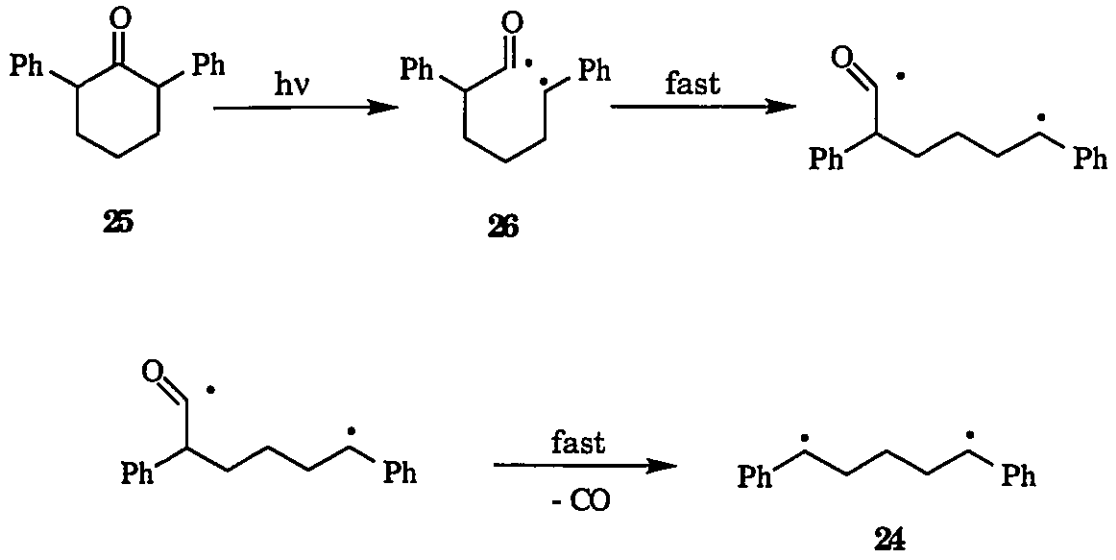

Scheme 5.7

It has been shown that the photolysis of **25** leads to the biradical **26**, which is followed by decarbonylation to give the triplet biradical **24** (Scheme 5.7). Although the lifetime for **26** is short, ~120 ns at 190 K,[162] it lives long enough so that the lowest energy conformation (the linear conformation shown in Scheme 5.7) is achieved before decarbonylation. Therefore, the incipient biradical is not in a conformation which allows rapid isc and cyclization and both olefins and cyclic products are formed.

It is expected that the primary intermediate formed upon photolysis would be the benzylic radical **27**. Cyclization to give the divalent iodine radical must be fast; the absorption band for LFP of **16** is formed within the

rise time of the LFP system, and the LDP experiments indicate that these intermediates must be formed well within the laser pulse. From the LDP experiments we estimate that **27** must be formed in less than two nanoseconds. The mechanism for LDP of **16** is shown in Scheme 5.9.

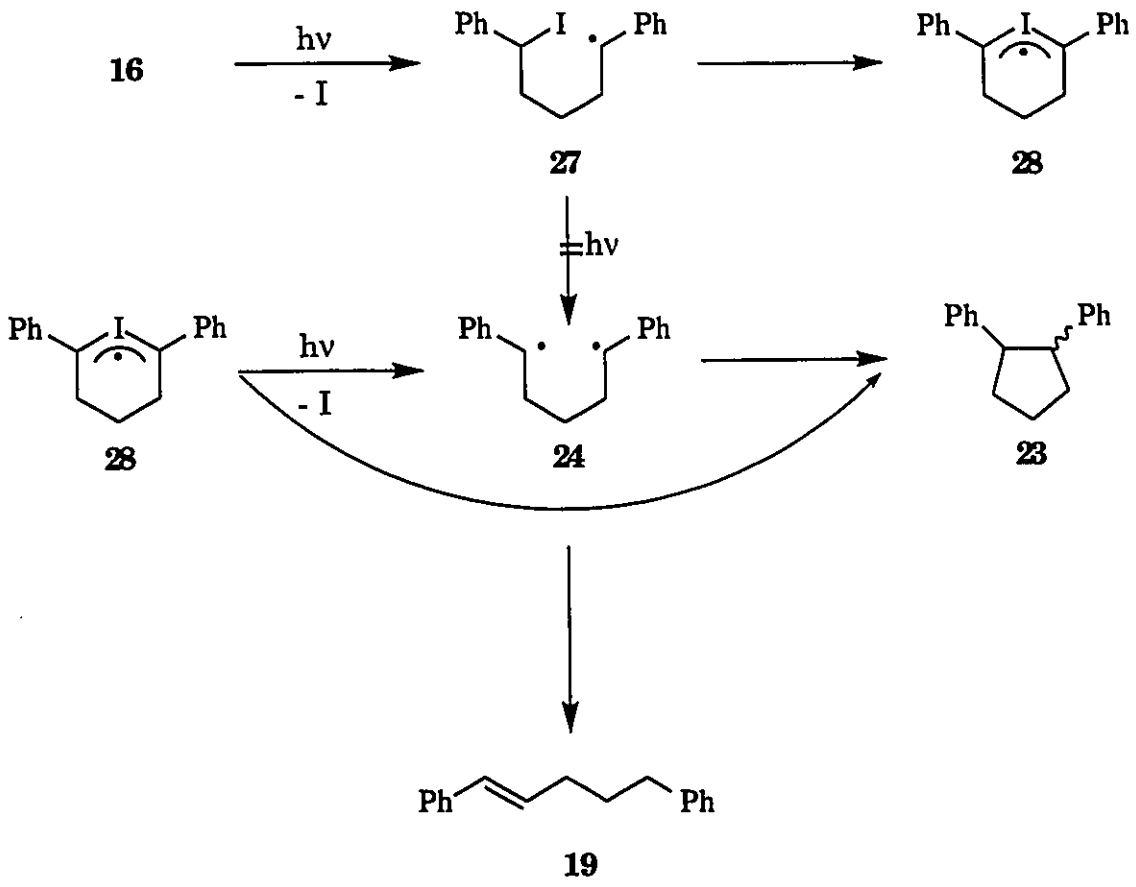

Scheme 5.9

Further evidence for formation of **28** as an intermediate can be seen from the two-laser two-colour LFP of **16**. If the triplet biradical were produced in a linear conformation, as would be expected from the benzylic radical, one would not expect instantaneous bleaching of the signal since the triplet biradical also absorbs very strongly at 320 nm with a lifetime of 900 ns in acetonitrile.[162] Although there may not be a jump in the

absorption signal (unless the extinction coefficient of the biradical was significantly larger than the precursor radical), it would be expected that the decay of the triplet biradical would be resolved after the 308 nm laser pulse. However, the bleaching of the signal at 320 nm is instantaneous.

5.3.3 Conclusion.

The 248 and 308 nm LFP of 1,5-diiodo-1,5-diphenylpentane (**16**) and 1,5-diiodohexane (**22**) cannot be explained on the basis of the carbon-centered radicals which would be expected from homolysis of a carbon-iodine bond. The hypervalent iodine radicals **28** and **29** have been proposed as an alternate structures to explain the anomalies present in the transient spectrum and the sluggish quenching by oxygen. LDP product studies and TLTC-LFP of **16** are consistent with this structural assignment. Although the evidence for these hypervalent iodine radicals is indirect, it would be difficult to explain the results presented here without invoking such an intermediate. Particularly compelling evidence is provided by the long wavelength absorption band (λ_{max} = 300 nm) produced upon 248 nm LFP of 1,5-diiodopenane **22**, and the cyclopentane products (**23**) from LDP of 1,5-diiodo-1,5-diphenylpentane.

5.4 Laser-Drop Photolysis of 2-Diazo-1,3-Indandione: Evidence for a Propadienone Intermediate.

The phototransformation of α-diazo ketones into ketenes involves the 1,2-migration of a carbon atom which has become known as the Wolff rearrangement. There is some controversy as to whether the migration of the carbon atom and loss of nitrogen occur in a concerted manner, or if it is

preceded by the loss of nitrogen to form an α-ketocarbene and/or an oxirene intermediate (Scheme 5.9).

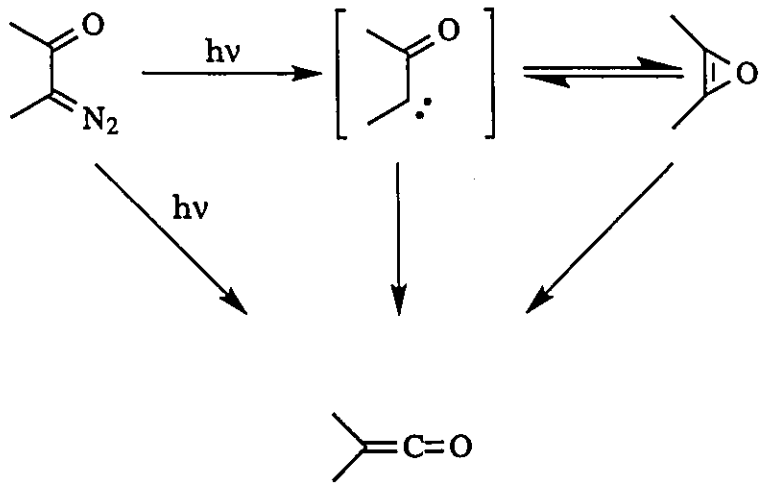

Scheme 5.9

A recent review on carbenes in matrices[20] lists ESR data for several triplet α-ketocarbenes. Chapman et al.[166,167] were the first to report the IRdetection of α-ketocarbenes generated by photolysis of α-diazoacenaphtaquinones in argon matrices at 15 K. Schector[168] was able to trap acenaphthyleneylidene with methanol to form the carbene insertion products. More recently Tomioka[169] has reported IR detection of an α–keto-α'-diazocarbene produced by photolysis of 1,3-bis(diazo)indan-2-one in an argon matrix at 10 K. As well, they were able to trap it in solution with methanol to form 1-diazo-3-methoxyindan-2-one. However, in both of the above examples there was no evidence for the formation of the ketenes in solution and only the carbene trapping products were formed. Thus, for cases where the carbenes can be efficiently trapped in solution the ketenes form only upon further photolysis of the ketocarbenes in matrices.[166,167,169]

For α-diazoketones which form the corresponding ketenes by way of the Wolff rearrangement the ketocarbene cannot usually be trapped in solution. In the case of 2-diazo-1,2-naphthoquinones Barra et al.[170] have shown that the Wolff rearrangement can be regarded as a concerted process in the nanosecond timescale.

Ketenes generated by the photolysis of α-diazo ketones can be trapped by nucleophiles at the oxy-substituted carbon to form acid enols which undergo tautomerization to the corresponding acid or acid derivative. When water is the nucleophile, a carboxylic acid is the ultimate product. This reaction has found numerous applications in the field of photoresist technology, especially in the case of diazonaphthoquinones.[1,171,172]

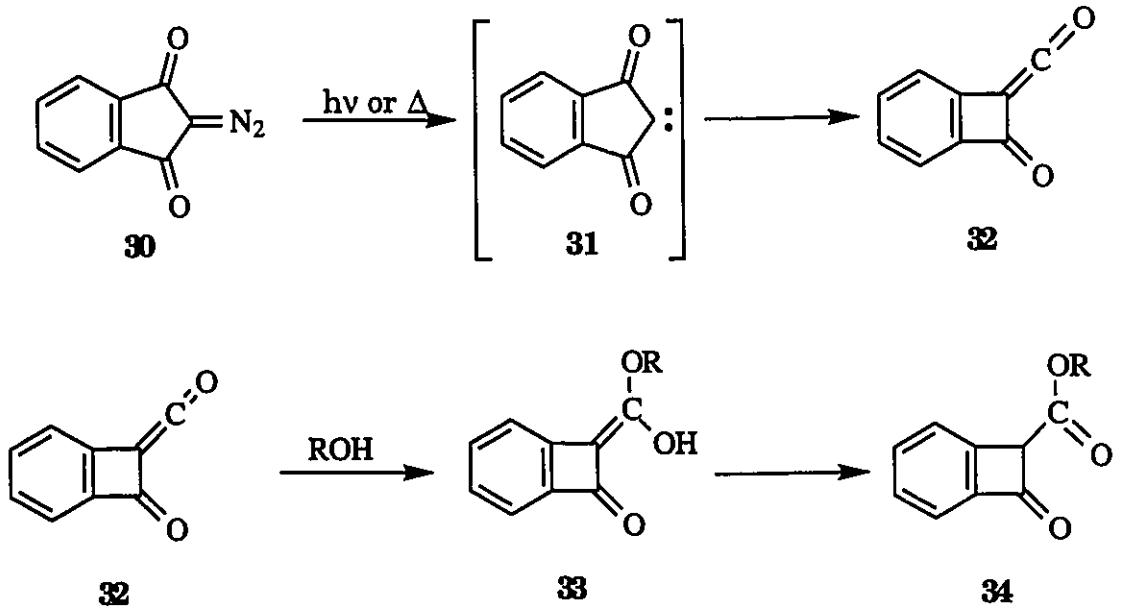

Scheme 5.10

In the case of cyclic α-diazoketones the Wolff rearrangement results in a ring contraction and is a useful method for the synthesis of benzocylobutene derivatives from diazoindanones.[173,174] Cava et al.[175,176]

reported that the gas phase pyrolysis (680 °C) of 2-diazo-1,3-indandione (**30**) in the presence of methanol gave satisfactory yields of the corresponding benzocyclobutenone-2-carboxylic acid methyl ester (**34** Scheme 5.10). However, the photolysis of **30** in methanol gave the diester of homophthalic acid (**37**) along with lesser amounts of 1,3-indandione and

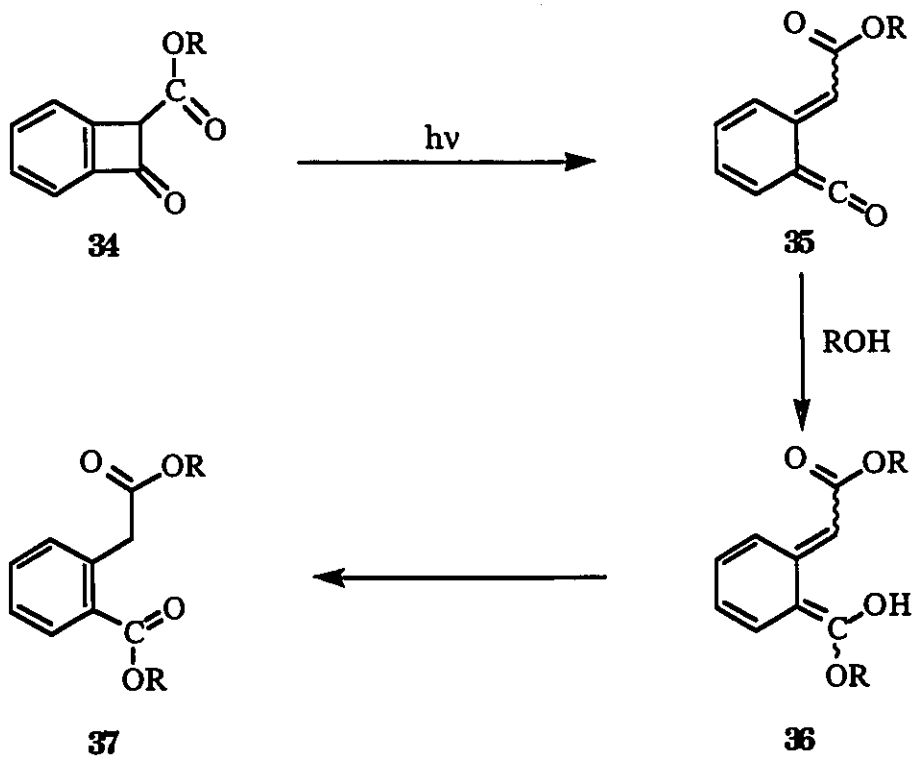

Scheme 5.11

3-methoxyisocoumarin. The authors proposed that **34** was formed, but that further photolysis of this compound resulted in its conversion to **37** by way of Scheme 5.11.

We reasoned that the photochemical preparation of the esters **34** should be possible under laser-drop conditions provided that their formation was slow enough so that they would not be formed within the

duration of the laser pulse and further photolyzed to give the diesters **37**. In this section we report the results of these experiments.

5.4.1 Results.

Laser-flash photolysis.[177] LFP (308 nm) of a 0.10 mM solution of **30** in acetonitrile results in immediate and permanent bleaching at wavelengths less than 340 nm and a weak absorption band centered at 360 nm which does not decay in the time scale of the LFP system (Figure 5.16). The bleaching is a result of the photolysis of the starting material which has a moderate absorption in this region. The absorption is assigned to the ketene **32**. There is no evidence for the intermediacy of the ketocarbene **31**, if it is formed it must be converted to the ketene within the risetime of the LFP system (~30 ns).

In contrast, 308 nm LFP of a 0.10 mM solution of **30** in methanol leads to the growth of two strong absorption bands centered at 300 and 390 nm (Figure 5.17). These bands grow in with a pseudo first order lifetime of 140 ns and subsequently decays with a first order lifetime of 56 μs (Figure 5.18). This spectrum is attributed to the enol ester **33**.

Low and high intensity photolysis. Irradiation of a 1.0 mM degassed solution of **30** in methanol at 300 nm (Rayonet) for 5 minutes results in ~40% conversion and the formation of **37** and **34** in a 0.80 ratio as determined by gas chromatography, no other products were found. Prolonged irradiation results in a decrease of this ratio. Irradiations in isopropanol resulted in a similar ratio for the corresponding ester and diester products when the conversion was ≤40%, however, the major product is 1,3-indandione, which accounted for 47% of the products formed at low conversions. Prolonged irradiation resulted in a complex mixture of products.

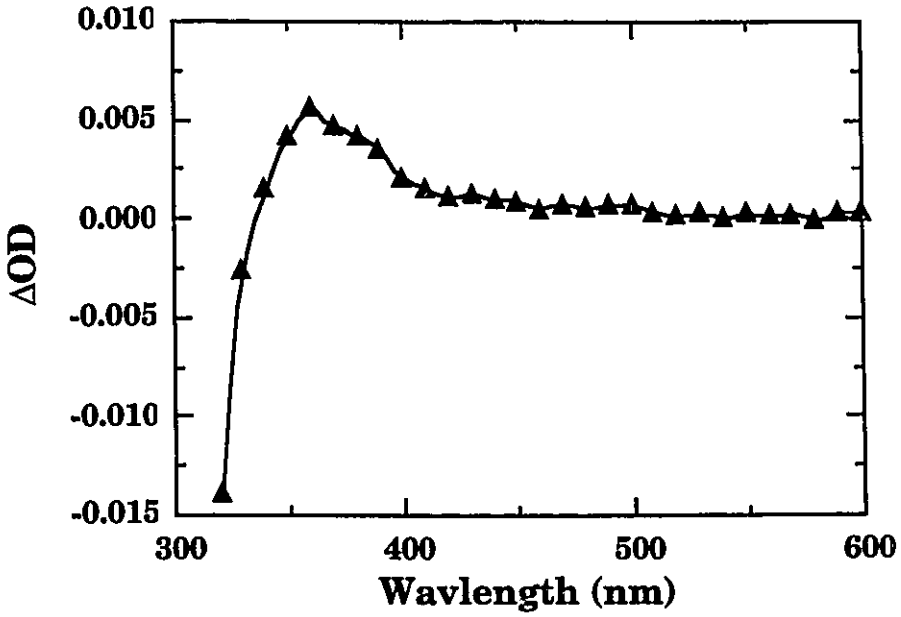

Figure 5.16: Transient spectrum obtained from 308 nm LFP of 0.10 mM solutions of **30** in acetonitrile.

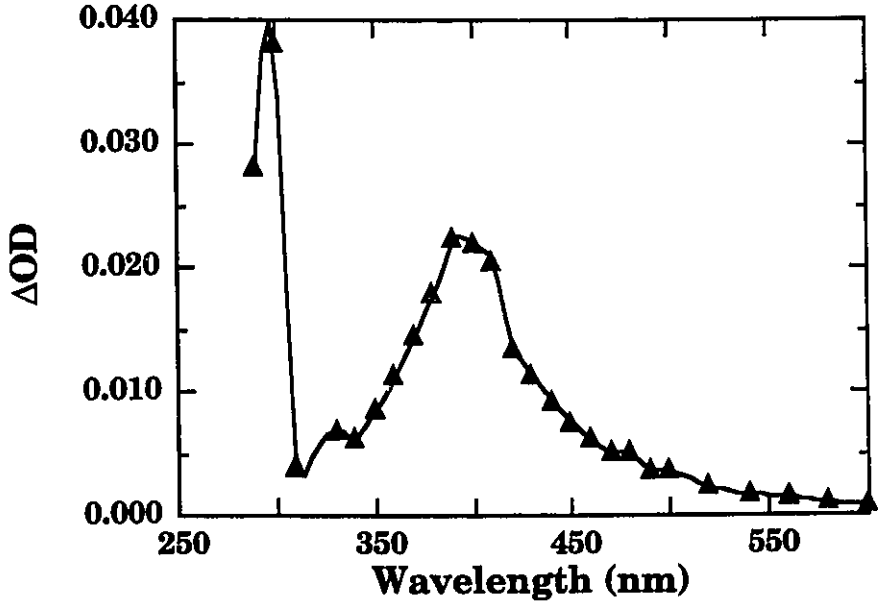

Figure 5.17: Transient spectrum obtained from 308 nm LFP of 0.10 mM solutions of **30** in methanol.

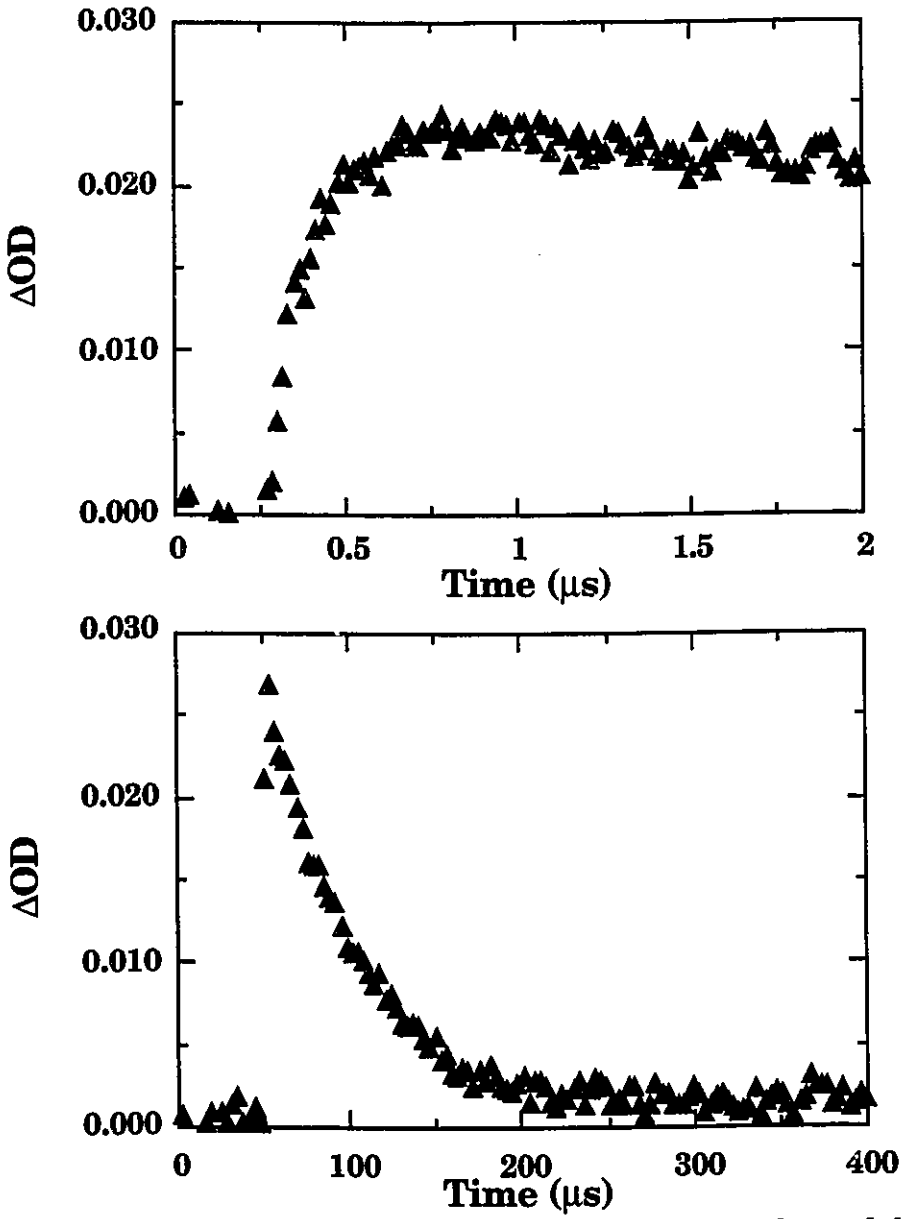

Figure 5.18: (Top) Growth of the enol ester **33** formed by trapping of the ketene **32** by methanol, monitored at 390 nm. (Bottom) Decay of **33** as monitored at 390 nm.

When 0.20 mM solutions of **30** in methanol were subjected to 308 nm LDP (100 mJ/pulse, one cycle) the conversion was 20% and both the diester and the monoester (**37** and **34**) were formed in a 1.25 ratio, these were the

only detectable products. The power dependency of the product ratio was done by attenuating the laser with precalibrated neutral density filters during LDP, it was found that the ratio **37/34** decreased with decreasing laser power. At 49% of the full laser power only the monoester was detected. A plot of the product ratio vs. % laser power is shown in Figure 5.19.

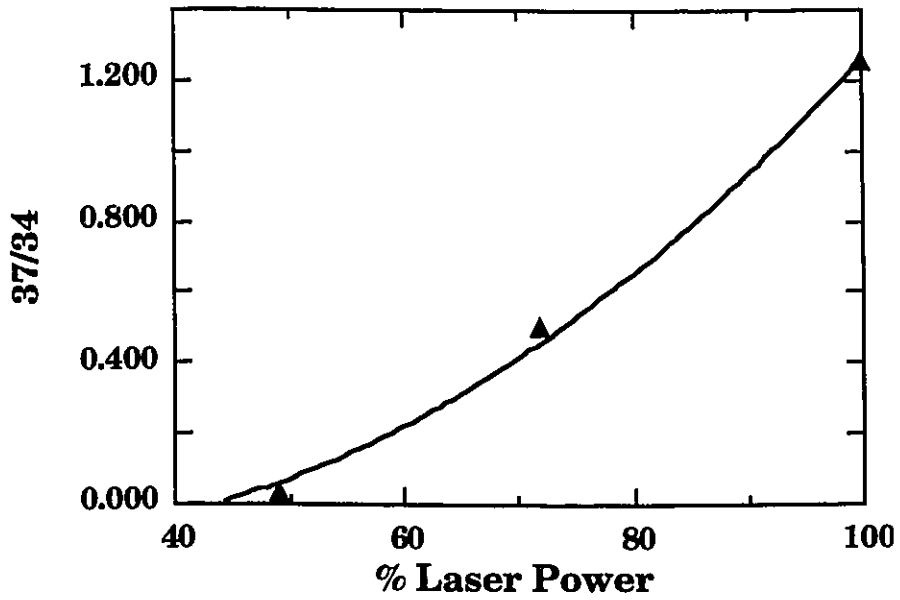

Figure 5.19: Ratio of the **37**-to-**34** as a function of laser power. 100 % laser power corresponds to ~100 mJ/pulse. The line in the graph is an arbitrary fit.

5.4.2 Discussion.

We could find no evidence for the formation of the ketocarbene **31** during LFP of **30** in acetonitrile. It is possible that this species lives long enough to abstract hydrogen from isopropanol when used as solvent. The formation of 1,3-indandione in isopropanol may result from the successive abstraction of two hydrogens from the solvent by the carbene **31**. When the solvent was methanol, 1,3-indandione was not formed. It should be pointed out that no O-H insertion products were found in either methanol or isopropanol. Previous studies have shown that α-ketocarbenes readily

insert into the O-H bond of alcohols.[168,169] It seems unlikely that the intermediacy of the carbene is involved in the formation of 1,3-indandione.

The LFP of **30** in methanol shows that neither the ester **34** nor its enol tautomer **33** are formed within the duration of the laser pulse. Thus it was expected that **37** would not be formed during laser-drop photolysis. However, this product was formed in substantial amounts as was the corresponding diester in isopropanol. The power dependency on the product ratio during LDP (Figure 5.19) indicates that **37** is formed by a multiple photon reaction. The order of multiple photon reactions (two- or three-photons) can sometimes be determined by plotting the ratio of the products (multi-/mono-photon products) against the power of the laser to the exponent which corresponds to the order (i.e. power^3 for a three photon reaction), when the correct order is chosen the plot will be a straight line.[90] However, we were unable to obtain enough points for such a determination.

Given that the spectrum from the photolysis of **30** in acetonitrile is dominated by bleaching of the starting material, and that the absorption band at 360 nm is small, it is not possible to examine the photochemistry of the ketene by TLTC-LFP. It should be pointed out that because the transient spectrum reports the change in absorbance (ΔOD, see Chapter 2), the bleaching signal below 340 nm does not mean that the ketene does not absorb at these wavelengths, only that the absorption coefficient for the ketene is smaller than that of the starting material. The photolysis of benzocyclobutenones is known to give ring opened o-xylylene type intermediates[178,179] and the photoinduced ring opening of **34** is so facile that the low-intensity photolysis of **30** in alcohols gives substantial amounts of the diester even at low conversions of starting material. Thus, under laser-drop conditions the ketene may absorb a second (or third) photon which

results in the formation of the propadienone intermediate **39**. This species can then be trapped by two molecules of alcohol to form the diester **37** (Scheme 5.12).

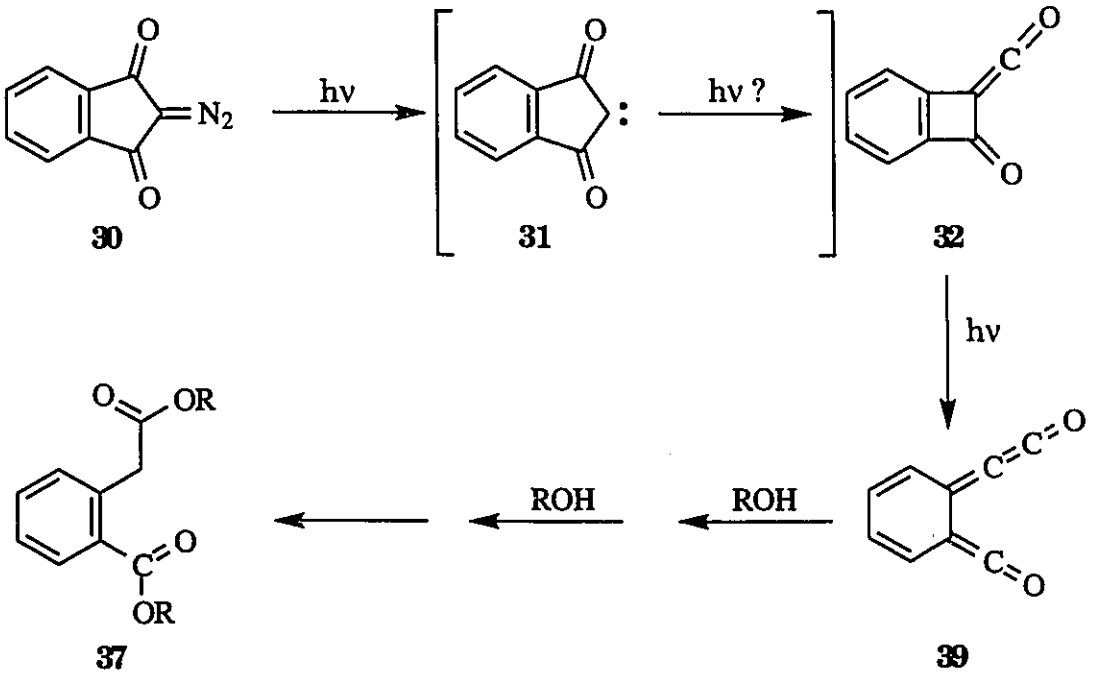

Scheme 5.12

Previous studies have shown that the electronic excitation of α-ketocarbenes results in a photoinduced Wolff rearrangement to form the corresponding ketene[166,167,169] (*vide supra*). Although we cannot determine from these experiments whether or not the carbene **31** is involved in the multiple photon reaction which results in the formation of the diester **37**, it is not possible to discount the involvement of the ketene **32**. Since **34** is not formed within the duration of the laser pulse it cannot be photolysed during the laser-drop experiments.

Simple propadienones (**41**) have been extensively studied by the flash vacuum pyrolysis of 5-alkylidene-1,3-dioxan-4,6-diones (**40**)[180-182] (Scheme

5.13). These workers found that the propadienones could be easily trapped by alcohols to form the corresponding acrylic acid esters. A later study by Wentrup et al.[183] unraveled the mechanism which leads to the formation of propadienones and also found that these species are remarkably stable in the gas phase, requiring temperatures as high as 800 °C before they isomerize to vinylketenes.

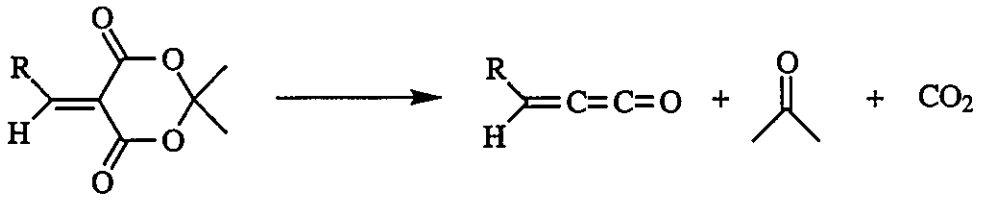

40 **41**

Scheme 5.13

Without spectroscopic information on the intermediates involved, it is impossible to predict the sequence of intermediates involved in the successive trapping of two molecules of alcohol by **39** to form the diester **37**. However, considering the long lifetime of the enol ester **34** (*vide supra*) and the previous work on propadienones,[180-182] it may be possible that the propadienone-ketene intermediate **39** will trap two molecules of alcohol to form the dienol diester **42** (Scheme 5.14) before either of the possible mono enol esters can tautomerize.

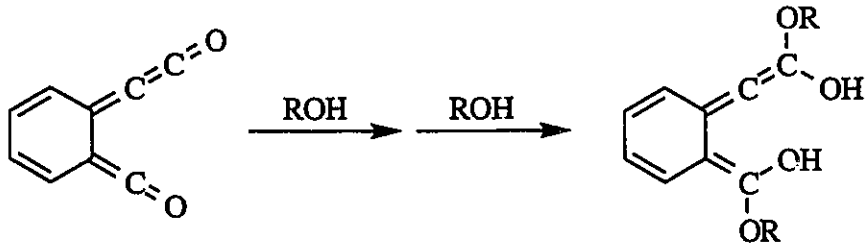

39 **42**

Scheme 5.14

It is unlikely that the low intensity photolysis of **30** in alcohols proceeds through the same mechanism as that of LDP. This is because the intermediate ketene has a much smaller extinction coefficient at the wavelengths used for low intensity irradiation (275 -325 nm), thus, the starting material would be an efficient internal filter at low conversions. As well, the ketene is to short-lived in methanol (~140 ns) to absorb a second photon under low intensity conditions. Therefore the low intensity irradiation of **30** must proceed through the mechanisms shown in Schemes 5.10 and 5.11.

5.4.3 Conclusion.

Laser flash photolysis combined with laser-drop photolysis have shown that the mechanism of conversion of 2-diazo-1,3-indandione (**30**) in alcohols to form the diester of homophthalic acid is dependent on the intensity of the irradiation source. Trapping by methanol is indirect evidence for the intermediacy of the propadienone-ketene intermediate **39** during laser-drop photolysis. Although the intermediacy of **42** is purely speculative, its unusual structure merits further attempts to characterize it spectroscopically.

5.5 The Two-Photon Chemistry of ortho-Methylbenzophenone.

The photoreduction of benzophenone in the presence of readily abstractable hydrogens to give benzopinacol is a well known reaction.[184] However, this reaction does not occur if the benzophenone is substituted at the ortho position by an alkyl group containing an α-hydrogen. In fact, Yang and Rivas[185] reported that ortho-benzylbenzophenone was photostable in hydrogen donating solvents. They discovered that the benzylic hydrogens

of the ortho-alkyl moiety could be exchanged for deuterium by photolysis in deuterated methanol. It was postulated that the triplet ketone abstracted one of the benzylic hydrogens of the ortho-alkyl moiety to form the photoenol **45** (Scheme 5.15). They reasoned that the intramolecular abstraction of hydrogen to form the photoenol was a reversible reaction and was responsible for the suppression of the expected photoreduction reaction to form the substituted benzopinacol. Proof for this intermediate was supplied by trapping it with dimethyl acetylenedicarboxylate to form the corresponding Diels-Alder adduct.[185]

Early conventional and laser flash photolysis studies[9,186] on the intermediates involved in the photolysis of ortho-methylbenzophenones found many absorption signals with lifetimes ranging from about 40 ns to several hundreds of seconds. However, many of the short-lived signals were misassigned to the triplet ketones and biradicals. Later investigations have shown that the triplet ketone is formed in the subnanosecond time scale and its lifetime is only ~3.5 ns.[187] Intramolecular hydrogen abstraction occurs only from the syn conformation of the triplet ketone to form the triplet biradical **44**.[187] The triplet biradical can interconvert between the syn- and anti-conformations before relaxation to form the enols occurs (14 ns),[188] thus, both the Z- and E-enols are formed. The Z-enol undergoes a 1,5-hydrogen shift to regenerate the starting ketone with a lifetime of about 77 ns.[188] The E-enol is very-long lived, up to 4 s depending upon the experimental conditions. The mechanism for the formation of the enols is shown in Scheme 5.15.

As early as 1965 Ullman and Huffman[189] reported that broadband irradiation of **43** in oxygenated solutions produced anthrone (**47**) in about a 1% yield. Porter and Tchir[9] detected an absorption signal (λ_{max} = 390 nm)

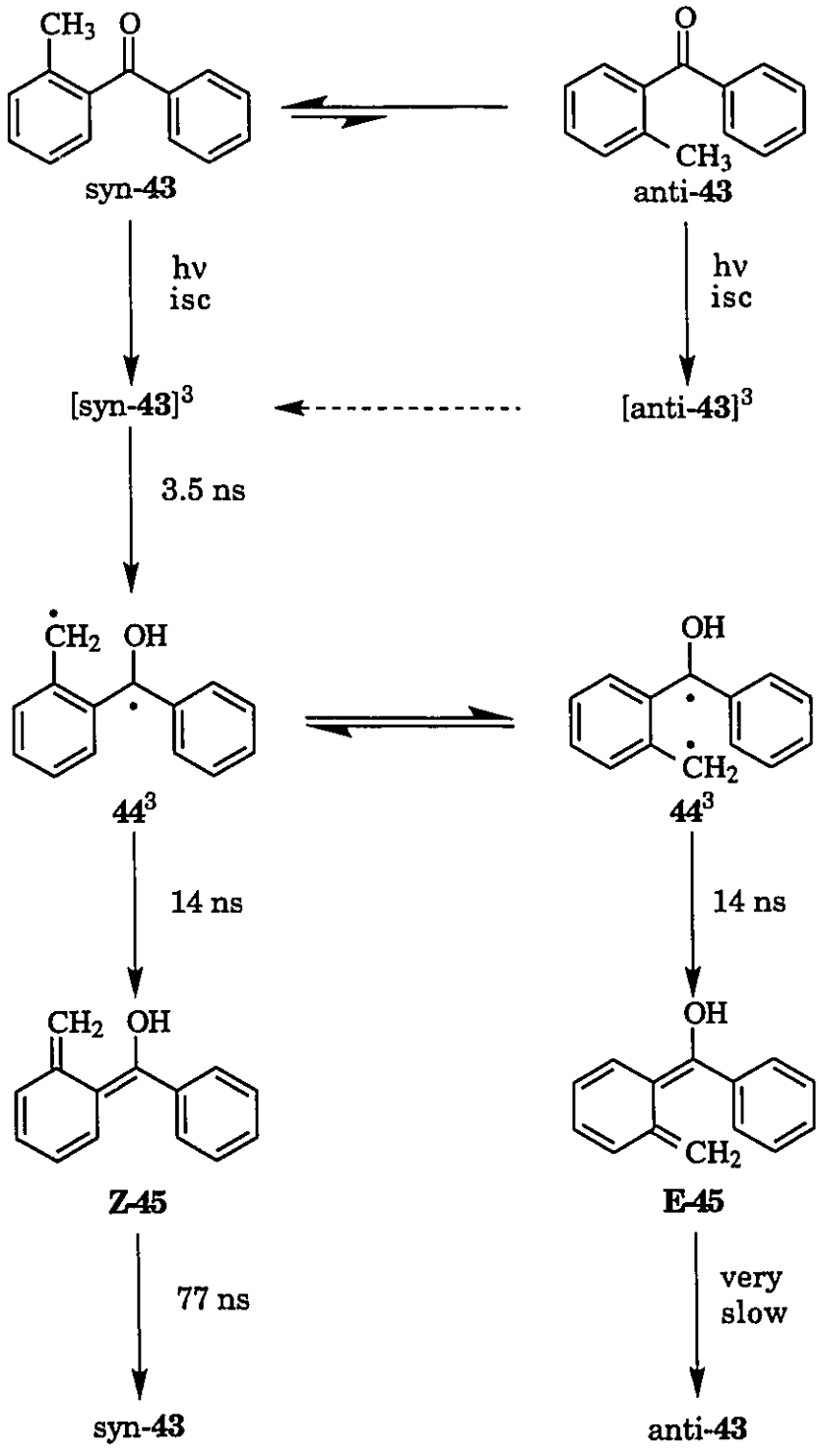

Scheme 5.15

Lifetimes indicated are for benzene as solvent and taken from ref. 188 except for the lifetime of [syn-**43**]^3 which is for ethanol as solvent and was taken from ref. 187.

which persisted for hours during the conventional flash photolysis of 2,4-dimethylbenzophenone. This signal was not present when 90% of the photolysis light between 380 and 550 nm was removed. They attributed the long-lived signal to the dihydroanthrone enol **46**, which was formed by the long wavelength photolysis of E-**45** (Scheme 5.16).

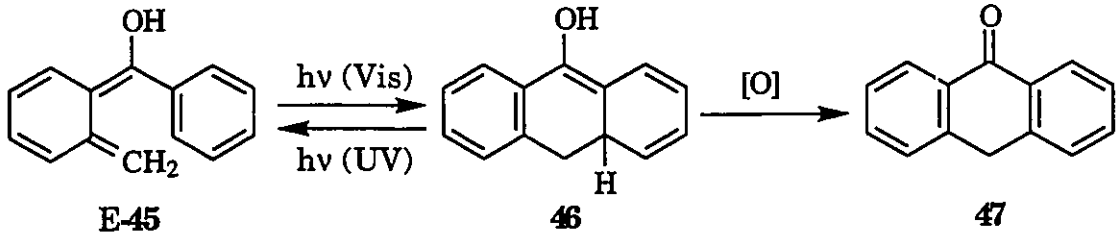

E-**45** **46** **47**

Scheme 5.16

Heindel et al.[190] showed that irradiation of **43** in benzene under a steady stream of air with a 350 nm Rayonet lamp supplemented by a long wavelength incandescent tungsten lamp produced anthraquinone in a 28% yield, along with 2-benzoylbenzaldehyde (**49**), 2-benzoylbenzoic acid (**50**) and 3-phenylphthalide (**51**). Irradiation with 350 nm by itself produced only **49**, **50**, and **51** but no anthraquinone (Scheme 5.17). These authors postulated that the anthrone produced as described by Porter and Tchir[9] could be photo-oxidized to produce anthraquinone.

Wilson and coworkers[191] have recently re-examined the photochemistry of **43** by laser-jet and conventional lamp photolysis. Low intensity irradiation (20 hours, 350 nm Rayonet lamp) of 54 mM deaerated solutions of **43** in benzene led to 89% conversion of starting material to give a complex mixture of products (products and percent yields given in Scheme 5.18). Laser-jet photolysis (argon ion cw laser, 2.85 W, 334 to 364 nm) of 20 mM deaerated solutions of **43** in benzene also led to a complex mixture of

products. However, the yield of anthrone (**47**) increased from 0.5% under low intensity conditions to 23% under laser-jet conditions (the yields of the other products were not given). A second laser-jet experiment was done with the crossed beams from two argon ion lasers, one with the UV output mentioned above and a second with output in the 458 to 514 nm range with 9.0 W of power. During this experiment the yield of anthrone was further enhanced to account for 34% of the products.

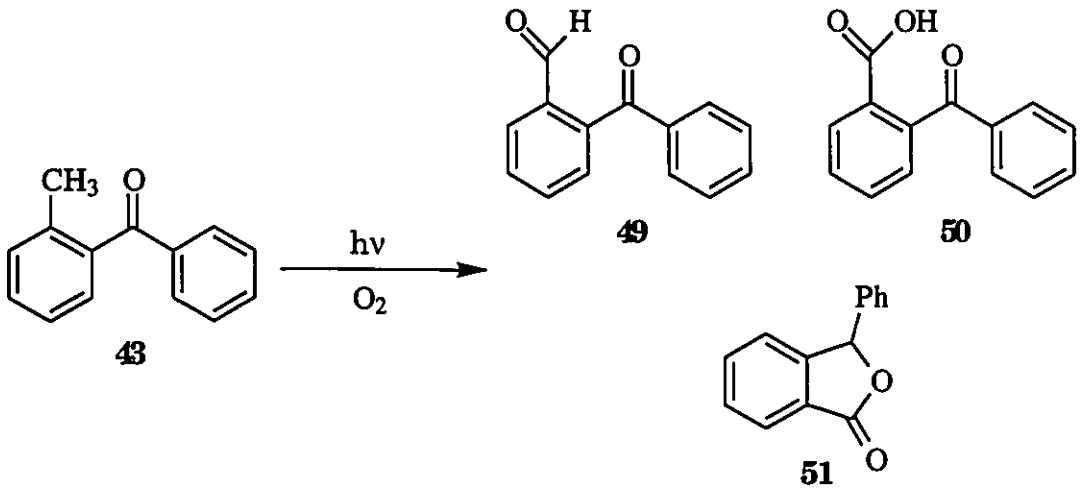

Scheme 5.17

Low intensity irradiation (11 hours, 350 nm Rayonet lamp) of 54 mM deaerated solutions of **43** in isopropanol led to 74% conversion and a much simpler product mixture. **52** and **53** were produced in 60% and 30% yields respectively, and an additional product, 2-methylbenzhydrol (**57**), was also formed in a 7% yield.[191] Laser-jet photolysis of isopropanol solutions of **43** were not reported.

Ishida and coworkers[188] produced Z- and E-**45** by pulse radiolysis of **43** in benzene solutions. In this case the reaction involves triplet energy transfer from triplet benzene formed by radiolysis. They confirmed the

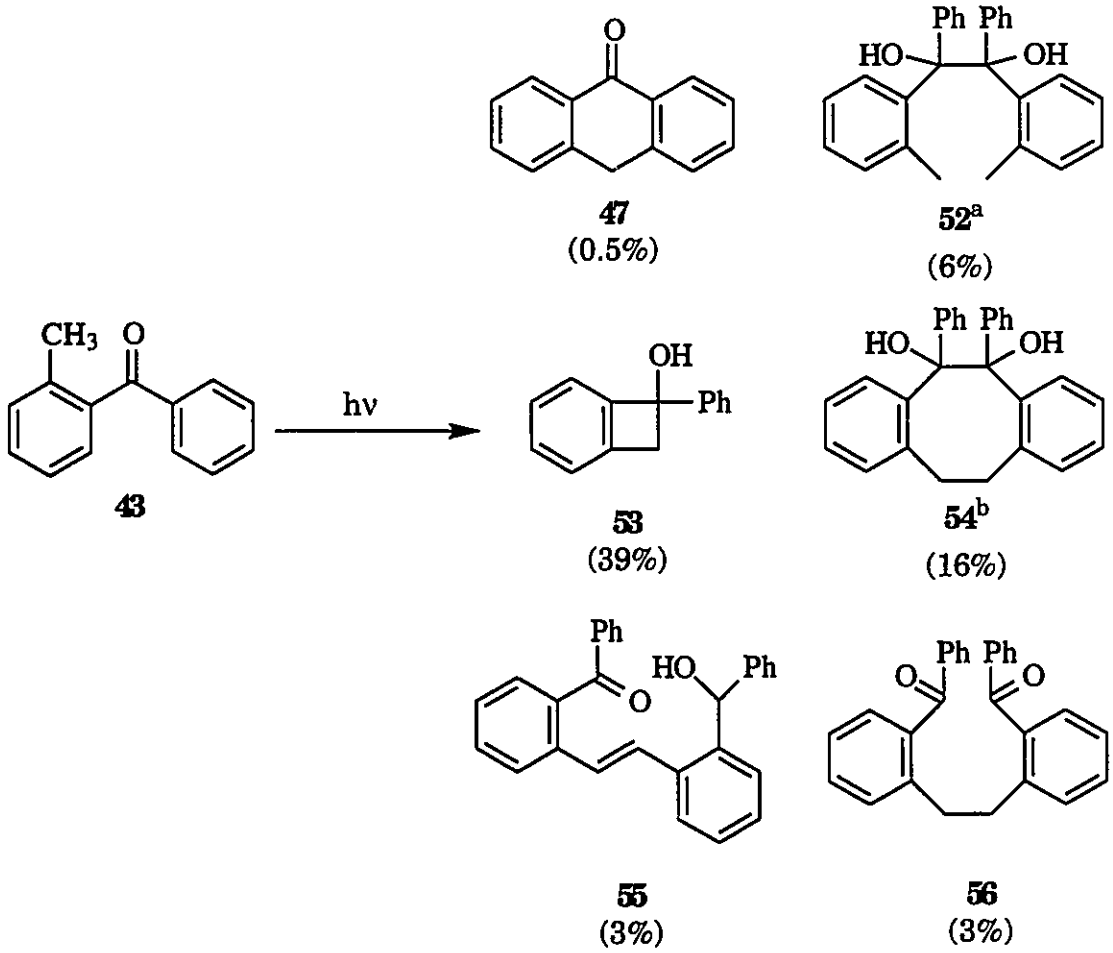

Scheme 5.18

[a] Meso and *d,l* forms present in a ratio of ca. 1:2. [b] Both syn- and anti-isomers, ratio varied from 5:1 to 9:1. Data taken from ref. 191.

lifetimes and mechanism for a number of the transients involved in the formation of these products in benzene as well as the rapid decay of Z-45 (λ_{max} = 390 nm, τ = 77 ns). The triplet ketone was found to have an absorption maximum at 535 nm and a lifetime of about 7 ns in benzene; this can be compared to 3.5 ns in ethanol as found by Das and Scaiano[187] by quenching with 2,5-dimethyl-2,4-hexadiene. The biradical 44 has a strong absorption at 330 nm in benzene with a lifetime of 14 ns,[188] the lifetime in

more polar solvents was found to be slightly longer, 26 ns in ethanol,[192] and 24 ns in 4:1 acetonitrile/water.[193]

Ishida et al.[188] were also able to confirm that E-**45** underwent photolysis at 460 nm by irradiating this species with a dye laser fired 2 μs after the electron pulse (an experiment very much like TLTC-LFP). E-**45** has an absorption maximum centered at ~420 nm and another band which extends into the UV. Photolysis of this species by the 460 nm pulse from the dye laser led to an increase in absorption at wavelengths ≤ 400 nm with a corresponding bleaching of the signals at wavelengths ≥430 nm. There was an isobestic region between 410 and 420 nm.

We decided to examine the laser-drop photochemistry of ortho-methylbenzophenone to compare the efficiency of the multiple photon reactions with those obtained during laser-jet photolysis.

5.5.1 Results.

Laser-flash photolysis. Figure 5.20 shows the transient spectra recorded 100 ns and 5 μs after the pulse from a 308 nm laser for 0.50 mM deaerated solutions of **43** in methanol. Note that the absorption maximum at the early time interval is at 400 nm and is shifted to 410 nm at the later time interval. The spectrum at 100 ns is due to both Z- and E-**45** and may also be contaminated by some contribution from **46**. The spectrum obtained 5 μs after the laser pulse may still be contaminated by some contribution from **46** since it is known that this species persists for hours in oxygen free solutions.[9]

TLTC-LFP experiments of identical solutions were done with a 440 nm pulse from the dye laser fired 1.5 μs after the 308 nm synthesis pulse. Figure 5.21 shows the transient spectra in the 350 to 450 nm region at time

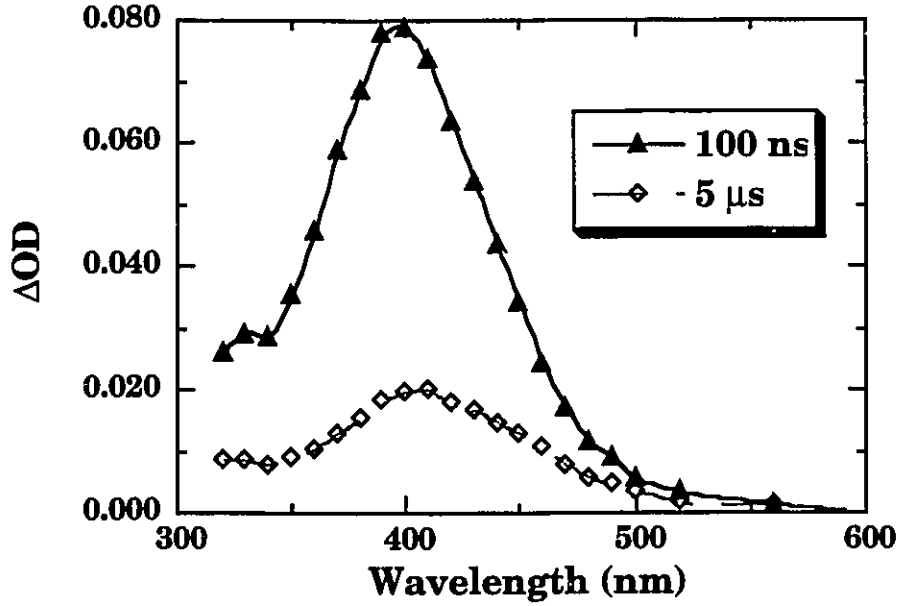

Figure 5.20: Transient spectra obtained from the 308 nm LFP of 0.50 mM deaerated solutions of **43** in methanol.

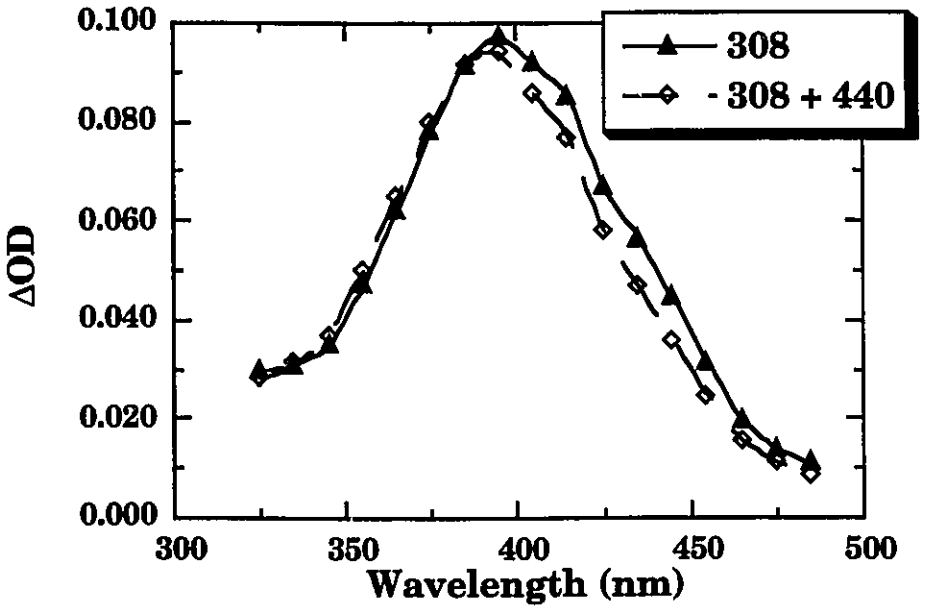

Figure 5.21: Transient spectra obtained from 308 nm and 308 + 440 nm TLTC-LFP of 0.50 mM deaerated solutions of **43** in methanol. Spectra obtained 100 ns before (triangles) and 100 ns after (diamonds) the firing of the second (440 nm) laser.

intervals 100 ns before and 100 ns after the dye laser pulse. Figure 5.22 shows the traces obtained at 355 and 455 nm. The bleaching at wavelengths > 405 nm and concurrent growth at wavelengths < 405 nm agree well with the results obtained by Ishida.[188]

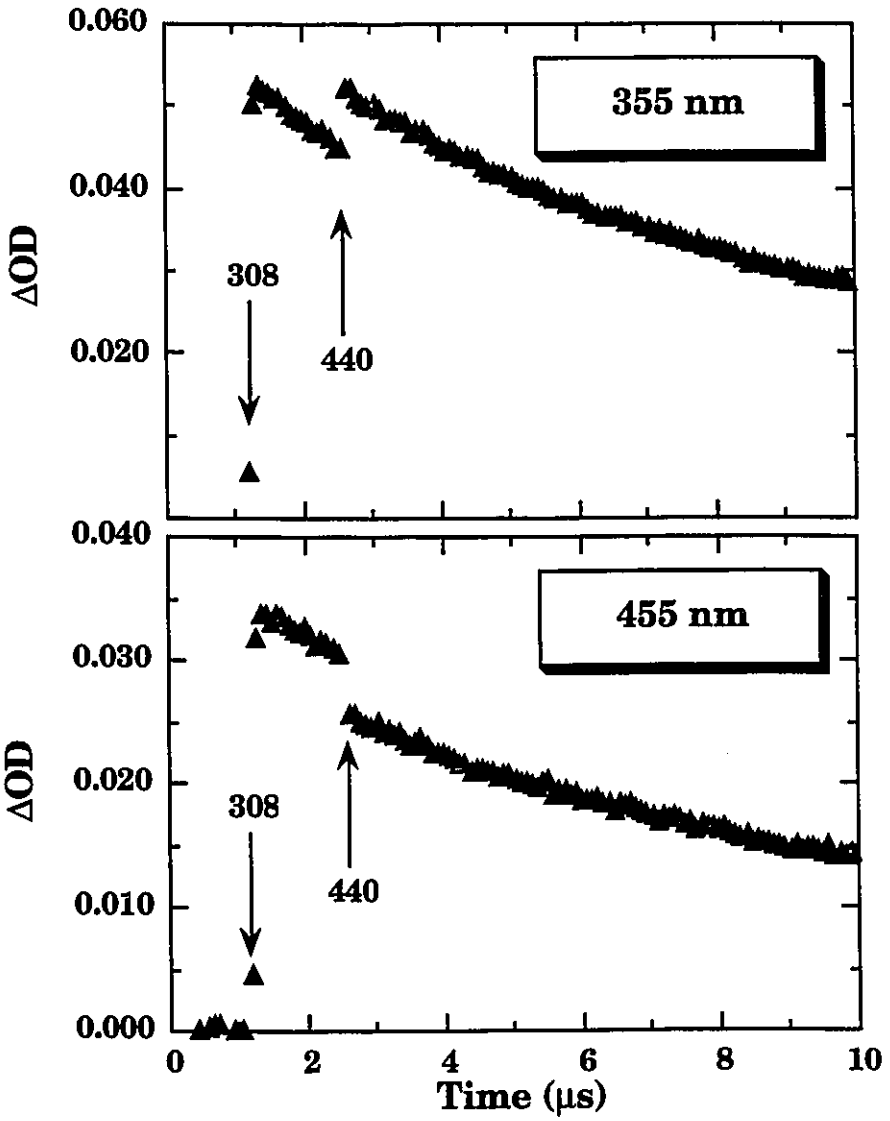

Figure 5.22: Decay traces from TLTC-LFP of 0.50 mM **43** in methanol. (Top) Jump in signal as monitored at 355 nm. (Bottom) Bleach of signal as monitored at 455 nm.

Low and high intensity photolysis. Low intensity photolysis (Rayonet, 300 nm) of deaerated 1.0 mM solutions of **43** in benzene showed no product

formation after 2 hours. In contrast, irradiation of an identical solution saturated with oxygen showed 37% conversion after 30 minutes. The three major products were **49**, **50**, and **51**. The distribution of these products varied, with **51** being larger at longer irradiation times, seemingly at the expense of **49**. Anthrone (**47**) was also present, but in much smaller amounts. The highest yield of **47** was ~1.5%. There were three other minor products which were not identified. The product distributions of a typical photolysis run are given in Table 5.4.

Table 5.4: Photolysis of **43** in oxygenated benzene.

Method	% Conv.	**49**	**50**	**51**	**47**
Rayonet [a]	37	18	32	44	~1
Laser-drop[b]	4	36	33	-	15

[a]Lamp irradiation at 300 nm [b]One cycle.

Laser-drop photolysis (308 nm) of 1.0 mM deaerated solutions of **43** in benzene also showed no product formation. However, 308 nm LDP of oxygen saturated solutions in benzene resulted in ~4% conversion after one cycle and the formation of **47** in a 15% yield, along with **49**, and **50**. There was one other major product (by HPLC) which could not be identified. Also, no phthalide **51** was detected from laser-drop photolysis. The product distributions for the 308 nm LDP of **43** are given in Table 5.4.

Molecular modeling. AM1-RHF calculations were done on E-**45** and **46** as well as the singlet excited state of E-**45** (E-**45***). The structures for the optimized geometries, as well as the bond orders for the central ring, are shown in Figure 5.23. Note that there is considerable bond formation

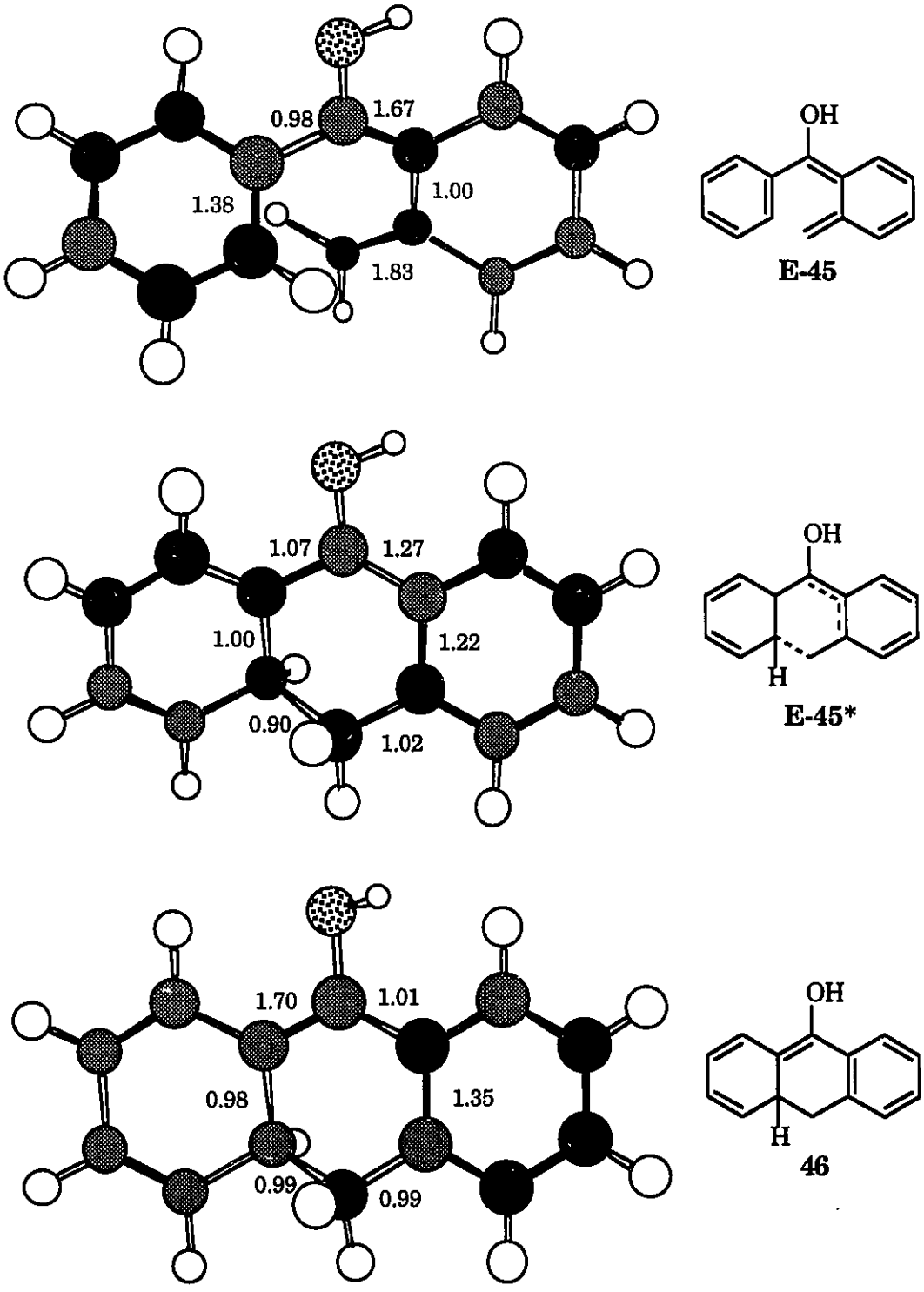

Figure 5.23: AM1-RHF calculated geometries and bond orders for the central rings for **E-45**, **E-45***, and **46**.

between the methylene carbon and the ortho carbon on the adjacent ring in E-**45*** with a calculated bond order of 0.90. Also, the bond orders for the external diene system of E-**45** have become much closer to the bond order of the product (**46**) in the excited singlet state E-**45***.

5.5.2 Discussion.

The TLTC-LFP results reported here are in excellent agreement with the pulse radiolysis-LFP results reported by Ishida.[188] The formation of **46** occurs on a time scale which is shorter than the pulse width of the dye laser (~15 ns). This is in accord with the AM1 calculations on the excited state of E-**45**. These calculations indicate that the excited state has substantial bond formation between the methylene carbon and the ortho carbon on the adjacent ring. The bond orders for E-**45*** can almost be described as an hybrid between the ground state reactant and product structures, but the geometry appears to be much closer to product. These calculations suggest that the reaction is an adiabatic process which occurs on the excited state surface, and it could be expected that the excited state of the enol would be very short-lived, certainly shorter than the time response of the LFP system.

Although Wilson et al.[191] reported that photolysis of **43** in benzene and isopropanol resulted in considerable conversion of starting material, we were unable to detect the loss of starting material during either low intensity irradiations or laser-drop photolysis. It should be mentioned that the irradiation times reported by Wilson were considerably longer than those reported here. As well, the laser-jet photolysis in benzene required 7 cycles to achieve ~30% conversion. Considering the high conversions which we have been able to achieve during LDP of other substrates, and the long

irradiation times reported by Wilson, it seems likely that the efficiency for product formation from the enols must be very small.

In contrast, the oxidatition of the enol to form benzoylbenzaldehyde (**49**) and benzoylbenzoic acid (**50**) is efficient enough to convert 37% of the starting material. The formation of 3-phenylphthalide (**51**) is most likely a result of the secondary photolysis of **49**. Scaiano et al.[194] have shown that the photolysis of this compound in benzene forms **51** in high yields. Confirmation of this secondary photolysis mechanism can be found in the LDP of oxygen saturated solutions of **43** in benzene. Under these conditions **51** could not be detected. This is because the oxidation of the enol to form **49** would not occur within the duration of the laser pulse, thus, **49** cannot be further photolyzed to form **51**.

The lifetime for the triplet biradical in benzene has been reported to be 14 ns,[188] thus the enols **45** would have been formed in significant quantities during the laser pulse to undergo absorption of a second photon to produce **46**. The 308 nm LDP of **43** shows a definite increase in the yield of anthrone when compared to the low intensity irradiations. However, it seems that the laser-jet is much more efficient for the production of anthrone from the photolysis of **43**. Not only are the yields of anthrone higher in the laser-jet, but the yields reported by Wilson[191] were for the photolysis of deoxygenated solutions.

Heindel et al.[190] have shown that the production of anthroquinone during the photolysis of **43** in aerated benzene does not occur in the absence of visible light. Wilson and coworkers[191] found that the efficiency of anthrone production during the LJP photolysis of **43** was increased by 50% when the visible light from a second laser was also focused on the microjet. These authors suggested that visible light induced the photoisomerization

of E-**45** to the dihydroanthrone **46**, but that UV light induces the reverse reaction as shown in Scheme 5.16. If this were the case then 308 LDP of **43** should not form the anthrone as a product. It is more likely that a pseudo-photostationary state is achieved in the laser-jet and that visible light shifts this pseudo-photostationary state towards **46**. This would explain the production of anthrone in significant yields by 308 nm laser-drop irradiation.

It should be pointed out that the triplet biradical is also sufficiently long lived, and has a suitable absorption at 308 nm, to undergo absorption of a second photon during laser-drop photolysis. However, it would not be possible to separate the photochemistry of these two intermediates during laser-drop photolysis.

5.5.3 Conclusion.

The systems discussed in the previous sections of this thesis have shown that laser-drop photolysis is a viable method for the production of semi-preparative amounts of multiple photon reaction products. In Chapter 4 a direct comparison was made between laser-drop and laser-jet photolysis which showed that, for the case of diphenylmethyl radicals, the efficiencies of the two methods were comparable. The investigation discussed above has shown that, in some cases, the laser-jet method may be preferable, especially when the transient to be excited absorbs at a longer wavelength than its precursor. It may be possible to overcome this problem with two-laser two-colour laser-drop photolysis (see Chapter 7).

5.6 Experimental.

Materials. Dicumyl peroxide (Aldrich) (**2**) was recrystallized twice from methanol. 2-Methylbenzophenone (Aldrich) (**43**) was purified by vacuum distillation. 1,5-dichloro-1,5-diphenylpentane (**21**) was a gift from Dr. H. Garcia and Dr. M. A. Miranda (Univ. Politécnica de Valencia, Valencia, Spain). 2-Diazo-1,3-indandione was a gift from Dr. J. Andraos (University of Ottawa, Ottawa, Canada).

t-Butyl-1,1-diphenylethyl peroxide (5) was prepared exactly as described by Falvey et al.[114] ^{1}H NMR ($CDCl_3$) δ ppm: 1.22 (s,9H), 2.00 (s, 3H), 7.20-7.42 (m, 10H). Although this compound appeared pure by NMR, HPLC analysis revealed an impurity which absorbed in the UV. Passage over alumina with a 90/10 mixture of hexane/ethyl acetate as eluent and recrystalyzation from methanol was adequate to remove this impurity.

1,5-diiodo-1,5-diphenylpentane (16) was prepared by the general procedure of Jung.[195] Argon was bubbled through a solution of 500 mg (1.96 mmol) of 1,5-diphenyl-penta-1,5-diol in 20 mL of dichloromethane contained in a 50 mL round-bottom flask equipped with a magnetic stir-bar. After 10 minutes, a septum cap was placed over the top of the flask and 1.9 mL (13.2 mmol) of trimethylsilyl iodide was added via syringe. The resulting mixture was stirred for 24 hours and then the reaction was quenched by the addition of 2 mL of water. This solution was extracted with three 30 mL portions of ether and then washed consecutively with 30 mL portions of water, 10% sodium thiosulfate solution, saturated bicarbonate solution, and saturated sodium chlorite. The organic layer was dried over anhydrous sodium sulfate, filtered, and concentrated by rotary evaporation to afford a yellow oil. The oil was then eluted through a silica column with dichloromethane and the solvent was removed by rotary evaporation to yield

840 mg (90%) of 1,5-diiodo-1,5-diphenylpentane (two diastereomers); ^{1}H NMR ($CDCl_3$) δ ppm: 1.1-1.8 (m, 2H) , 1.9-2.25 (m, 2H), 2.25-2.5 (m, 2H), 5.1 (t, 2H), 7.2-7.5 (m, 10H); ^{13}C NMR ($CDCl_3$) δ ppm: 28.9 (t), 30.1 (t), 33.1 (t), 33.4 (t), 40.2 (d), 120.9 (d), 127.9 (d), 128.7 (d), 143.5 (s), 143.6 (d). Elemental analysis; Calculated: C, 42.88; H, 3.81; I, 53.31. Found: C, 42.96; H, 3.85; I, 53.53.

General Techniques. Products from the photolysis of **2** and **5** were quantified by HPLC analysis (**2** - internal standard: benzene; **5** - internal standard: 1,4-di-t-butylbenzene) and identified by comparison to authentic samples.

Products from the low-intensity photolysis of **16** were analyzed by GC and GC-MS and compared to authentic samples synthesized by alternate routes. These product studies were done by Dr. H. Garcia and Dr. M. A. Miranda (Valencia). Details to be published elsewhere.[196] The products from LDP of **16** were quantified by ^{1}H NMR using the signals from the benzylic hydrogens from **16** (5.1: t, 2H), the benzylic hydrogens from **23** (cis and trans; 3.04-3.12: m, 2H and 3.40-3.48: m, 2H) and the olefinic hydrogens from **19** (trans; 6.20 - 6.50: m, 2H)

Products from the photolysis of 2-diazo-1,3-indandione, **30,** were identified by GC-MS. These products were quantified by GC with 1,4-di-t-butylbenzene as internal standard.

Products **49** and **51** (from the photolysis of **43**) were identified by GC-MS. These products were quantified by GC with 1,4-di-t-butylbenzene as internal standard. Products **47** and **50** were quantified by HPLC with 1,4-di-t-butylbenzene as internal standard, these products were also identified by HPLC and comparison to authentic samples (benzoylbenzoic acid, **50**, did not pass through the GC column).

Thermolysis of 5 was done by adding 50 mg of **5** to 25 mL of t-butyl benzene, this solution was then purged with dry nitrogen for 30 minutes. The solution was then refluxed (bp = 169 °C) for 90 minutes under a slow steady stream of nitrogen. GC analysis showed a complex mixture of products, no benzophenone or acetophenone was detected.

Chapter 6. Investigations Concerning Drop Explosion During Laser-Drop Experiments.

6.1 Introduction.

Irradiation of a small droplet of solution by the focused output from a 308 nm excimer laser (~ 10 ns, 60 - 130 mJ/pulse), as described in Chapter 4, causes it to burst in a manner which appears to be similar to the ablation of organic polymers by pulsed UV lasers.[197-199] The mechanism by which the drops explode could have important consequences on the chemistry which occurs within the drop, or its fragments, after irradiation by the laser pulse. The deposition of such a large amount of energy in such a short time frame could very well cause an extreme change in temperature, which in turn could alter the mechanism by which the reactions inside the drop occur (as compared to low-intensity lamp irradiations). Thus, it is important to ascertain whether the change in chemistry which occurs upon laser-drop photolysis is due to multi-photon chemistry or extreme temperatures inside the drops.

In 1982 Srinivasan and co-workers[200,201] reported that irradiation of organic polymers by pulsed UV lasers causes the material at the surface of the polymer to be etched to a depth of 0.1 μm to several microns. The principal advantages of UV laser radiation over either visible or IR laser radiation is the lack of detectable thermal damage to the substrate and the control which can be exercised over the depth of etching by adjusting the number of pulses and/or the fluence of the laser. Because of the control which can be exercised over the etching of material, ablative photodecomposition (APD) has found some lithiographic[202] and medical[203,204] applications.

The physicochemical mechanism (or mechanisms) which are responsible for APD are not clearly understood and there is much debate as to whether it is a predominantly photochemical or photothermal phenomenon. At lower wavelengths (≤ 193 nm), photochemical bond scission is a possible mechanism since there is sufficient energy (> 145 kcal/mol) to break the carbon-carbon single bonds of the polymer backbone. At longer wavelengths, there is not enough energy to break bonds in a monophotonic process and either a photothermal or multiphotonic mechanism must be responsible for the ejection of material at these longer wavelengths.

For most materials, significant etching occurs only when the laser fluence is above a certain threshold. Plots of etch depth/pulse versus the log of the laser fluence give an S-shaped curve[198] such as that shown in Figure 6.1. The threshold fluence is difficult to pinpoint because the etch curve approaches the abscissa asymptotically. The initial region of slight etching is followed by a region which rises steeply in a linear fashion and then levels off at larger fluences. The threshold fluence varies with the wavelength of the laser and the type of material, with larger threshold fluences needed at longer wavelengths (for most polymers the absorption decreases with increasing wavelength). Clean etching at longer wavelengths is observed only for materials with strong absorption at that specific wavelength.[199] If the material does not absorb at the wavelength used, clean etching and control over depth of etching are no longer observed. This has been interpreted as indicating that the photoablation changes from being a predominantly photochemical mechanism to a photothermal process.[198]

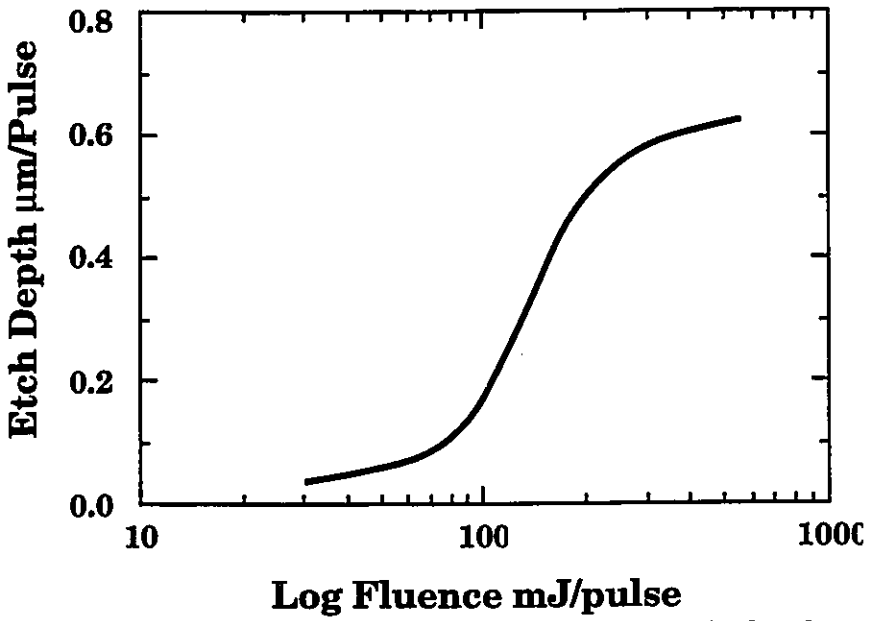

Figure 6.1: Plot showing typical behavior of etch depth with laser fluence.

Since the original reports on APD by Srinivasan et al.[200,201] there have been numerous investigations on the physical aspects of the polymer surface after ablation and the depth of etching as a function of the wavelength of the laser and the material which is irradiated. Although this approach is of great importance for the technological implications of APD, it gives little information as to the dynamics and make-up of the ejection of material during, and immediately after, the laser pulse. Several groups have used various approaches to gain some insight into the processes that lead to the ejection of material.

When a polymer (or other) surface is irradiated by a laser pulse of sufficient fluence to cause ablation a loud audible report can be heard and a bright plume of material is ejected from the surface that produces an intense emission at continuous and discrete wavelengths. Koren and Yeh[205,206] have observed and characterized the emissions resulting from APD for various polymers and graphite in air, helium and under vacuum

with 193, 248 and 351 nm lasers. At fluences near the threshold levels a long-lived (~1 μs), unresolved continuum emission was observed; this was attributed to hot, polyatomic fragments. At fluences above the threshold levels, discrete emissions from C_2, C and CN fragments were observed with 193 and 248 nm lasers, as well as short- and long-lived continuum emissions. It is interesting that CN emissions were observed for polymers (and graphite) which do not contain nitrogen as long as the irradiation was done under an air environment. The short-lived continuum emission was attributed to the free (electron)-to-bound transitions which occur in a plasma. No CN emissions for any of the polymers studied were observed when a 351 nm laser was used. At even higher laser fluences emissions from carbon ions begin to appear.

Another interesting feature found in the investigations by Koren and Yeh[205,206] was a correlation between the rough-to-smooth transition of the ablated polymer surface and the appearance of the C_2 and CN emissions. The authors attribute this to the ablation of the larger polyatomic fragments (which are responsible for the long-lived continuum emission) into the smaller diatomic species. This ablation of the larger fragments would also occur on the surface of the polymer, leaving a smoother etch pit. It was also found that 351 nm ablation does not leave a smooth etch pit, or produce CN emissions, regardless of the laser fluence. These results indicate that ablation above the threshold limits for 193 and 248 nm lasers are caused by multiphoton absorptions while a photothermal mechanism is consistent with 351 nm ablation.

The material which is etched from a polymer surface due to APD is ejected with considerable velocity and directionality. The dynamics of this plume has been the subject of much research. Laser-induced fluorescence

(LIF) has been used to determine the velocity distributions for specific diatomic fragments in the plume for PMMA ablated with a 248 nm laser.[207] It was found that C_2 and CN fragments reach velocities as high as 1×10^6 cm/s, (for comparison, the speed of sound in air is 3.3×10^5 cm/s). However, super-sonic speeds for these fragments were found even when the laser fluence was below the threshold level. Although the intensities from the C_2 emissions increased by a factor of 200 when the laser fluence was increased from below the threshold value (150 mJ/cm^2) to well above it (650 mJ/cm^2), the maximum velocities increased by only 30%. The authors note that production of these fragments, from the polymer, at this velocity would require the energy from three 248 nm photons.[198] It is also interesting that these velocities correspond to a translational temperature of many tens of thousands degrees, but an analysis of the rotational spectrum of the fluorescence shows a rotational temperature of only ~1000 K.[208] This supports a statistical thermodynamic process without complete energy randomization for the thermalization of the ejected diatomic species as suggested by Koren and Yeh.[205,206]

Nanosecond photographic techniques have also been employed in the determination of the velocities of the ejected material caused by APD.[58-61] These studies found that APD (193, 248 and 308 nm) causes a blast wave to be ejected from the surface of a polymer in a hemispherical manner at velocities $>10^5$ cm/s, followed by the ejection of a stream of larger particles normal to the polymer surface traveling at sub-sonic velocities. The blast wave was attributed to small diatomic species, and the larger particles to smaller fragments from the original polymer.

The spectroscopic studies by Koren and Yeh[205,206] and a later study by Davis and co-workers[209] found that the short-lived continuum emission at

fluences above the threshold value began before the laser pulse was over. However, the time response of their detector (30 ns) was not fast enough to resolve the build-up of the emission. A photoacoustic investigation by Dyer and Srinivasan[210] found that a stress wave actually begins a few nanoseconds after the start of the laser pulse for a strongly absorbing polyimide film (Kapton^{TM}) with both 193 and 308 nm laser irradiation, with this time delay shortened with increasing laser fluence. As well, the duration of the signal was shortened with increasing laser fluence for the 308 nm laser, decreasing from about 70 ns to ≤ 25 ns at fluences above the threshold level. For PMMA, at 193 nm, there are two stress waves at fluences close to the threshold region; the authors attribute this behavior to a thermoelastic stress wave preceding the ablation stress wave. At higher fluences the stress wave due to ablation begins to overlap the thermoelastic wave but both are still evident in the oscillogram. The authors conclude that, although temperatures as high as 800 K are reached, this in itself is not adequate to account for the rapid ejection of material and a substantial photochemical process must be responsible.

Another aspect of the APD of polymers which do not have significant absorption at the wavelengths of the laser is the need for *incubation pulses*. UV laser ablation is usually carried out with a succession of pulses and the etch depth is a linear function of the number of pulses. Measurements of the etch depth per pulse are usually calculated by dividing the total depth by the number of pulses; this type of measurement assumes that the etch depth per pulse is constant. This assumption has been found to be correct when a large number of pulses are used. However, it has been shown that the first few pulses do not etch the material significantly, and in fact sometimes cause a slight elevation at the surface of the material.[59] Kuper

and Stuke[211] detected a buildup of new absorptions in PMMA subject to UV radiation and suggested that incubation pulses were necessary to change the absorption properties of the virgin, non-absorbing material so that subsequent pulses are no longer irradiating a non-absorbing surface.

Recently, Srinivasan and Ghosh[212] have reported that liquid benzene can also undergo APD with 248 and 308 nm laser pulses. With 248 nm laser pulses at fluences of 100 to 400 mJ/cm^2 these authors report the formation of dimeric products which are not formed at lower laser fluences, at even higher laser fluences the solutions turn black and elemental carbon precipitates from the solution. Similar results were obtained by irradiation with 308 nm laser pulses, however, the APD threshold was 1000 mJ/cm^2. Since benzene does not absorb at 308 nm the authors attributed the APD at this wavelength to multiphoton excitation of benzene. It is noteworthy that 248 nm laser irradiation of liquid acetone at the same fluences did not cause ablative decomposition.

In view of the extreme temperatures which have been shown to occur during the APD of organic polymers, regardless of whether it is due to a photothermal or photochemical mechanism, gives rise to some concern as to the temperature changes which occur in the solvent during laser-drop photolysis. We felt that it was necessary to address this issue and attempts to measure the temperature of the drop using pyrene excimer thermometry,[213] as well as nanosecond photographs of the exploding drops are described in this chapter.

6.2 Results.

6.2.1 Fluorescence Spectra in Drops.

Emission from an excited molecule which forms a complex with a ground state molecule (or molecules) will frequently be at longer wavelengths than emission from the uncomplexed excited molecule. If this complex is only stable in the excited state and dissociates into its component parts after transition to the ground state it is known as an exciplex, if the complex is between an excited and ground state of the same molecule it is called an excimer.[131,214] Because there is no association of the ground state molecules the emission shows no vibrational structure. The excimer emission of pyrene is well known and has often been used to probe molecular mobility in constrained media. At ambient temperatures an equilibrium can be achieved between the excimer and monomer species. At higher temperatures the equilibrium is shifted towards the monomers, causing a greater degree of emission from the monomer species. Thus, the ratio of the monomer-to-excimer emissions can also be used to probe the temperature in environments where an equilibrium can be established.[215]

As mentioned in Chapter 4, when methanol solutions of 1,1-diphenylacetone were subject to 308 nm LDP a bright green emission could be seen originating from the drop prior to its explosion. The emission spectrum (Figure 4.6) agrees well with previously reported spectra for the excited diphenylmethyl radical.[26,92] When drops of spectral grade methanol or acetonitrile were subject to 308 nm LDP no emissions could be detected either by the naked eye or with LFP fluorescence detection. It is interesting that true fluorescence from the drops is easily discernible by the naked eye, the entire drop is illuminated so that it looks like a small, coloured 'light bulb'. By contrast, when a drop with no fluorescent material is irradiated,

only a small portion of the drop is illuminated, in the size and shape of the laser beam as it impinges upon the drop, this is probably due to scattered light from the surface of the drop.

The emission spectrum from LDP (fluence: ~500 mJ/cm^2) of deaerated, 160 μM solutions of pyrene in hexane clearly show both monomer and excimer emissions centered at 390 and 470 nm respectively. By comparison, the LFP emission spectrum for the same solutions (at ~25 ^{o}C) in a conventional laser-flash cell show two bands centered at 390 and 460 nm. Figure 6.2 shows these emission spectra normalized at 380 nm. The apparent red-shift of the LDP emission is likely due to the large errors (± 10%) introduced in the emission intensities due to the non-uniformity of the drop size during data acquisition.

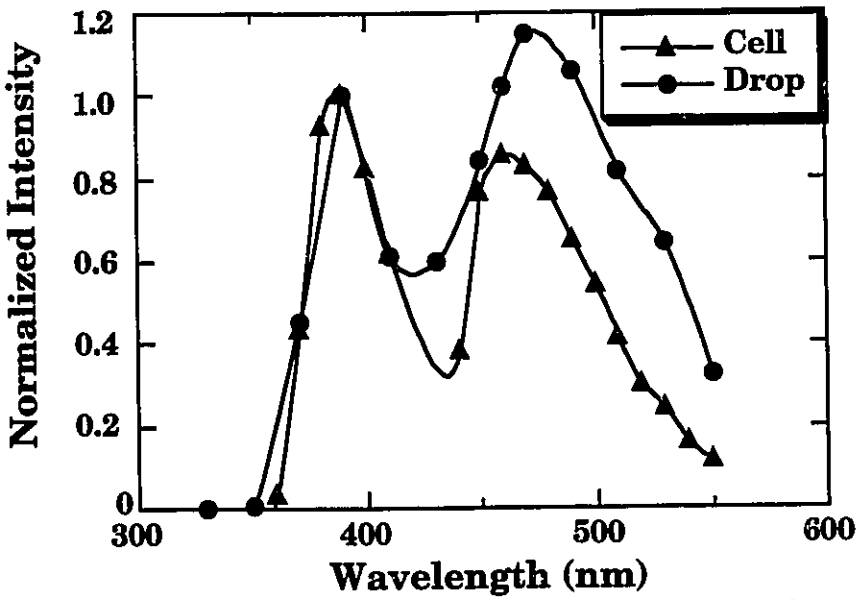

Figure 6.2: Fluorescence spectra of 160 μM pyrene in hexanes. Under normal and laser-drop conditions.

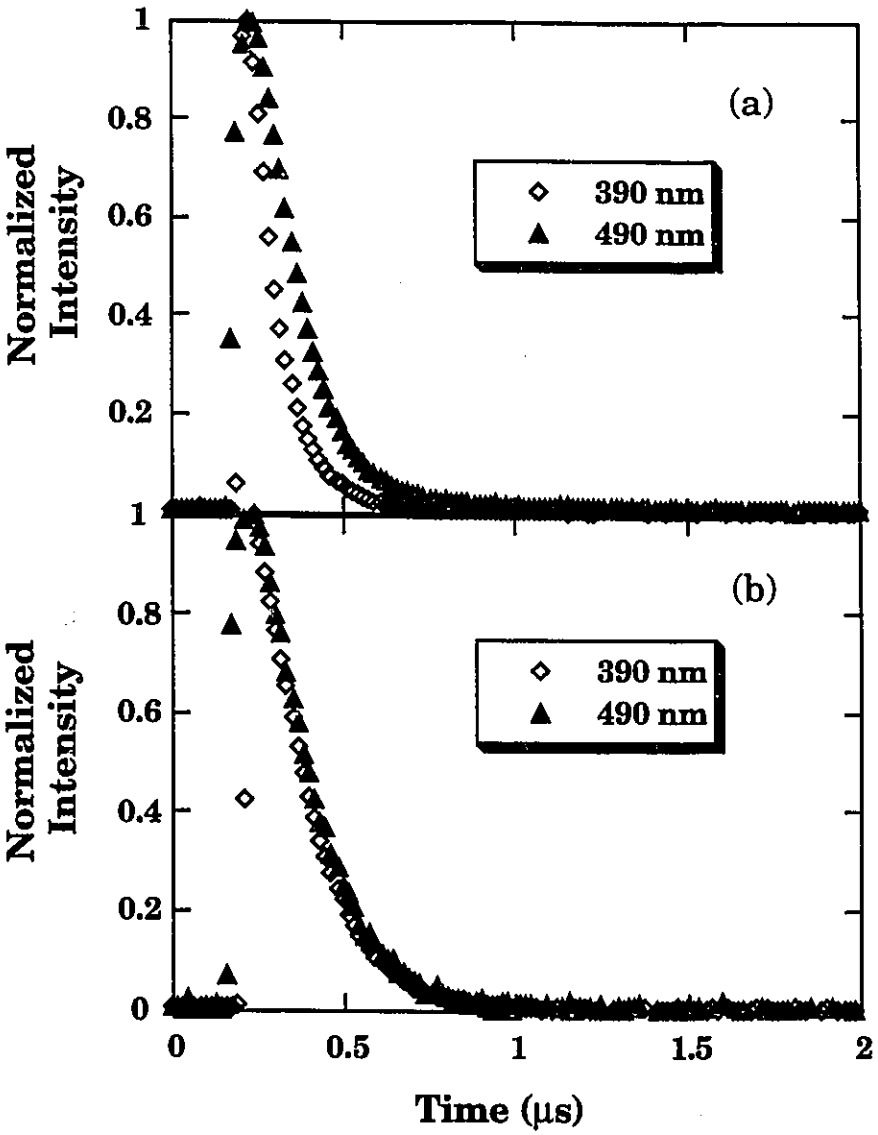

Figure 6.3: Fluorescence decays of the monomer and excimer emissions from 160 μM pyrene in hexanes. (a) Under laser-drop conditions. (b) In a LFP cell under normal LFP conditions.

Wells and Melton[213] have shown that the ratio of monomer to excimer emission of pyrene increases with increasing temperature. The results shown in Figure 6.2 would appear to indicate that the temperature of the drops actually decreases upon laser-drop irradiation. In order for pyrene emission thermometry to accurately measure temperatures it is

essential that a state of equilibrium between the excited singlet and the excimer is achieved. If an equilibrium between these two species is achieved, the lifetimes for the excited singlet and the excimer would be identical. The lifetimes for the excited singlet and the excimer during LDP are 89 and 125 ns respectively. Figure 6.3a shows the decay traces for the emissions from LDP at 390 and 490 nm. The lifetimes for the emissions from both bands in the conventional laser cell are the same, 160 ns, as shown in Figure 6.3b.

It is known that molecular oxygen can quench the fluorescence from both the monomer and the excimer,[214] with the excimer exhibiting more efficient quenching than the monomer. It is clear from the lifetimes that this is not the case here since the monomer emission is shorter-lived, indicating that the non-equilibrium state must be due to factors other than oxygen contamination. It has been previously shown that the lifetime for the excited diphenylmethyl radical is considerably shorter under laser-drop conditions (section 4.2.2), and in micelles.[93] It seems likely that the high concentration of excited states under laser-drop conditions is responsible for the non-equilibrium behavior in this case.

6.2.2 Nanosecond Photography.

Photographs of the drops can be taken during the course of their explosion using a conventional camera and film by using a flash source that is shorter than the dynamics of the explosion. We have modified a technique described by Srinivasan[58-61] which utilizes the narrow pulse width of an excimer laser as the flash for the camera. This method was developed in collaboration with Dr. B. R. Arnold. This is done in a manner similar to a TLTC-LFP experiment, except in this case the second laser is

used to irradiate a 460 nm fluorescent laser dye held in a quartz test tube. The light emitted from the dye (460 nm) is used to expose the film and capture the image of the exploding drop for a period of ~10 ns. By selecting different time delays for the firing of the second laser the dynamics of the explosion can be seen as a series of photographs. These photographs were scanned and converted to digital images. The digital images could be enlarged and either viewed on the computer screen or good quality facsimiles printed from a laser printer. Figure 6.4 shows the actual size of one such photographic facsimile along with the same imaged enlarged 8 times. Full experimental details for this technique are given in Chapter 2.

Figure 6.5 shows a photograph during LDP of a droplet of hexane containing 160 μM pyrene. This photograph was taken without the photographic 'flash' laser, thus, the pyrene emission was the source of light for the film, and the exposure time was approximately 125 ns (the lifetime of the excimer emission under laser-drop conditions, *vide infra*). It can be seen from this photograph that the entire drop is illluminated by the pyrene emission. Note also that this droplet was irradiated just before it would have dropped spontaneously from its increasing weight. Smaller drops are more spherical in shape (as can be seen from Figure 6.4).

Figure 6.6 shows photographs for the LDP of acetone and acetonitrile at delay times of 1, 2, 5, and 10 μs after the LDP laser pulse, the arrows show the direction of the LDP laser pulse. Acetonitrile is transparent at 308 nm while acetone has an extinction coefficient of ~5 $M^{-1}cm^{-1}$ (for acetone vapor),[216] making the drops virtually opaque at this wavelength. Note that there is a small amount of fluorescence at the edge of the drops in the photographs of the acetone drops, this appears as a zero time 'ghost' image in all of the acetone pictures. This ghost image is less evident in the

acetonitrile pictures, but a ghost image of the drop can be seen in the 2 ms picture (Figure 6.7). The syringe needle has an outside diameter of 0.80 mm and was used to calculate the diameter of the drops, and the distance traveled by the ejected material. The acetone drops averaged 2.2 ± 0.2 mm in diameter (5.6 ± 1.5 μl) and the acetonitrile drops averaged 2.4 ± 0.2 mm in diameter (7.2 ± 1.6 μl). The laser fluence for these pictures was ~800 mJ/cm^2.

After 1 μs the acetonitrile drop is still mostly intact, but there appears to be some damage to the side opposite to the site of irradiation. The acetone drop clearly shows that some material has been ejected to a distance of about 300 μm in the direction opposite to the laser. After 2 μs the acetonitrile shows ejection of material in the same direction as the laser pulse. The material ejected from the acetone drop is spreading out as well as moving away from the drop to about 600 μm. At 5 μs it is obvious that the material ejected from the acetone drop is moving away and spreading out in a fan-like fashion. Although the material ejected from acetonitrile shows some spread, it is moving away in a more cylindrical fashion than the acetone drops. After 10 μs, the ejected material from the acetonitrile drop has begun to lose its cylindrical shape.

The distances traveled by the material ejected from the acetonitrile drop are 800 and 1700 μm at 4 and 7 μs respectively. It should be noted that the errors in the calculation of distances may be as large as 25% at early time delays (≤2 μs) and are minimum distances since it is assumed that the ejected material is traveling in the plane of the two-dimensional photographs. The error in measurements at longer time scales would be considerably less due to a smaller angle of deviation from the photographic plane (because the material spreads laterally as well as linearly), however,

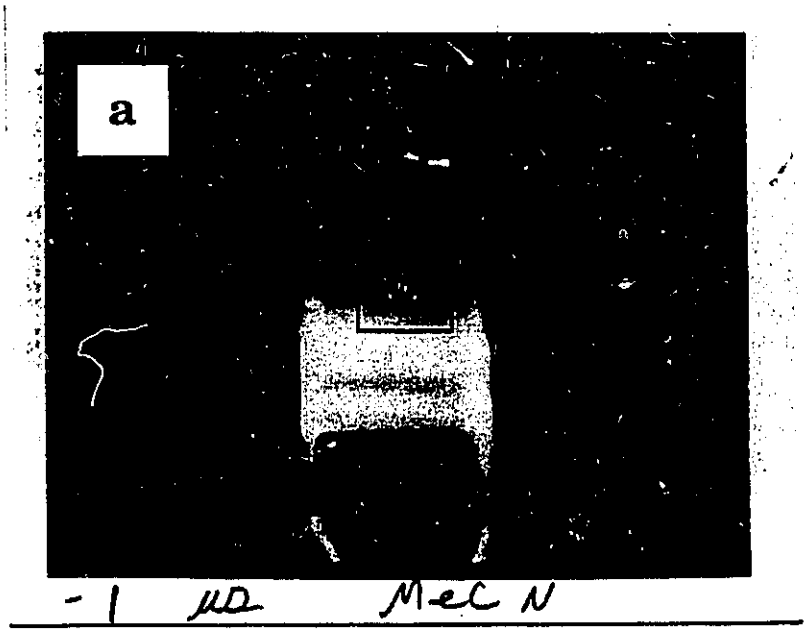

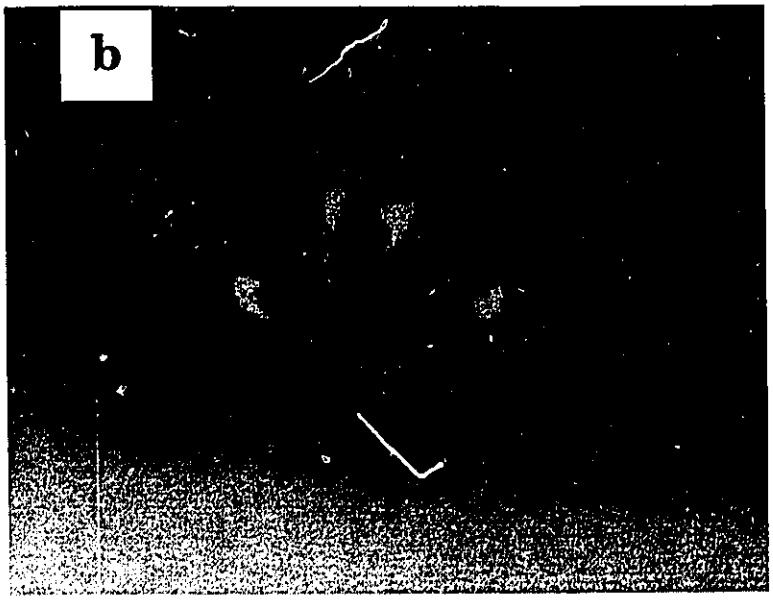

Figure 6.4: Scanned image of Polaroid photograph of acetonitrile 1 μs after the LDP laser pulse; a) actual size, b) enlarged ~8 times.

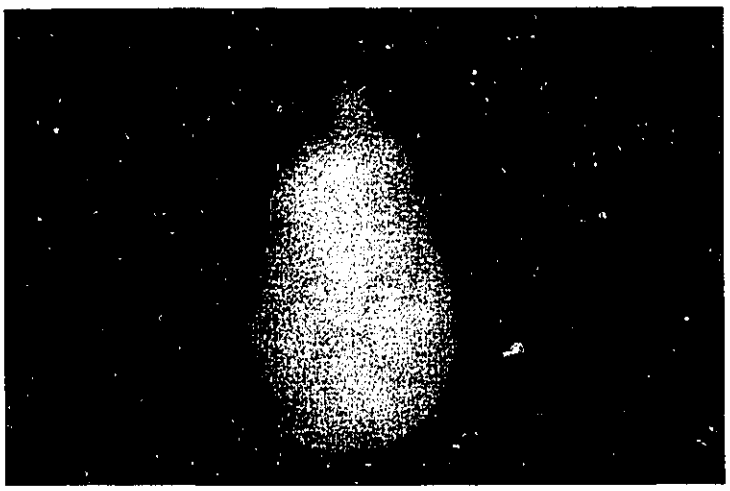

Figure 6.5: Photograph of hexane drop containing 160 μM pyrene. No flash laser used (see text).

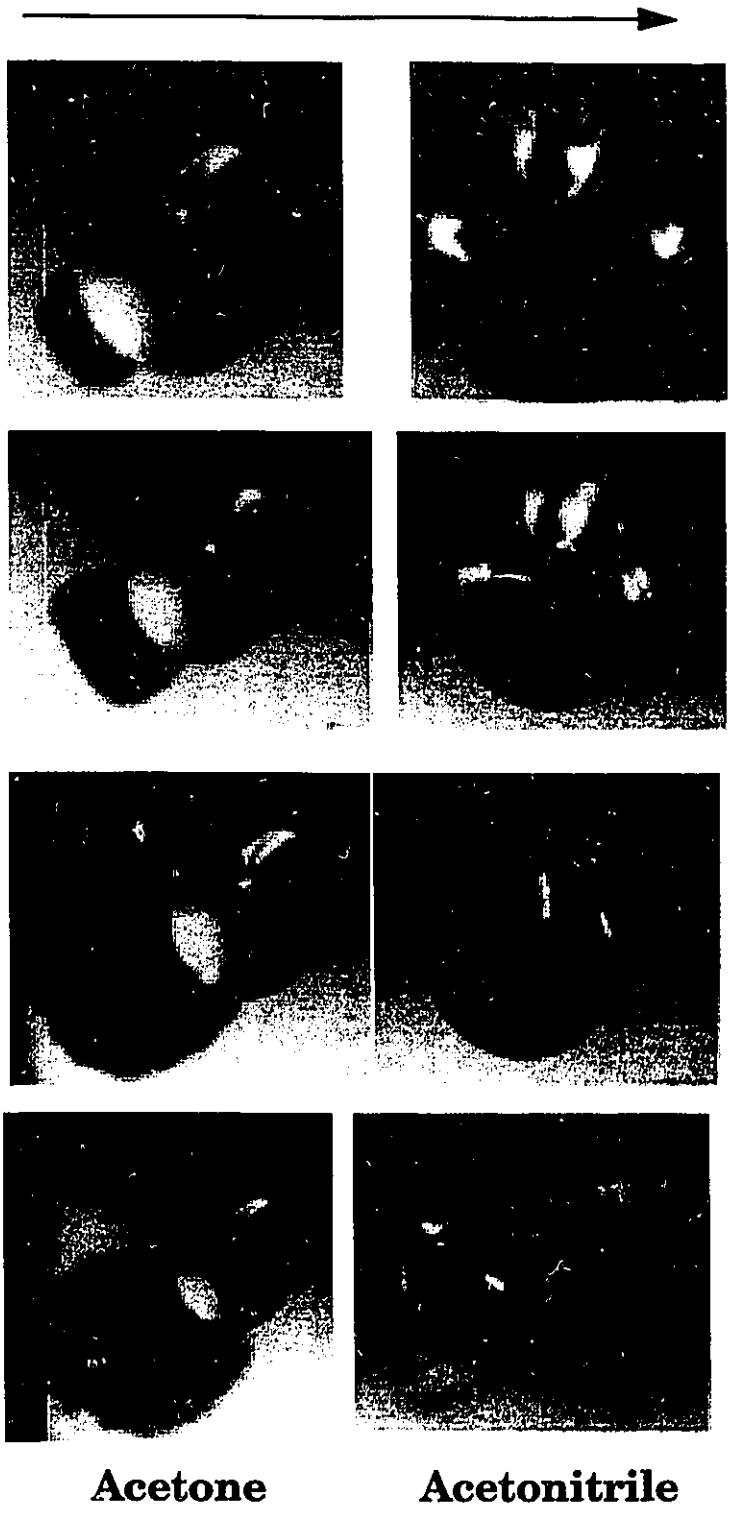

Figure 6.6: Nanosecond photographs of acetone and acetonitrile at delay times of: a) 1 μs, b) 2 μs, c) 5 μs, d) 10 μs. Arrow at the top of the pictures indicates the direction of the laser.

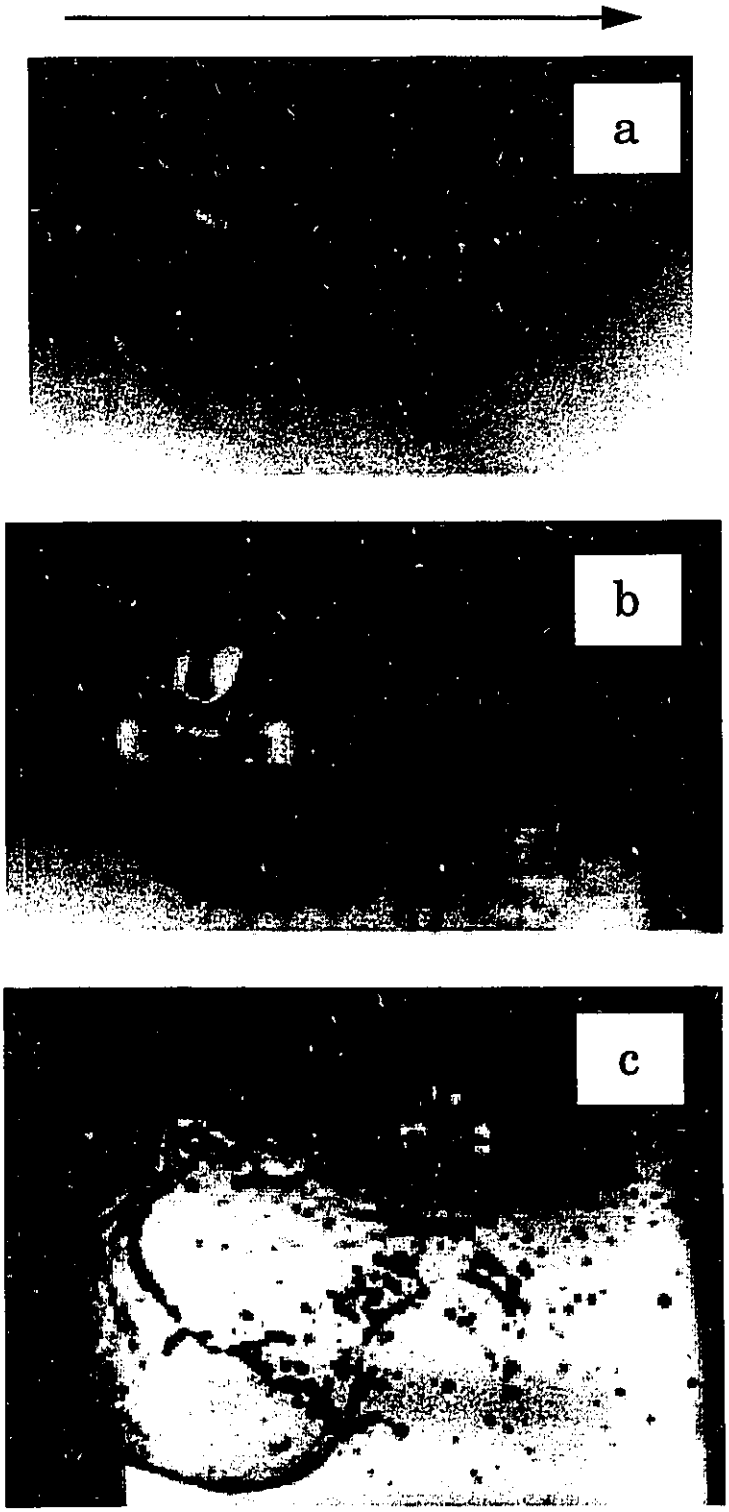

Figure 6.7: Nanosecond photographs of acetonitrile at delay times of: a) 30 μs, b) 100 μs, c) 2 ms. Arrow at the top of the pictures indicates the direction of the laser.

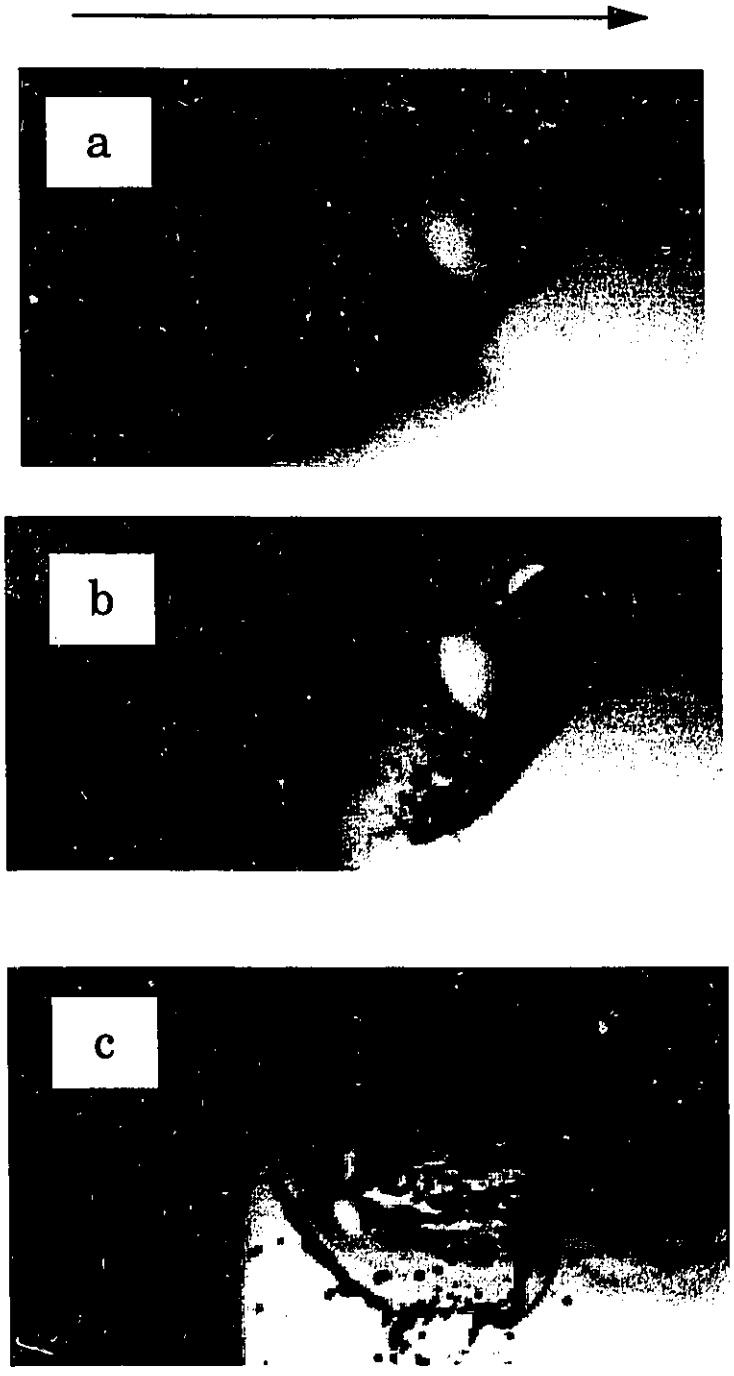

Figure 6.8: Nanosecond photographs of acetone at delay times of: a) 30 μs, b) 200 μs, c) 2 ms. Arrow at the top of the pictures indicates the direction of the laser.

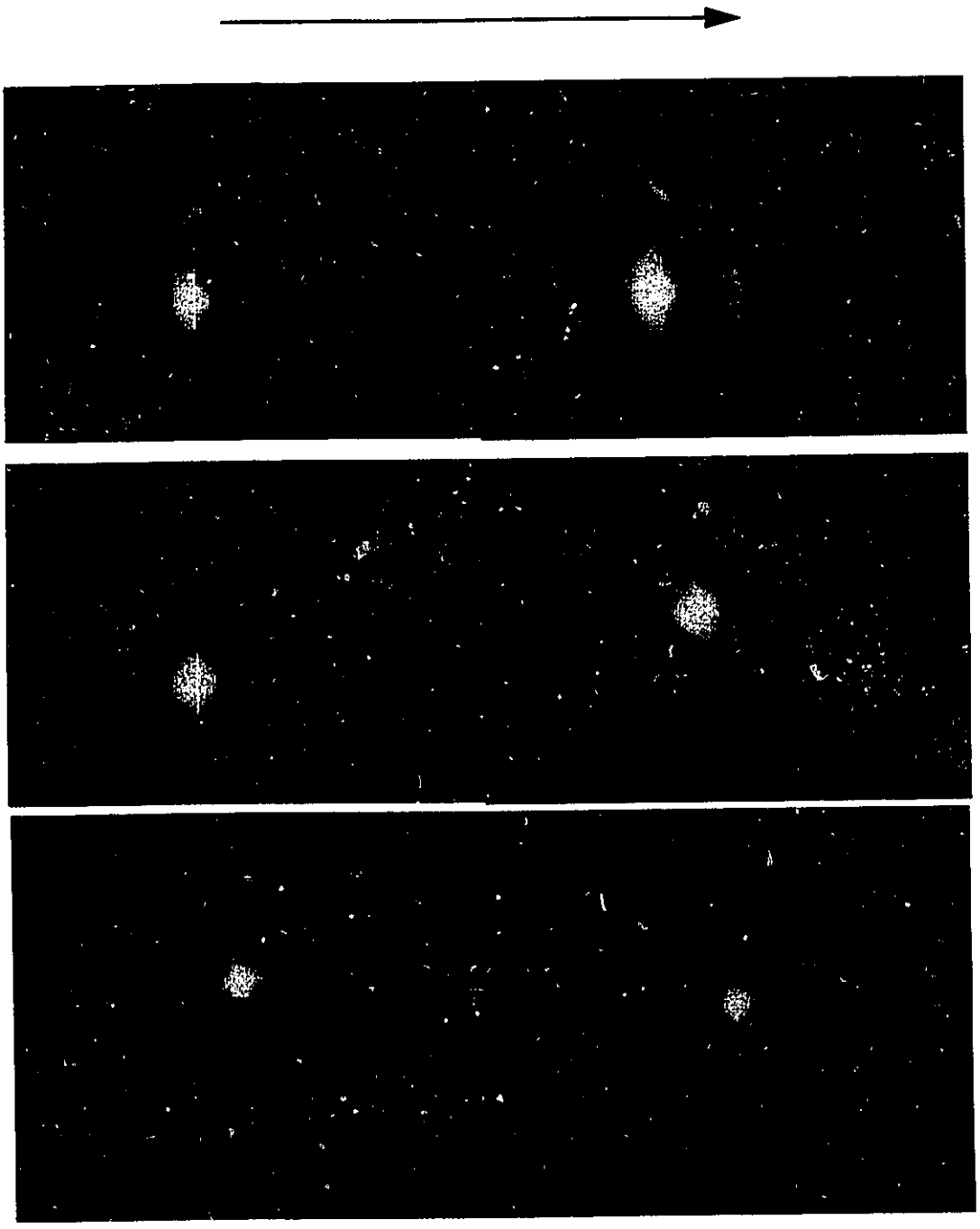

Figure 6.9: Nanosecond photographs of hexane drops with 9-bromophenanthrene at delay times of: a) 1 μs, b) 3 μs, c) 4 μs, d) 8 μs, e) 15 μs, f) 30 μs. Arrow at the top of the pictures indicates the direction of the laser.

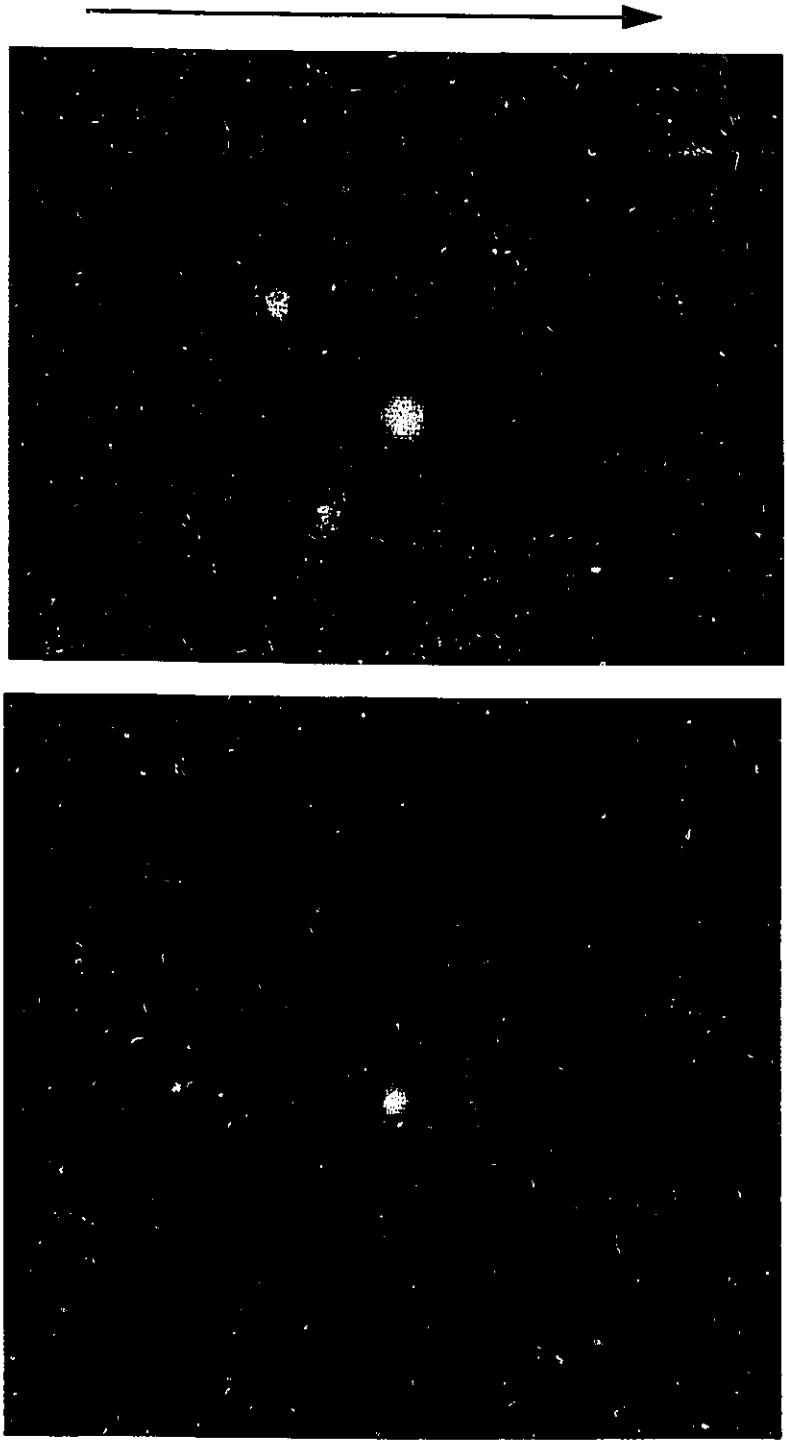

Figure 6.10: Nanosecond photographs of hexane drops with 9-bromophenanthrene at delay times of: a) 100 μs, b) 1 ms. Arrow at the top of the pictures indicates the direction of the laser.

velocities determined by the distance traveled between two time delays will still have a large error associated with them because of the large error at earlier time delays. The ejected material at the front of the moving stream of material from both drops have initial velocities of about 300 m/s.

Up to about 10 μs the bulk of the drops were still intact (had not yet fragmented). The material ejected from the acetone drop is made up of a much smaller fragments and appears as a finer 'mist' than the material ejected from the acetonitrile drop. Figure 6.7 shows the acetonitrile drops at longer delay times. At about 30 μs the remaining portion of acetonitrile began to lose its cohesion and starts to be destroyed. It is clear in the 100 μs delay photograph that a large portion of the remaining acetonitrile drop is moving in a direction that is opposite to that of the initially ejected material. At 2 ms the drop has been removed from the needle and virtually destroyed. Figure 6.8 shows the acetone drops at longer delay times. At 30 μs the acetone drop shows a deformation on the side of the drop opposite to that of the initially irradiated edge. The back of this deformation is approximately half the distance from the irradiated edge of the drop as the material which was initially ejected in the opposite direction. As well, there is considerable movement of material in all directions away from the irradiated edge of the drop. At 100 μs the acetone drop has begun to 'open' up, with material moving away from the irradiated edge in all directions.

Photographs were also taken of cyclohexane drops containing 9-bromophenanthrene at a concentration such that the absorption through the diameter of the drops was ~0.15. This absorption corresponds approximately to the absorption of drops for the LDP product studies mentioned in previous chapters (except for the LDP of cumyl peroxides where the absorptions were considerably less). The average diameter for

these drops was 2.7 ± 0.2 mm (10.3 ± 2.0 μl). These pictures also show a strong ghost image, but it is most probably reflected laser light, since these were the first photographs taken, there was no 345 nm cut-off filter placed in front of the camera lens. A photograph taken with no flash source shows a weak fluorescence emanating from the drop in the same manner as the pyrene drop in Figure 6.4, the scattered laser light also appears in this photograph and is much stronger than the fluorescence.

Figure 6.9 shows these drops at delay times from 1 to 30 μs. No visible damage is seen in these drops until 3 μs, when some material is ejected from the side of the drop opposite to that of the irradiated edge. At 4 μs it is evident that material is ejected from both sides of the drop. In the 8 and 15 μs photographs the damage to the drop has progressed, but appears similar to the 4 μs drop. At 30 μs a new area of damage appears on the upper right hand portion of the drop. Figure 6.10 shows the drop at longer delay times, the drops appear to be disintegrating in all directions After 1 ms the drop is completely destroyed, Figure 6.10 shows the drop at delay times of 100 μs and 2 ms, there is approximately equal amounts of material on both sides of the ghost image.

6.3 Discussion.

Because there was no equilibrium established between the excited singlet of pyrene and the pyrene excimer during LDP it was not possible to use their relative emission intensities to determine quantitatively the temperature of the drops.[213] However, in spite of this, since the changes in pyrene emission are not dramatic, the temperature probably does not change much. Particularly, when the lifetimes for the excimer emission in the drop and the cell are considered (125 and 160 ns respectively). The

shortened lifetime of the excimer in the drops is more likely due to the non-equilibrium state than any temperature increase in the solvent.

The emission studies are also informative because of the lack of emissions from either diatomic species or the free-to-bound emissions found in a plasma. These emissions are easily detectable during the APD for a number of organic polymers[205,206] and can in fact be seen by the naked eye.[198] This indicates that the liquids are not undergoing ablative photodecomposition.

The nanosecond photographs of drops during LDP indicate that different mechanisms are responsible for the destruction of the drops for acetone and acetonitrile. This is most probably a result of the different absorptivities of the two drops. In the case of acetone, which is virtually opaque at 308 nm, 90% of the energy from the laser pulse is deposited in the first 150 μm of the drop (this corresponds to the distance at which the absorbance is 1, c = 13.6 M, $\varepsilon = 5\ M^{-1}cm^{-1}$). This represents a volume of about 0.5 μl, if 90 mJ (90% of 100 mJ, the energy of the laser pulse) are deposited and converted into heat in this volume of acetone, the temperature change would be 160° (C = 0.31 cal/K.g).

Although it is difficult to quantify the amount of energy which is converted into heat under laser-drop conditions, it seems very likely that the actual temperature increase in the case of acetone would be enough to superheat the liquid, which in turn results in a rapid volume increase due to vaporization. This volume increase will cause the pressure of the liquid inside the drop to increase. Since the penetration of the energy is limited to just inside the edge of the drop, the rapid volume explosion would first be seen at this edge. Once the volume explosion has overcome the surface tension of the drop at this edge, material will be ejected because of the

pressure differential between the inside and outside of the drop. This in turn will begin to push the bulk of the drop in the opposite direction (conservation of momentum), in much the same manner as a balloon when a small hole is made in one side (of course this must be done without popping the balloon). As the volume expansion progresses, it will begin to open up the drop from the irradiated edge as seen in the photographs.

In the case of acetonitrile, the drop is transparent at the wavelength of the laser, and the laser light will penetrate further than the acetone drops. From the photographs it is clear that the material is ejected from the side opposite to the irradiated edge, which is exactly opposite to the case of acetone. Thus it is safe to assume that the light does indeed penetrate further into the acetonitrile drop.

It is well known that when light traveling through a transparent medium encounters a boundary leading into another transparent medium, part of the light is reflected and part enters the second medium. The light which enters the second medium will be deflected at the boundary by an angle which depends on the angle of incidence and the refractive index of the two media. Lenses make use of this principle to focus an image by the refraction of light through a transparent, spherical surface. Since the acetonitrile drops are transparent spheres, they will act as a lens and concentrate the incident laser irradiation inside the drop during laser-drop photolysis. The focal length of a lens is dependent on the radius of curvature of the surface and its index of refraction[202] and is given by equation 6.1 where f is the focal length of the lens, n is the refractive index of the lens material, and r is the radius of curvature of the spherical surface. Application of equation 6.1 to drops of acetonitrile with r = 1.2 μm

$$f = nr/(n-1) \qquad (6.1)$$

(n = 1.34) gives a focal length of 4.7 μm. The refractive index used in this calculation is the refractive index for acetonitrile at the sodium D line (589 nm), strictly speaking, it should be the value at the wavelength of the laser, however, the refractive index for organic liquids does not change considerably with wavelength and in fact increases with decreasing wavelength which would result in a shorter focal length.

When the laser pulse first enters the acetonitrile drop it has insufficient flux to cause localized heating of the solvent. As the light penetrates further into the drop, it becomes focused by the lensing action of the drop. At some point before it exits the acetonitrile drop the flux must become sufficient to heat the drop to an extent which is large enough to cause a volume expansion which results in the ejection of material in a manner similar to that for the acetone drops. Judging by the fact that material is ejected from the rear of the drop it seems likely that the light penetrates well past the mid-point of the drop before it causes any significant heating.

The exact mechanism which is responsible for the heating of the solvent at some threshold level is hard to surmise, it could be that small amounts of impurities in the solvent are responsible for the initial absorptions which cause the absorption of the drop to increase. This impurity mechanism has been proposed for the ablative destruction of quartz by lasers which emit at wavelengths at which the material is apparently transparent.[57] Another possibility is that micron sized dust particles in the solvent act as black bodies which cause localized heating.

Although the model discussed above for the destruction of absorbing and non-absorbing drops is speculative in nature, more information would be needed to characterize the exact mechanism, it is fully consistent with the photographs. Furthermore, it can be used to explain the dynamics of the drops doped with 9-bromophenanthrene. In this case the flux needed to cause a volume explosion is smaller due to the absorbing dopant, thus the explosion occurs at a smaller penetration depth inside the drop, if this volume explosion transpires near the center of the drop, ejection of material will begin at both sides of the drop simultaneously. As well, destruction of these drops does not begin until about 3 μs after the laser pulse, and the material is ejected at a much lower velocity, about 65 m/s. This indicates that a large portion of the initial momentum of the volume explosion has been transferred to a greater mass of material. The initial absorption of the doped drops cannot be used to determine the transmittance of light (and thus penetration depth) because the transients produced also have large extinction coefficients at the wavelength of the laser and the absorbance of the drops will change during the course of laser pulse. This is, for example, the case for 9-bromophenanthrene.[217]

The actual temperature changes which occur during LDP could not be adequately determined from the studies discussed here, but further discussion of some the chemistry which has been mentioned in previous chapters is informative for a qualitative sense of the temperature changes which may occur. Consider that the conversion for the LDP of 1,1-diphenylacetone in methanol is 19% after one cycle (see section 4.2.2), if this reaction were due solely to an increase of the temperature, then at least 19% of the volume of the drop must be subject to the temperature changes necessary to overcome the activation barrier for this reaction. This

corresponds to a volume of ~2 μl; if 100 mJ are deposited and converted into heat in this volume of methanol, the temperature change would be 20°, thus the temperature inside the drop would be around 45° C. This upper limit to Δt indicates that insufficient thermal energy is released to cause the cleavage of a carbon-carbon bond.

It should also be considered that any increase in the temperature of the solvent after LDP would be quickly dissipated as the ejected material comes in contact with the walls of the laser-drop cell, certainly any temperature increase will not last more than a few seconds, and probably much less. It would require very extreme temperatures to convert 19% of the starting material in such a short time. Thus when the starting material conversions are taken into account, along with the heat capacities of the solvents, any temperature increase in the drops (or its fragments) is insufficient to account for the differences seen in the chemistry of the intermediates.

6.4 Conclusion.

The destruction of small liquid drops by their irradiation with the focused output from a 308 nm pulsed laser has been shown to occur in the μs time scale. A model has been proposed which adequately explains this phenomenon for both absorbing and non-absorbing drops. Although the temperature increase which must accompany the explosion could not be measured quantitatively, emissions from pyrene suggest that the temperature increase is not more than a few tens of degrees. The high conversion of substrates subject to laser-drop irradiation cannot be explained by thermal process and must be the result of photochemical processes.

6.5 Experimental.

Details for fluorescence LFP and nanosecond photography are given in Chapter 2. The Polaroid photographs were scanned by a Microtek 600GS digital scanner with Adobe Photoshop 2.5.1 software. The scanned images were enlarged for viewing and printing. No digital enhancement was done on the scanned images.

Chapter 7: Final Comments and New Directions

We have shown that the selectivity for the fragmentation pathways of radicals can be severely altered by electronic excitation of the radical. The α,α-dialkoxybenzyl radicals discussed in Chapter 3 show little selectivity from the excited state. It is interesting that the excited 1,1-diphenylethoxyl radical shows very little selectivity towards β-scission, producing both methyl and phenyl radicals in almost equal amounts, while the excited cumyloxyl radical shows complete selectivity to form only methyl radicals (Chapter 5). It is known that substitution has a large effect on the position of the visible absorption band of benzyloxyl type radicals.[108,115] Thus, it is certain that one aromatic ring must be involved in the electronic transition responsible for the visible absorption band. It would be interesting to study the effect of substitution on the aromatic rings of the 1,1-diphenylethoxyl radical towards the selectivity of the β-scission reaction from the excited radical. It is feasible that, depending on the electronic nature of the aromatic substituent(s), some selectivity for the ejection of the phenyl radicals may be observed.

Although indirect evidence for hypervalent iodine radicals such as those discussed in Chapter 5 has been previously reported,[142-146] and there is at least one case where the detection of such a radical has been "tentatively" proposed,[156] the report contained herein is, to date, the best evidence for such a radical intermediate. Since it is now known that these radicals have suitable absorption properties for LFP investigations it should be possible to examine the reactivity of these species with various substrates and in different solvents. Preliminary LFP investigations on the

photochemistry of 1,5-diiodopentane in polar solvents show drastically different behavior than the same compounds in cyclohexane. Considering the stability of iodonium ions, it would be interesting to examine the electron donor properties of these types of radicals. Measurement of their oxidation potentials by photomodulation voltammetry should be possible.[218]

This thesis has reported the LDP results for a number of chemical systems. As one might guess, we have investigated a number of other chemical systems which were not reported because the laser-drop and low intensity photolysis gave the same products and product ratios. A few systems were not pursued because of the complexity of the laser-drop photolysis products. Chart 7.1 shows the structures for the compounds which were subject to LDP but not pursued. A general procedure for laser drop photolysis is to dilute the compound to be studied in the desired solvent so that the 308 nm absorption in a 1 cm cell is between about 0.3 and 1.0. If the extinction coefficient is very large it may be necessary to photolyze a large quantity in order to get enough product for analysis.

As can be seen from Chart 7.1 we have tried LDP on a number of α-diazoketones. All of these compounds are known to form ketenes upon photolysis. It was hoped that the two-photon chemistry of these compounds would result in the further photolysis of the ketenes to form the corresponding carbenes by photodecarbonylation. However, the photochemistry of these compounds was not altered by 308 nm laser-drop photolysis. A large part of this problem may be the small extinction coefficients of the ketenes at 308 nm. This problem may be overcome by using shorter wavelength pulsed lasers for the LDP laser. We have limited ourselves to the 308 nm excimer laser because, until recently, it was the only laser we had available which could deliver more than ~30 mJ/pulse of

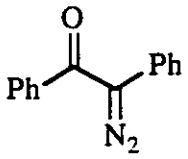

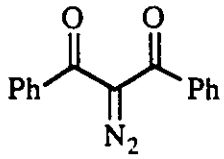

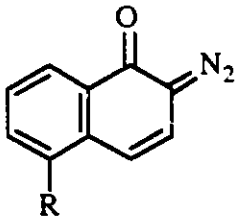

R = H, SO_3Ph, SO_3Me

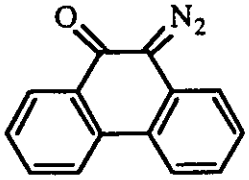

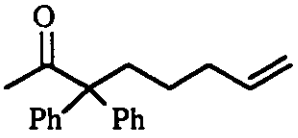

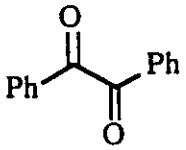

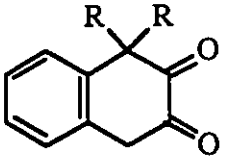

R = H, Me

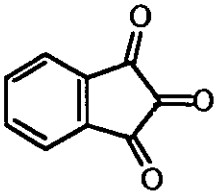

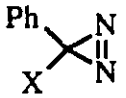

X = Cl, Br

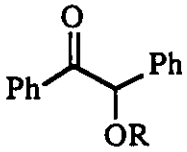

R = Me, i-Pr

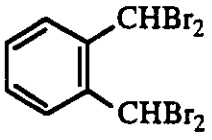

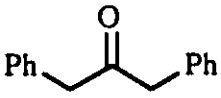

Chart 7.1

UV radiation. Attempts were made to use some of the other lasers for LDP, but the conversions were very small which made product analysis difficult. Another problem which arises with these short wavelengths is that the

extinction coefficients are often so large that the compounds must be diluted to μM concentrations or less. This means that large amounts of solution would have to be photolyzed in order to obtain semi-preparative amounts of product.

One of the excimer lasers has recently been equipped to operate with a Kr/F_2 gas mixture which gives ~120 mJ/pulse at 248 nm. Many of the α-diazoketones listed in Chart 7.1 should be re-examined using 248 nm LDP. As well, photons of this wavelength are much higher in energy than 308 nm photons; this may result in different phenomena and/or chemistry during LDP as has been proposed for the case of ablative photodecomposition (see Chapter 6). Srinivasan has investigated the products which result from the APD of liquid benzene at 248 nm.[212] Although they reported several products, the conversions were very low because these experiments were done on bulk liquids with several laser shots. It should be possible to produce these products in much higher yields with 248 nm LDP.

As section 5.5 showed, the LDP of ortho-methylbenzophenone was not quite as efficient as the LJP of the same compound.[191] One reason for the difference in efficiency may be that the argon ion laser has longer wavelength emissions (333 - 364 nm) than what we have used for laser-drop photolysis. Wilson also showed that the efficiency could be increased by the additional output from another cw laser which emitted in the visible region of the spectrum.[191] It may be possible to perform two-laser two-colour laser drop photolysis experiments. This technique would overcome the problems which occur when the transients produced absorbs in a different region than their precursors. The nanosecond photographs (Chapter 6) have shown that there is sufficient time between the firing of the laser and the

destruction of the drops so that a second laser could impinge upon the drop before it has been destroyed. There may be some initial problems associated with the spatial overlap of the focused laser beams, but it is not expected that these problems would be insurmountable.

An in depth study of the processes involved in the destruction of the drops during LDP was beyond the scope of this thesis. We have done some preliminary investigations into these processes (Chapter 6) and proposed a model which adequately describes the dynamics of drop explosion for strongly absorbing, weakly absorbing, and transparent drops. Additional nanosecond photographic experiments under variable conditions (flux, effect of dopants, etc.) would be helpful in assessing the validity of this model. Also, our investigation could not quantify the thermal changes which occur during LDP, but it seems that the overall temperature changes (the average temperature increase for the entire drop) are not large. Time resolved Raman spectroscopy could possibly be used to quantify the thermal changes, as well as the dynamics of these changes, which occur during LDP.

Claims to Original Research

1. Development of the laser-drop photolysis technique. This technique is suitable for the preparation of multiple photon reaction products in semi-preparative yields utilizing pulsed lasers.

2. The first reports on the selectivity of the fragmentation pathways for electronically excited radicals. This includes the quantum yield for the fragmentation of α,α-dimethoxybenzyl radical (0.80), an important intermediate involved in free radical photopolymerizations. Also the first report for photoinduced β-scission of t-alkoxyl radicals.

3. Detection of a hypervalent iodine radical. This is the first report to detect and characterize the ground state, as well as the excited state, reaction pathways for such a radical.

4. Nanosecond photographs of the dynamics of the explosion of small liquid drops subject to high-intensity, pulsed, UV radiation.

5. The intermediacy of an unusual propadienone-ketene intermediate, and the possible intermediacy of a dienol diester, in the high-intensity photolysis of 2-diazo-1,3-indandione.

References

(1) Roth, H. D. *Angew. Chem. Int. Ed. Engl.* **1989**, *28*, 1193.

(2) Laidler, K. J. *Chemical Kinetics;* 3rd ed.; Harper & Row: New York, 1987

(3) Norrish, R. G. W.; Porter, G. *Nature* **1949**, *164*, 658.

(4) Kasha, M. *Disc. Faraday Soc.* **1950**, *9*, 14.

(5) Bodenstein, M.; Brenschade, W.; Schumacher, H. J. *Z. Phys. Chem. B* **1935**, *28*, 81.

(6) Bodenstein, M.; Brenschade, W.; Schumacher, H. J. *Z. Phys. Chem.* **1938**, *40*, 120.

(7) Briers, E.; Chapman, O. L.; Walter, E. *J. Chem. Soc.* **1926**, 562.

(8) Porter, G. *Proc. R. Soc. London, Ser. A* **1950**, *200*, 284.

(9) Porter, G.; Topp, M. R. *Proc. R. Soc. London, Ser A* **1970**, *315*, 173.

(10) Scaiano, J. C. *Acc. Chem. Res.* **1983**, *16*, 234.

(11) Schmidt, J. A.; Hilinski, E. F. *Rev. Sci. Instrum.* **1989**, *60*, 2902.

(12) Wilson, R. M.; Schnapp, K. A. *Chem. Rev.* **1993**, *93*, 223.

(13) Griffin, G. W. *Angew. Chem. Int. Ed. Eng.* **1971**, *10*, 537.

(14) Muller, J. F.; Muller, D.; Deury, H. J.; Michl, J. *J. Am. Chem. Soc.* **1978**, *100*, 1629.

(15) Sheridan, R. S. *Organic Photochemistry*; Marcell Dekker: New York, 1987, Volume 8.

(16) Whittle, E.; Dows, D. A.; Pimentel, G. C. *J. Chem. Phys.* **1954**, *22*, 1943.

(17) Norman, I.; Porter, G. *Nature* **1954**, *174*, 508.

(18) Duncan, I. R. *Chem. Soc. Rev.* **1980**, *9*, 1.

(19) Wright, B. B. *Tetrahedron* **1985**, *41*, 1517.

(20) Sander, W.; Bucher, G.; Wierlacher, S. *Chem. Rev.* **1993**, *93*, 1583.

(21) Banks, J. T.; Scaiano, J. C. *J. Am. Chem. Soc.* **1993**, *115*, 6409.

(22) Scaiano, J. C.; Tanner, M.; Weir, D. *J. Am. Chem. Soc.* **1985**, *107*, 4396.

(23) Scaiano, J. C.; Johnston, L. J. *Pure Appl. Chem.* **1986**, *58*, 1273.

(24) Scaiano, J. C.; Johnston, L. J.; McGimpsey, W. G.; Weir, D. *Acc. Chem. Res.* **1988**, *21*, 22.

(25) Scaiano, J. C.; Johnston, L. J. *Organic Photochemistry*; Marcell Dekker: New York, 1989, Volume 10.

(26) Bromberg, A.; Schmidt, K. H.; Meisel, D. *J. Am. Chem. Soc.* **1984**, *106*, 3056.

(27) Bromberg, A.; Schmidt, K. H.; Meisel, D. *J. Am. Chem. Soc.* **1985**, *107*, 83.

(28) Itoh, M.; Tokumura, K.; Tanimoto, Y.; Okada, Y.; Takeuchi, H.; Obi, K.; Tanaka, I. *J. Am. Chem. Soc.* **1982**, *104*, 4146.

(29) Tokumura, K.; Udagawa, M.; Itoh, M. *J. Phys. Chem.* **1985**, *89*, 5147.

(30) Redmond, R. W.; Wayner, D. D. M.; Kanabus-Kaminska, J. M.; Scaiano, J. C. *J. Phys. Chem.* **1989**, *93*, 6397.

(31) Wilson, R. M.; Hannemann, K.; Schnapp, K. A.; Memarian, H. R.; Azadnia, A. In *SPSE Proceedings: Summer Symposium on Photochemistry for Imaging*; SPSE - The Society for Imaging Science and Technology: White Bear Lake, Minnesota, 1988; pp Pages.

(32) Wilson, R. M.; Schnapp, K. A.; Hannemann, K.; Ho, D. M.; Memarian, H. R.; Azadnia, A.; Pinhas, A. R.; Figley, T. M. *Spectrochim. Acta* **1990**, *46A*, 551.

(33) Wilson, R. M.; Adam, W.; Oestriche, R. S. *The Spectrum* **1991**, *4*, 8.

(34) Ashkin, A.; Dziedzic, J. M. *Phys. Rev. Lett.* **1977**, *38*, 1351.

(35) Ashkin, A.; Dziedzic, J. M. *Appl. Opt.* **1981**, *20*, 1803.

(36) Owen, J. F.; Chang, R. K.; Barber, P. W. *Opt. Lett.* **1981**, *6*, 540.

(37) Tzeng, H.-M.; Wall, K. F.; Long, M. B.; Chang, R. K. *Opt. Lett.* **1984**, *9*, 499.

(38) Qian, S.-X.; Snow, J. B.; Tzeng, H.-M.; Chang, R. K. *Science* **1986**, *231*, 486.

(39) Hammett, L. P. *J. Am. Chem. Soc.* **1937**, *59*, 96.

(40) Hammond, G. S. *J. Am. Chem. Soc.* **1955**, *77*, 334.

(41) Rüchardt, C. *Angew. Chem. Int. Ed. Eng.* **1970**, *9*, 830.

(42) Ritchie, C. D. *J. Am. Chem. Soc.* **1972**, *5*, 348.

(43) Richard, J. P.; Jencks, W. P. *J. Am. Chem. Soc.* **1982**, *104*, 4689.

(44) Ta Shma, J. P.; Rappoport, Z. *J. Am. Chem. Soc.* **1983**, *105*, 6082.

(45) Huyser, E. S.; Wang, D. T. *J. Org. Chem.* **1964**, *29*, 2720.

(46) Kochi, J. K. *J. Am. Chem. Soc.* **1962**, *84*, 1193.

(47) Scaiano, J. C.; Chen, C.; McGarry, P. F. *J. Photochem. Photobiol. A: Chem* **1991**, *62*, 75.

(48) Bohne, C.; Konuk, R.; Scaiano, J. C. *Chem. Phys. Lett.* **1988**, *152*, 156.

(49) Wilkinson, F.; Willsher, C. J.; Casal, H. L.; Johnston, L. J.; Scaiano, J. C. *Can. J. Chem.* **1986**, *64*, 539.

(50) Asmus, K. D.; Janata, E. In *The Study od Fast Processes and Transient Species by Electron Pulse Radiolysis*; J. Basendale and F. Busi, Ed.; Reidel Publishing: 1982; pp 91.

(51) Arnason, J. T.; Guèrin, B.; Kraml, M. M.; Mehta, B.; Redmond, R. W.; Scaiano, J. C. *Photochem. Photobiol.* **1992**, *55*, 35.

(52) Belt, S. T.; Scaiano, J. C.; Whittlesey, M. K. *J. Am. Chem. Soc.* **1993**, *115*, 1921.

(53) Evans, C. Ph. D. Thesis, University of Ottawa, 1989.

(54) McGarry, P. F. Ph. D. Thesis, University of Ottawa, 1992.

(55) Scaiano, J. C. *J. Am. Chem. Soc.* **1980**, *102*, 7747.

(56) Goldschmidt, C. R.; Ottolenghi, M.; Stein, G. *Isr. J. Chem.* **1970**, *8*, 29.

(57) Ihlemann, J. *Appl. Surf. Sci.* **1992**, *54*, 193.

(58) Srinivasan, R.; Braren, B.; Casey, K. G.; Yeh, J. T. C. *Appl. Phys. Lett.* **1989**, *55*, 2791.

(59) Srinivasan, R.; Braren, B.; Casey, K. G. *J. Appl. Phys.* **1990**, *68*, 1842.

(60) Srinivasan, R.; Braren, B.; Casey, K. G. *Pure Appl.Chem.* **1990**, *62*, 1581.

(61) Srinivasan, R. *J. Appl. Phys.* **1993**, *73*, 2743.

(62) Huang, R. L.; Lee, K. H. *J. Chem. Soc.* **1964**, 5957.

(63) Huang, R. L.; Lee, K. H. *J. Chem. Soc.* **1964**, 5963.

(64) Sandner, M. R.; Osborn, C. L. *Tetrahedron Lett.* **1974**, *15*, 415.

(65) Baumann, H.; Timpe, H. J.; Zubarev, V. E.; Fok, N. V.; Melnikov, M. Y. *J. Photochem.* **1985**, *30*, 487.

(66) Fischer, H.; Baer, R.; Hany, R.; Verhoolen, I.; Walbiner, M. *J. Chem. Soc. Perkin Trans. 2* **1990**, 787.

(67) Phan, X. T. *J. Radiat. Curing* **1986**, 11.

(68) Borer, A.; Kirchmayr, R.; Rist, G. *Helv. Chim. Acta* **1978**, *61*, 305.

(69) Fouassier, J.-P.; Merlin, A. *J. Photochem.* **1980**, *12*, 17.

(70) Groenenboom, C. J.; Hageman, H. J.; Overeem, T.; Weber, A. J. M. *Makromol. Chem.* **1982**, *183*, 281.

(71) Jaegermann, P.; Lendzian, F.; Rist, G.; Möbius, K. *Chem. Phys. Lett.* **1987**, *140*, 615.

(72) Jent, F.; Paul, H.; Fischer, H. *Chem. Phys. Lett.* **1988**, *146*, 315.

(73) Huang, R. L.; Lee, T.-W.; Ong, S. H. *J. Chem. Soc. (C)* **1969**, 40.

(74) Chick, W. H.; Ong, S. H. *J. Chem. Soc., Chem. Commun.* **1969**, 216.

(75) Santhosh, C.; Mishra, P. C. *J. Photochem. Photobiol. A: Chem* **1990**, *51*, 245.

(76) Wintgens, V.; Johnston, L. J.; Scaiano, J. C. *J. Am. Chem. Soc.* **1988**, *110*, 511.

(77) Heller, H. G.; Langan, J. R. *J. Chem. Soc., Perkin Trans. II* **1981**, 341.

(78) The estimate of 78 is based on the product of the methyl:ethyl (6.5) and ethyl:isopropyl (12) ratios of reactivities, see table 3.1.

(79) Crawford, R. J.; Raap, R. *Can. J. Chem.* **1964**, *43*, 126.

(80) Mendenhall, G. D. *Tetrahedron Lett.* **1983**, *24*, 451.

(81) Loucks, L. F.; Liu, M. T. H.; Hooper, D. G. *Can. J. Chem.* **1979**, *57*, 2201.

(82) Kiefer, H.; Traylor, T. G. *Tetrahedron Lett.* **1966**, *7*, 6163.

(83) Heller, H. G. In *Electronic Materials: From Silicon to Organics*; L. S. Miller and J. B. Mullin, Ed.; Plenum Publ.: New York, 1991; pp 471

(84) Johnston, L. J.; Scaiano, J. C. *J. Am. Chem. Soc.* **1986**, *108*, 2349.

(85) Banks, J. T.; Scaiano, J. C.; Adam, W.; Oestrich, R. S. *J. Am. Chem. Soc.* **1993**, *115*, 2473.

(86) Arnold, B. R.; Scaiano, J. C. *Macromolecules* **1992**, *25*, 1582.

(87) Arnold, B. R.; Scaiano, J. C.; McGimpsey, W. G. *J. Am. Chem. Soc.* **1992**, *114*, 9978.

(88) Bohne, C.; Boch, R.; Scaiano, J. C. *J. Org. Chem.* **1990**, *55*, 5414.

(89) Arnold, B. R.; Scaiano, J. C. *Unpublished results.* **1993**,

(90) Adam, A.; Oestrich, R. S. *J. Am. Chem. Soc.* **1992**, *114*, 6031.

(91) Neville, A. G.; Brown, C. E.; Rayner, D. M.; Lusztyk, J.; Ingold, K. U. *J. Am. Chem. Soc.* **1991**, *113*, 1869.

(92) Weir, D.; Scaiano, J. C. *Chem. Phys. Lett.* **1986**, *128*, 156.

(93) Scaiano, J. C.; Shi, J. L. *Chem. Phys. Lett.* **1990**, *173*, 271.

(94) Faria, J. L.; Steenken, S. *J. Am. Chem. Soc.* **1990**, *112*, 1277.

(95) Redmond, R. W.; Scaiano, J. C.; Johnston, L. J. *J. Am. Chem. Soc.* **1990**, *112*, 398.

(96) Pryor, W. A. *Free Radicals in Biology*; Academic Press: New York, 1976; Vol. 3.

(97) Carter, W. P. L.; Darnall, K. R.; Lloyd, A. C.; Winer, A. M.; Pitts, J. N., Jr. *Chem. Phys. Lett.* **1976**, *42*, 22.

(98) Pitts, J. N.; Finlayson, B. J. *Angew. Chem., Int. Ed. Engl.* **1975**, *14*, 1.

(99) Ingold, K. U. *Pure Appl. Chem.* **1967**, *15*, 49.

(100) Walling, C. *Pure Appl. Chem.* **1967**, *15*, 69.

(101) Howard, J. A.; Bennett, J. E.; Brunton, G. *Can. J. Chem.* **1981**, *59*, 2253.

(102) Wong, P. C.; Griller, D.; Scaiano, J. C. *J. Am. Chem. Soc.* **1982**, *104*, 5106.

(103) Howard, J. A.; Scaiano, J. C. In *Landolt-Börnstein. Numerical Data and Functional Relationships in Science and Technology. New Series*; H. Fischer, Ed.; Springer-Verlag: Berlin, 1984; Vol. 13d; pp 431.

(104) Walling, C.; Padwa, A. *J. Am. Chem. Soc.* **1963**, *85*, 1593.

(105) Walling, C.; Wagner, P. J. *J. Am. Chem. Soc.* **1964**, *86*, 3368.

(106) Neta, P.; Dizaroglu, M.; Simic, M. G. *Isr. J. Chem.* **1984**, *24*, 25.

(107) Neville, A. G.; Brown, C. E.; Rayner, D. M.; Lusztyk, J.; Ingold, K. U. *J. Am. Chem. Soc.* **1989**, *111*, 9269.

(108) Avila, D. V.; Brown, C. E.; Ingold, K. U.; Lusztyk, J. *J. Am. Chem. Soc.* **1993**, *115*, 466.

(109) Weiland, H. *Chem. Ber.* **1911**, *44*, 2250.

(110) Maillard, B.; Ingold, K. U. *J. Am. Chem. Soc.* **1976**, *98*, 1224.

(111) Kochi, J. K.; Krusic, P. J. *J. Am. Chem. Soc.* **1969**, *91*, 3940.

(112) Shevlin, P. B.; Hansen, H. J. *J. Org. Chem.* **1977**, *42*, 3011.

(113) Effio, A.; Griller, D.; Ingold, K. U.; Scaiano, J. C.; Sheng, S. J. *J. Am. Chem. Soc.* **1980**, *102*, 6063.

(114) Falvey, D. E.; Khambatta, B. S.; Schuster, G. B. *J. Chem. Phys.* **1990**, *94*, 1056.

(115) Avila, D. V.; Lusztyk, J.; Ingold, U. *J. Am. Chem. Soc.* **1992**, *114*, 6576.

(116) Paul, H.; Small, R. D., Jr.; Scaiano, J. C. *J. Am. Chem. Soc.* **1978**, *100*, 4520.

(117) Baignée, A.; Howard, J. A.; Scaiano, J. C.; Stewart, L. C. *J. Am. Chem. Soc.* **1983**, *105*, 6120.

(118) Tokumura, K.; Nosaka, H.; Ozaki, T. *Chem. Phys. Lett.* **1990**, *169*, 321.

(119) Tokumura, K.; Ozaki, T.; Nosaka, H.; Saigusa, Y.; Itoh, M. *J. Am. Chem. Soc.* **1991**, *113*, 4974.

(120) Maillard, B.; Ingold, K. U.; Scaiano, J. C. *J. Am. Chem. Soc.* **1983**, *105*, 5095.

(121) Howard, J. A.; Ingold, K. U. *Can. J. Chem.* **1969**, *47*, 3796.

(122) Lissi, E. *Can. J. Chem.* **1974**, *52*, 2491.

(123) Burkey, T. J.; Majewski, M.; Griller, D. *J. Am. Chem. Soc.* **1986**, *108*, 2218.

(124) Scaiano, J. C.; Wubbels, G. G. *J. Am. Chem. Soc.* **1981**, *103*, 640.

(125) Avila, D. V.; Ingold, K. U.; DiNardo, A. A.; Zerbetto, F.; Zgierski, M. Z.; Lusztyk, J. *J. Am. Chem. Soc.* **1994**, *in preparation.*

(126) Dewar, M. J. S.; Zoebisch, E. G.; Healy, E. F.; Stewart, J. J. P. *J. Am. Chem. Soc.* **1985**, *107*, 3902.

(127) Baker, J. *J. Comp. Chem.* **1986**, *7*, 385.

(128) Avila, D. V. unpublished results. Note that if $\Delta H = 0$ the same condition can be met, however, this appears highly unlikely.

(129) Porret, D.; Goodev, C. G. *Proc. Roy. Soc. A* **1958**, *31*, 165.

(130) Wagniere, G. H. *The chemistry of the carbon-halogen bond*; Wiley: New York, 1973.

(131) Kopecky, J. *Organic photochemistry: a visual approach*; VCH Publishers: New York, 1992.

(132) Kropp, P. J.; Worsham, P. R.; Davidson, R. I.; Jones, T., H. *J. Am. Chem. Soc.* **1982**, *104*, 3972.

(133) Kropp, P., J.; Sawyer, J. A.; Snyder, J. J. *J. Org. Chem.* **1984**, *49*, 1583.

(134) Perkins, R. R.; Pincock, R. E. *Tetrahedron* **1975**, *20*, 943.

(135) Kropp, P., J.; Poindexter, G. S.; Pienta, N. J.; Hamilton, D. C. *J. Am. Chem. Soc.* **1976**, *98*, 8135.

(136) Dannenberg, J. J.; Dill, K. *Tetrahedron Lett.* **1972**, *13*, 1571.

(137) Bakale, D. K.; Gillis, H. A. *J. Phys. Chem.* **1970**, *74*, 2074.

(138) Varvoglis, A. *Synthesis* **1984**, 709.

(139) Crivello, J. V.; Lam, J. H. W. *Macromolecules* **1977**, *10*, 1307.

(140) Pappas, S. P. *J. Imaging. Technol.* **1985**, *11*, 146.

(141) Baumann, H.; Timpe, H. *Acta Polymer* **1986**, *37*, 309.

(142) Bunnett, J. F.; Wamser, C. C. *J. Am. Chem. Soc.* **1966**, *88*, 5534.

(143) Brydon, D. L.; Cadogan, J. I. *J. Chem. Soc., Chem. Commun.* **1966**, 744.

(144) Brydon, D. L.; Cadogan, J. I. *J. Chem. Soc. C* **1968**, 819.

(145) Tanner, D. D.; Reed, D. W.; Setiloane, B. P. *J. Am. Chem. Soc.* **1982**, *104*, 3917.

(146) Devoe, R. J.; Sahyun, M. R. V.; Schmidt, E.; Serpone, N.; K., S. D. *Can. J. Chem.* **1988**, *66*, 319.

(147) Farnham, W. B.; Calabrese, J. C. *J. Am. Chem. Soc.* **1986**, *108*, 2449.

(148) Wittig, G.; Schöllkopf, U. *Tetrahedron* **1958**, *3*, 91.

(149) Reich, H. J.; Phillips, N. H.; Reich, I. L. *J. Am. Chem. Soc.* **1985**, *107*, 4101.

(150) Perkins, C. W.; Martin, J. C.; Arduengo, A. J.; Lau, W.; Alegria, A.; Kochi, J. K. *J. Am. Chem. Soc.* **1980**, *102*, 7753.

(151) Perkins, C. W.; Clarkson, R. B.; Martin, J. C. *J. Am. Chem. Soc.* **1986**, *108*, 3206.

(152) Perkins, C. W.; Martin, J. C. *J. Am. Chem. Soc.* **1986**, *108*, 3211.

(153) Thaler, W. *J. Am. Chem. Soc.* **1963**, *85*, 2607.

(154) Shea, K. J.; Skell, P. S. *J. Am. Chem. Soc.* **1973**, *95*, 283.

(155) Olah, G. A. *Halonium Ions*; Wiley Interscience: New York, 1975

(156) Chateauneuf, J.; Lusztyk, J.; Ingold, K. U. *J. Org. Chem.* **1990**, *55*, 1061.

(157) Peyman, A.; Beckhaus, H.-D.; Rüchardt, C. *Chem. Ber.* **1988**, *121*, 1027.

(158) Chatgialoglu, C. In *Handbook of Organic Photochemistry*; J. C. Scaiano, Ed.; CRC Press: Boca Raton, Florida, 1989; Vol. II; pp 3

(159) Bartl, J.; Steenken, S.; Mayr, H.; McClelland, R. A. *J. Am. Chem. Soc.* **1990**, *112*, 6918.

(160) Adam, W.; Oestrich, R. S. *J. Am. Chem. Soc.* **1993**, *115*, 3455.

(161) Zimmt, M. B.; Doubleday, C. J.; Turro, N. J. *J. Am. Chem. Soc.* **1986**, *108*, 3618.

(162) Zimmt, M. B.; Doubleday, C. J.; Gould, I. R.; Turro, N. J. *J. Am. Chem. Soc.* **1985**, *107*, 6724.

(163) Plummer, B. F.; Chihal, D. M. *J. Am. Chem. Soc.* **1971**, *93*, 2071.

(164) Pappas, S. P.; Zehr, R. D., Jr. *J. Am. Chem. Soc.* **1971**, *93*, 7112.

(165) Kubo, Y.; Togawa, S.; Yamane, K.; Takuwa, A.; Araki, T. *J. Org. Chem.* **1989**, *54*, 4929.

(166) Hayes, R. A.; Hess, T. C.; McMahon, R. J.; Chapman, O. L. *J. Am. Chem. Soc.* **1983**, *105*, 7787.

(167) McMahon, R. J.; Chapman, O. L.; Hayes, R. A.; Hess, T. C.; Krimmer, H. P. *J. Am. Chem. Soc.* **1985**, *107*, 7597.

(168) Chang, S.; Shankar, B. K. R.; Shechter, H. *J. Org. Chem.* **1982**, *47*, 4226.

(169) Murata, S.; Yamamoto, T.; Tomioka, H. *J. A. Chem. Soc.* **1993**, *115*, 4013.

(170) Barra, M.; Fisher, T. A.; Cernigliaro, G. J.; Sinta, R.; Scaiano, J. C. *J. Am. Chem. Soc.* **1992**, *114*, 2630.

(171) Reiser, A. *Photoreactive Polymers: The Science and Technology of Resists*; John Wiley and Sons: New York, 1989, pp 409.

(172) Marignier, J. L. *Nature* **1990**, *346*, 115.

(173) Cava, M. P.; Litle, R. L.; Napier, D. R. *J. Am. Chem. Soc.* **1958**, *80*, 2257.

(174) Klundt, I. L. *Chem. Rev.* **1970**, *70*, 471.

(175) Cava, M. P.; Spangler, R. J. *J. Am. Chem. Soc.* **1967**, *89*, 4550.

(176) Spangler, R. J.; Kim, J. H.; Cava, M. P. *J. Org. Chem.* **1977**, *42*, 1697.

(177) Andraos, J.; de Lucas, N.; Scaiano, J. C. *Unpublished results.* **1994**.

(178) Boate, D. R.; Johnston, L. J.; Kwong, P. C.; Lee-Ruff, E.; Scaiano, J. C. *J. Am. Chem. Soc.* **1990**, *112*, 8858.

(179) Boch, R.; Bradley, J. C.; Durst, T.; Scaiano, J. C. *Tetrahedron Lett.* **1994**, *35*, 19.

(180) Brown, R. F. C.; Eastwood, F. W.; Harrington, K. J. *Aust. J. Chem.* **1974**, *27*, 2373.

(181) Brown, R. F. C.; McMullen, G. L. *Aust. J. Chem.* **1974**, *27*, 2385.

(182) Brown, R. F. C.; Eastwood, F. W.; McMullen, G. L. *J. Am. Chem. Soc.* **1976**, *98*, 7421.

(183) Wentrup, C.; Lorencak, P. *J. Am. Chem. Soc.* **1988**, *110*, 1880.

(184) Scaiano, J. C. *J. Photochem.* **1973/74**, *2*, 81.

(185) Yang, N. C.; Rivas, C. *J. Am. Chem. Soc.* **1961**, *83*, 2213.

(186) Zwicker, E. F.; Grossweiner, L. I.; Yang, N. C. *J. Am. Chem. Soc.* **1963**, *85*, 2671.

(187) Das, P. K.; Scaiano, J. C. *J. Photochem.* **1980**, *12*, 85.

(188) Ishida, A.; Yamamoto, K.; Takamuku, S. *Bull. Chem. Soc. Jpn.* **1992**, *65*, 3186.

(189) Ullman, E. F.; Huffman, K. R. *Tetrahedron Lett.* **1965**, 1863.

(190) Heindel, N. D.; Molnar, J.; Pfau, M. *J. Chem. Soc., Chem. Commun.* **1970**, 1373.

(191) Wilson, R. M.; Hanneman, K.; Peters, K.; Peters, E. M. *J. Am. Chem. Soc.* **1987**, *109*, 4741.

(192) Das, P. K.; Encinas, M. V.; Small, R. D., Jr.; Scaiano, J. C. *J. Am. Chem. Soc.* **1979**, *101*, 6965.

(193) Nakayama, T.; Hamanoue, K.; Hidaka, T.; Okamoto, M.; Teranishi, H. J. *J. Photochem.* **1984**, *24*, 71.

(194) Netto-Ferreira, J. C.; Scaiano, J. C. *Can. J. Chem.* **1993**, *71*, 1209.

(195) Jung, M. E.; Ornstein, P. L. *Tetrahedron Lett.* **1977**, 2659.

(196) Banks, J. T.; Scaianc, J. C.; Garcia, H.; Miranda, M. A. *To be published.* **1994.**

(197) Srinivasan, R. *Science* **1986**, *234*, 559.

(198) Srinivasan, R.; Braren, B. *Chem. Rev.* **1989**, *89*, 1303.

(199) Yeh, J. T. C. *J. Vac. Sci. Technol. A* **1986**, *4*, 653.

(200) Srinivasan, R.; Mayne-Banton, V. *Appl. Phys. Lett.* **1982**, *41*, 576.

(201) Srinivasan, R.; Leigh, W. J. *J. Am. Chem. Soc.* **1982**, *104*, 6784.

(202) Linsker, R.; Srinivasan, R.; Wynne, J. J.; Alens, D. R. *Lasers Surg. Med.* **1984**, *4*, 2.

(203) Trokel, S. T.; Srinivasan, R.; Braren, B. *Am. J. Ophtamol.* **1983**, *96*, 710.

(204) Cole, H. S.; Liu, Y. S.; Phillip, H. R. *Appl. Phys. Lett.* **1986**, *48*, 76.

(205) Koren, G.; Yeh, J. T. C. *J. Appl. Phys.* **1984**, *56*, 2120.

(206) Koren, G.; Yeh, J. T. C. *Appl. Phys. Lett.* **1984**, *44*, 1112.

(207) Srinivasan, R.; Braren, B.; Dreyfus, R. W. *J. Appl. Phys.* **1987**, *61*, 372.

(208) Srinivasan, R. *Polymer Degradation and Stability* **1987**, *17*, 193.

(209) Davies, G. M.; Gower, M. C.; Fotakis, C.; Efthimiopoulos, T.; Argyrakis, P. *Appl. Phys.* **1985**, *A36*, 27.

(210) Dyer, P. E.; Srinivasan, R. *Appl. Phys. Lett.* **1986**, *48*, 445.

(211) Kuper, S.; Stuke, M. *Appl. Phys. B* **1988**, *44*, 199.

(212) Srinivasan, R.; Ghosh, A. P. *Chem. Phys. Lett.* **1988**, *143*, 546.

(213) Wells, M. R.; Melton, L. A. *J. Heat Transfer* **1990**, *112*, 1008.

(214) Förster, T. *Angew. Chem. Int. Ed. Engl.* **1969**, *8*, 333.

(215) Gossage, H. E.; Melton, L. A. *Appl. Optics.* **1987**, *26*, 2256.

(216) Lambert, J. B.; Shurvell, H. F.; Lightner, D. A.; Cooks, G. R. *Introduction to Organic Spectroscopy.*; Macmillan: New York, 1987, pp 454.

(217) Scaiano, J. C.; Arnold, B. R.; McGimpsey, W. G. *J. Am. Chem. Soc.* **1994**, *In press.*

(218) Wayner, D. D. M.; Griller, D. *J. Am. Chem. Soc.* **1985**, *107*, 7764.